CRANFIELD UNIVERSITY

S B Ferreira

THERMOECONOMIC ANALYSIS AND OPTIMISATION OF BIOMASS FUEL GAS TURBINES

SCHOOL OF ENGINEERING

PhD THESIS

CRANFIELD UNIVERSITY

SCHOOL OF ENGINEERING

PhD THESIS

Academic Year 1998-2002

S B Ferreira

THERMOECONOMIC ANALYSIS AND OPTIMISATION OF BIOMASS FUEL GAS TURBINES

Supervisor: P Pilidis

October 2002

This thesis is submitted for the degree of Philosophy Doctor

Abstract

The ready availability of biomass in Brazil makes this type of fuel a major candidate to integrate the country's energy matrix. Although this fuel is used as a primary energy source, its use for electricity generation is still modest. On the other hand, high efficiency and power density achieved by modern gas turbine engines make them a promising option for the power generation market. Thus, this thesis has as main objective to analyse the marriage between the solid fuel, biomass in this case, and gas turbines.

Two main types of power plants are studied; the biomass integrated gasification gas turbine cycle (BIGGT) and the externally fired cycle (EFGT), which for the first time is thoroughly studied for the use of biomass fuel, plus the intercooled and recuperated variants of these power plants. The results are compared with the ordinary natural gas fuelled cycle. The method involves on- and off-design point performance and exergy analysis. The economic performance and optimisation for each cycle is also explored in order to assess their feasibility. The optimisation technique adopted is the Genetic Algorithm (GA) connected to the conventional hill-climbing methodology. This merge uses the GA to identify the region of optimum values, which are then passed on to the hill-climbing algorithm. In this way the long time demanded by the GA to converge is shortened and the unreliability of the hill-climbing method in finding the global optimum is overcome.

The codes developed for design-point performance analysis and optimisation, compared with a commercial package, proved reliable and robust. The tools developed for exergy analysis (on- and off-design) are also robust and flexible, with the capability of analysing and calculating the properties of mixtures made of 23 different gases. The emissions equations are sufficiently accurate for the purposes of this thesis. The relationship proposed for calculating the variable operating and maintenance costs proved to be consistent with the current knowledge.

The results show that the optimised cycles are competitive with current technology in terms of cost of electricity, the EFGT being the more competitive biomass cycle, with costs of electricity (US$ 0.07/kWh) comparable with those of the natural gas fuelled power plants. The BIGGT in its turn shows a cost of electricity 29 percent higher than its natural gas and externally fired counterparts (US$0.09/kWh) counterparts. The method used to work out the best investment – the required revenue (RR) method – demonstrated that the EFGT is again comparable with the NGGT cycle, with its RR being only 7 percent higher. The BIGGT cycle shows a higher RR due to its costly gasification/cleaning system. The minimisation of the exergy destruction ratio indicates that little improvement would be achieved after the reduction of this parameter, and a penalty – an 85 percent increase in the cost of electricity – must be paid.

The environmental advantage of the biomass-fuelled cycles over the natural gas cycle is clear, making these systems very promising as low emissions alternatives. Both BIGGT and EFGT cycles presented very low CO_2 emissions. Regarding NO_x emissions, the EFGT cycle has the lowest rates, whereas the BIGGT has the highest.

Acknowledgements

Firstly, I would like to thank my supervisor, Professor Pericles Pilidis for his guidance and also for the opportunities given during my work in Cranfield.

To the School of Engineering staff, mainly Mrs. Barbara McKenzie and Ms. Caroline Heaton, for the invaluable support and logistics, my most sincere gratitude.

To all friends, from all over the world made in these four years in England, a big thank you for just being friends.

My gratitude to Professor Marco Antônio Rosa do Nascimento, from Universidade Federal de Itajubá – Brasil, who introduced me to the marvellous world of gas turbines.

The support given by CAPES/Brasil, the sponsoring agency that financially supported me for four years is acknowledged, with special thanks to Mrs. Vanda Lucena.

To my parents, Humberto and Doca, and my brother, Christian, who supported me in all projects I undertook during my life. "Thanks" does not express my gratitude for the love given. I just hope I can do at least the same for my "little one".

To my beautiful wife, Marta, who is indeed more than a partner, all my love and gratitude for the support during the twelve wonderful years we have been together. Of course, to my little daughter Beatriz, whose name means happiness and that is exactly what she is.

List of contents

List of figures

List of tables

Nomenclature

Symbols

$\dot{C}$ and $\dot{Z}$	–	cost rates
$\dot{S}$	–	entropy rate, [W/K]
$\dot{E}$	–	exergy rate, [W]
m	–	mass flow, [kg/s]
$\bar{s}$	–	molar entropy, [J/mol-K]
$\overline{HHV}$	–	molar higher heating value, [J/mol]
$\overline{R}$	–	universal gas constant, [J/mol-K]
$\dot{W}$	–	work
Δ	–	difference (of temperature, pressure, etc.)
η	–	efficiency
ε	–	exergetic efficiency
φ	–	heat exchanger effectiveness
A	–	area, [m^2], or activity ratio for emission calculations
c	–	average cost per unit of exergy, [$/GJ]
CH_4	–	methane
CO	–	carbon monoxide
CO_2	–	carbon dioxide
C_p	–	specific heat at constant pressure, [J/kg]
C_v	–	specific heat at constant volume, [J/kg]
E	–	emission
EF	–	emission factor
f	–	exergoeconomic factor
FAR	–	fuel to air ratio
h	–	specific enthalpy, [J/kg]
H_2	–	hydrogen
H_2O	–	water

m	–	mass, [kg]
NO_x	–	nitrogen oxides
OPR	–	overall pressure ratio
P	–	pressure, either [bar] or [atm]
PR or *R*	–	pressure ratio
r	–	relative cost difference
s	–	specific entropy, [J/kg-K]
SO_2	–	sulphur dioxide
T	–	temperature, either [K] or [^oC]
TET	–	turbine entry temperature, either [K] or [^oC]
TBO	–	time between overhauls, in [hours [h]
t_{op}	–	time of operation
U	–	overall heat exchange (or transfer) coefficient, $\left[\frac{W}{m^2.K}\right]$
UR	–	relative humidity
V	–	velocity, [m/s]
x	–	molar fraction
y_D	–	exergy destruction ratio

Subscripts

∞	–	polytropic
(v)	–	vapour
a	–	actual
amb	–	ambient
b	–	biomass
cc	–	combustion chamber
comp or c	–	compressor
D	–	destruction
e or out	–	exit or outlet
exh	–	exhaust
f	–	fuel
g	–	gas

G	–	gasifier
gen	–	generation
GT	–	gas turbine
HX	–	heat exchanger
i	–	inlet
is	–	isentropic
L	–	losses
o	–	reference
p	–	products
r	–	reactants
sat	–	saturation
t	–	turbine
tot	–	total
u	–	useful

Superscripts

CH	–	chemical
KN	–	kinetic
PH	–	physical
PT	–	potential

Abbreviations

a	–	ash
BIGCC	–	biomass integrated gasification combined cycle
BIGICR	–	biomass integrated gasification intercooled and recuperated gas turbine
BIGGT	–	biomass integrated gasification gas turbine
BOP	–	balance of the plant
CerHx	–	ceramic heat exchanger
CHP	–	combined heat and power
CoE	–	cost of electricity
CRF	–	capital recovery factor
CV	–	calorific value

daf	–	dry ash free
DC	–	direct costs
DFCT	–	direct coal-fired gas turbine
DP	–	design-point
EFCC	–	externally fired combined cycle
EFGT	–	externally fired gas turbine
FBC	–	fluidised bed combustor
FC	–	fixed carbon
FCI	–	fixed investment costs
GA	–	genetic algorithm
GEF	–	global environmental fund
HA	–	hybrid algorithm
HHV	–	higher heating value
HP	–	high pressure
HRSG	–	heat recovery steam generator
IC	–	internal combustion engine or indirect costs
ICEFGT	–	intercooled externally fired gas turbine
IGCC	–	integrated gasification combined cycle
LCV	–	low calorific value
LHV	–	lower heating value
LP	–	low pressure
LPG	–	liquefied petroleum gas
LPT	–	low pressure turbine
NGGT	–	natural gas fuelled gas turbine
NPOP	–	population size
O&M	–	operating and maintenance
OD	–	off-design
PEC	–	purchased equipment cost
PEI	–	purchased equipment installation
PFBC	–	pressurised fluidised bed combustor
RR	–	required revenue
SCR	–	selective catalytic reduction

UNDP	–	United Nations Development Program
VIGV	–	variable inlet guide vane
VM	–	volatile matter
VO&M	–	variable operating and maintenance costs
w	–	water or moisture content

THE ROAD TO WISDOM

_by_ Piet Hein (1905-1996), Danish poet and scientist

The road to wisdom? – Well, it's plain
and simple to express:
Err
and err
and err again
but less
and less
and less.

CHAPTER I – GENERAL INTRODUCTION AND THESIS OVERVIEW

Introduction

The new scenario of the energy market in Brazil, with privatisation, future emission constraints, and the pursuit of alternative forms of energy generation, have led to the search for new power generation technologies and improvements in the existing ones. One of the most promising practices is to combine gas turbines and local biomass fuels, be it dedicated plantations or residues from agro-industries.

In Brazil, especially, biomass is a readily available fuel, and one of the most available residues from agro-industry is sugarcane bagasse. Although this sort of industry has been using bagasse as fuel for many years, the efficiencies achieved in the old steam cycles are much lower than those of modern gas turbine combined cycles. Furthermore, the potential role of this industry and a well-defined policy for independent private producers are the latest incentive for the use of more efficient cycles.

The widespread approach, as far as gas turbines are concerned, is to use biomass integrated gasification gas turbine cycles (BIGGT), which has been analysed by several authors (Lora et al. 2000b, Lora et al. 2000a, Bridgwater, 1995, Bhattacharya, 1993; Hall et al. 1995, Junior Isles, 1998, Turn, 1999a). However, gasification is a very costly process with large energy drains. The externally fired gas turbine cycle (EFGT) is proposed as another form of biomass utilisation, and seems equally promising in terms of efficiency and power (Ferreira et al. 2001b). The competitive cost of electricity in the EFGT cycle is also a very attractive point to be considered.

Objectives and thesis overview

The objectives of the work described in this thesis are:

1. Propose and study in detail the use of biomass fuels in externally fired cycle, regarding design- and off-design performance, and economic implications of

the use of such fuel. So far the externally fired cycle has been studied for coal applications only.

2. Carry out a design-point performance analysis and optimisation of both BIGGT and EFGT cycles, using the conventional natural gas fired cycle (NGGT).
3. Conduct an economic analysis and optimisation of these cycles using a novel tool, namely Hybrid Algorithm: Genetic Algorithm + Hill Climbing.
4. Propose a tool for economic assessment of the gas turbine cycles operating under off-design conditions, which can be used as a real time economic assessment of the cost of electricity.
5. Conduct on-design and off-design exergetic analyses in order to identify the components that are major sources of losses, and evaluate the cost-effectiveness of investing in these components.

This thesis is divided in seven chapters, which will be described in the paragraphs that follow. The first chapter is the current one and intends to clarify its objectives and contributions, and also give an overview of the content of the other chapters.

Chapter II defines the term biomass and describes it as a fuel. The main thermochemical characteristics, such as moisture content, ash content, volatile matter, fixed carbon, and heating value, and their effect on the biomass performance as a fuel are discussed and compared with more commonly-used fuels. A general overview of its potential as a primary energy source is also presented. The Brazilian scenario is emphasised in order to show the potential of biomass as a source in that particular country. The economic point of view – including land use, transport and handling – of the use of biomass are thoroughly discussed, and the chapter ends with a description of the environmental advantages of this type of fuel.

Chapter III explains the technologies available for the use of solid fuels in gas turbines, and the main advantages and drawbacks of those technologies are presented. The gasification process is discussed in detail, and the main types of gasifiers are described and classified accordingly to their oxidant, operating pressure, and calorific values yielded. The gas turbine cycles potentially available are also described and a

thorough discussion about their design-point performance, including exergetic analysis, plus an analysis of the implications of low calorific value fuels in gas turbines is presented. The cleaning system is described and the technological alternatives discussed under the specifications demanded by the gas turbine manufacturers. The EFGT cycle is introduced and the main thermodynamic and technological issues regarding the use of a heat exchanger in substitution for the conventional combustion chamber are carefully examined. Finally, an estimate and discussion about the emissions regarding CO_2 and NO_x is presented for each cycle.

Chapter IV is a brief discussion about the main issues relating to the use of gas turbines in combined cycle power plants. The on- and off-design performances are examined, regarding changes in ambient parameters and load demand. Because the steam part of combined cycles is not the object of study of this thesis, only the single-pressure mode steam cycles is presented, which is enough to give an idea of the capabilities of the combined cycles.

Chapter V describes the method adopted for the exergetic analysis carried out in this work. Exergy is defined and a justification of the use of such a technique, instead of the current energy analysis, is conducted. A description of the methods used to calculate the exergy content of streams and fuels is given, and the main parameters used for exergetic analysis such as exergy efficiency, exergy destruction, and exergy destruction ratio are discussed. The exergoeconomic method is also described, together with the equations used to calculate individual component costs. The optimisation using Hybrid Algorithm (HA) is carried out followed by the economic and exergoeconomic analyses of the optimum designs.

Chapter VI presents the results of the off-design performance of each cycle regarding changes in ambient temperature and load. The control parameters are TET^{l} and VIGVs. A part-load exergy analysis is carried out in order to assess the sensitivity of each component to load variations, and also to identify the critical components, i.e., those that are the main source of irreversibilities. A method for off-design estimate of the variable operating and maintenance (VO&M) costs is proposed and applied to three case studies regarding three major cities in Brazil and their demand curve within one year.

Finally, Chapter VII presents the conclusions on the findings and results of this work and recommends future goals related to the gas turbine cycles studied.

[1] Throughout this thesis the nomenclature used us as close as possible to that suggested in Ramsden, K. W., 2002.

CHAPTER II – BIOMASS: A GENERAL OVERVIEW

Introduction

Due to the growing scarcity of fossil fuels, the increasing energy demand all around the globe, and the mounting concern about greenhouse gas emissions, research centres around the world have been conducting technical and economic assessments for alternative energy sources.

Renewable sources of energy are the primary focus of the investigations being conducted; however, not all countries have the right renewable resources to generate the amount of power required. A common characteristic is that all these regions have an immense potential for a special type of renewable energy, biomass, either from plantations or in the form of residues from certain industries.

The term biomass refers to renewable organic matter. This work focuses on the use of two main types of biomass: sugarcane bagasse, a fibrous residue from the sugarcane milling process, and eucalyptus, from dedicated plantations. In this particular case biomass is the plant material derived from the reaction between CO_2 in the air, water, and sunlight, via photosynthesis, to produce the carbohydrates that form the building blocks of a plant (McKendry, 2002a).

Brazil has a special potential for the use of renewable sources of energy, and as such the focus of this study, funded by a Brazilian research agency, will be the two principal potential types of biomass produced that country; the aforementioned sugarcane bagasse and eucalyptus.

The use of biomass for power generation

Biomass has been used as a primary energy resource since the discovery of fire, initially as a heat source only. With the industrial revolution and the invention of the boiler and steam engine, biomass started to be used for shaft-power and electricity generation in those countries where coal was either in short supply or of poor quality. Sometimes used as a complement for coal, in many countries biomass completely substituted this fuel, becoming the main source of energy.

Table 1 – Estimated potential supplies of biomass for energy (10^3 MJ/year) in the mid-21st century (Larson, 1993)

Region	Recoverable residues			Biomass plantations	Total potential
	Crop	Forest	Total		
US/Canada	1.70	3.80	5.50	34.80	40.30
Europe	1.30	2.00	3.30	11.40	14.70
Japan	0.10	0.20	0.30	0.90	1.20
Australia & New Zealand	0.30	0.20	0.50	17.90	18.40
Former URSS	0.90	2.00	2.90	46.50	49.40
Latin America	2.40	1.20	3.60	51.40	55.00
Africa	0.70	1.20	1.90	52.90	54.80
China	1.90	0.90	2.80	16.30	19.10
Other Asia	3.20	2.20	5.40	33.40	38.80
TOTAL	**12.50**	**13.70**	**26.20**	**265.50**	**291.70**

Table 1 gives the estimated potential supplies of biomass for the 21st century. The potential for developing countries of Latin America and Africa is enormous, closely followed by the former URSS and the United States and Canada.

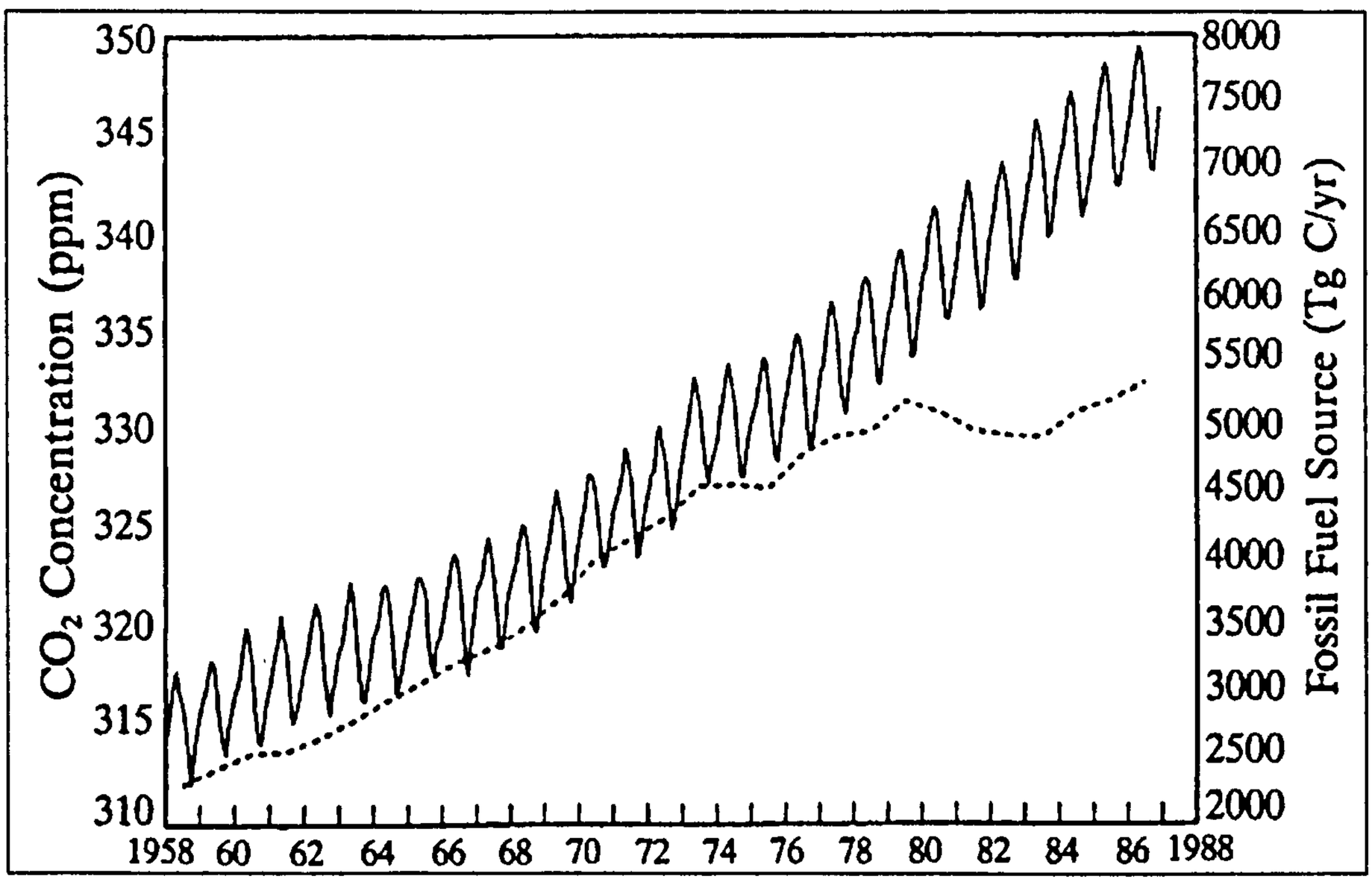

Figure 1 – The increase in the concentration of global atmospheric CO_2 (solid oscillating curve) and CO_2 emissions from the burning of fossil fuels (dotted line) (Levine, J. S., 1991)

Furthermore, biomass can make a large contribution to minimising the global emission of greenhouse gases, mainly CO_2. Due to increasing demand for energy, the use of fossil fuels has substantially increased since the end of the World War II.

Figure 1 illustrates the CO_2 emissions and shows the increase in global atmospheric CO_2 and CO_2 from fossil fuel sources from 1958 to 1988. The annual

oscillation in the curve for the concentration of global atmospheric CO_2 emissions is due to the seasonal cycle of photosynthetic activity.

The Brazilian case

Brazil is a vast country with a population of 174 million people, economic growth of around 3.5 percent per year. Such an immense developing economy inevitably places a strain on the country's resources, and amongst the basic needs energy is of paramount importance in maintaining its growth rate. Electricity is the main form of energy used in this tropical country, with an increase rate of 4.5 percent per year. Even in the "cold" South, heating is not a concern, apart from the heat for industrial use.

Unlike most countries, Brazil has never made particular use of coal as a source of energy, due, mainly, to its low quality and the difficulty of its exploitation. Biomass played a large part until 1940, when it represented 75 percent of the total energy consumed in the country (Leite, Antonio Dias, 1997). Nowadays the predominant renewable source in this energy matrix is the hydraulic energy, with hydropower plants generating more than 90 percent of the total electricity demanded (Instituto Brasileiro de Geografia e Estatistica - IBGE, 2001). As for primary energy sources, 66 percent of the primary energy production comes from renewable sources; biomass contributing to 20 percent of the total primary energy production, sugarcane by-products representing 10 percent, and wood 11 percent (Figure 2) (Ministerio das Minas e Energia - Brazilian Government, 2001).

The main biomass fuels used for electricity generation are sugarcane industry residues, of which bagasse, which is a fibrous residue matter from the sugarcane processing, is the major contributor. This fuel has played a large part in the power generation for the sugar and alcohol mills for years. With the instability of the international market for sugar and alcohol, along with the increasing demand, electricity has become the main asset of the large mills. However, the use of biomass in old and poorly efficient steam cycles represents a waste of fuel and money to the producer. Employing modern and more efficient cycles, production could reach up to 80 kWh/ton of sugarcane, against the actual 20-30 kWh/ton of sugarcane (Nogueira et al. 1995). The use of such a fuel would also contribute to the diversification of the energy matrix,

avoiding the dependence on the hydraulic energy. The sugarcane mills in Brazil are self-sufficient in terms of power generation, with an installed capacity of 600 MW_e (Coelho et al. 1999).

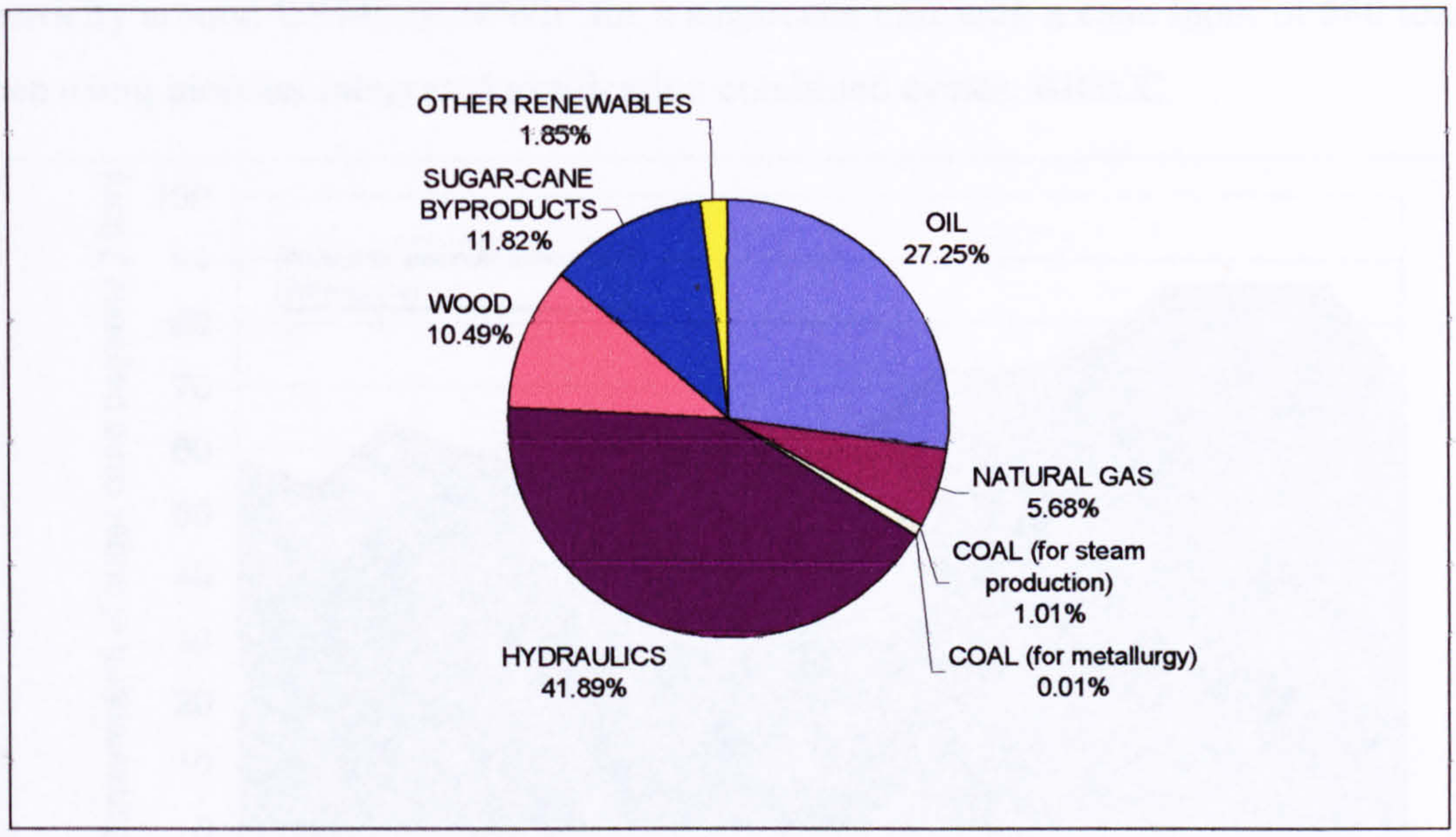

Figure 2 – Primary fuel sources in the Brazilian energy matrix (Ministerio das Minas e Energia - Brazilian Government, 2001)

As an example of the biomass potential, let us cite the sugarcane production in the State of São Paulo. Responsible for 59 percent of the sugarcane produced in Brazil[2], in this State the plantations yield an average of 76 ton/ha (Instituto de Economia Agricola, 2001) of cane and an average of 7-13 ton/ha of straw. After milling and juice extraction 12 percent of the sugarcane becomes bagasse (Nogueira, L. A. H., Lora, E. S., Trossero, M. A., and Frisk, T., 2000), yielding an average of 9.12 tons of bagasse per hectare. Figure 3 shows the total bagasse production in Brazil from 1985 to 2001, and the amount of this fuel used for power generation.

Apart from the alcohol production and the bagasse residue, if just 50 percent of the straw (cane tips) were used for power generation, 25 percent of the Brazilian import of petroleum could be saved. Another good example is the wood industry, which generates up to 50 percent of residues from the process (Oliveira et al. 1999), and most of the time the residues are thrown away instead of being utilised as fuel for power/heat generation.

Among many others, biomass could become one of the major energy sources in this new scenario. Using already proven technology and considering emissions taxation it is possible to generate power at reasonable prices. Walter et al. 1999, project a cost of electricity around US$40,00/MWh[3] for a sugarcane mill with a cane input of 580 ton/h, when using biomass integrated gasification combined cycles, BIGCC.

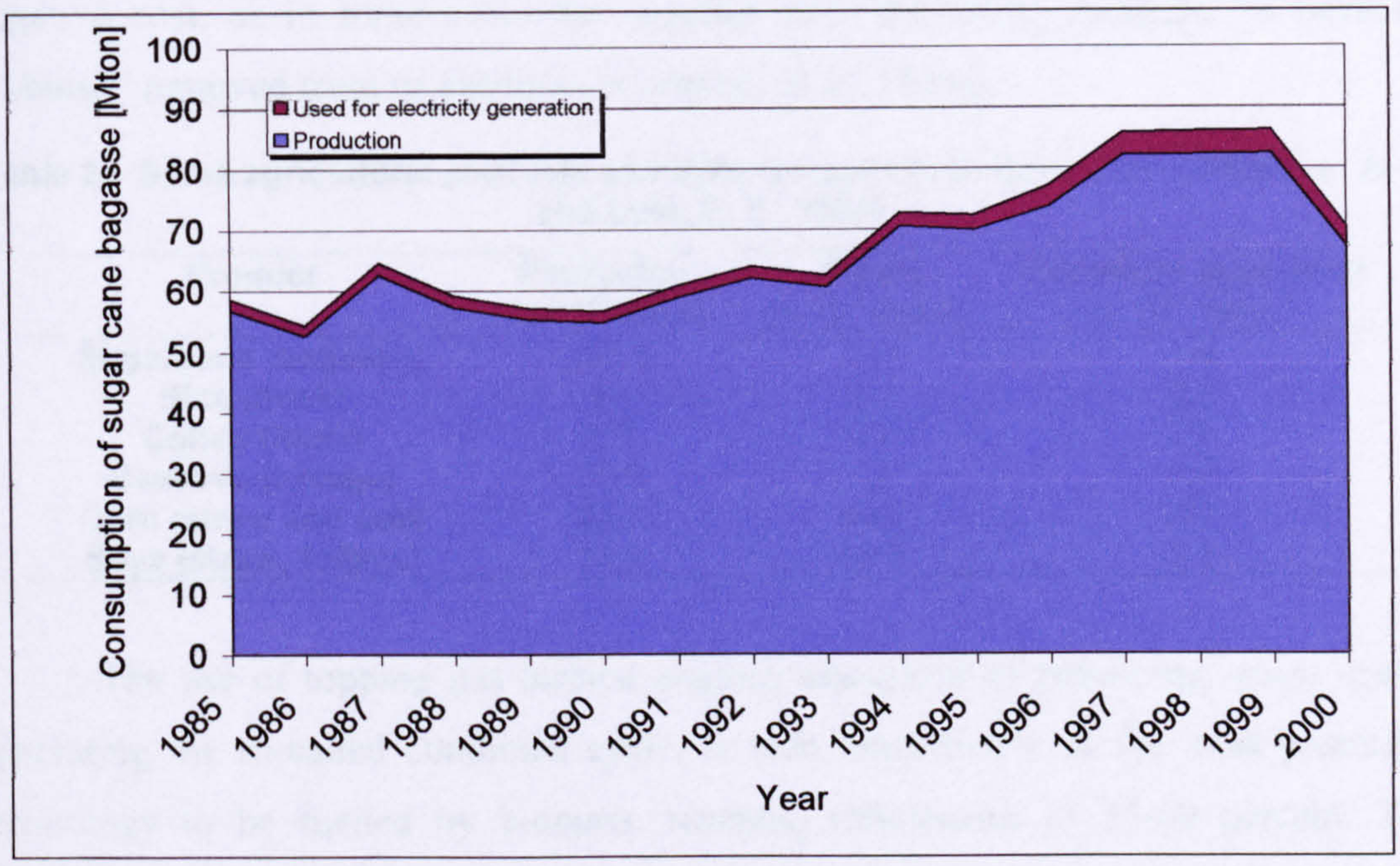

Figure 3 – Sugarcane bagasse production and the amount of this fuel used for power generation in Brazil (Ministerio das Minas e Energia - Brazilian Government, 2001)

Last but not least, another example of the biomass fuel capacity in Brazil is the northeastern region, which has a potential of 50 million ha for eucalyptus plantation, yielding 12,600 GJ/yr, at an average cost of US$2.11/GJ[4] (Consonni et al. 1996a). This scenario would allow a cost of electricity (CoE) of 5.7 ¢/kWh[5] as against 6.2 ¢/kWh of a hydroelectric power plant (Consonni et al. 1996a), the predominant primary source of energy in the country.

Other biomass fuels and/or residues can also contribute to the energy matrix, reducing the reliance on hydroelectric power plants, which can be severely affected by

---

[2] The sugarcane production reached 332,898,019 ton in 2000 (Secretaria de Politica Agricola - Brasil, 2001 & Instituto de Economia Agricola, 2001).

[3] In 1995 US$, non-fuel O&M US$ 8.2/MWh, fuel cost US$ 7.5/ton and US$ 10.0/ton, capacity factor 0.80.

[4] According to Consonni et al. 1996a, these costs include 85 km transport and chipping. The moisture content of the delivered chips is 33 percent due to some natural drying that occurs between harvest and delivery.

[5] Utility financing, with biomass price US$ 2.00 per GJ and US$ 2000.00 per kW installed (Consonni et al. 1996a).

draughts, as in 2001, and fossil fuels. Table 2 gives a clear picture of the potential for this type of fuel for the country.

It is clear that a more rational use of these resources could save a large quantity of fossil fuels, reducing the emission of gases that contribute to the greenhouse effect, particularly CO_2. Furthermore, biomass is a relatively cheap fuel, sometimes with a negative cost, as in some cases the supplier pays the utility company to have the "rubbish" removed from its premises (Consonni et al. 1996a).

Table 2 – Some agricultural products and their residues in Brazil in 1991 (Cortez, L. A. B. and Lora, E. S., 1997)

Product	Production (x 10^{-6} tons)	Waste (x 10^{-6} tons)[6]	Petroleum equivalent (x 10^{-6} tons)[7]
Sugarcane (bagasse)	260,8	39,1	7,4
Rice (husk)	9,5	2,7	0,6
Coffee (husk)	3,1[8]	2,1	0,5
Cassava (foliage)	24,5	7,3	1,9
Corn (straw and cob)	23,7	31,4	8,2
Soya (straw, foliage)	14,9	35,8	9,3

The use of topping gas turbine engines associated to bottoming steam cycles, generating the so-called combined cycle, is seen immediately as the most promising technology to be fuelled by biomass, reaching efficiencies of 55-60 percent. Two approaches will be described and analysed later in this thesis; the biomass integrated gasification/gas turbine, BIGGT, and the externally fired gas turbine cycle, EFGT.

Biomass compared with other energy sources

When compared with other sources of energy, biomass shows considerable advantages. Wind power is unreliable and the capacity factor (period of time in which the power plant is available) is very much dependent on the location. Geothermal power plants are still very expensive. Finally, normal hydropower plants flood a large amount of nearly flat land, which could be used for crop plantations.

Compared with its main counterpart, fossil fuels, biomass presents a number of advantages and few drawbacks, as will be discussed in the following sections.

---

[6] Dry basis.

[7] tEP, tons petroleum equivalent.

[8] Coconut coffee.

Thermal properties of biomass

Each type of biomass has its own set of characteristics that define its performance as a fuel, either in a direct burning device or in a gasifier. The most important properties concerning thermal conversion of biomass are (Quaak, P., Knoef, H., and Stassen, H., 1999):

1. Moisture content;
2. Ash content;
3. Volatile matter content(*VM*) and fixed carbon (*FC*);
4. Alkali metal content;
5. Heating value (or calorific value);
6. Bulk density.

Moisture content

Biomass is composed of three main parts:

1. Water (*w*);
2. Ash (*a*);
3. Dry and ash free matter (*daf*), i.e., the remaining components of the biomass.

The moisture content in the biomass (*m*) refers to the quantity of water in the matter, expressed as a percentage of its total weight, which can be expressed in three different ways:

1. *Wet basis*: the weight of the amount of water present in the biomass is expressed as a percentage of the sum of the weight of the water, ash, and the remaining material present on that particular biomass, thus:

$$m = \frac{w}{w + a + daf} \qquad [1]$$

2. *Dry basis*: the weight of the amount of water present in the biomass is expressed as a percentage of the ash and the remaining material "dry" matter present in the biomass:

$$m = \frac{w}{a + daf} \quad \textbf{[2]}$$

3. *Dry-ash-free basis*: the weight of the amount of water present in the biomass is expressed as a percentage of the dry-ash-free matter:

$$m = \frac{w}{daf} \quad \textbf{[3]}$$

Furthermore, the moisture content can be divided into:

1. *Intrinsic*: the moisture content of the material without the influence of weather effects;
2. *Extrinsic*: the influence of prevailing weather conditions during harvesting on the overall biomass moisture content.

In practical terms it is the extrinsic moisture content that is of concern, as the intrinsic moisture content is usually only achieved, or applicable, under laboratory conditions (McKendry, 2002a).

The moisture content affects the biomass properties as a fuel (Figure 4), so it is very important to specify the basis in which the biomass is being represented. Furthermore, the moisture content in the biomass can vary from as little as 10 percent, for cereal grain for instance, to as much as 50-70 percent, for plantations or forest residues.

Ash content

Ash is regarded as the inorganic component of the biomass, and can be expressed in the same way as the moisture content. In general, the ash content is expressed in a dry basis (Table 3).

The *inherent ash value* – an integral part of the plant structure, which consists of a wide range of elements – represents less than 0.5 percent in wood, 5 to 10 percent in diverse agricultural crop materials, and up to 40 percent in rice husks.

The ash content and composition of the biomass affects its behaviour under the high temperatures of combustion and gasification. Dependent on the magnitude of the ash content, the available energy of the fuel is reduced proportionately (McKendry, 2002a).

Melted ash can also cause problems in both combustors and gasifiers such as clogged ash-removal caused by slagging ash to severe operating problems in fluidised-bed systems (Quaak, P., Knoef, H., and Stassen, H., 1999).

Volatile matter content and fixed carbon

The chemical energy in solid fuels is stored in two forms:

1. *Volatile matter (VM)*: the portion driven-off as a gas (including moisture) by heating (950°C for 7 minutes);
2. *Fixed carbon (FC)*: the mass remaining after the release of volatiles, excluding ash and moisture content.

The significance of the *VM* and *FC* content is that they provide a measure of the ease with which the biomass can be ignited and subsequently gasified, or oxidised, depending on how the biomass is going to be utilised as an energy source. Table 3 shows typical compositions for different biomass fuels and coals.

Biomass typically has a high volatile matter content, whereas coal has a low volatile matter content, or, in the case of anthracite coal, a negligible one. As will be seen later in this thesis, this characteristic makes biomass a more suitable fuel for gasification than coal.

Table 3 – Typical proximate of gasification feedstatock (dry basis)

Fuel	Proximate analyses (% weight)			LHV (MJ/kg)
	VM	FC	Ash	
Biomass				
Eucalyptus[9]	82.55	16.93	0.52	19.35
Wood[10]	82.6	13.7	0.1	21.0
Bark[10]	70.6	27.2	2.2	22.0
Bagasse[9]	73.78	14.95	11.27	17.33
Coals				
Ill. N°6 betumin.[9]	37.50	43.40	18.18	26.67
W. Kentucky bet.[9]	33.12	48.18	18.70	27.81
Texas lignite[10]	38.9	44.5	16.6	29.6

Alkali metal content

The alkali metal content (Na, K, Mg, P, and Ca) is especially important for any thermo-chemical conversion processes. The reaction of alkali metals with silica present in the ash produces a sticky, mobile liquid phase, which leads to blockages of airways in the furnace and gasifier.

When using a gas turbine engine as a prime mover these contaminants are of special concern due to the sensitivity of such an engine to contaminants, as will be discussed later.

Heating value (or calorific value)

The heating value, or calorific value (CV) of a material is an expression of the energy content, or heat value, released when burnt in air. The CV is usually measured in terms of the energy content per unit mass, or volume. The CV of a fuel can be expressed in two forms (McKendry, 2002a):

1. *The gross CV, or higher heating value (HHV)*: the total energy content released when the fuel is burnt in air, including the latent heat contained in the water vapour, and therefore represents the maximum amount of energy potentially recoverable from a given biomass source;
2. *The net CV, or lower calorific value (LHV)*: the total energy content released when the fuel is burnt in air, not including the latent heat contained in the

[9] Source: Larson, 1993

[10] Source: Larson et al. 1989

water vapour. Because in practical terms the latent heat contained in the water vapour cannot be effectively used, the LHV is the appropriate value to use for the energy available for the subsequent use.

Biomass always contains some water, which is released as vapour upon heating. This implies that the evaporation process absorbs some of the heat released during the chemical reactions. For this reason, the LHV decreases as the moisture content of the biomass increases (Figure 4).

At a moisture content of approximately 87 percent (wet basis) the LHV would be zero. In practice, the maximum allowable moisture content must be 55 percent (wet basis) to ignite the fuel and extract energy from it.

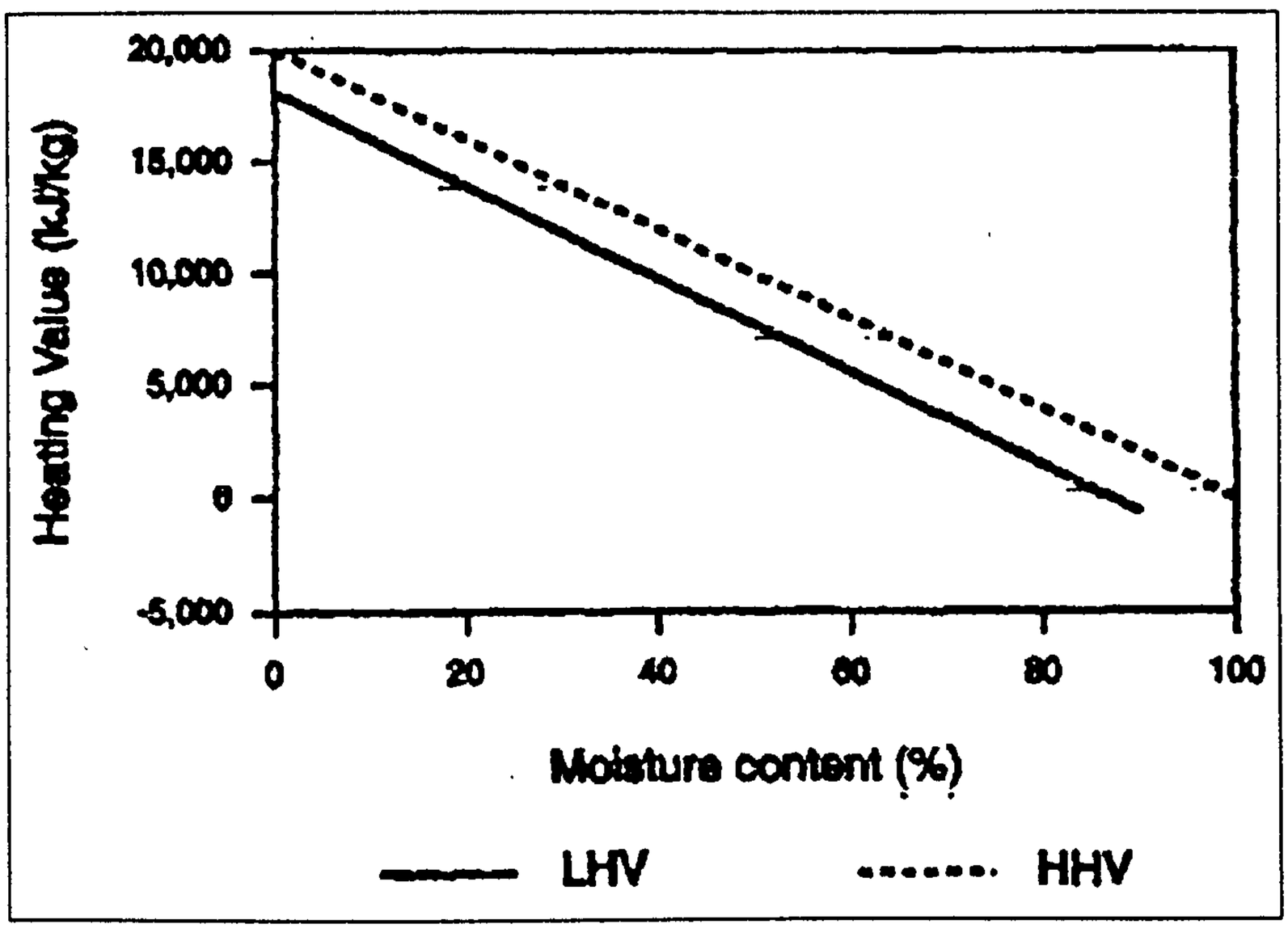

Figure 4 – Calorific value of biomass as a function of moisture content (Quaak, P., Knoef, H., and Stassen, H., 1999)

Bulk density

Bulk density refers to the weight of material per unit of volume, and can be expressed in two ways: *as-produced* and *as-processed.* The importance of the as-produced bulk density is in relation to transport and storage costs. The density of the processed product impacts on fuel storage requirements, the sizing of the materials handling system, and how the material is likely to behave during subsequent thermo-

chemical processing, either as a fuel or as a feedstock (McKendry, 2002a). Biomass bulk densities show extreme variation, from 150 to 200 kg/m^3 for solid wood (Table 4).

Together with the heating value, bulk density determines the energy density. In general, biomass energy densities are approximately one-tenth of that of fossil fuels (Quaak, P., Knoef, H., and Stassen, H., 1999).

Table 4 – Bulk density of selected biomass sources (McKendry, 2002a)

Biomass	Bulk density [kg/m^3], daf
Wood	
Hardwood chips	230
Softwood chips	180-190
Pellets	560-630
Sawdust	120
Planer shavings	100
Straw	
Loose	20-40
Chopped	20-80
Baled	110-200
Moduled	100-1250
Hammermilled	20-110
Cubed	320-670
Pelleted	560-710

The economic point of view

The usual way of using solid fuel for power generation used to be the steam cycle, using a boiler to burn the fuel and generate steam, which is then expanded in a steam turbine. The efficiency for this kind of power plant varies from 18 percent to 30 percent[11]. From the mid-80s, with the gas turbine/combined cycles proving their potential for high efficiency, a new approach started to be studied, and this is the integrated gasification combined cycle (IGCC) with efficiencies ranging from 22 percent to 48 percent[11], in the case of biomass, the BIGCC.

Another proposed technology using biomass gasification is the internal combustion engine. The gas can be used either in compression ignition engines (diesel) or spark ignition (gasoline) engines. Due to its easy maintenance and engine robustness, this technology is suitable for remote regions, such as the inner Amazon region. Biogas can replace from 75 percent to 90 percent of the diesel required in an engine, and electricity costs as low as ¢ 10.00/kWh have been estimated (Larson, 1993); however, its low exhaust temperature makes it unsuitable for combined cycle applications.

Internal combustion engines are not within the scope of this work, therefore little attention will be given to them.

From the economic point of view biomass is still an expensive option for power generation, as far as BIGGT or BIGCC systems are concerned, but this situation could change with the application of carbon taxes (Traverso et al. 2002) and agricultural incentives. Furthermore, with further technological development, costs are expected to drop considerably. Table 5 gives an overview of the estimate of different projected BIGCC technologies. The difference in the costs is due to the capacity of the power plants and also the technology involved in the gasification island.

Table 5 – Estimate costs for different BIGCC power plants (Turn, 1999c)

	PRI	Tecogen	Ebasco	NREL	GEF	Average
Capital cost [$/kWe]	3005.0	1850.0	1706.0	1588.0	1500.0	1929.8
Plant size [MWe]	50.0	50.0	64.0	56.0	32.0	50.4
Efficiency	27.8	23.0	28.7	36.0	40.0	31.1
Electricity cost [¢/kWh]						
Capital	4.2	2.6	2.4	2.6	3.2	3.0
Fuel	4.1	2.1	1.7	2.4	1.3	2.3
O&M	3.0	2.9	3.0	1.1	0.7	2.1
TOTAL [¢/kWh]	**11.3**	**7.6**	**7.1**	**6.1**	**5.2**	**7.5**
Total less fuel [¢/kWh]	**7.2**	**5.5**	**5.4**	**3.7**	**3.9**	**5.1**

The GEF (Global Environment Fund) shows costs of the tenth power plant, i.e., it is considered that the more plants that are designed and built, the more the costs will be reduced due to the experience acquired in the previous projects. The first GEF project, the WBP/SIGAME (Table 6), which has been developed in the state of Bahia, Brazil, has an estimated capital cost of US$ 2 750/kW$_e$ (Bridgwater, 1995). This project is a joint venture that involves a private company, Shell Brasil S.A., public companies CHESF, *Companhia Hidro Elétrica do São Francisco*, and ELETROBRAS, and international funding agencies like United Nations Development Program (UNDP), the World Bank, and the GEF (Carpentieri et al. 1998).

The project has two main objectives (McGowin et al. 1998):

1. *Short-term objective*: to establish a globally replicable prototype unit on a commercial scale for the cogeneration of electricity based on the gasification

[11] For power plants capacity ranging from 10MWe to 100 MWe (Bridgwater, 1995).

of wood chips and sugarcane bagasse. No native forests will be used in fulfilling this objective.

2. *Long-term objective*: to reduce global warming by lowering CO_2 emissions, which would be produced by conventional thermal generation.

Table 6 – Characteristics of the Brazilian BIGCC project

	Units	Quantity
Gas turbine engine	GE-LM2500	1
Plant performance		
Gross capacity	MW	40.40
Auxiliary power	MW	8.14
Net capacity	MW	32.26
Annual capacity factor	%	85
Annual generation	MWh/yr	240,208
Net thermal efficiency (LHV)	%	40.7
Net plant heat rate	KJ/kWh	8,848
Biomass heat content	MJ/kg_{dry}	18.4
Fuel consumption		
Biomass fuel	ton_{dry}/h	15.52
LPG	Kg	6
Diesel oil	Ton	0.10
Auxiliary power consumption		
Gas compression	MWh	4.90
BOP	MWh	3.24
Fuel price[12]	U$/GJ	1.96

McGowin et al. 1998, also emphasise the environmental and social benefits of this project:

1. Employment and income growth in rural areas – this would avoid the still very large migration of the northeastern population to the more economically developed Southeast;
2. Increased capital investment in the power sector;
3. Economic support to industries that already use biomass, such as sugarcane mills;
4. Verification of the benefits of plantations for energy production and decentralised electricity generation.

[12] Including stumpage, harvesting, transport, and handling costs (drying and processing).

The purpose of this work is to use biomass as a source of fuel for a utility company. However, so far biomass has been seen as a fuel suitable mainly for self-production of electricity. In this case the fuel will have a nearly zero cost, depending on the fuel source. Costs related to handling, storage and pre-treatment must be considered. If the company intends to generate electricity and heat through biomass purchase, many other parameters will affect the final price of biomass and must be taken into consideration such as transportation, climate, soil quality, land rent, labour costs, etc (Larson et al. 1997). However, the fact that the fossil fuels have increased in price over the last five years must also be taken into consideration. Another parameter to consider is the emissions tax, which can have a considerable effect on the final cost of electricity. This, in the near future, could take biomass off the self-production scenario and place it in the merchant power plants market.

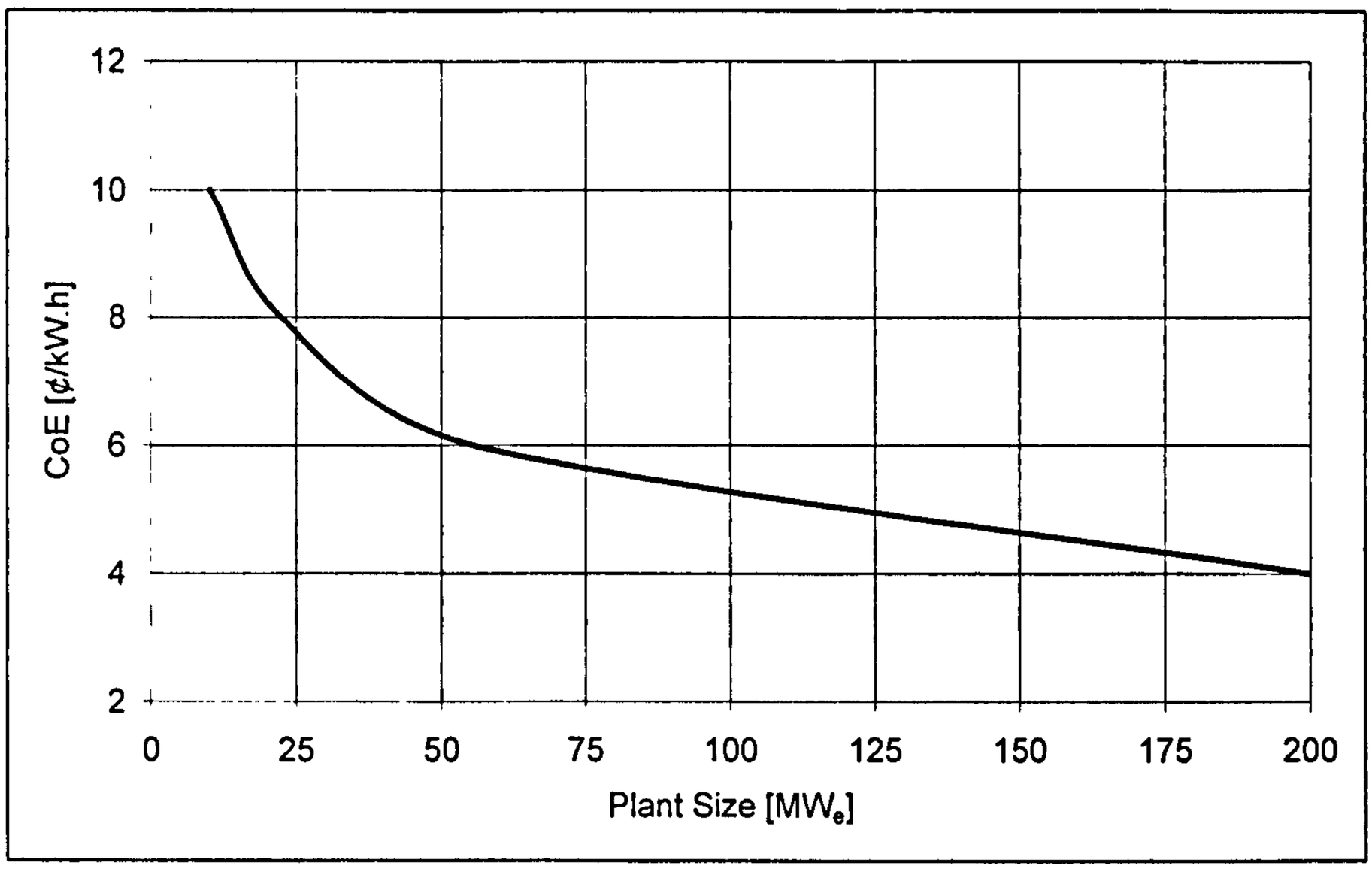

Figure 5 – Cost of electricity for BIGCC systems[13] (Craig et al. 1994)

The generation costs will also be very much dependent on the type of cycle to be used, for instance, steam cycle, gasification (gas turbine or internal combustion engine), combined cycle, or the externally fired gas turbine/combined cycle (EFCC). Each concept offers advantages and drawbacks, which will be carefully analysed throughout

[13] Includes all costs: pre-treatment, handling, fuel transport, etc.

the development of this work. Figure 5 shows the trend line for the cost of electricity (CoE) in BIGCC systems.

Land use

Due to its low calorific value, biomass is a land-intensive renewable energy source. For electricity production, biomass is considerably more land-intensive than are other renewable technologies such as solar and wind technologies. Depending on the efficiency and power of the cycle, biomass can be as land-intensive as a hydropower plant (Table 7).

However, in the Brazilian scenario two situations must be considered. The first is electricity generation from sugarcane bagasse; in this case the biomass consists of residues from the cane harvesting and milling, i.e., the plantation is already there, even considering merchant plants that would buy the residues from the mills. The second is the decentralised electricity production in remote areas of the country. In some of those areas, such as the northeastern region, deforestation has reached the point when the desertification of some areas is imminent, and plantations would contribute to the recovery of those areas.

Table 7 – Land requirement for electricity generation from renewables (Larson, 1993)

	Land requirement for electricity [ha/MW]
Biomass	235
Solar photovoltaic	1.3
Solar thermal	4.0
Wind	4.7-16
Hydraulic	16-900

Biomass transport

Due to its low energy density[14] the cost of delivering the biomass is heavily dependent on the distance it has to travel. Another parameter to influence the delivered price of biomass is the layout and quality of the road system around the power plant.

Due to the size of the country, transport is an issue that must be taken into consideration. Most of the Brazilian population is concentrated in the industrialised southeastern region. Big hydroelectric power plants in this area are economically and environmentally unaffordable, and, from the strategic standpoint, diversification of the

[14] Sugarcane bagasse, for example has a LHV = 18 MJ/kg.

energy matrix is welcome. Therefore, other energy sources must be added to the grid, and biomass, as already shown, is one of the best and most abundant fuels. The high number of industries in the region favours the residue generation and guarantees the fuel supply.

Biomass transport costs in US$/ton are typically expressed as a fixed cost, regarding loading and unloading, plus a cost that varies with distance (Larson et al. 1997). According to Turnbull, 1996, transportation by truck of wood wastes and agricultural residues to a conversion facility more than 80-120 km away is neither economically nor environmentally reasonable.

Handling and pre-treatment

All the technology regarding biomass handling and pre-treatment is readily available. The capital cost of the whole pre-treatment part of the system is about US$ 600.00/kWe at 20 MWe, and offers some economy of scale, falling to around US$ 300.00/kWe at 100 MWe (Bridgwater, 1995).

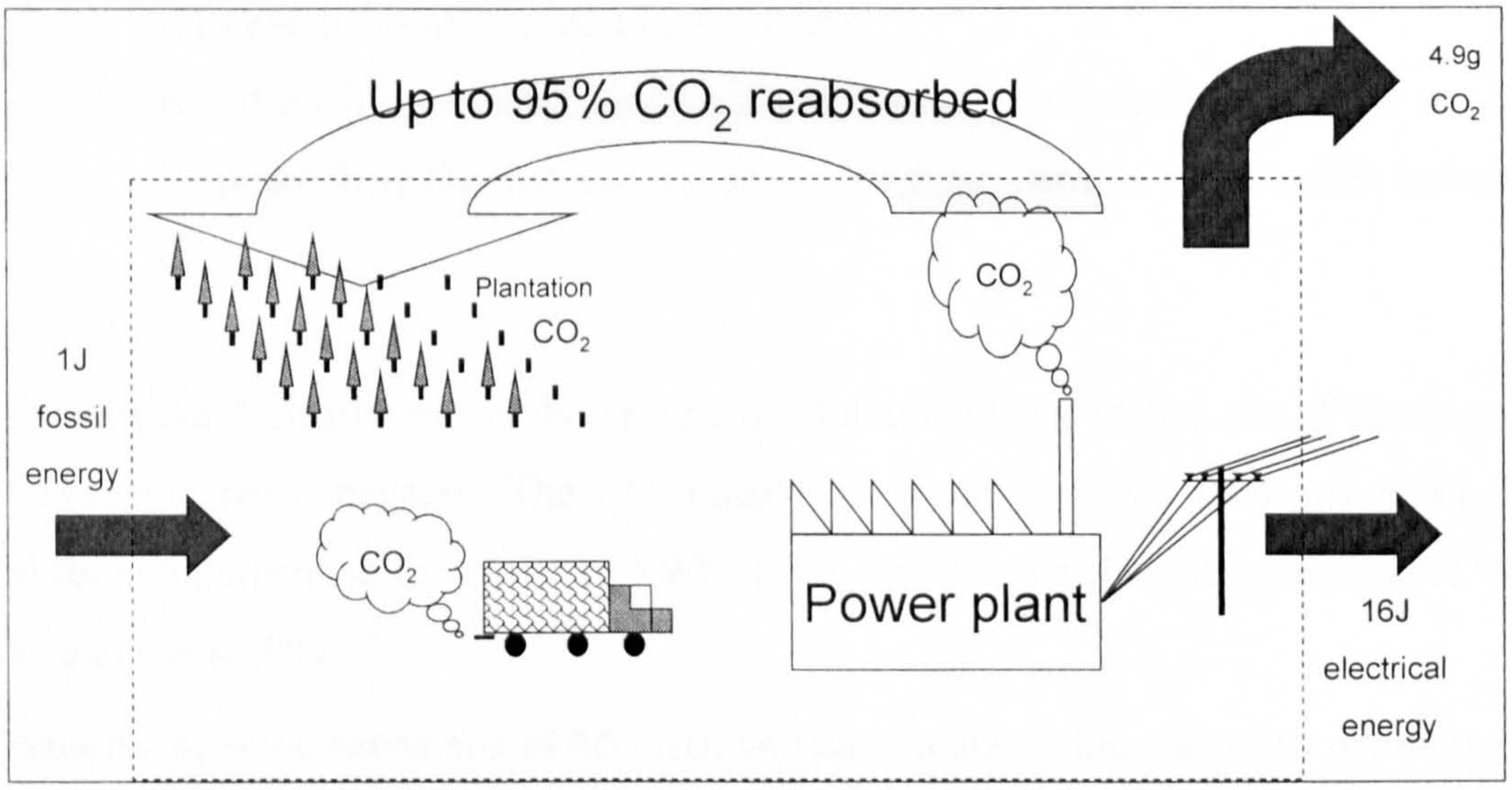

Figure 6 – Carbon cycle in a power station fired by biomass

The environmental point of view

Fossil fuels consist basically of organic matter (biomass) that has been deteriorating for millions of years, yielding a high energy content, non-renewable fuel. Burning "old" biomass produces "new" CO_2, whilst biomass from plantations is "new" biomass which absorbs CO_2 to build its carbonic structure.

The environmental advantages of the use of biomass as a power generation fuel can be summarised in six main points:

1. The low level of pollution. When used in a sustainable way, biomass can reduce by up to 95 percent the CO_2 emission (Turnbull, 1996), as the plantations sequestrate the CO_2 in order to use the carbon to build the structure of the trees; the remaining 5 percent is due to transport (Lora, 2001) (Figure 6);
2. As a renewable source, the planted areas can be re-used for the same purpose, i.e., energy plantation (Cortez, L. A. B. and Lora, E. S., 1997);
3. Biomass is a relatively cheap source of energy; in developing countries it still is the cheapest fuel, either related to its weight or related to heat per unit;
4. Its low ash and sulphur concentrations avoid particulate emissions and SO_2 formation;
5. Energy plantations do not damage the environment because it is possible to reforest devastated areas to plant them;
6. Residues from certain industrial and agricultural processes can be used as biomass fuel, for instance sugarcane bagasse, wastes from coffee industry, etc.

Figure 7 clearly shows the environmental advantages of the use of biomass, in this case sugarcane bagasse. The CO_2 emissions are much lower than any other fuel used for comparison, at only 0.02 kg/kWh. Table 8 shows the specific emissions of SO_2, NO_x, and particulate.

Table 8 – Specific emissions of SO_2, NO_x and particulate during electricity generation using fossil fuels and sugarcane bagasse [g/kWh] (Lora et al. 2000a)

	Natural gas	Coal	Fuel oil	Bagasse (BIG/GT)
SO_2	0.00	0.72 – 24.26	0.23 – 7.92	0.00
NO_x	1.07	3.69	1.76	1.38
Particulate	0.02	1.51 – 302.52	0.29	0.19 – 8.16

Sulphur is seldom found in biomass fuels, which explains the zero SO_2 emissions in the sugarcane bagasse. Particulate is of especial concern for biomass systems; however, the use of the correct cleaning technology can easily make this figure

fall within the limits established by either local legislation or engine requirements. NO_x is also of concern, but again, several already proven technologies can help in controlling its emissions.

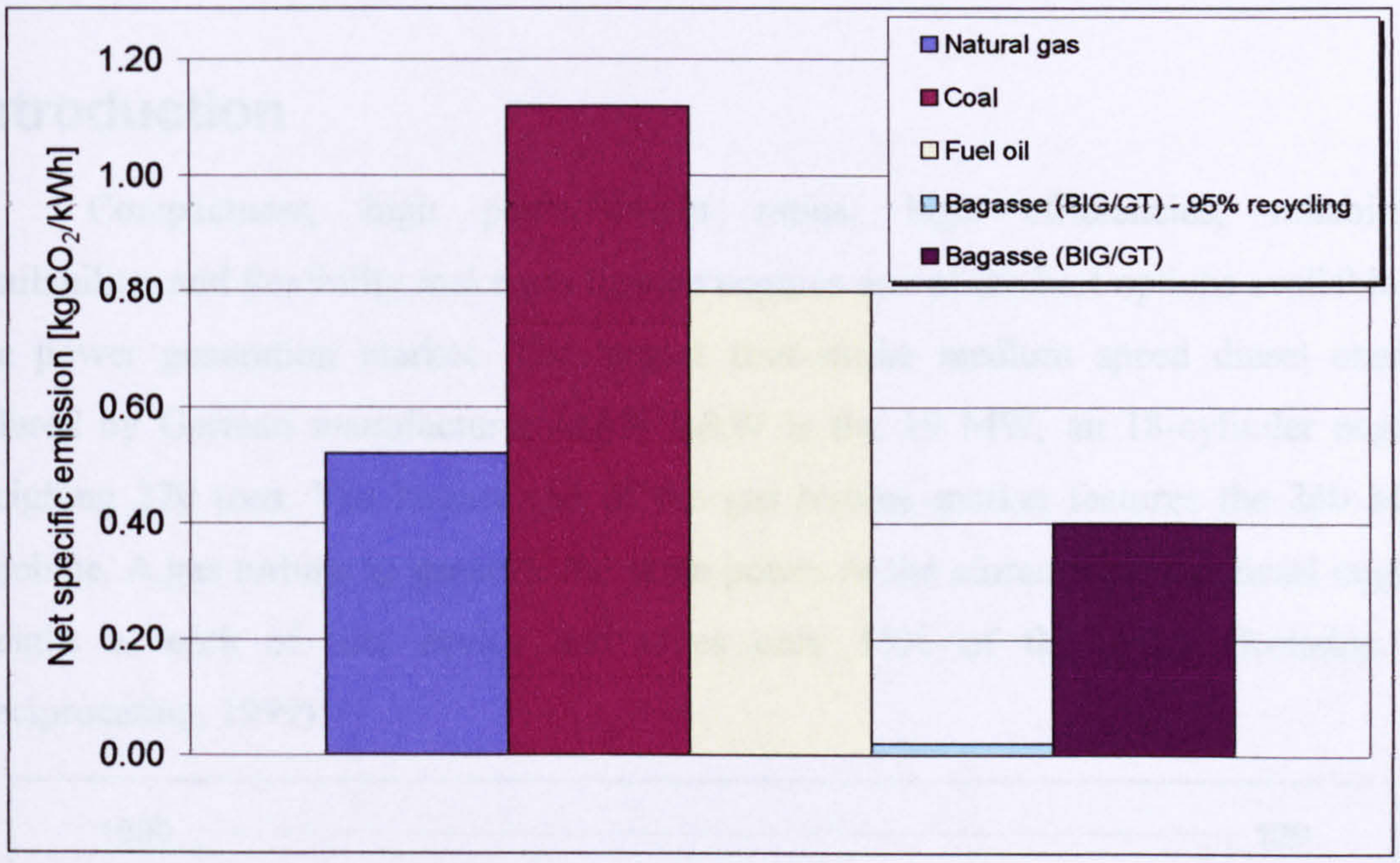

Figure 7 – Specific emissions of CO_2 during electricity generation using fossil fuels and sugarcane bagasse [kg/kWh] (Lora et al. 2000a)

CHAPTER III – METHODS FOR USING BIOMASS IN GAS TURBINES

Introduction

Compactness, high power/weight ratios, high efficiencies, reliability, availability, and flexibility make gas turbine engines one of the best options available to the power generation market. The largest four-stroke medium speed diesel engine offered by German manufacturer MAN B&W is the 19 MW, an 18-cylinder engine weighing 270 tons. The largest end of the gas turbine market features the 260 MW machine. A gas turbine to generate the same power as the aforementioned diesel engine weighs a tenth of that device and takes only 15% of the space (Rotating or Reciprocating, 1999).

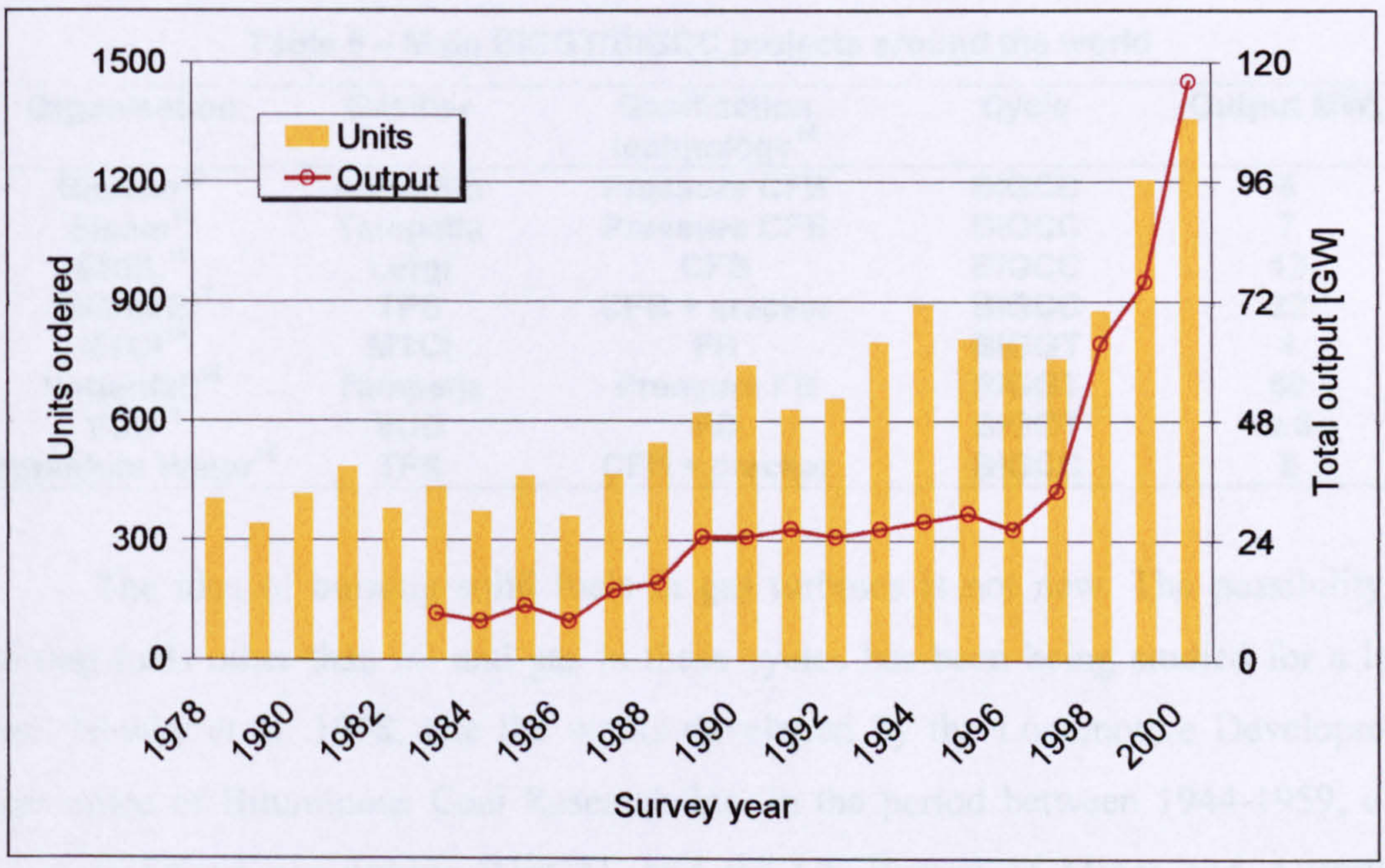

Figure 8 – Gas turbine order trends (McNeely, 2001)

For these reasons orders for gas turbine engines have been growing fast in the last 10 years, with a growth of 55% over 2000, and the total output increasing from 41,390 MW to 117,240MW (Figure 8), particularly with sales concentrated in medium sized and aeroderivative engines. South America alone had an increase of 204% in large gas turbine units (McNeely, 2001).

When the bottoming steam cycle is added to the system, comprising the so-called combined cycle, the efficiencies achieved with the use of gas turbine engines are of the order of 57-60%. The design of such gas turbines, like the GT26 and the MS9001H, are based on:

1. Increased gas cycle efficiency – that is, lower fuel consumption;
2. Increased specific work – reduced capital cost;
3. Increased exhaust gas temperature – improved performance of steam bottoming cycle (Carcasci et al. 2000).

Given all the advantageous characteristics of the gas turbines, these engines are very promising prime movers to be used in conjunction with biomass fuels. Several projects around the world are focused on the BIGGT/BIGCC systems, as shown in Table 9.

Table 9 – Main BIGGT/BIGCC projects around the world

Organisation	Gasifier	Gasification technology[15]	Cycle	Output MW_e
Bioflow[16]	Ahlström	Pressure CFB	BIGCC	6
Elsam[16]	Tampella	Pressure CFB	BIGCC	7
ENEL[16]	Lurgi	CFB	BIGCC	12
SIGAME[17]	TPS	CFB + cracker	BIGCC	32
MTCI[16]	MTCI	FB	BIGGT	4
Vattenfall[16]	Tampella	Pressure FB	BIGGT	60
VUB[16]	VUB	FB	BIGGT	0.6
Yorkshire Water[16]	TPS	CFB + cracker	BIGCC	8

The idea of burning solid fuels in gas turbines is not new. The possibility of burning fuels other than oil and gas in these cycles has been being studied for a long time. Newby et al. 1998, cite the works developed by the Locomotive Development Committee of Bituminous Coal Research Inc. in the period between 1944-1959, on a direct coal-fired gas turbine (DFCT), and the US Bureau of Mines and Australian Aeronautical Research Laboratories, from 1948 to 1970. According to the authors a major challenge has been the development of in-situ removal of sulphur, alkali vapour,

[15] FB = fluidised bed; CFB = circulating fluidised bed

[16] Source: Bridgwater, 1995

[17] Source: Turn, 1999b

and particulate to low enough levels to permit its use in combustion turbine power systems without additional, external gas cleaning. Consonni et al. 1996d, cite the works developed by Sultzer Escher-Wyss in the 1930s and the efforts of a consortium started in 1987 in the USA, a project in a 2 MW and a 44 MW facility. In Italy an small-scale project, 500 kW, involves more than fifty organisations.

However, the use of solid fuels directly into the combustion chamber leads to problems such as erosion and corrosion of the expander blades. The costs of maintenance become extremely high and the engine life is severely shortened. The use of pressurised fluidised bed combustors is an option, but it would be economically feasible only at power plants larger than 70 MW (Ward et al. 1983), which fall outside the power range for economically feasible biomass systems[18] – 20 to 70 MW (Consonni et al. 1996b). Another drawback is the low efficiency of this cycle, for the bed temperature must be low enough to allow low NO_x production, and the hot gas filter must be efficient enough to control the particulate emission (Consonni et al. 1996d).

This chapter will describe and discuss the advantages and drawbacks of two approaches to using solid fuel in gas turbines, the BIGGT and EFGT, described earlier. The aspects related to intercooling and recuperation will also be discussed.

The gasification process

Before moving on to particular aspects of the gas turbine, it is necessary to understand the gasification process. The issues related to the gasification chemical kinetics will not be dealt with in this thesis. The detailed description of these processes can be found elsewhere (Desrosiers, R., 1981, Souza-Santos, 1989, Wang et al. 1993, Bettagli et al. 1995, Ergudenler et al. 1997, Mansaray et al. 2000, and Mathieu et al. 2002).

Gasification technology is more than a century old, and the use of gasifiers for operating engines – internal combustion engines – was established by 1900. Gasifier-engine systems were used successfully during World War I. During World War II, more than one million gasifiers were in use producing gas fuel for trucks, buses, taxis, boats, trains, etc (Bhattacharya, 1993).

---

[18] This limitation is mainly due to transport costs, as discussed earlier.

Gasification also offers potential environmental advantages when compared with combustion systems. The fuel gas produced by gasifiers is lower in both volume and temperature than the fully combusted product from a combustor. These characteristics provide an opportunity to clean and condition the fuel gas prior to use. Combustion of the resulting gaseous fuel can be more accurately controlled than combustion of solid biomass. As a result, the overall emission, particularly NO_x, from gasification based power systems can be reduced (Stevens, 2001).

Thermochemical gasification

The gasification process that relates to gas turbine applications is the thermochemical conversion, which provides low to medium calorific value gases in a large and constant mass flow rate supply.

Thermochemical gasification is the conversion by partial oxidation at elevated temperature of a carbonaceous feedstock such as biomass or coal into a gaseous energy carrier (Bridgwater, 1995). This process occurs in the following three steps:

1. *Drying*: the drying process evaporates the moisture.
2. *Pyrolysis*: refers to a complex set of reactions during which the volatile components of the feedstock vaporise at temperatures below 600°C and leave behind fixed carbon (char) and ash. Biomass consists of 75-85 percent volatile matter, compared with half or less with coal, so pyrolysis plays a larger role in the gasification of biomass. Moreover, biomass pyrolyses at lower temperatures than coal, as shown in Figure 9 (Larson et al. 1989). Products of pyrolysis include water vapour, heavy hydrocarbon compounds – tars and oils – that condense at relatively high temperatures, and char.
3. *Gasification*: or partial oxidation of the solid char, pyrolysis tars and pyrolysis gases. With biomass, a relatively small amount of char remains after pyrolysis due to its low fixed carbon fraction. Much of the char is burnt to provide heat to the pyrolysis process and to gasify any remaining char. Because biomass chars are much more reactive than coal chars[19], biomass

[19] 10-30 times more reactive, according to Larson et al. 1989

gasifiers can operate at lower temperatures than coal gasifiers to achieve the same conversion rates.

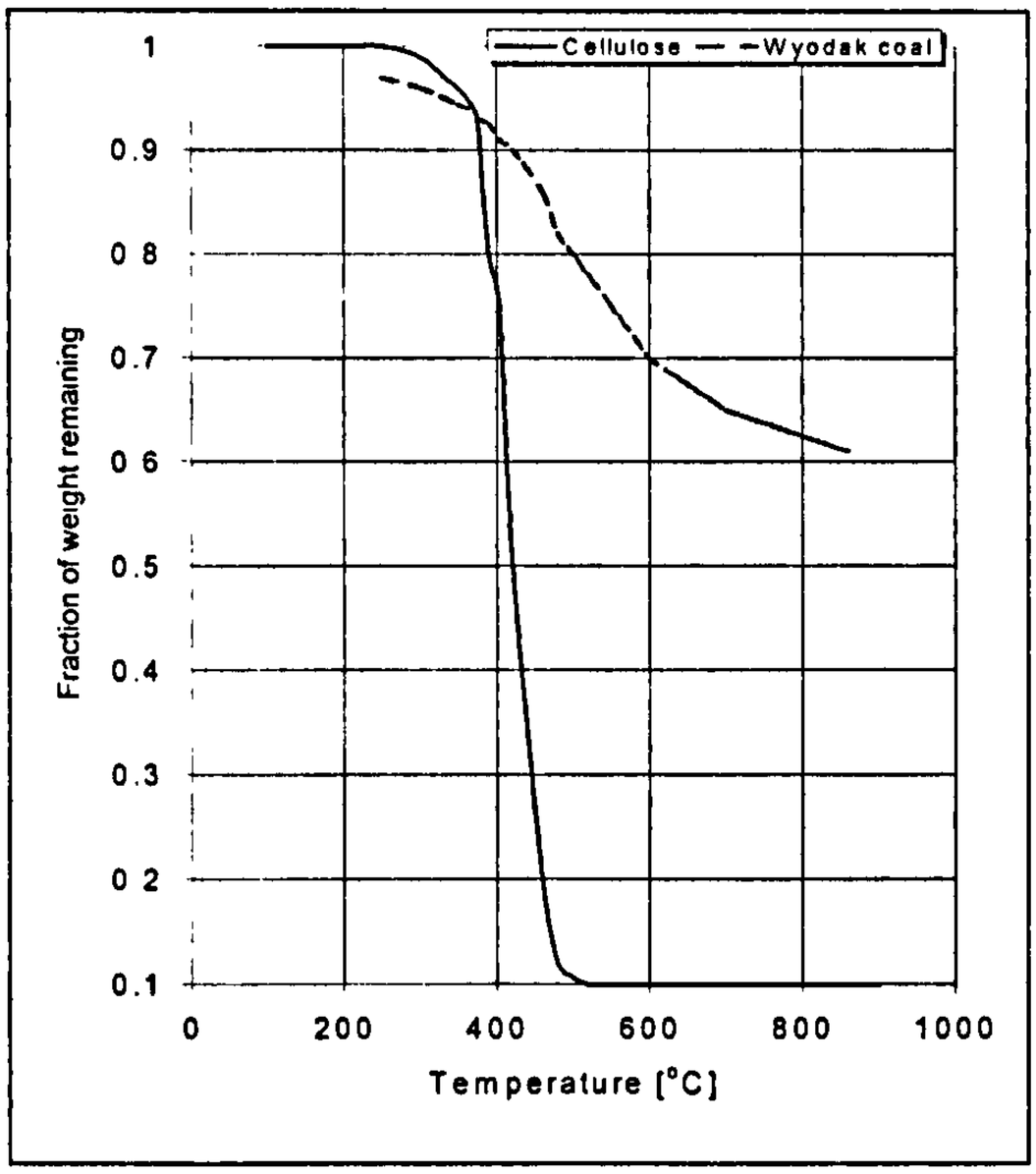

Figure 9 – Weight loss as a function of pyrolysis temperature for coal and cellulose (a major component of biomass) (Larson et al. 1989)

Generally pyrolysis proceeds much more rapidly than gasification, and the latter is thus the rate-controlling step. The gas, liquid, and solid products remaining from the pyrolysis process then react with the oxidising agent – usually air – to give permanent gases (CO, CO_2, H_2) and lesser quantities of hydrocarbon gases. Many of the reactions are catalysed by the alkali metals present in wood ash, but still do not reach equilibrium (Bridgwater, 1995).

The chemistry and practical operational aspects of gasification are influenced by four main parameters:

1. *Temperature*: this parameter affects gasification rates and reactor design. Operating temperatures influence the design of ash removal systems. Both slagging and dry-ash gasifiers have been developed for coal. Biomass and coal ash have comparable melting temperatures (1100-1200°C), but since biomass can be gasified at lower temperatures, most biomass gasifiers utilise dry ash removal systems. Moreover, a much lower ash content than coal further simplifies ash removal from biomass gasifiers.

2. *Pressure*: has a modest effect on gasification chemistry, but an important effect on system design and cost (Figure 10). Higher pressure permits higher processing rates for a given reactor size. In a fluidised bed gasifier, throughput (ton/h) increases from m_o to m as pressure increases from p_o to p, approximately according to:

$$\frac{m}{m_o} = \left(\frac{p}{p_o}\right)^{0.6} \qquad [4]$$

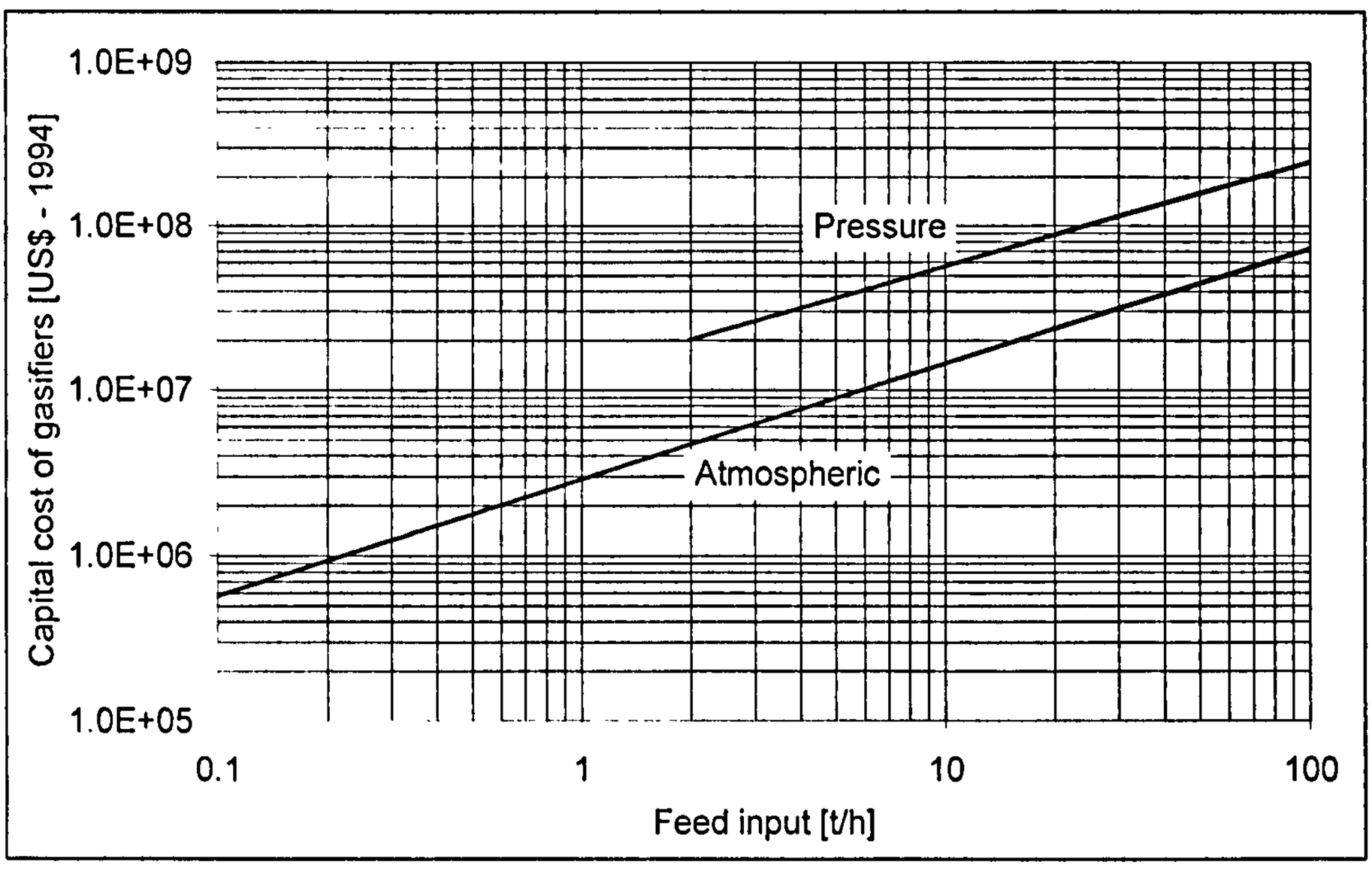

Figure 10 – Installed plant costs for gasification systems (Bridgwater, 1995)

The ability to use smaller reactors leads to savings in materials and in field construction costs. Drawbacks of higher pressure operation are the increased complications for feeding and the increased risk of clinker formation in hot spots within the oxidation zone. Gas composition and heating value are not significantly affected by gasification pressure.

3. *Presence of moisture*: in some gasifiers, steam is injected to provide some of the required moisture, since water in the feedstock is driven off during pyrolysis and is thus unavailable for reaction. In some gasifiers, additional steam is used to maintain the reacting bed below the specified temperature,

typically that of ash melting. Excess moisture acts to dilute the heating value of the raw gas. The lower limit on the heating value of gas for stable gas turbine combustion appears to be about 3.0 MJ/Nm^3. This sets an upper limit on the acceptable moisture content of the feedstock of 25-30 percent (Larson et al. 1989).

4. *Type of oxidant*: oxygen or air is the oxidant in most gasifiers, and steam is sometimes used as an additional reactant. Using oxygen produces a better quality gas; an average of 12 MJ/Nm^3 (compared with an average of 38 MJ/Nm^3 for the natural gas). Air gasification produces a gas with about half of that calorific value due to the diluting effect of the nitrogen, but this is still sufficient for gas turbine combustion. Steam is used to increase the hydrogen content in the flue gas. With respect to its calorific value (CV) the produce gas is classified into three main categories (McKendry, 2002b):

Low CV	4-6 MJ/Nm^3	Using air or steam /air
Medium CV	12-18 MJ/Nm^3	Using oxygen or steam
High CV	40 MJ/Nm^3	Using hydrogen or hydrogenation.

It is worth remembering that, due to its simplicity and low cost, the gasification modell in this thesis uses an atmospheric gasifier.

Gasification technology

Several different configurations of reactors have been developed for gasification systems. Each one has different characteristics and applications, advantages and drawbacks, which will be summarised in following items. According to the type of bed, gasifiers can be classified into fixed bed (Figure 11) and fluidised bed reactors (Figure 12 and Figure 13).

The fixed bed reactors can be further classified into updraft and downdraft gasifiers. The fluidised bed can be classified into three distinct new types: bubbling fluid bed, circulating fluid bed, and twin bed gasifiers.

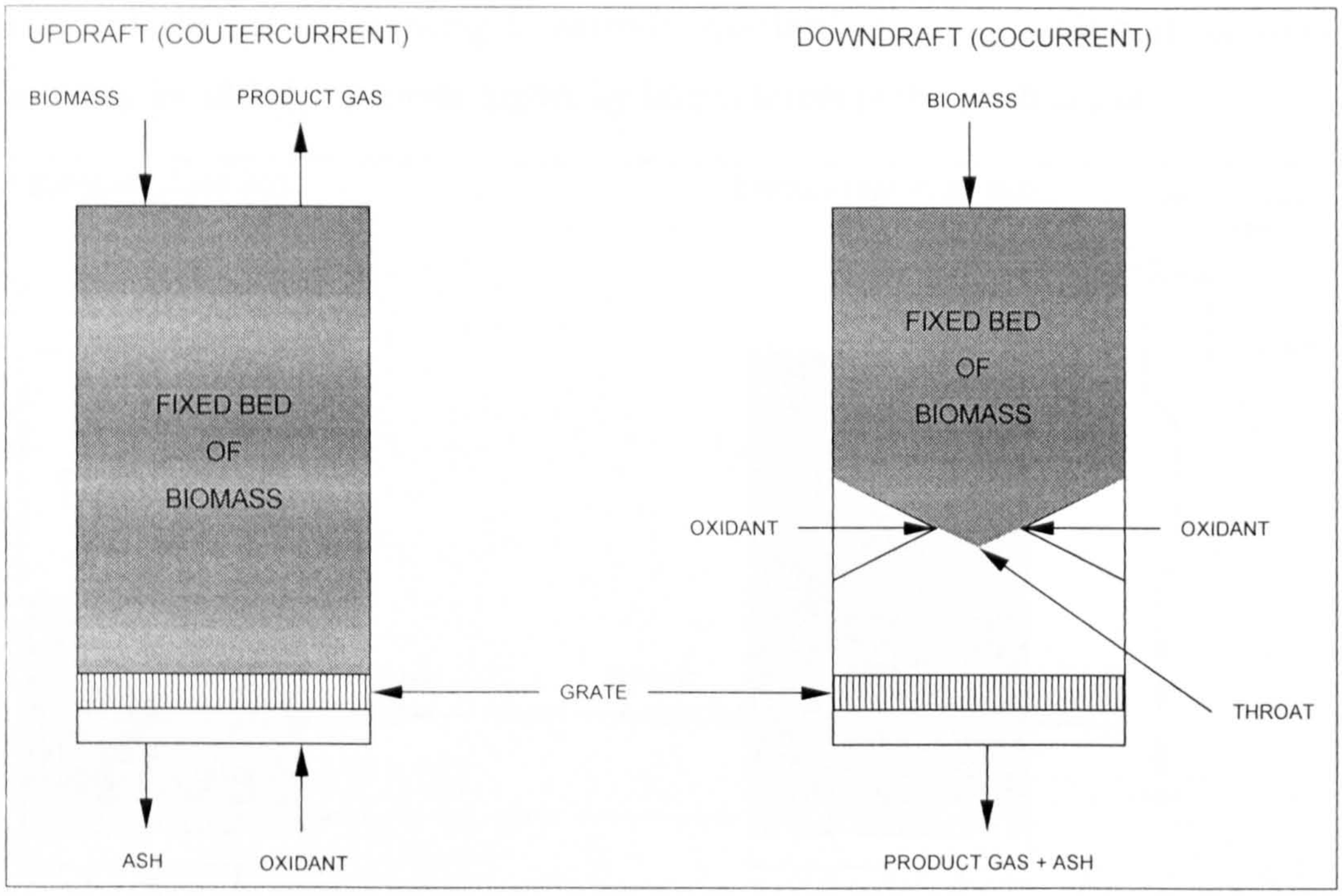

Figure 11 – Downdraft and updraft fixed bed gasifiers

Fixed bed gasifiers

The updraft gasifier

In the updraft gasifier biomass is input on the upper part of the gasifier, making its way down the reactor, while the oxidant is input on the lower part of the gasifier (countercurrent configuration). The product gas moves up. The following sequence of events then takes place:

1. Biomass is first dried by the hot gas product moving up;
2. Biomass is pyrolysed, the vapour from pyrolysis is taken upwards by the upflowing hot product gas. Char remains from this process;
3. The remaining char continues going down the reactor to be gasified.

Tars are present in the vapour from pyrolysis. Part of this tar condenses on the cool descending biomass, and another amount is carried out of the gasifier – around 20 percent. The condensed tars are recycled back to the reaction zones, where they are further cracked to gas and char. In the bottom of the gasification zone the solid char

from pyrolysis and tar cracking is partially oxidised by the incoming air or oxygen. Steam may be added to provide higher hydrogen levels in the product gas.

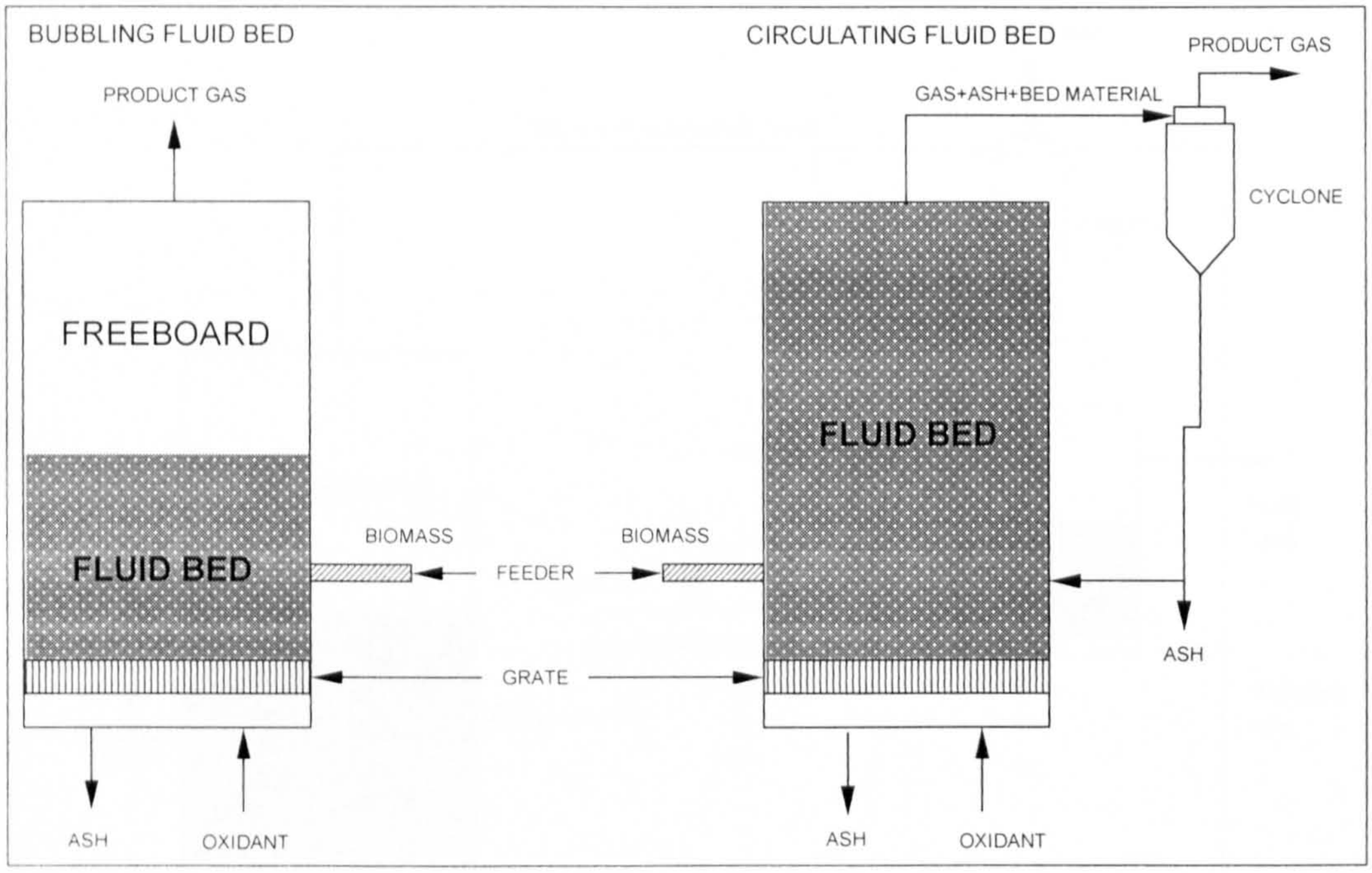

Figure 12 – Single and circulating fluidised bed gasifiers

The product gas from an updraft gasifier has a significant proportion of tars and hydrocarbons, which contribute to a high calorific value gas. However, for certain applications, such as gas turbines, the tars must be removed. The main advantages of these gasifiers are simple construction and high thermal efficiency[20].

The downdraft gasifier

As in the updraft gasifier, in the downdraft gasifier biomass is input on the upper part of the reactor. However when it reaches the throat (Figure 11), which supports the solid matter and where most of the gasification occurs, the oxidant is injected and makes its way down together with the solid matter (cocurrent configuration). The reaction products are intimately mixed in the turbulent high-temperature region around the throat, which aids tar cracking. Some tar cracking also occurs below the throat on a residual charcoal bed, where the gasification process is completed (Bridgwater, 1995). This reactor delivers a relatively clean gas, as due to low velocities at the top of the

---

[20] The sensible heat of the gas produced is recovered by direct heat exchange with the entering feedstock, which is dried, preheated and pyrolysed before the gasification zone.

gasifier, the product gas has a relatively low concentration of particulate (Larson et al. 1989).

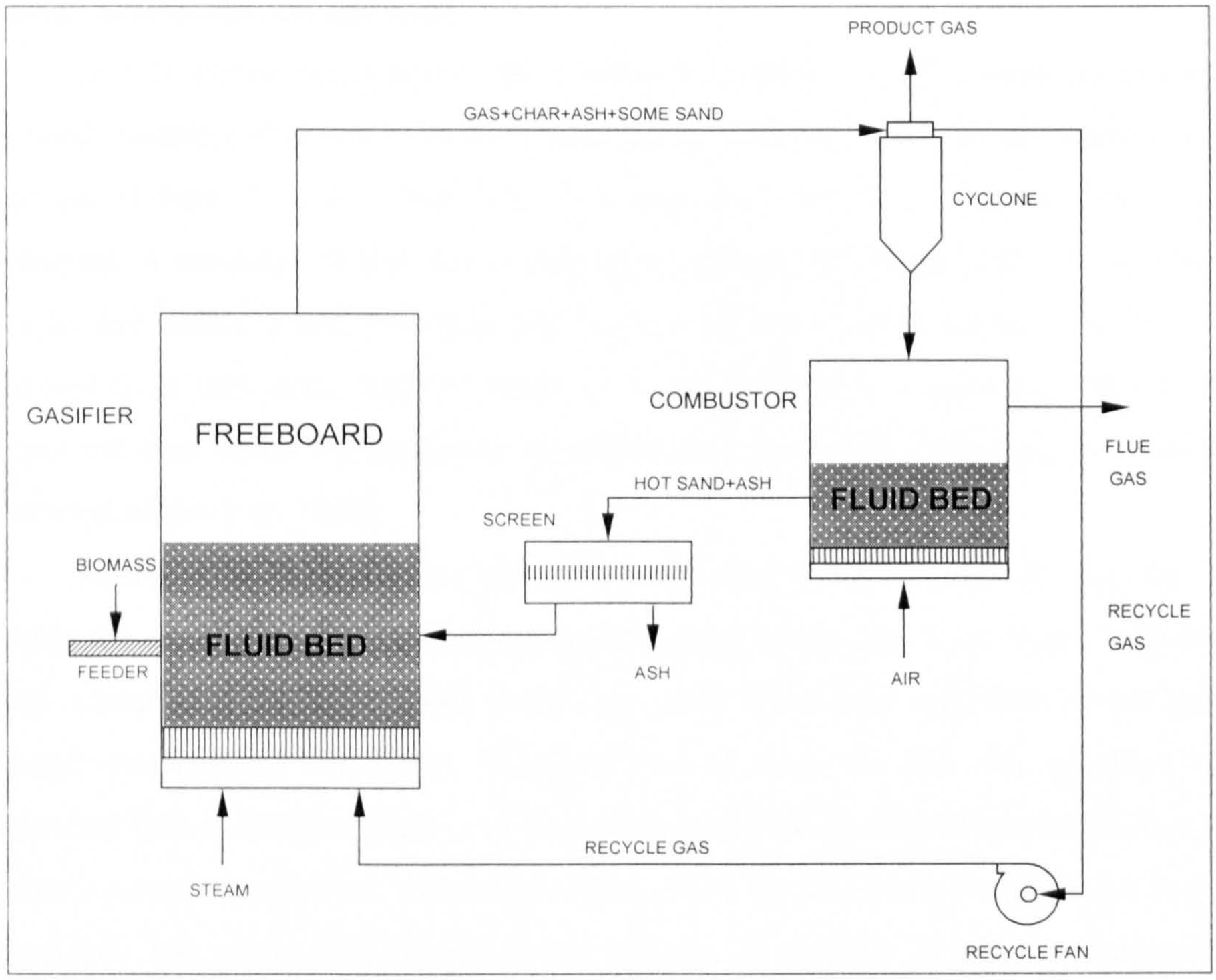

Figure 13 – Twin fluidised bed gasifier

Downdraft gasifiers are simple, reliable and proven for certain fuels. However, some restrictions on fuel characteristics apply, such as: relatively dry (~30 wt-percent), low ash content (< 1wt-percent), and low proportion of fine and coarse particles (not smaller than ~ 1 cm and not larger than ~ 30 cm in the longest dimension). Owing to the low content of tars in the gas, this configuration is generally favoured for small-scale electricity generation with internal combustion engines. The physical limitations on the diameter and particle size relation mean that there is a practical upper limit to the capacity of this configuration (~500 kg/h or 500 kWe) (Bridgwater, 1995).

Fluidised bed gasifiers

Bubbling bed (or Single bed)

In a fluidised bed gasifier, the feedstock is typically fed continuously and is fluidised, together with an inert heat distributing material[21], by oxidant and/or steam injection (Figure 12). The bubbling fluid-bed was the first fluidised bed design developed. A variation of this, the circulating fluidised bed (Figure 12) was developed later. In any fluidised bed, pyrolysis and char conversion occur throughout the bed. The excellent heat and mass transfer leads to a fairly uniform temperature distribution around the bed, better fuel-moisture utilisation, and faster reactions than in fixed bed reactors (Larson et al. 1989).

Reaction temperature is kept relatively low (~800-850°C) to prevent ash melting, by control of blast air rates and good mixing of the bed. As a result, little or no steam is needed for cooling, unlike in the fixed bed. While peak temperatures are lower, average temperatures are higher (fluidised bed gasifiers are the only gasifiers with isothermal bed operation), leading to the conversion of a significant amount of tars and oils into permanent gases. Carbon conversion of 98 percent has been achieved in pilot scale tests. The particulate loading in the raw gas is one to two orders of magnitude greater than with fixed beds (Larson et al. 1989).

Loss of fluidisation due to bed sintering is one of the commonly encountered problems, depending on the thermal characteristics of the ash. Alkali metal compounds from the biomass ash form low melting eutectics with the silica in the sand, which is the usual fluidising medium. This results in agglomeration and bed sintering with eventual loss of fluidisation (Bridgwater, 1995).

Circulating fluidised bed

Due to the high velocities in the circulating fluidised bed, a large amount of solids is entrained in the product gas. This system has been designed to re-circulate the solid matter into the gasifier to improve carbon conversion efficiency compared with the

---

[21] Silica sand is the most common material, although alumina and other refractory oxides have been used to avoid sintering, and catalysts have also been used to reduce tars and modify product gas composition.

bubbling fluidised bed design. The hot gas produced is, in most cases, used in close-coupled process heat or in boilers for sensible heat recovery.

This configuration has been extensively developed for woodwaste conversion in pulp and paper mills for firing lime and cement kilns and steam raising for electricity generation (Bridgwater, 1995).

Twin fluid bed gasifiers

These are used to give a gas of higher heating value from reaction with air than is obtained from a single air-blown gasifier (Figure 13). The gasifier is in effect a pyrolyser, heated with hot sand from the second fluid bed, which is heated by burning the product char in air before recirculation to the first reactor. Sometimes steam is added to encourage the shift reaction to generate hydrogen and to encourage carbon-steam reactions (Bridgwater, 1995).

Table 10 summarises the characteristics of each of the gasifiers described in previous sections.

Table 10 – Typical gasifier characteristics (all air-blown) (Bridgwater, 1995)

	Temperature [°C]					Capacity	MWe	
	Reaction	Exit	Tars	Partic.	Scalability	[ton/h]	Min.	Max.
Downdraft	1000	800	v. low	mod.	poor	0.5	0.1	1
Updraft	1000	250	v. high	mod.	good	10	1	10
Single	850	800	fair	high	good	10	1	20
Circulating	850	850	low	v.high	v.good	20	2	100
Twin	800	700	high	high	good	10	2	50

Pressurised vs. atmospheric operation

The advantages and drawbacks of both pressurised and atmospheric operation have not been well defined yet. The Brazilian project, for instance, uses both.

Pressurised systems have the following features:

1. Feeding is more complex and very costly;
2. Capital costs are much higher than an atmospheric system (Figure 10);
3. Gas is supplied to the turbine at high pressure, removing the need for gas compression and also permitting relatively high tar contents in the gas; such tars need to be completely burnt in the gas turbine combustor;

4. Hot gas cleanup with mechanical filters, such as sintered metal or ceramic candles usually reduces thermal and pressure energy losses;
5. Overall system efficiency is higher owing to retention of sensible heat and chemical energy of tars in the product gas and the avoidance of a fuel gas compression stage ahead of the turbine (Bridgwater, 1995).

Atmospheric gasifiers have the following significant features:

1. For gas turbine applications the product gas is required to be sufficiently clean for compression before the turbine;
2. Atmospheric systems have a potentially much lower capital cost at smaller capacities of below 30 MWe (Bridgwater, 1995).

Feedstock pre-treatment

The level of pre-treatment required for biomass gasification depends on the technology adopted. The main areas of concern can be summarised as follows:

1. *Drying*: the biomass moisture content must be between 10-15 percent before the feedstock enters the gasifier.
2. *Particle size*: in most gasifiers, gas has to pass through the biomass and the feed has to have sufficient compressive strength to withstand the weight of the feed above. Typical particle sizes are 20-80 mm.
3. *Fractionation*: nitrogen and alkali metals are critical in certain biomass feedstocks, as they are partially carried over into the gas stream. Small particles tend to contain less nitrogen and alkalis, so fractionation into fine and coarse particles helps to produce a gas with fewer impurities (McKendry, 2002b).

Feedstock properties

The biomass properties, beyond affecting the combustion process, significantly influence the gasification process and gasifier performance, especially the following characteristics:

1. *Moisture content*: apart from the ignition problem and the reduction of the heating value of the fuel, a high moisture content reduces the temperature achieved in the oxidation zone, resulting in the incomplete cracking of the hydrocarbons released from the pyrolysis zone. Increased levels of moisture and the presence of CO produces H_2 by the water shift reaction, and in turn the increased H_2 content of the gas produces more CH_4 by direct hydrogenation. However, the gain in H_2 and CH_4 of the gas does not compensate for the loss of energy due to the reduced CO content of the gas (McKendry, 2002b).

2. *Ash content:* High mineral matter can make gasification impossible. The oxidation temperature is often above the melting point of the biomass ash, leading to clinkering/slagging problems in the hearth and subsequent fuel blockages. Clinker is a problem for ash contents above 5 percent, especially if the ash is high in alkali oxides and salts (McKendry, 2002b).

Thermodynamic properties of gases

In order to have an efficient tool to calculate thermodynamic properties of several chemical elements present in the gases from the gasification process, a set of polynomial equations has been used to calculate specific heat, enthalpy, and entropy.

These polynomial equations have been developed by McBride et al. 1993. Together with the respective set of coefficients, they can be easily inserted in a computer code. The following dimensionless form was chosen:

$$\frac{C_p^0(T)}{R} = a_1 + a_2 T + a_3 T^2 + a_4 T^3 + a_5 T^4 \qquad [5]$$

$$\frac{H^0(T)}{RT} = a_1 + a_2 \frac{T}{2} + a_3 \frac{T^2}{3} + a_4 \frac{T^3}{4} + a_5 \frac{T^4}{5} + \frac{b_1}{T} \qquad [6]$$

$$\frac{S^0(T)}{R} = a_1 \ln T + a_2 T + a_3 \frac{T^2}{2} + a_4 \frac{T^3}{3} + a_5 \frac{T^4}{4} + b_2 \qquad [7]$$

where $T \equiv$ is the temperature of the element, in K;

$R \equiv$ is the universal gas constant, 8314.51 $\left[\frac{J}{mol.K}\right]$;

$a_{i=1,\ldots,5}$, b_1 and b_2 ≡ are the coefficients[22];

C_p^0 ≡ is the heat capacity at constant pressure for standard state[23], $\left[\frac{J}{mol.K}\right]$;

H^0 ≡ is the enthalpy, either $\{H^0(T) - H^0(0)\} + H^0(0)$ or

$\{H^0(T) - H^0(298.15)\} + H^0(298.15)$, $\left[\frac{J}{mol}\right]$;

S^0 ≡ is the entropy at temperature T for standard state, $\left[\frac{J}{mol.K}\right]$.

The equations are valid within the range 200 to 6000 K. The gaseous species, the focus of this work, are generally considered stable at 298.15 K and 1 bar. Two temperature ranges were defined in order to fit the results given by the equations, the first range is between 200 and 1000 K, and the second is between 1000 K and 6000 K.

Of course not all the gases were taken into consideration in this work. Only 22 species plus liquid water[24] were selected, trying to embrace the most common species present in natural gas and gases derived from gasification of coal and biomass. These species are: CH_4, C_2H_6, C_3H_8, C_4H_{10}, C_5H_{12}, C_2H_2, C_7H_8, Ar, H_2, N_2, O_2, CO_2, CO, NO, N_2O, NO_2, NH_3, H_2S, $H_2O_{(g)}$, $H_2O_{(l)}$, S_2, SO_2, and SO_3.

The validation of the equations is based on Saad, M., 1997. A comparison between the thermodynamic properties presented by that author was carried out, and good correlation between equations and the tables was found, as can be seen in the following eight gaseous species selected for the validation: NO_2, NO, H_2, $H_2O_{(v)}$, CO, CO_2, N_2, and O_2.

Figure 14 and Figure 15 show the validation for the eight gases aforementioned. When these curves were being built a little distortion was observed for temperatures just above 3000 K. Because the air, gaseous fuels, and combustion product temperatures are far below 3000 K for industrial gas turbine calculations, the errors above that temperature will be disregarded during the calculations, so that there are no implications in the final results.

---

[22] The coefficients can be found in the Appendix C.

[23] According to McBride et al. 1993, this is ideal gas at standard pressure of 1 bar.

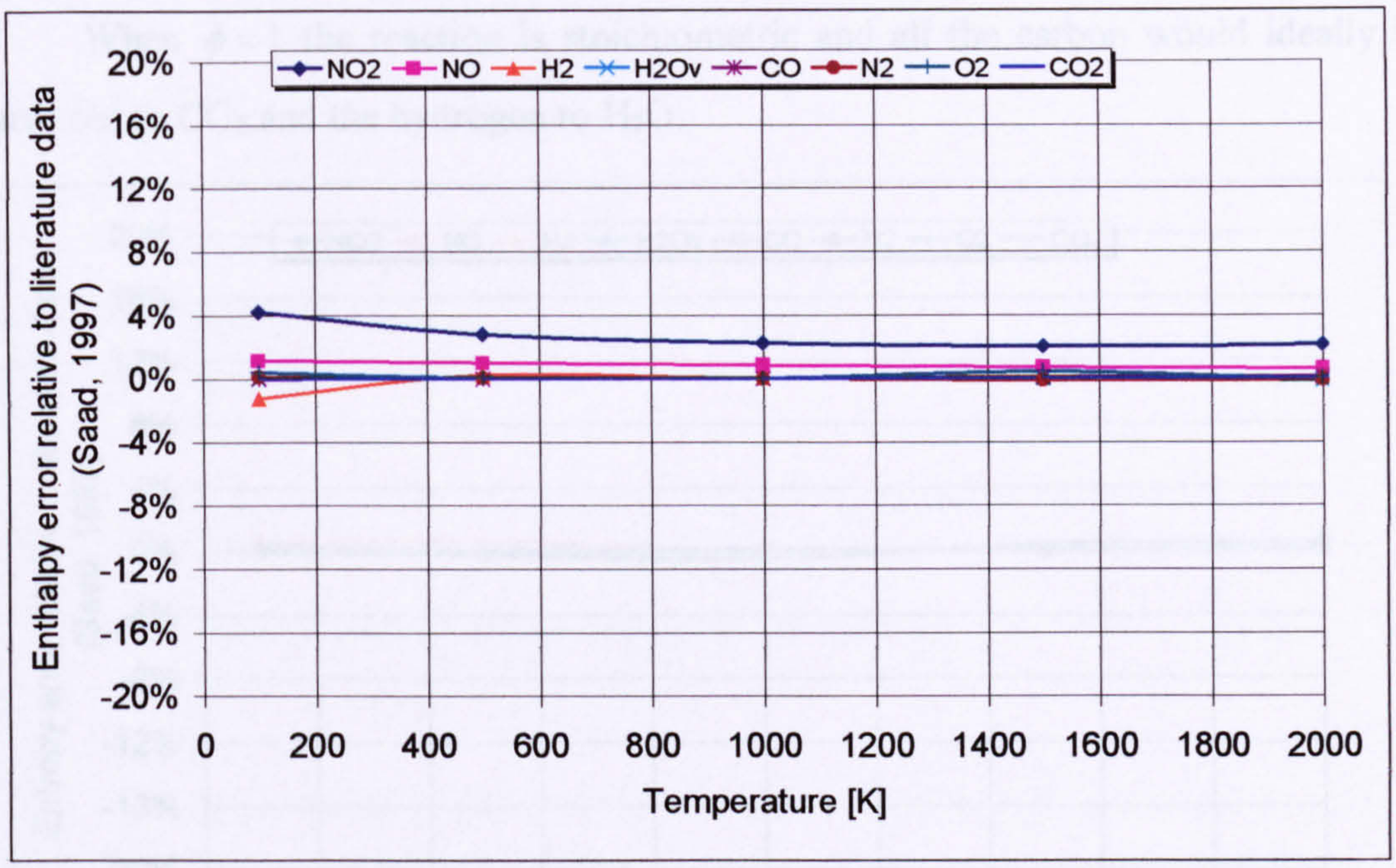

Figure 14 – Enthalpy error relative to literature data for different gases

Combustion calculations

The gaseous fuels comprise a significant number of components, such as CH_4, C_2H_6, CO_2, CO, N_2, H_2O, etc. Due to this variety of gases, it is necessary to gather all components in just one fuel of the form $C_aH_bO_dN_eAr_fS_g$, thus facilitating the calculations of the coefficients in the reaction of combustion.

Assuming that air is composed of O_2, N_2, CO_2, H_2O, and Ar, it can be represented as $C_AH_BO_DN_EAr_F$. Thus, the combustion equation is written as:

$$C_aH_bO_dN_eAr_fS_g + \phi^{-1}\alpha(C_AH_BO_DN_EAr_F) \Rightarrow \beta CO_2 + \gamma H_2O_{(v)} + \psi N_2 + \varepsilon SO_2 + \varphi Ar + \lambda O_2 \quad \textbf{[8]}$$

where $\phi = \dfrac{\overline{AFR}_{stoic}}{\overline{AFR}} \equiv$ is the equivalence ratio;

$\overline{AFR}_{stoic} \equiv$ is the molar air-to-fuel ratio stoichiometric;

$\overline{AFR} \equiv$ is the actual molar air-to-fuel ratio.

---

[24] Among 1130 species – gaseous, liquid and solid.

When $\phi = 1$ the reaction is stoichiometric and all the carbon would ideally be converted to CO_2 and the hydrogen to H_2O.

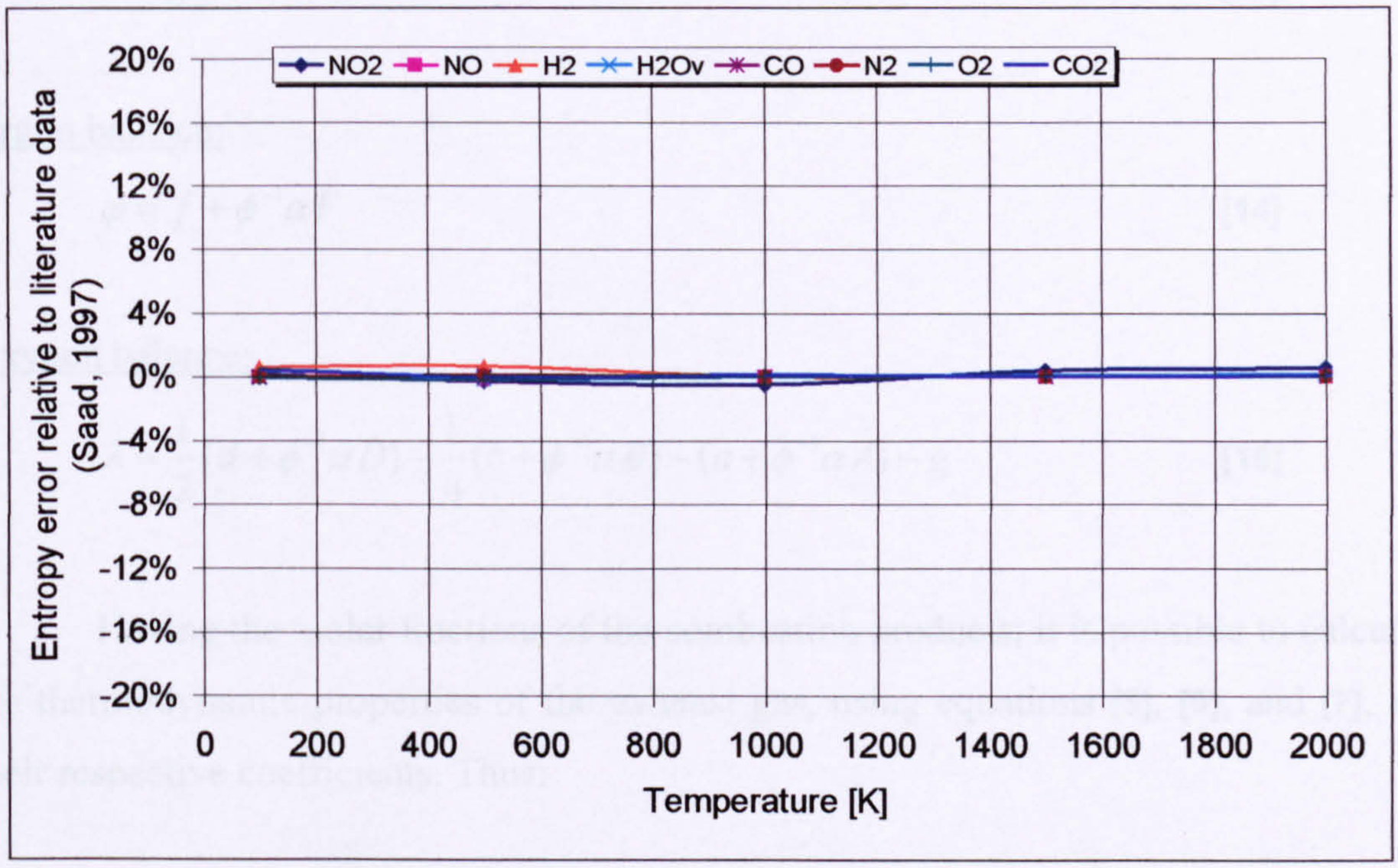

Figure 15 – Entropy error relative to literature data for different gases

The coefficients α, β, γ, ψ, ε, and φ, are calculated as follows:

$$\alpha = \frac{\left[d - 2(a+g) - \frac{b}{2}\right]}{\left[2A + \frac{B}{2} - D\right]} \qquad [9]$$

Carbon balance:

$$\beta = a + \phi^{-1}\alpha A \qquad [10]$$

Hydrogen balance:

$$\gamma = \frac{1}{2}(b + \phi^{-1}\alpha B) \qquad [11]$$

Nitrogen balance:

$$\psi = \frac{1}{2}(e + \phi^{-1}\alpha E) \qquad [12]$$

Sulphur balance:

$$\varepsilon = g \qquad [13]$$

Argon balance:

$$\varphi = f + \phi^{-1}\alpha F \qquad [14]$$

Oxygen balance:

$$\lambda = \frac{1}{2}(d + \phi^{-1}\alpha D) - \frac{1}{4}(b + \phi^{-1}\alpha B) - (a + \phi^{-1}\alpha A) - g \qquad [15]$$

Having the molar fractions of the combustion products, it is possible to calculate the thermodynamic properties of the exhaust gas, using equations **[5]**, **[6]**, and **[7]**, and their respective coefficients. Thus:

$$\overline{TP}_{gas} = \sum_{i=1}^{r} x_i \cdot \overline{TP}_i \qquad [16]$$

where $\overline{TP}_{gas} \equiv$ molar physical property (heat capacity, enthalpy, entropy, exergy or molar weight) of the mixture;

$\overline{TP}_i \equiv$ molar physical property of the i^{th} gas component; ($i = 1, \ldots, r$);

$x_i \equiv$ mole fraction of the i^{th} species; ($i = 1, \ldots, r$).

The simple and the intercooled and recuperated gas turbine cycles

The simple cycle

The simplest gas turbine cycle consists of a compressor, a combustion chamber, and an expander, which delivers shaft power to the compressor and to an electricity generator.

The choice between a single- and two-shaft gas turbine is dependent on the application and size of the engine. This thesis will focus on the aeroderivative gas

turbine. As seen in Larson, 1993, BIGGT systems are characterised by high conversion efficiencies and low expected unit capital costs ($/kW) in the 5-100 MW_e size range.

It is worth pointing out that cogeneration systems have been successfully built using both single- and two-shaft gas turbines (Figure 16) (Cohen, H., Rogers, G. F. C., and Saravanamuttoo, H. I. H., 1996).

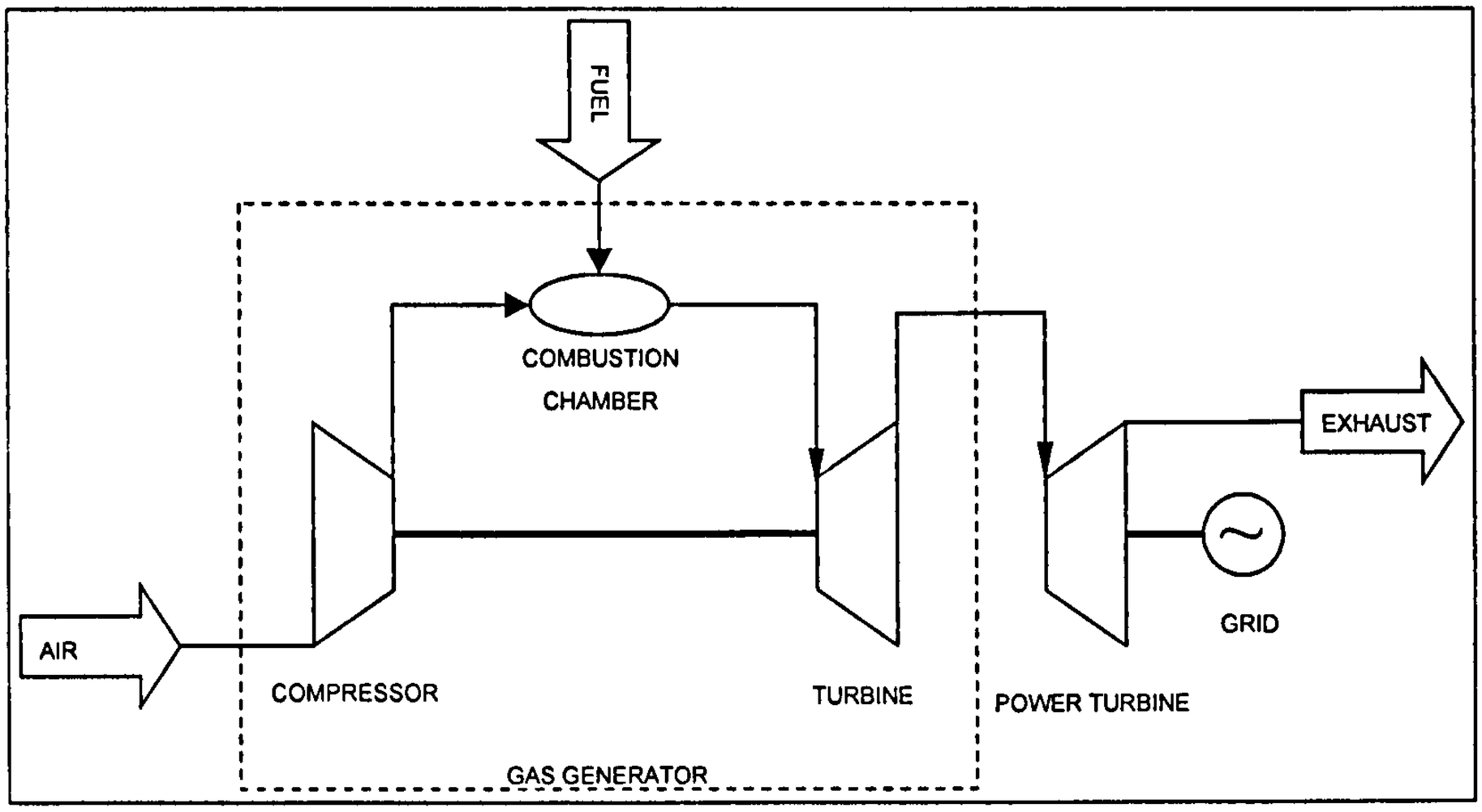

Figure 16 – Two-shaft gas turbine engine

The intercooled and recuperated cycle

Intercooling and heat recuperation are two ways used to improve cycle power output and efficiency. The first consists of splitting the compression process into a low pressure compression and a high pressure compression, decreasing the work needed to increase the pressure of the working fluid. The second consists of preheating the working fluid, in this case air, before it enters the combustion chamber, using the hot exhaust gases, diminishing the energy (fuel) input to the cycle (Figure 17).

Each process has a different aim. Intercooling intends to increase specific power, while recuperation aims to increase efficiency.

Intercooling

An ideal thermodynamic cycle analysis shows that the addition of the intercooler (IC), to the gas turbine cycle would increase the specific power at the cost of an efficiency reduction. Power is increased because the second stage, high-pressure

compressor (HPC), starts at lower temperatures and therefore requires less work. However, for the same pressure ratio (*PR*) the heat input must increase in order to compensate for the heat removed from the compressor (Alves et al. 2001).

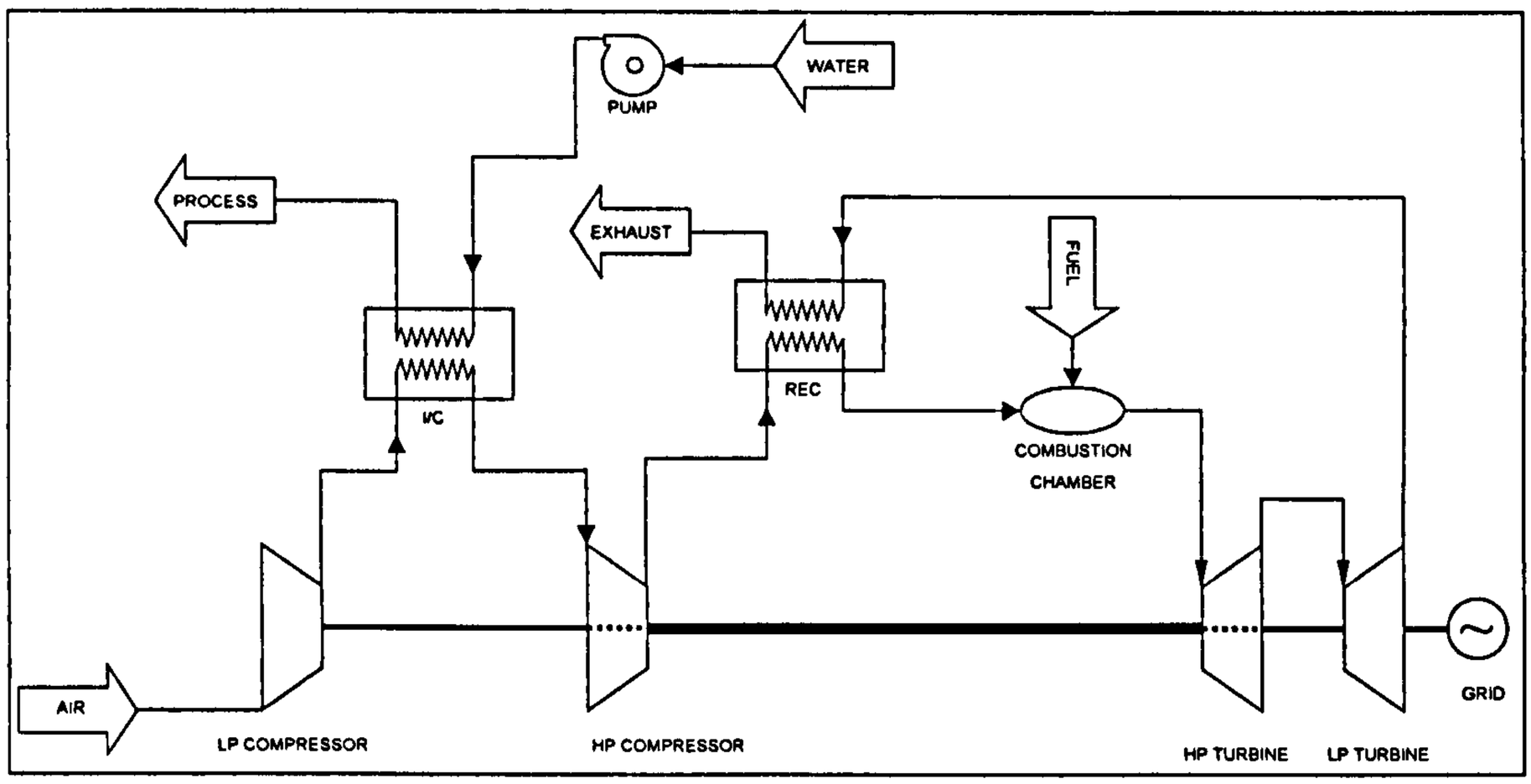

Figure 17 – Intercooled/recuperated gas turbine engine

An important benefit of the intercooled cycle is that by reducing compressor work, it reduces the sensitivity of the cycle to component losses. Also, the introduction of intercooling will allow the adoption of a significantly higher pressure ratio (*PR*), because it reduces the compressor exit temperature and increases the pressure ratio for the optimum thermal efficiency.

Assuming that the air is intercooled to the low-pressure compressor (LPC) inlet temperature (T_1), and neglecting the losses in the heat exchanger, it can be seen in Figure 18 that the maximum specific work is reached when the LP and HP pressure ratio are equal, i.e.:

$$PR_{OPTIMUM} = \sqrt{OPR} \qquad [17]$$

where $PR_{OPTIMUM}$ ≡ optimum pressure ratio for each individual compressor;

OPR ≡ overall pressure ratio.

Recuperation

The loss of efficiency resulting from the presence of the intercooler can be overcome with the use of a heat exchanger to pre-heat the air, before it enters the

combustion chamber, using the hot exhaust gases. This heat exchanger is called the recuperator (Figure 17). The cycle is called the intercooled/recuperated gas turbine cycle.

To enhance thermal efficiency in the intercooled cycle without introducing a recuperator, the overall pressure ratio of the engine must be increased. Three aspects limit the overall pressure ratio in a simple cycle gas turbine:

1. For a given turbine entry temperature, there is an optimum pressure ratio which gives the highest efficiency.
2. Due to the need to cool the turbine, a higher compressor exit temperature will require a large air bleed and this will have a negative impact on the cycle.
3. When operating in a combined cycle, there must be a compromise between the pressure ratio and a suitable engine exhaust temperature (Alves et al. 2001).

Figure 18 shows a comparison between the intercooled and the intercooled/recuperated cycles. The superiority of the second, in terms of thermal efficiency, is clearly seen. However, due to the backpressure at the exhaust of the engine, caused by the presence of the recuperator, its specific work is penalised. Even at pressure ratio 60, the optimum intercooled and recuperated cycle is more efficient than the intercooled-only cycle.

The use of intercooled/recuperated cycles in power generation has not been recorded in electricity market applications. These cycles are generally used for ship propulsion due to their capability to operate efficiently in part-load conditions (Walsh, P. P. and Fletcher, P., 1998).

The BIGGT cycle

The biomass integrated gasification/gas turbine (BIGGT) is made of the following main components:

1. *The gasification island (or gasifier)*: this system receives the solid biomass and, through thermochemical processes, converts it into a low calorific gas.
2. *The gas cleaning system*: the gas leaving the gasifier is full of particulates, alkali metals, tars, and other contaminants. The cleaning system has the difficult task of making this gas acceptable within the limits of the gas turbine engine manufacturer.
3. *The gas turbine engine*.

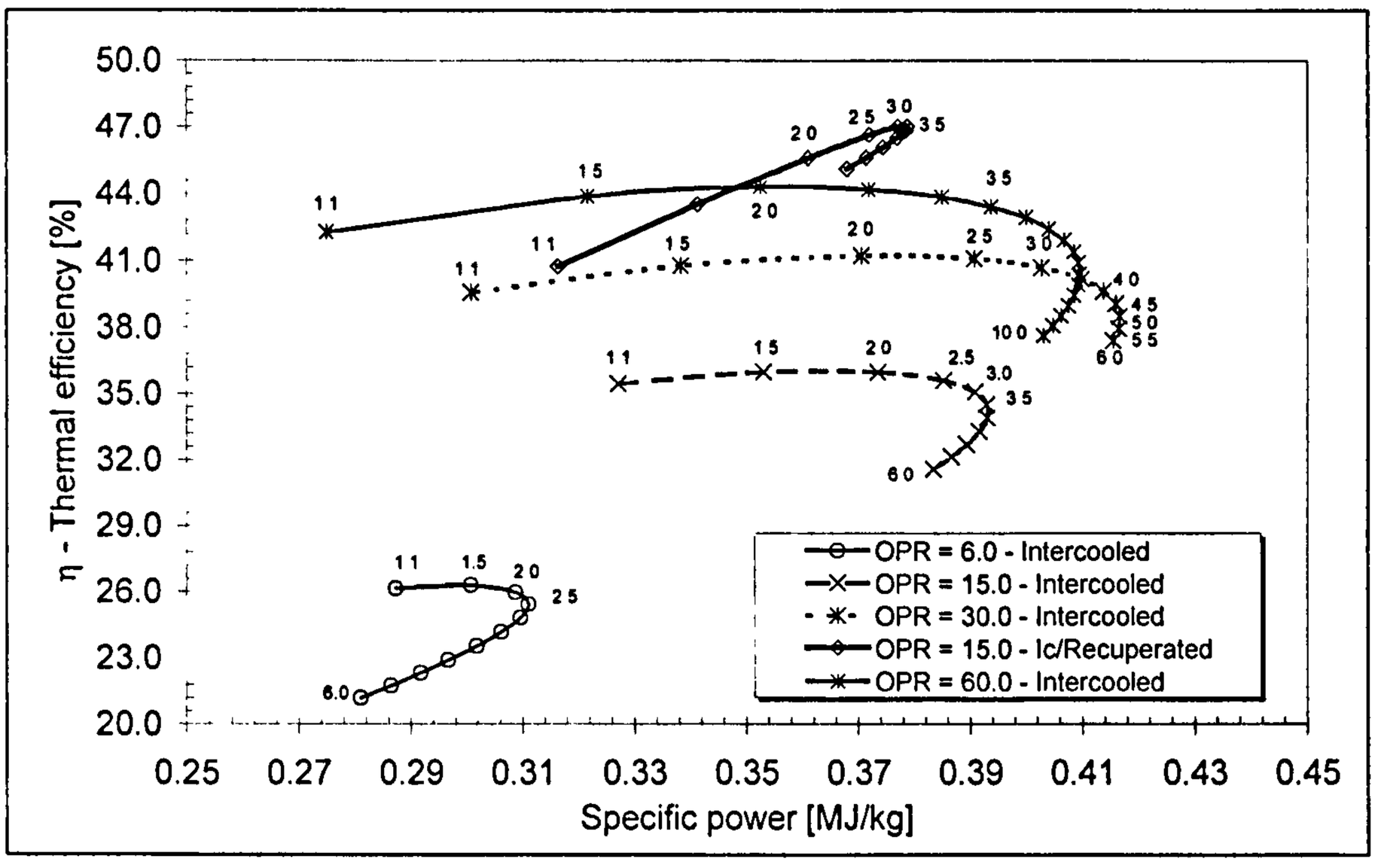

Figure 18 – Optimum pressure ratio for the LPC in an intercooled gas turbine cycle and comparison with an intercooled/recuperated gas turbine

The gas turbine engine receives the low calorific fuel as energy input (Figure 19). Although it appears to be nearly the same process as in a natural gas fired plant, the use of such a different fuel can cause serious trouble to the engine and ancillary devices, as will be discussed later in this chapter. Moreover, the presence of the gasification system severely penalises the system in terms of size, cost, and thermal efficiency.

The main aspects of concern in such a cycle can be summarised as:

1. The efficiency losses in the gasification and cleaning system;
2. The low calorific value of the fuel supplied;
3. The cleanliness of the fuel.

Such a system is under demonstration in several countries, including Brazil, and the prospects are promising. However, several difficulties have to be overcome in order to make this cycle economically feasible.

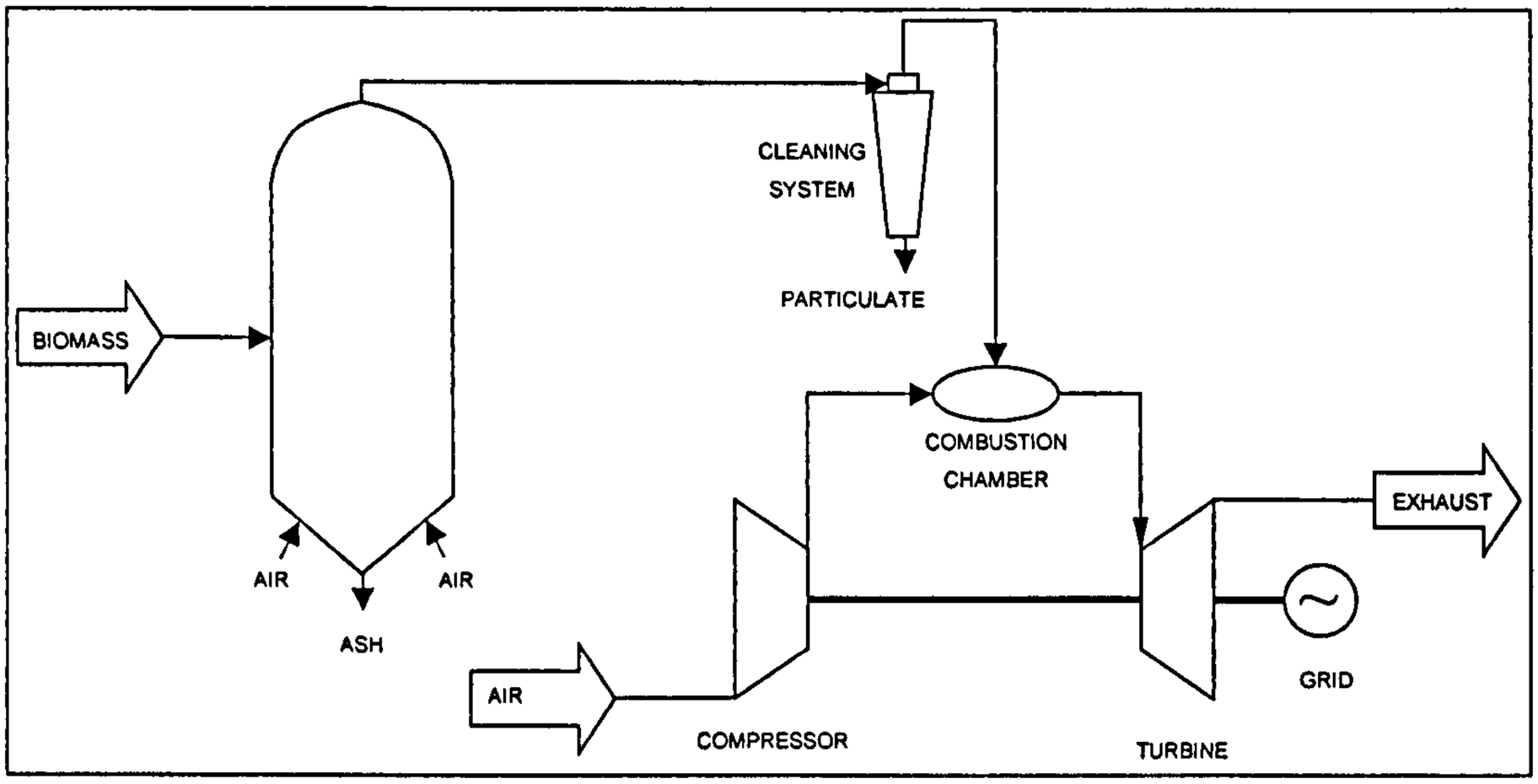

Figure 19 – Scheme of a BIGGT system

The losses in the gasification process

The gasification system receives a solid fuel with a reasonable calorific value (16-22 MJ/kg) and transforms it into a low calorific value gas (4-11 MJ/kg). The gas produced can be used in wider range of applications than the solid fuel, but this flexibility comes at the expense of the energy content of the fuel.

The gasification efficiency (η_G) is defined as the ratio of the heat content of the fuel gas generated by the gasification of the biomass and the heat content of the wood when totally burnt:

$$\eta_G = \frac{m_g \, LHV_g}{m_b \, LHV_b} \qquad [18]$$

where $m_g \equiv$ mass flow of the gas produced;

$LHV_g \equiv$ lower heating value of the gas produced;

$m_b \equiv$ mass flow of solid fuel (biomass);

$LHV_b \equiv$ lower heating value of the solid fuel (biomass).

The gas turbine engine cycle efficiency is:

$$\eta_{GT} = \frac{\dot{W}_u}{\dot{m}_g \, LHV_g} \qquad \textbf{[19]}$$

where $W_u \equiv$ useful work from the gas turbine cycle considering all the off-takes for the BIGGT system.

Combining equations **[18]** and **[19]** it is possible to derive the following relationship for the overall BIGGT efficiency:

$$\eta_{BIGGT} = \eta_G \cdot \eta_{GT} \qquad \textbf{[20]}$$

Gasification efficiencies range from 65-75 percent for fixed bed gasifiers and from 80-85 percent for fluidised bed gasifiers, according to Larson et al. 1989. Assuming $\eta_G = 80\%$ and a typical $\eta_{GT} = 36\%$ the overall efficiency of the system is substantially reduced to $\eta_{BIGGT} = 29\%$, demonstrating the penalisation imposed by the gasification system.

The cleaning system and gas cleanup

Gas turbine engines are very sensitive machines and the presence of contaminants in the fuel gas can cause serious damage to injectors, filters, and hot parts in general, including erosion and corrosion of the turbine blades. The presence of the contaminants also has an impact regarding the emissions issue, mainly NO_x emissions.

Systems producing either fuel or synthesis gas must deal with the cleanup of five primary contaminants:

1. Particulates;
2. Alkali compounds;

3. Tars;
4. Nitrogen-containing components;
5. Sulphur[25].

Table 11 shows some limits for contaminants present in the fuel for two gas turbine manufacturers. These values are probably conservative and will be well established when more operating experience is available.

Table 11 – Gas turbine fuel specifications (Schmitz et al. 2000)

Fuel gas requirements	Siemens KWU	Allison (> 11.8 MJ/scm)
Sulphur – S	n.a.[26]	236.0 mg/MJ
Halides – Cl, F, Br	n.a.	17.8 μg/MJ
Alkali – Na, K	7.1 μg/MJ	11.7 μg/MJ
Vanadium – V	Σ(Pb,V)	11.7 μg/MJ
Lead – Pb	11.9 μg/MJ	11.7 μg/MJ
Zinc – Zn	n.a.	11.7 μg/MJ
Iron – Fe	n.a.	11.7 μg/MJ
Copper – Cu	n.a.	4.7 μg/MJ
Calcium – Ca	238.0 μg/MJ	11.7 μg/MJ
Magnesium – Mg	n.a.	35.0 μg/MJ
Particles	404.0 μg/MJ < 2μm 374 μg/MJ > 10 μm undue	> 0.3 μm undue

Particulates

Particulates, even in relatively small quantities, can cause turbine blade erosion. Lightweight aeroderivative gas turbines are especially susceptible. As a result, manufacturers specify stringent particulate limits. For example, General Electric (GE) specifications for its turbines (both heavy-duty and aeroderivative varieties) require a total concentration below 1 ppmw at the turbine inlet, with 99 percent of the particles less than 10 μm diameter. This corresponds to a particulate concentration in uncombusted low-heating-value gas of about 3-5 ppmw. Since particulate concentrations in raw gas from most fluidised bed gasifiers will be 5000 ppmw to 10,000 ppmw or higher, it is likely that very high efficiency filtration (ceramic or sintered-metal) and/or wet scrubbing of the raw gas will be required (Consonni et al. 1996a).

[25] Sulphur is a major concern for gas from coal gasification.

[26] n.a. ≡ not available

Alkali metals

Alkali metals corrode the turbine blades. Gas turbine manufacturers specify maximum allowable alkali concentrations of about 4 ppbw in the combustion products for aeroderivative gas turbines and two or three times this level for heavy-duty gas turbines. The 4 ppbw corresponds to about 20 ppbw in uncombusted low-heating-value gas. During biomass gasification, alkali metals such as sodium and potassium contained in the feedstock are vaporised and leave the gasifier with the product gas.

At exit temperatures in excess of about 600°C, these metals will remain in the vapour phase and their concentration will far exceed maximum concentrations tolerable to the gas turbines. For removal, the key step is cooling the gas in the presence of solids or liquids on which the condensed vapours can be deposited and removed from the gas stream. Alternatively, wet scrubbing can be used, which would result in more significant cooling and provide essentially complete alkali removal. According to Neilson, 1998, in the mid 1980s GE M&I experienced premature corrosion of turbine blades running in high alkali environments.

Tars

Tars form during the gasification of biomass and account for 0.5 to 1.5 percent by mass of the product gas from a typical fluidised-bed gasifier, depending on temperature. If tars condense on cool surfaces, severe operating problems can result, including constricted piping or clogged valves. Tars will often constitute such an important energy component of the fuel gas that removing them from the gas would result in a loss of system efficiency.

Two approaches are being taken for dealing with tars in BIGGT systems. In the approach pursued by Bioflow and Enviropower, two gasifier manufacturers, dolomite in the fluid bed acts as both the bed material and tar-cracking catalyst. Dolomite leaving the gasifier is recycled back through a cyclone to the reactor. The product gas is then cooled to 350°C to 400°C, enough to condense alkali vapours, but not enough to condense any but the heaviest tars the gas may contain. Thus, there appears to be a temperature window of 300°C to 600°C within which problems with both condensed tars and vaporised alkalis might be avoided.

A second approach involves the use of dolomite or some other catalyst in a separate reactor placed immediately after the gasifier. Additional air is provided to the catalytic "cracker" to maintain an elevated temperature. The second reactor leads to the production of a gas with very low levels of tar, so that cold, wet scrubbing can be used with relatively little loss of chemical energy (Consonni et al. 1996a). However, in tests with nickel catalysts almost complete removal of tar could be observed at 900°C, making Ni-based catalysts very promising for hot gas cleaning (Schmitz et al. 2000).

Nitrogen oxides

Nitrogen oxides (NO_x) can be produced in a gas turbine combustor from nitrogen in the combustion air (thermal NO_x) or from compounds produced during gasification from nitrogen in the feedstock (fuel-bound NO_x). Thermal NO_x is the dominant concern in the combustion of natural gas, because of the high flame temperature generated. Thermal NO_x formation with the combustion of low heating value gas is likely to be very low due to the lower flame temperatures. Fuel-bound NO_x is potentially more problematic, although for low-nitrogen biomass fuel-bound NO_x may not be a problem except where NO_x emissions standards are quite strict. Nitrogen typically leaves a fluidised-bed gasifier primarily as ammonia (NH_3), with an order of magnitude less leaving as hydrogen cyanide (HCN). Pressurisation increases the NH_3 and decreases HCN concentrations, and when dolomite is used for tar cracking, the HCN concentration is reduced significantly. Followed by a wet scrubbing step, the gasifier can completely remove ammonia, thereby essentially eliminating fuel-bound NO_x.

Alternatively, catalytic decomposition or selective oxidation of NH_3 at elevated temperature may be possible. If fuel-bound NO_x is unacceptably high, an economically undesirable fallback option is selective catalytic reduction (SCR) technology applied to the stack gas (Consonni et al. 1996a), or, if the NO_x emissions are not too strict, steam injection is a cheaper option. The choice between these two methods depends on the strictness of local regulations. Although the SCR method is more expensive, emission targets lower than 10 ppmvd are easily achieved (Agazzani et al. 1997b).

Detailed information about methods for gas turbine cleanup can be found in Stevens, 2001. For further information on NO_x formation mechanisms please refer to Tariq et al. 1996, Singh, 1998 and Lefebvre, A. H., 1998.

Gas turbine performance with low calorific value fuels

In general the gas turbines available in the market have been designed for a high calorific value fuel, such as natural gas and fuel oil. Gasified biomass, as a general rule, has a tenth of the calorific value of natural gas, compromising the performance of individual components, and consequently the cycle as a whole.

Because of the low calorific value (LCV) of the gas derived from biomass, more fuel mass flow is needed to achieve the desired turbine entry temperature (*TET*). This larger amount of fuel leads to mass imbalance between the compressor and turbine, causing the pressure ratio to rise and the compressor operating point to move towards surge (Figure 20). This leads to the need of using variable inlet guide vanes (VIGVs) or bleed valves at low power settings, or alternatively to the need for redesigning the turbine nozzle guide vanes. A redesign of the combustion chamber is also needed to accommodate the large fuel mass flow (Ferreira et al. 2001a).

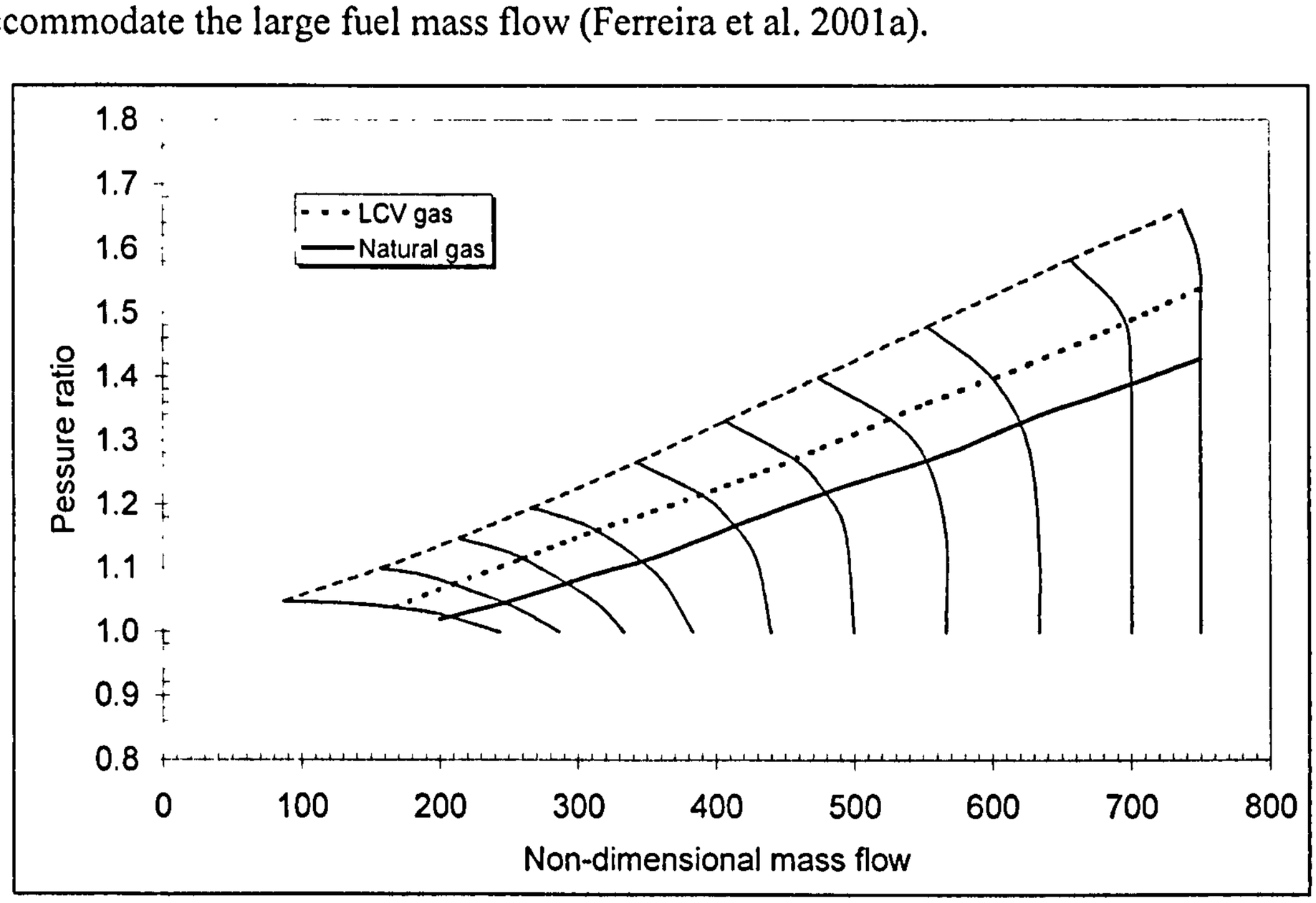

Figure 20 – Compressor working lines for LCV gas and natural gas fired gas turbine

In the Brazilian BIGCC project, a modified aeroderivative engine is being used. This engine has been designed to operate in the steam injected gas turbine (STIG)

mode. Therefore, the gas turbine area has been already designed for large mass flows. This gas turbine model, a GE LM2500PH, has been successfully tested using LCV fuels, and emissions results are very promising (Neilson et al. 1999).

Neilson, 1998 indicates four major areas where modifications are needed for the STIG engine to operate with gasified biomass:

1. Singular annular combustor with larger swirler to accept the fuel nozzle;
2. Unique fuel nozzle with dual inner circuits for start gas and biogas delivery to the combustor;
3. Start fuel manifold to deliver starting fuel to fuel nozzles;
4. Biogas manifold to deliver biomass gas to fuel nozzles.

Another feedstock property that influences the performance of the cycle is the moisture content of the fuel, as described in Hughes et al. 1998. These authors have found that for a given raw-biomass moisture content, reducing the feed-biomass moisture increases efficiency, but at a decreased rate, suggesting a trade-off between efficiency and additional dryer capacity (cost). If air-drying to 30 percent raw moisture content were achieved outside the cycle, the efficiency would be comparable with zero percent raw biomass moisture, without any further drying. In this situation, it might be more cost-effective to eliminate the dryer. One option to reduce the cost of biomass drying is the use of the heat available in gas turbine exhaust gases.

The externally fired gas turbine (EFGT) cycle

The EFGT cycle is found in two distinct versions:

1. *The parallel EFGT*: in this version the compressed air from the compressor goes through a heat exchanger, where it is heated up, is expanded in a turbine, and is released either to the atmosphere or into a heat recovery system (Figure 21). The combustion air is supplied at ambient temperature. If discharged to the atmosphere the heat available in the turbine exhaust is completely wasted. On top of that the heat exchanger exhaust contains a fair amount of energy being wasted.

2. *The series EFGT*: in this version the expanded hot air goes into a combustion chamber (Figure 22). The recuperative nature of this cycle makes it more efficient than the parallel EFGT; moreover the optimum is achieved at low pressure ratios[27] (Figure 23).

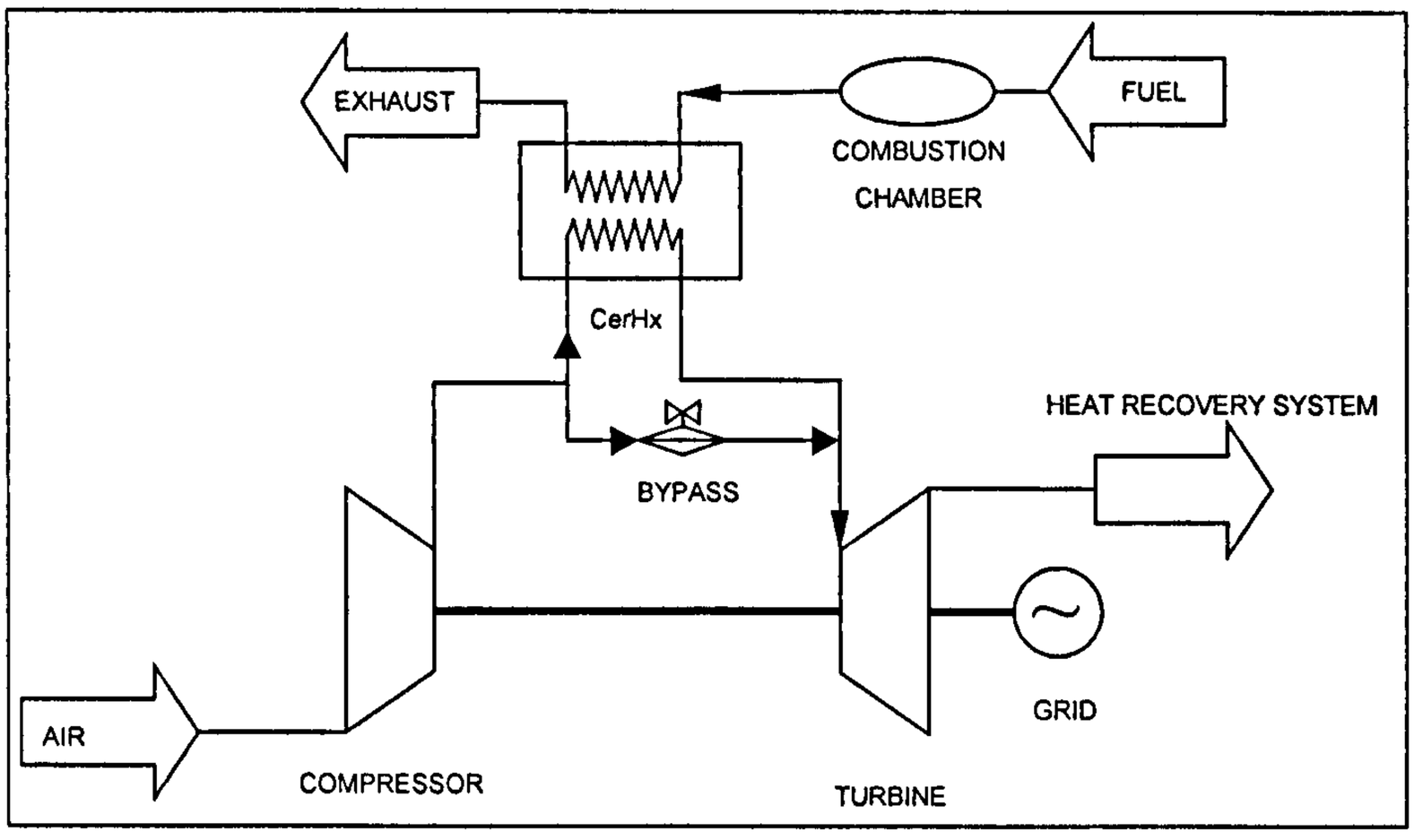

Figure 21 – Schematic of a parallel EFGT

The high efficiency of the series EFGT is the reason for its choice for the present thesis. Thus, from this point onwards, the term EFGT refers to the series externally fired gas turbine arrangement. Moreover, the very high temperature in the heat exchanger exhaust of the parallel EFGT (1172 K for its optimum pressure ratio of 15) is far above the limit supported by the state-of-the-art HRSGs (around 610°C according to Dechamps, 1999), making this stream unsuitable for combined cycle applications, unless some of the heat is dissipated before entering the HRSG.

The main drawback of the EFGT cycle, when compared with the conventional cycle fuelled by fossil fuels, is the low efficiency when a high temperature heat exchanger is not used. Due to the temperature constraints of the heat exchanger, the turbine entry temperature is much lower than that of the conventional cycle (Larson et al. 1988). The development of heat exchangers that can withstand higher temperatures at reasonable costs will change this situation, allowing efficiencies as good as those of a

---

[27] It is pointed out that the calculations where carried out for a simple cycle, a combined cycle configuration will allow high efficiencies for both cycles.

conventional cycle. Another problem is related to the deterioration of the heat exchanger performance due to slagging – deposition of solid particulates in the ceramic heat exchanger tubes.

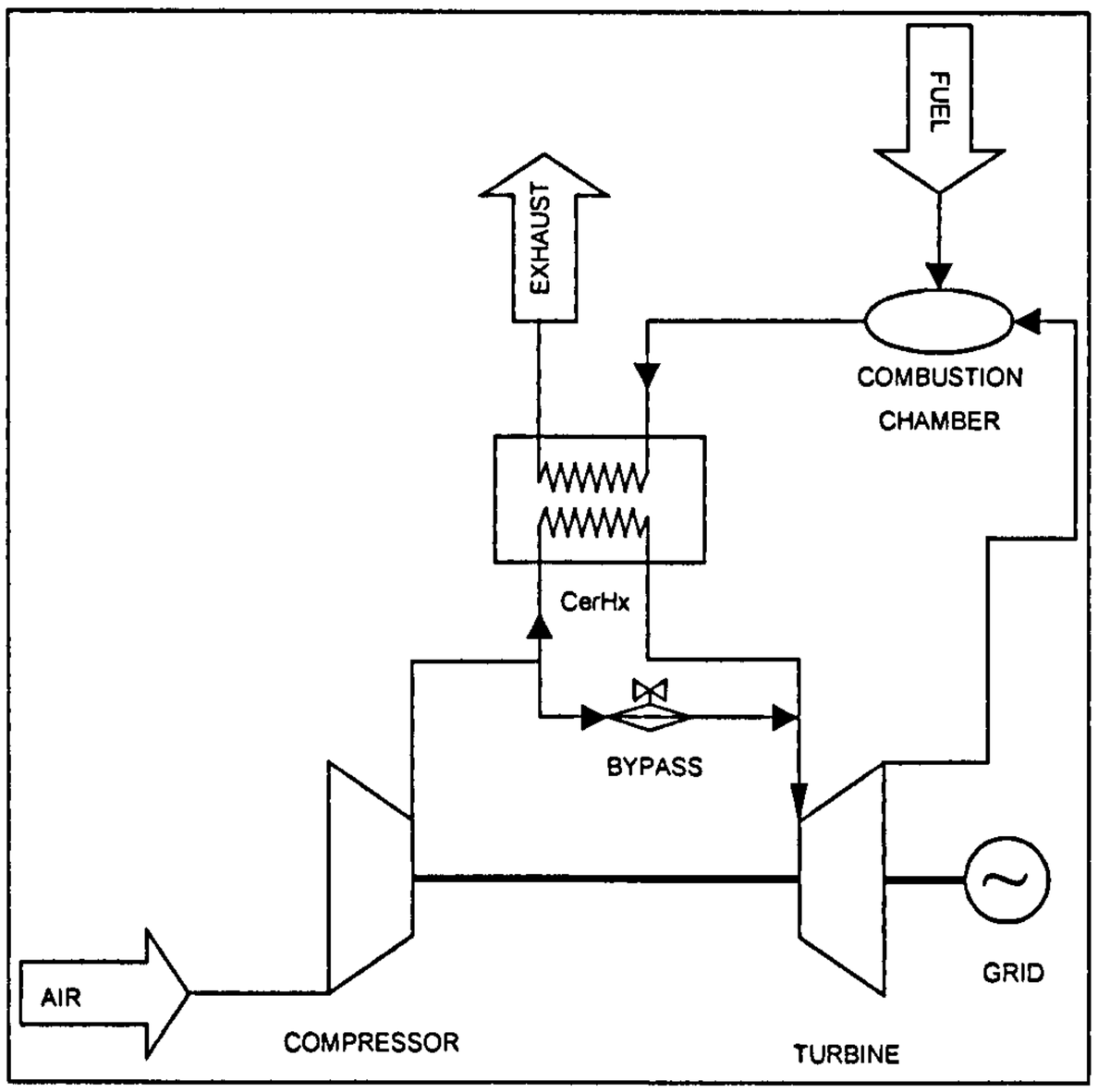

Figure 22 – Schematic of a series EFGT

On the other hand there are several advantages in using the EFGT cycles fuelled by biomass. The first is that the gasification system is no longer needed. As already noted, this device is very costly and introduces large losses into the overall cycle efficiency, not to mention its bulk. The second advantage is the versatility of the combustion chamber, i.e., many different fuels can be burnt, allowing the use of that which is the cheapest or readily available. The pre-treatment needed is modest when compared with other cycles. These points are of great relevance when considering biomass fuels. Finally, the working fluid is clean air, which means that the maintenance costs will drop and the engine life will be lengthened.

NO_x emissions are an issue to be investigated. Some estimates will be presented later in this thesis.

The heat exchanger

Once the turbine entry temperature is imposed by the heat exchanger capacity, this device must be capable of withstanding very high temperatures for the sake of the

cycle efficiency. Many researchers and research centres (Ward et al. 1983, Lahaye et al. 1989, Ranasinghe et al. 1989, Solomon et al. 1996, and Jolly et al. 1998) have been trying to develop a heat exchanger specifically to be used in EFGT cycles.

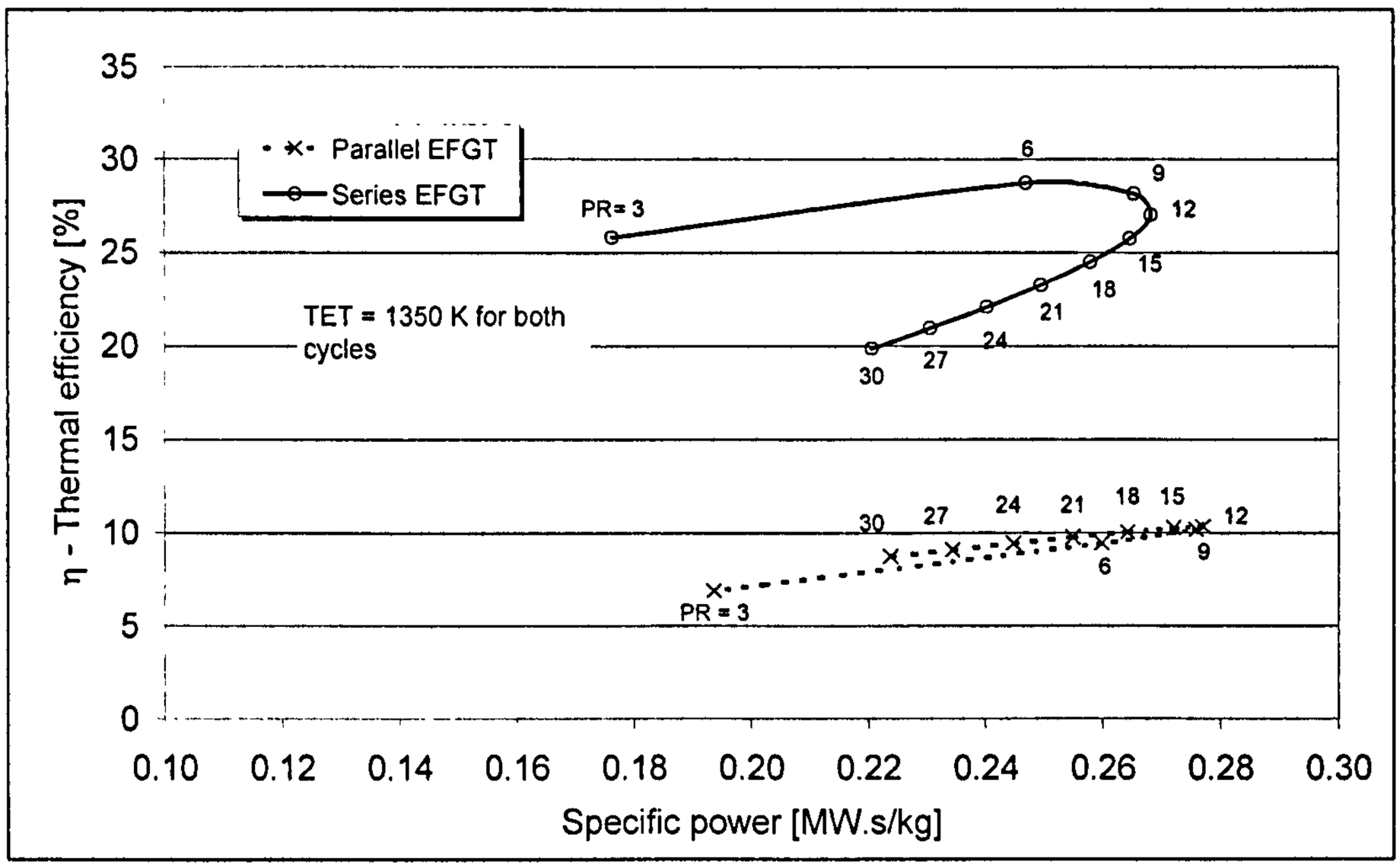

Figure 23 – Comparison between the performance of a parallel and a series EFGT

Conventional materials used in high temperature heat exchangers, such as super-alloys, are not suitable for highly efficient EFGT cycles. The use of ceramics has been seen as the most promising solution to the problem. The leading materials for high temperature pressurised heat exchanger applications are silicon carbide (SiC) based ceramics due to their relatively low cost and demonstrated fabrication technology relative to alternate refractory materials (Steen et al. 2000).

Although some researchers say that state-of-the-art ceramics are still unsuitable for use in EFGT engines (Solomon et al. 1996), there are records of ceramic heat exchangers working with products from coal combustion for approximately 500 hours at temperatures of up to 1535°C (1808K) (Lahaye et al. 1989), and 1388°C (1661K) (Solomon et al. 1996). This EFGT cycle presented thermal efficiency of 34%, with overall pressure ratio (OPR) of 10, and turbine entry temperature (*TET*) of 1150°C (1423K). With the development of ceramic materials and techniques to minimise the damage caused by fuel contaminants it is reasonable to expect that in a few years high efficiency EFGTs may be commercially available. It is worth pointing out that the experimental period of this operation is still insufficient to have a clear view of the

performance of the ceramic heat exchanger, although the same authors mention the use of ceramic heat exchangers in some industries.

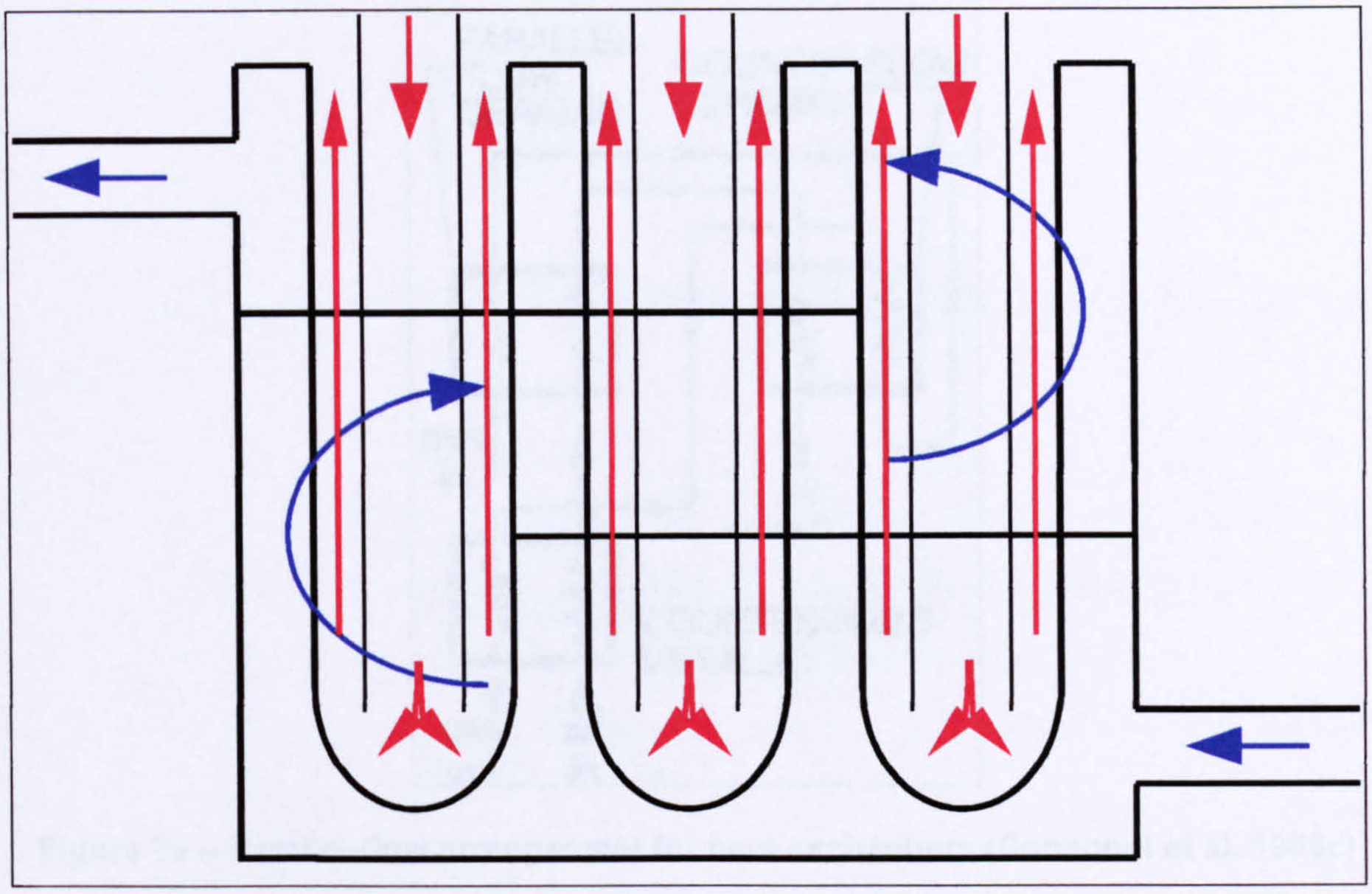

Figure 24 – Bayonet tube arrangement for heat exchangers

Jolly et al. 1998, proposed the use of bayonet tube arrangements in the ceramic heat exchangers for externally fired gas turbines (Figure 24). A bayonet element is made of two concentric tubes; the outer tube is plugged at one end and the inner tube is open at both ends. The air enters the inner tube and reverses its flow at the end to travel through the annulus (or vice-versa). The combustion products flow across the bayonet elements in the shell side of the heat exchanger. The use of such elements is justified by their capacity to expand or contract under the influence of very large temperature differences, minimising thermal stress.

Consonni et al. 1996c, suggest the use of a parallel-flow arrangement (Figure 25), combining the use of metallic and ceramic heat exchangers. According to those authors, the proposed arrangement, in the worse case scenario, allows a total heat transfer surface about 50 percent less than the normal counter flow arrangement. This considerably reduces the costs of the heat exchangers.

Despite all the attempts to develop a suitable heat exchanger for EFGT cycles, such a device would be available at high costs for a long life prototype application. For this reason in this thesis the heat exchanger outlet temperature at its cold side is

constrained at 1350K, meaning temperatures of 1435K in the hot side inlet of the heat exchanger for the EFGT simple cycle.

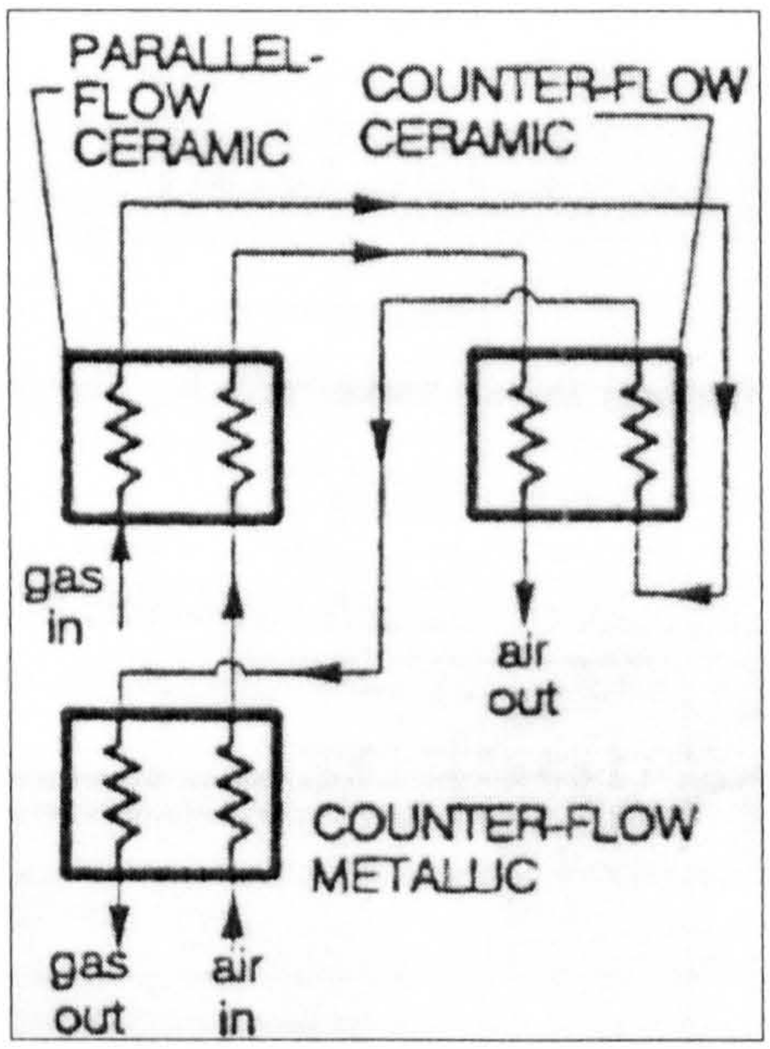

Figure 25 – Parallel-flow arrangement for heat exchangers (Consonni et al. 1996c)

The very high exhaust temperatures also suggest that this cycle is suitable for combined gas/steam cycles. Actually, the steam cycle can be optimised independently of the gas turbine cycle, once the HRSG inlet gas temperature can be adjusted without interfering with the gas turbine engine (Lahaye et al. 1989).

Key problems with this cycle are:

1. Thermal inertia of the heat exchanger, which would not allow quick acceleration of the engine;
2. Heat-ups, shutdowns and thermal transients would be a cause of stress material;
3. Slagging and fouling in the heat exchanger;
4. Performance improvements rely not only on gas turbine advancements, but also on the progress of ceramic heat exchangers (Consonni et al. 1996d).

Erosion can be controlled through the control of the velocity of the particles at the heat exchanger intake. According to Ranasinghe et al. 1989, the maximum allowable velocity of the dust-laden flue gases to prevent tube erosion, is given by:

$$V = \frac{0.0037674}{\sqrt{m}} \qquad [21]$$

where $V \equiv$ denotes the velocity in m/s;

$m \equiv$ denotes the mass of the impacting particles.

Despite all the cited handicaps they are compensated by the following main advantages:

1. With no flame upstream, the temperature entering the gas turbine is particularly uniform, implying lower thermal stresses and cooling flows.
2. The working fluid is clean air, reducing maintenance costs.
3. Gas cleaning is not as demanding as in pressurised fluidised bed combustors (PFBC) and BIGGT, because the gases produced by combustion flow downstream the turbine.
4. Unlike gasification systems, any kind of fuel can be burnt in the combustor.
5. The absence of a chemical section makes this cycle more familiar for utilities used to operate conventional steam plants (Consonni et al. 1996d).

The combustor

The combustor to be used on the EFGT cycle is a controversial issue. On one hand, Lahaye et al. 1989 state that the technology is readily available, including low-NO_x, high-efficiency suspension burners, and fluid beds. On the other hand, Consonni et al. 1996d and Elmegaard et al. 2002 have pointed out that the design of a combustor to be used in the EFGT cycle is a technology still to be developed.

Engine components performance calculations

The performance of each type of cycle has been calculated using subroutines developed specifically for this thesis. The programming language used is Fortran90, chosen for its modularity (Ellis, T. M. R., Philips, I. R., and Lahey, T. M., 1997) and

also because it intends to contribute to TURBOMATCH, a code developed at Cranfield for gas turbine performance calculations.

Subroutines to calculate design-point performance of the various engine components have been developed, and they are described in the following sections. All subroutines are contained in one module, making it easy to call just the subroutines needed for a specific cycle.

Air composition

The air composition by volume is calculated using the equations given in Table 12. Given the relative humidity (UR), altitude (AL), and ambient temperature (T_{amb}), its possible to calculate the air composition using the following equations (Ferreira, 1998):

$$P_{amb} = 101325.0 \times e^{-11.6\times10^{-5}\times AL} \quad \textbf{[22]}$$

where P_{amb} ≡ is the ambient pressure, [Pa];

AL ≡ is the local altitude, [m].

$$P_{sat} = e^{\left[\sum_{i=1}^{9} a_i T_{amb}^{i} + 10\,4592 + \frac{-3968.06}{T_{amb}-39.573}\right]} \quad \textbf{[23]}$$

where P_{sat} ≡ is the saturation pressure for the water in the air, [Pa];

T_{amb} ≡ is the ambient temperature, [K];

a_i ≡ are coefficients as follows:

$$a_1 = -0.44897\times10^{-2}; a_2 = -0.417520\times10^{-4}; a_3 = 0.368510\times10^{-6}$$
$$a_4 = -0.101520\times10^{-8}; a_5 = 0.865310\times10^{-12}; a_6 = 0.903668\times10^{-15}$$
$$a_7 = -0.199690\times10^{-17}; a_8 = 0.779287\times10^{-21}; a_9 = 0.191482\times10^{-24}$$

Compressor

The subroutine for compressor performance calculations receives as input the working fluid mole composition, the pressure ratio, the inlet temperature and the polytropic efficiency. The output value is the outlet temperature. Intake pressure losses, bleeding, and compressor work are calculated externally.

Given the working fluid mole composition it is possible to calculate its heat capacity using the formula described in **Thermodynamic properties of gases**. The outlet temperature is calculated through an iterative process inside the subroutine. The inlet and other outlet thermodynamic properties are calculated using the pressure, temperature, and gas mole composition for each station using the formulae from **Thermodynamic properties of gases**.

Table 12 – Coefficients for the calculation of air composition by volume

Compound	Mole fraction
O_2	$0.2099\left(1-UR\frac{P_{sat}}{P_{pamb}}\right)$
N_2	$0.7804\left(1-UR\frac{P_{sat}}{P_{pamb}}\right)$
Ar	$0.0094\left(1-UR\frac{P_{sat}}{P_{pamb}}\right)$
CO_2	$0.0003\left(1-UR\frac{P_{sat}}{P_{pamb}}\right)$
H_2O	$UR\frac{P_{sat}}{P_{amb}}$

Turbine

The subroutine for the turbine performance calculations receives as input the inlet pressure, the outlet pressure, the gas mole composition the turbine entry temperature, and the polytropic efficiency of the turbine, and returns the outlet temperature.

Again the inlet and other outlet thermodynamic properties are calculated using the pressure, temperature, and gas mole composition for each station using the formulae from **Thermodynamic properties of gases**.

Nozzle cooling only is assumed; that means that the mixing of the flow from compressor bleeding and combustion chamber takes place in the first inlet nozzle guide vane. The properties for the mixed stream are calculated in the subroutine MIXER.f90.

The subroutines for compressor and turbine have been previously developed by Ferreira, 1998.

Mixer

The subroutine mixer, as just mentioned, calculates the temperature of the flow going into the turbine. It receives as input the mole composition of the two flows to be mixed, their mass flows and their temperatures, returning the mixed flow mole composition, mass flow and temperature. The mixed flow pressure is assumed to be the same as the combustor outlet pressure.

The inlet and other outlet thermodynamic properties are calculated using the pressure, temperature, and gas mole composition for each station, using the formulae from **Thermodynamic properties of gases.**

Combustor

The combustor is a special part of the calculations and a dedicated module has been developed for this component. This module contains three subroutines for combustion calculations, and they are:

1. *Subroutine REACT_LHV*: this subroutine receives as input a gaseous fuel mole composition and returns its *LHV* based on the method described in **The calorific value and the chemical exergy of a gaseous fuel**, equation **[44]**;
2. *Subroutine FUEL_CHEMICAL_EXERGY*: it receives as input a gaseous fuel mole composition and returns its chemical exergy based on the method described in **The calorific value and the chemical exergy of a gaseous fuel**, equation **[45]**;
3. *Subroutine FAR_FINDER*: it receives as input the fuel *LHV*, its mole composition and temperature, the air mole composition and its temperature, and the efficiency of combustion. The returned values are the fuel to air ratio and the combustion products mole composition. The calculation is based on the mass balance and energy balance within the combustor, and equations are as follows:

$$\dot{m}_p = \dot{m}_{air} + \dot{m}_{fuel} \qquad [24]$$

where $m_p \equiv$ is the mass flow of the combustion products, [kg/s];

m_{air} ≡ is the air mass flow, [kg/s];

$\dot{m}_{fuel}$ ≡ is the fuel flow, [kg/s].

As already demonstrated by Cohen, H., Rogers, G. F. C., and Saravanamuttoo, H. I. H., 1996, the problem of calculating the fuel to air ratio can be solved with the following approach. Since the process is adiabatic with no work transfer, the energy balance is given by:

$$\dot{m}_p h_p - (\dot{m}_{air} h_{air} + \dot{m}_{fuel} h_{fuel}) = 0 \qquad \textbf{[25]}$$

where h_p ≡ is the specific enthalpy of the combustion products, [J/kg];

h_{air} ≡ is the specific enthalpy of the air, [J/kg];

h_{fuel} ≡ is the specific enthalpy of the fuel, [J/kg].

Using equation **[24]**, equation **[25]** becomes:

$$(\dot{m}_{air} + \dot{m}_{fuel})h_p - (\dot{m}_{air} h_{air} + \dot{m}_{fuel} h_{fuel}) = 0 \qquad \textbf{[26]}$$

It is known that the mass fuel-to-air-ratio $FAR = \frac{\dot{m}_{fuel}}{\dot{m}_{air}}$, thus equation **[26]** becomes:

$$(1 + FAR)h_p - (h_{air} + FAR \times h_{fuel}) = 0 \qquad \textbf{[27]}$$

Making use of the enthalpy of reaction (ΔH_r) at a reference temperature[28] (T_r) equation **[27]** can be expanded and adjusted to become:

$$FAR = \frac{h_p(T_r) - h_p + h_a - h_p(T_r)}{h_p - h_p(T_r) + \Delta H_r + h_f(T_r) - h_f} \qquad \textbf{[28]}$$

[28] Usually T_r = 298.15 K.

Equation **[28]**; however, gives the theoretical fuel-to-air-ratio. The actual fuel-to-air-ratio (FAR_a) is found using the following equation:

$$\eta_{cc} = \frac{FAR}{FAR_a} \qquad \textbf{[29]}$$

where $\eta_{cc} \equiv$ is the combustion efficiency.

Thus:

$$FAR_a = \frac{h_p(T_r) - h_p + h_a - h_p(T_r)}{\eta_{cc}\left(h_p - h_p(T_r) + \Delta H_r + h_f(T_r) - h_f\right)} \qquad \textbf{[30]}$$

As already mentioned, the heating value of a fuel is numerically equal to the enthalpy of combustion, but have the opposite sign. Thus:

$$FAR_a = \frac{h_p(T_r) - h_p + h_a - h_p(T_r)}{\eta_{cc}\left(h_p - h_p(T_r) - LHV + h_f(T_r) - h_f\right)} \qquad \textbf{[31]}$$

Heat exchanger

The final subroutine needed to carry out the calculations is the one that calculates the performance of a heat exchanger. The heat exchanger effectiveness (φ) is defined as (Cohen, H., Rogers, G. F. C., and Saravanamuttoo, H. I. H., 1996):

$$\varphi = \frac{T_{c_{out}} - T_{c_{in}}}{T_{h_{in}} - T_{c_{in}}} \qquad \textbf{[32]}$$

where $T_{c_{out}} \equiv$ is the cold stream outlet temperature, [K];

$T_{c_{in}} \equiv$ is the cold stream inlet temperature, [K];

$T_{h_{in}} \equiv$ is the hot stream inlet temperature, [K].

A good estimate of the heat exchanger surface area (A_{HX}) in [m^2], is given by (Ganapathy, V., 1991):

$$A_{HX} = \frac{\dot{Q}}{U \times \Delta T_{\log}} \qquad [33]$$

where $\dot{Q} \equiv$ is the heat exchange rate, [J/s];

$U \equiv$ is the overall heat exchange coefficient, $\left[\frac{W}{m^2 \cdot K}\right]$;

$\Delta T_{\log} = \frac{\Delta T_{MAX} - \Delta T_{MIN}}{\ln\left(\Delta T_{MAX} / \Delta T_{MIN}\right)} \equiv$ is the log-mean temperature difference.

Engine performance validation

This section describes the calculation methods for the three gas turbine cycles that are the basis of study in this thesis, and also the validation of the results against a commercial software called GateCycle®. The codes have been developed such that they calculate the thermodynamic performance, and also carry out the exergy and economic analyses.

Another reason to develop this simple code is the fact that GateCycle® is not an open source code, therefore it is not possible to link GateCycle® to GENIAL, the genetic algorithm code used for the optimisation studies.

The natural gas fuelled gas turbine, NGGT, is the benchmark for the other two cycles, the EFGT and the BIGGT.

The natural gas cycle

The NGGT cycle is the reference for comparison with the EFGT and BIGGT cycles, therefore the calculations for this cycle have been carried out using GateCycle®. No optimisation has been carried out for this cycle. The data for the performance calculation, such as component efficiencies, are based on current technological state for aeroderivative engines (International Turbomachinery Handbook 2000/2001, 2001).

Validation for the code BIGGT.f90

In order make sure that the code used to calculate the performance of the BIGGT cycle – called BIGGT.f90 – is giving sensible results, a validation against GateCycle® has been carried out. The data for the components are presented in Table 13; these data are the same inputs for both codes. Table 14 gives the fuel composition used in the simulation.

Table 13 – Design data for the simulation of the BIGGT cycle

	BIGGT
PR	3 to 30
m_{air}	100 kg/s
TET	1450 K
$\eta_{\infty c}$	0.87
$\eta_{\infty t}$	0.88
$(\Delta P/P_{in})_{cc}$	0.04
η_{cc}	0.99
η_{gasif}	0.75

The model is for a one-shaft gas turbine. The gasification efficiency (η_{gasif}) has been chosen based on the earlier discussion about gasifiers. The fuel data comes from Codeceira-Neto et al. 1999, and is in accordance with the average sugarcane bagasse composition in the north-eastern region of Brazil.

Table 14 – Fuel data for the simulation of the BIGGT cycle

Biomass		Biogas	
Component	**Mole fraction**	**Component**	**Mole fraction**
		N_2	48.40
Carbon	39.53	**CO**	21.00
Hydrogen	32.56	CO_2	9.70
Oxygen	13.89	H_2	14.50
Moisture	14.02	CH_4	1.60
		$H_2O_{(v)}$	4.80
LHV [MJ/kg]	**18.43**	**LHV**	**4.46 MJ/kg**

The comparison between the two codes is shown in Figure 26. It is seen that the maximum error given by BIGGT.f90 relative to GateCycle® is less than 2 percent for all parameters – compressor work (CW), fuel compressor work (FCW), turbine work (TW), useful work (UW), exhaust temperature (Texh), specific fuel consumption (SFC), and thermal efficiency (Thef).

These results indicate that the code performs well for the purposes of this work.

Validation for EFGT.f90

Another simple code – EFGT.f90 – has been developed to carry out the performance of the externally fired gas turbine. Again GateCycle® has been used as a reference code. Table 15 shows the design data used to carry out the performance of the EFGT cycle.

Table 15 – Design data for the simulation of the EFGT cycle

	EFGT
PR	3 to 30
$\dot{m}_{air}$	100 kg/s
TET	1350 K
$\eta_{\infty c}$	0.87
$\eta_{\infty t}$	0.88
$(\Delta P/P_{in})_{cc}$	0.02
η_{cc}	0.99
$(\Delta P/P_{in})_{CerHx}$	0.04
U	30 $W/m^2 \cdot K$
φ_{CerHx}	0.80

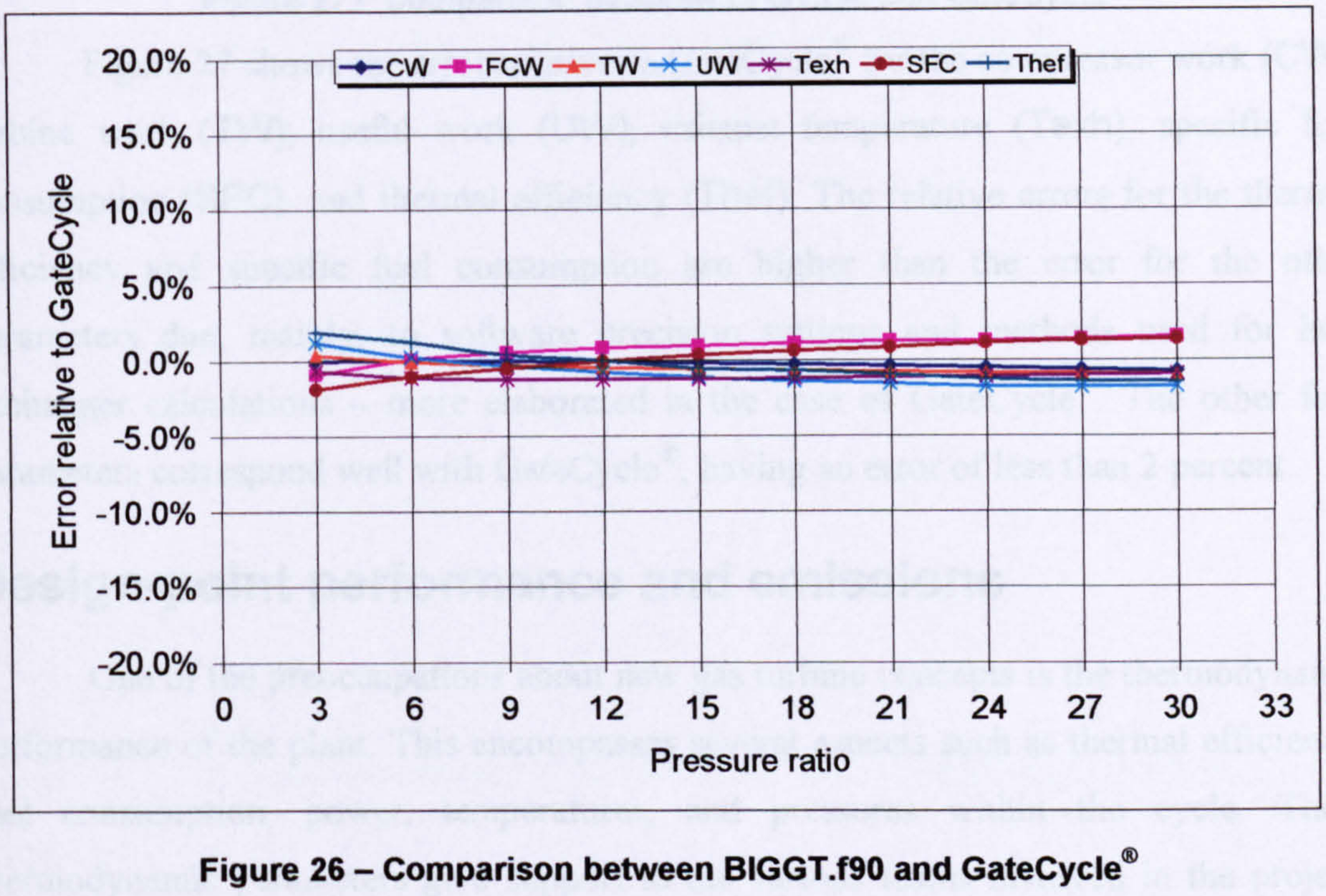

Figure 26 – Comparison between BIGGT.f90 and GateCycle®

The model is a one-shaft gas turbine. Pressure losses in the ceramic heat exchanger $\left(\left(\Delta P/P_{in}\right)_{CerHx}\right)$ are assumed the same for both the hot and cold side, and the overall heat exchange coefficient (U) has been chosen in accordance with values given

in the literature (Consonni et al. 1996c and Luzzatto et al. 1997). The solid fuel used is the biomass presented in Table 14.

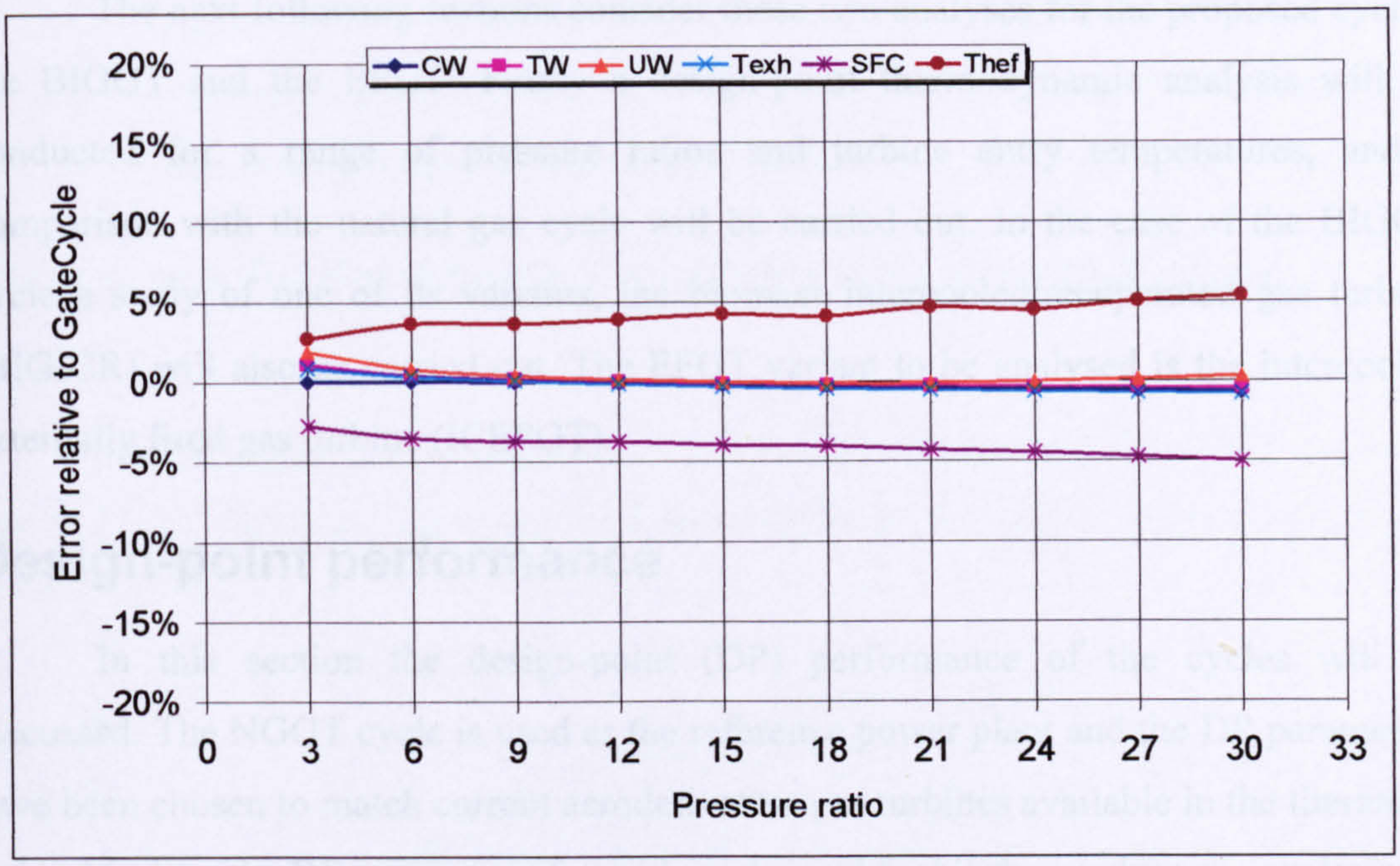

Figure 27 – Comparison between EFGT.f90 and GateCycle®

Figure 27 shows the error relative to GateCycle® for the compressor work (CW), turbine work (TW), useful work (UW), exhaust temperature (Texh), specific fuel consumption (SFC), and thermal efficiency (Thef). The relative errors for the thermal efficiency and specific fuel consumption are higher than the error for the other parameters due, mainly, to software precision settings and methods used for heat exchanger calculations – more elaborated in the case of GateCycle®. The other four parameters correspond well with GateCycle®, having an error of less than 2 percent.

Design-point performance and emissions

One of the preoccupations about new gas turbine concepts is the thermodynamic performance of the plant. This encompasses several aspects such as thermal efficiency, fuel consumption, power, temperatures, and pressures within the cycle. These thermodynamic parameters give support to the various teams involved in the project, e.g., component integration, aerodynamics, etc.

Another very important parameter to be considered during the conceptual design of a power plant is the amount of pollutants – CO_2, NO_x, unburned hydrocarbons,

particulate, etc. – released by the system. This information helps on deciding the right combustion technology to be adopted.

The next following sections consider these two analyses for the proposed cycles, the BIGGT and the EFGT. Firstly a design-point thermodynamic analysis will be conducted for a range of pressure ratios and turbine entry temperatures, and a comparison with the natural gas cycle will be carried out. In the case of the BIGGT cycle a study of one of its variants, the biomass intercooled/recuperated gas turbine (BIGICR) will also be carried out. The EFGT variant to be analysed is the intercooled externally fired gas turbine (ICEFGT).

Design-point performance

In this section the design-point (DP) performance of the cycles will be discussed. The NGGT cycle is used as the reference power plant and the DP parameters have been chosen to match current aeroderivative gas turbines available in the literature. Table 16 gives the DP parameters for each cycle used in this thermodynamic analysis.

Table 16 – Design data for the simulation of the studied cycles

	NGGT	BIGGT	EFGT
PR	3 to 30		
Bleed	6% of compressor intake		
$\dot{m}_{air}$	100 kg/s		
TET	1100 to 1600 K		
η_c	0.88		
η_t	0.89		
$(\Delta P/P_{in})_{cc}$	0.04	0.04	0.02
η_{cc}	0.99	0.99	0.99
φ_{CerHX}	-	-	0.90
η_{gasif}	-	0.75	-
U	-	-	30 $W/m^2 \cdot K$

Natural gas fuelled engine compared with gasified biomass fuelled engine

Figure 28 shows a comparison between the DP performance for the NGGT power plant and the BIGGT power plant. Two main characteristics are noticeable:

1. *Low efficiency of BIGGT*: the heavy penalty imposed by the gasification and cleaning system is clearly depicted in Figure 28;
2. *Higher specific power of BIGGT*: due to the much higher fuel flow the combustion gases are in a much larger volume than in the NGGT case. This large amount of gas produces more useful work for a given *TET*.

Natural gas fuelled engine compared with externally fired engine

Still in Figure 28 the comparison between the NGGT and the EFGT cycles is depicted. The dotted line shows the limit temperature for the ceramic heat exchanger.

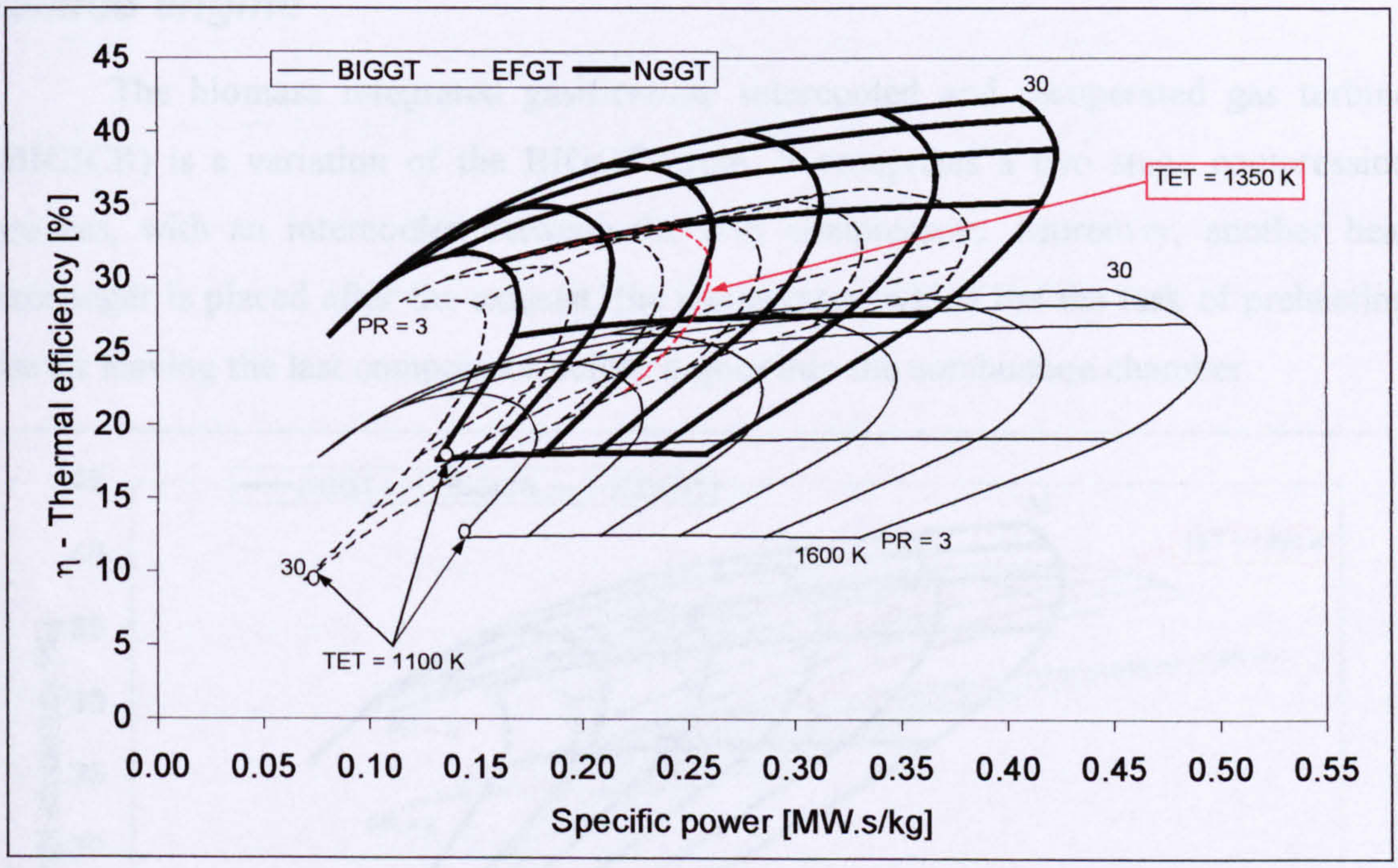

Figure 28 – Comparison between NGGT, BIGGT, and EFGT cycles

The EFGT power plant shows a good rate of efficiency compared with the NGGT power plant, and a much higher rate of efficiency compared with the BIGGT system. However the specific power is not as high as the BIGGT, though comparable with the NGGT. In this case the mass flow through the expander is lower in the EFGT than in the NGGT, due to the fact that only hot air goes through the turbine. The pressure losses imposed by the heat exchanger also affect the thermal efficiency and specific work of the EFGT cycle. In the NGGT case the expansion is to atmosphere,

whereas in the EFGT, the expander must overcome the pressure losses in the heat exchanger and the combustor.

Another interesting fact is that the efficiency of the EFGT cycle reaches its maximum at low pressure ratios. This is due to the recuperative nature of the cycle, that is, the lower the pressure ratio the higher the exhaust temperature. As the air that goes into the combustor is hot air from the free power turbine, the hotter this air the less fuel is necessary to achieve the high temperatures demanded for high efficiency.

Natural gas, gasified biomass, and externally fired engines compared with intercooled and recuperated gasified biomass fuelled engine

The biomass integrated gasification/ intercooled and recuperated gas turbine (BIGICR) is a variation of the BIGGT cycle. It comprises a two stage compression process, with an intercooler between the two compressors. Moreover, another heat exchanger is placed after the exhaust, the recuperator, which has the task of preheating the air leaving the last compressor before it goes into the combustion chamber.

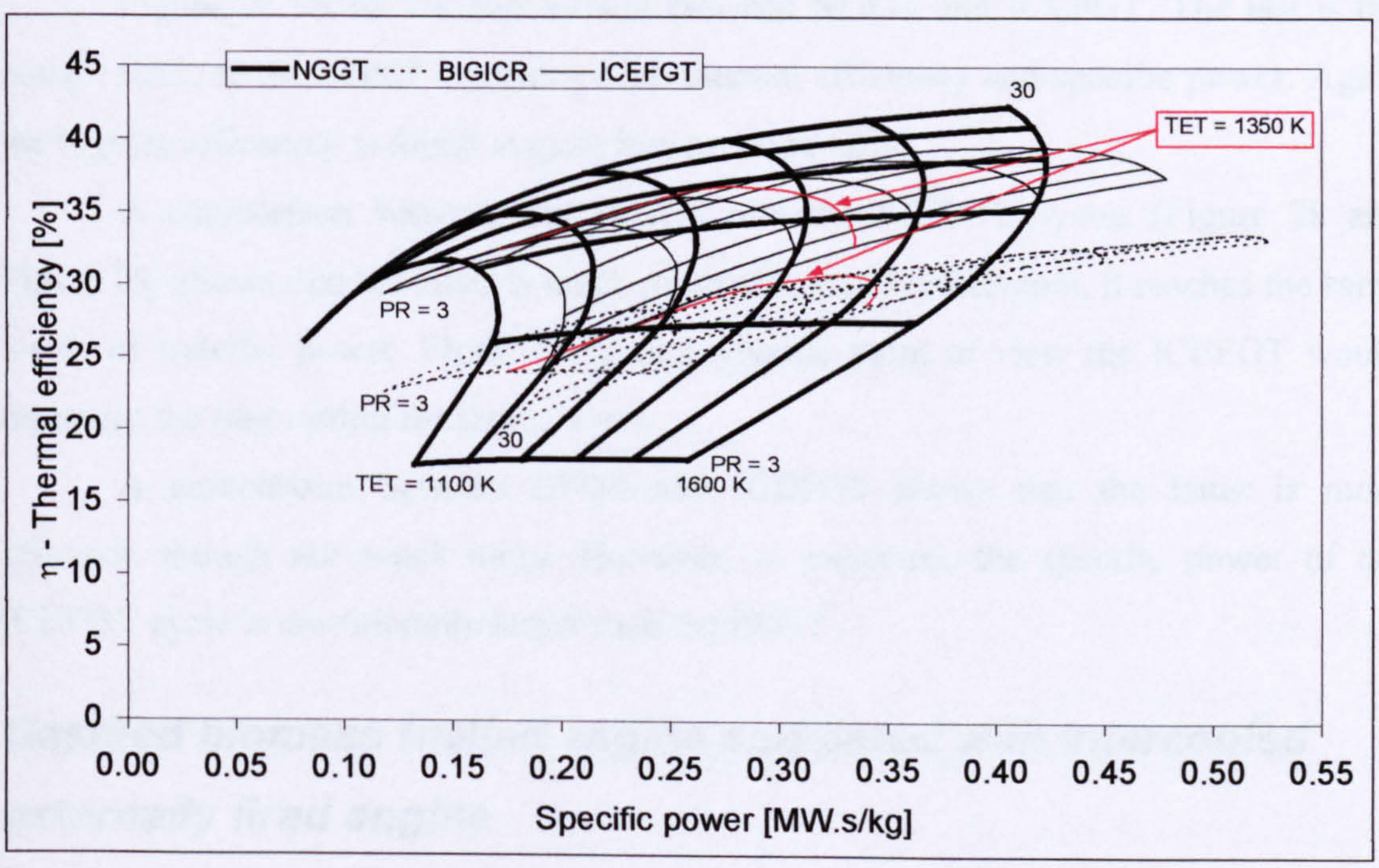

Figure 29 – Comparison between NGGT, BIGICR, and ICEFGT cycles

Figure 29 shows the comparison between the performance of the NGGT and the BIGICR gas turbines. The NGGT plant is still more efficient, showing that the heat

recuperation does not have a great impact due to the presence of the gasification and fuel cleaning system.

However, in terms of specific power it is even higher than the BIGGT cycle (Figure 28 and Figure 29). In terms of efficiency, when compared with the BIGGT system, the BIGICR presents thermal efficiency 17 percent higher. Again it is interesting to note that the efficiency is high for moderate pressure ratios, as in the EFGT cycle, due to its recuperative nature.

Comparing the EFGT and the BIGICR cycles (Figure 28 and Figure 29), the former is more efficient for low pressure ratios. On the other hand, the BIGICR has the higher specific power.

Natural gas, gasified biomass, and externally fired engines compared with intercooled externally fired engine

The intercooled externally fired gas turbine has a two stage compression process with an intercooler in between. A recuperator is pointless in this cycle due to its inherent recuperative nature.

Figure 29 shows the comparison between NGGT and ICEFGT. The last is the closest cycle to the NGGT regarding both thermal efficiency and specific power. Again the highest efficiency is found at quite low pressure ratios.

A comparison between the BIGGT and the ICEFGT cycles (Figure 28 and Figure 29) shows that the latter is much more efficient. Furthermore, it reaches the same levels of specific power. From the thermodynamic point of view the ICEFGT would represent the best option for biomass use.

A comparison between EFGT and ICEFGT shows that the latter is more efficient, though not much more. However, as expected, the specific power of the ICEFGT cycle is considerably larger than the EFGT.

Gasified biomass fuelled engine compared with intercooled externally fired engine

An interesting comparison is that between the two most complex biomass cycles, the BIGICR and the ICEFGT (Figure 29). The latter is superior to the former in

terms of efficiency; however, the BIGICR still maintains its high specific power, again due to the larger fuel mass flow going through the turbine.

However, as already discussed, intercooling and recuperation would increase the complexity of already complex cycles, and the use of such devices is not yet common practice. Another observation is that combined cycles would allow much higher efficiency and power, and the intercooled/recuperated cycles do not offer the possibility of implementing such technology due to their low exhaust temperature.

After this general overview of the performance of the cycles, a more specific comparison can be made. The intention is to find the locus of the maximum efficiency for each analysed cycle.

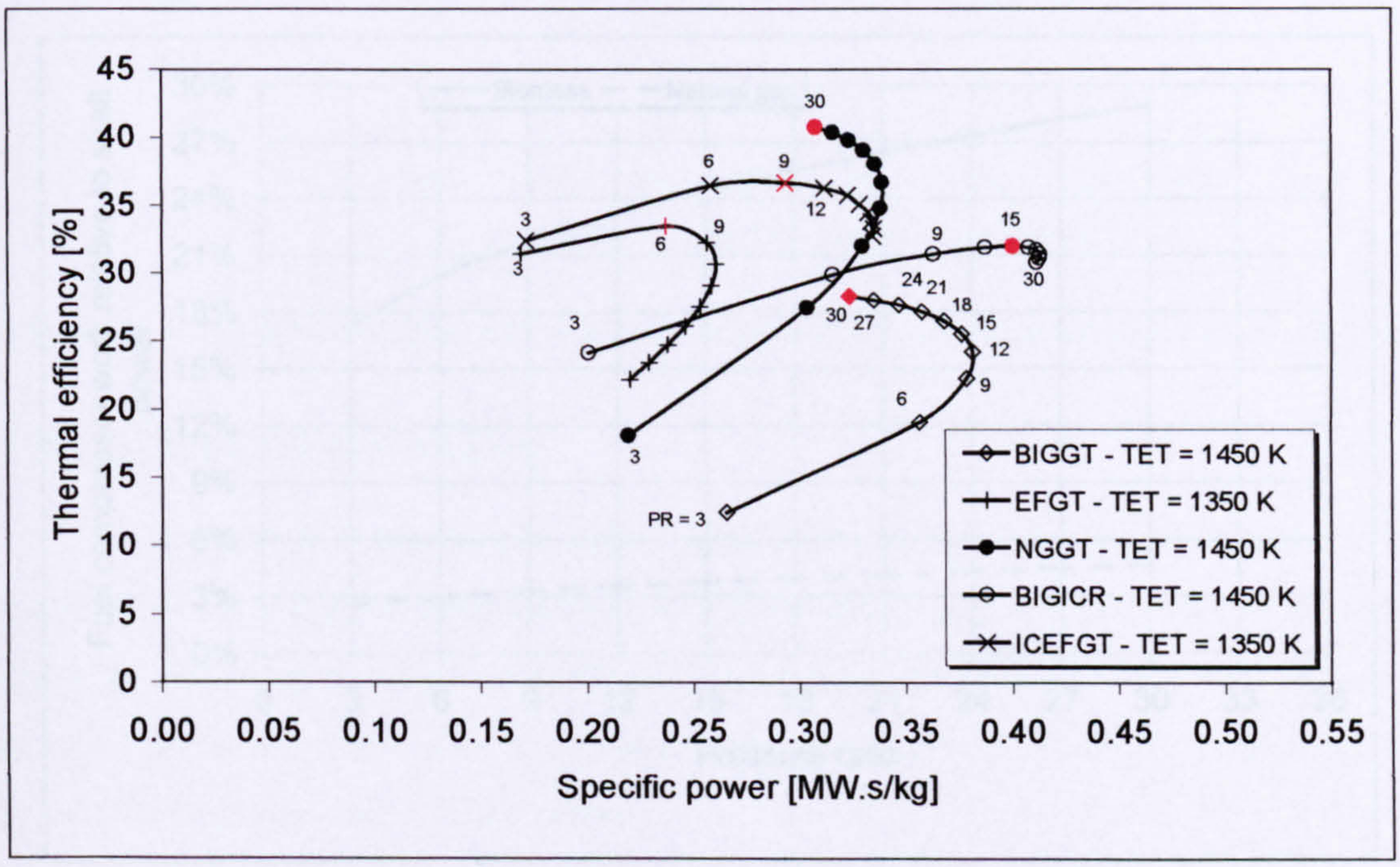

Figure 30 – Comparison between all cycles considering TET limitations

In Figure 30 the *TET* has been limited to 1450 K for the NGGT, BIGGT, and BIGICR cycles, and to 1350 K for the EFGT, and ICEFGT cycles. It has been mentioned before that the maximum efficiencies are achieved at low pressure ratios for the externally fired cycles; however, no values were assigned to these pressure ratios. In this figure the red marks represent the maximum thermal efficiency for each cycle. It shows clearly these maxima: for the EFGT cycle $PR_{opt} = 6$, and for the ICEFGT, $PR_{opt} = 9$. For the NGGT and BIGGT cases the maximum efficiencies are found at the maximum *PR*, i.e. $PR_{opt} = 30$. The BIGICR cycle finds its optimum at $PR_{opt} = 21$.

The effect of fuel compression

In order to inject fuel into the combustion chamber, this fluid must be compressed to overcome the pressure into the combustor and pressure losses that occur on fuel nozzle injectors and ancillary equipment.

When operating on natural gas the fuel compressor work is usually neglected during calculations, for it represents no more than 4 percent at high pressure ratios, due to the small amount of fuel (Figure 31). However, because biogas has a tenth of the natural gas calorific value the fuel flow can be up to 10 times larger. In this case, neglecting the fuel compressor work can have a misleading effect on the conclusions of both thermodynamic and economic assessment.

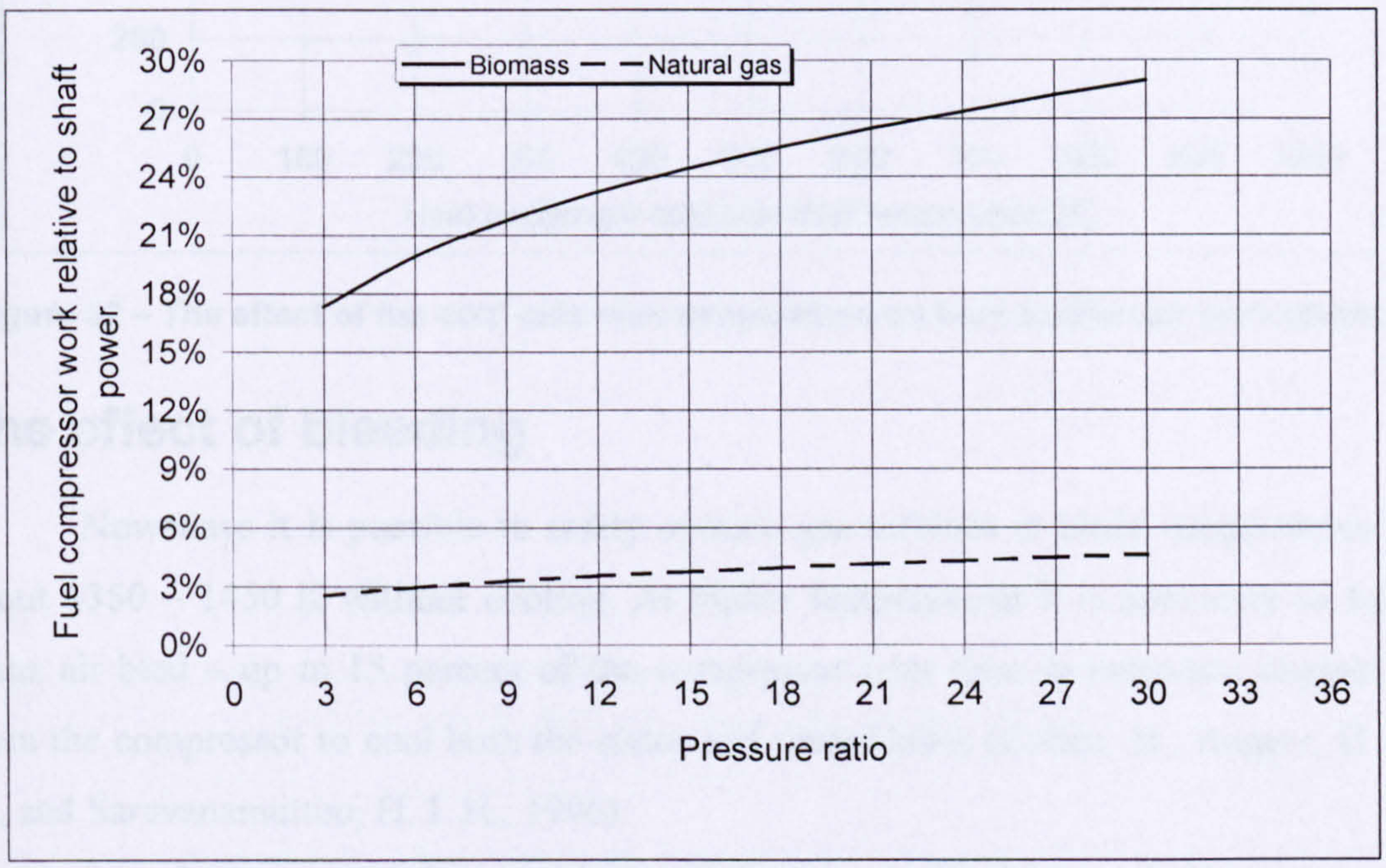

Figure 31 – Fuel compressor work for natural gas and gasified biomass

The effect of intercooling on the heat exchanger

The use of an intercooler has effects on both BIGGT and EFGT cycles. On the BIGGT cycle it decreases both the air temperature before the combustor and exhaust temperature increasing power, but negatively affecting efficiency, as already discussed.

On the EFGT cycle, as the cold side inlet temperature decreases, due to the use of intercooling, the hot side inlet temperature must increase to achieve the same *TET*, as demonstrated in Figure 32. This increase in the combustion products temperature

entering the heat exchanger can reach unbearable levels for this device, making the ICEFGT an infeasible cycle for state-of-the-art heat exchanger technologies.

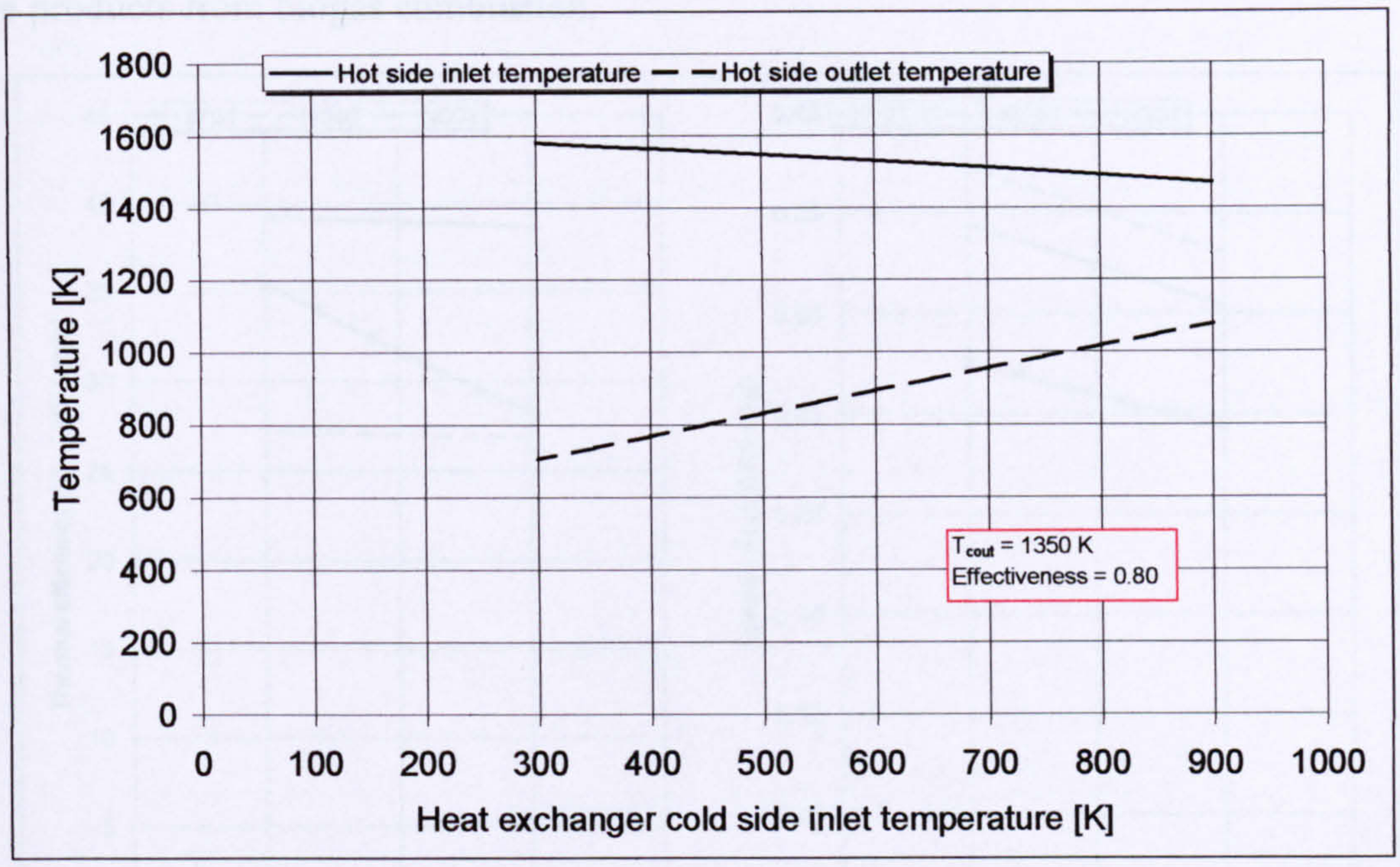

Figure 32 – The effect of the cold side inlet temperature on heat exchanger performance

The effect of bleeding

Nowadays it is possible to safely operate gas turbines at blade temperatures of about 1350 – 1450 K without cooling. At higher temperatures it is necessary to have some air bled – up to 15 percent of the compressor inlet flow in industrial engines – from the compressor to cool both the stator and rotor blades (Cohen, H., Rogers, G. F. C., and Saravanamuttoo, H. I. H., 1996).

In order to assess the sensitivity of the two main objects of this thesis, the BIGGT and the EFGT, a calculation has been carried out, as demonstrated in Figure 33. The *TET* has been considered the same for all cycles, i.e., *TET* = 1450 K. It is seen that the NGGT and the BIGGT cycles are quite insensitive to bleeding in terms of efficiency, whilst the externally fired engine has a severe drop in its thermal efficiency (Figure 33(a)).

The higher sensitivity to bleeding demonstrated by the EFGT cycle is explained by the air properties, such as specific heat, shown in Figure 34. The specific heat at constant pressure (*Cp*) for the pure air is considerably lower than the *Cp* for the combustion products. The mixing of "cold" air from the compressor decreases even

further the value of *Cp*, penalising the efficiency of the EFGT cycle. It can also be noticed that the combustion products from the natural gas have a slightly lower *Cp* than the products from biogas combustion.

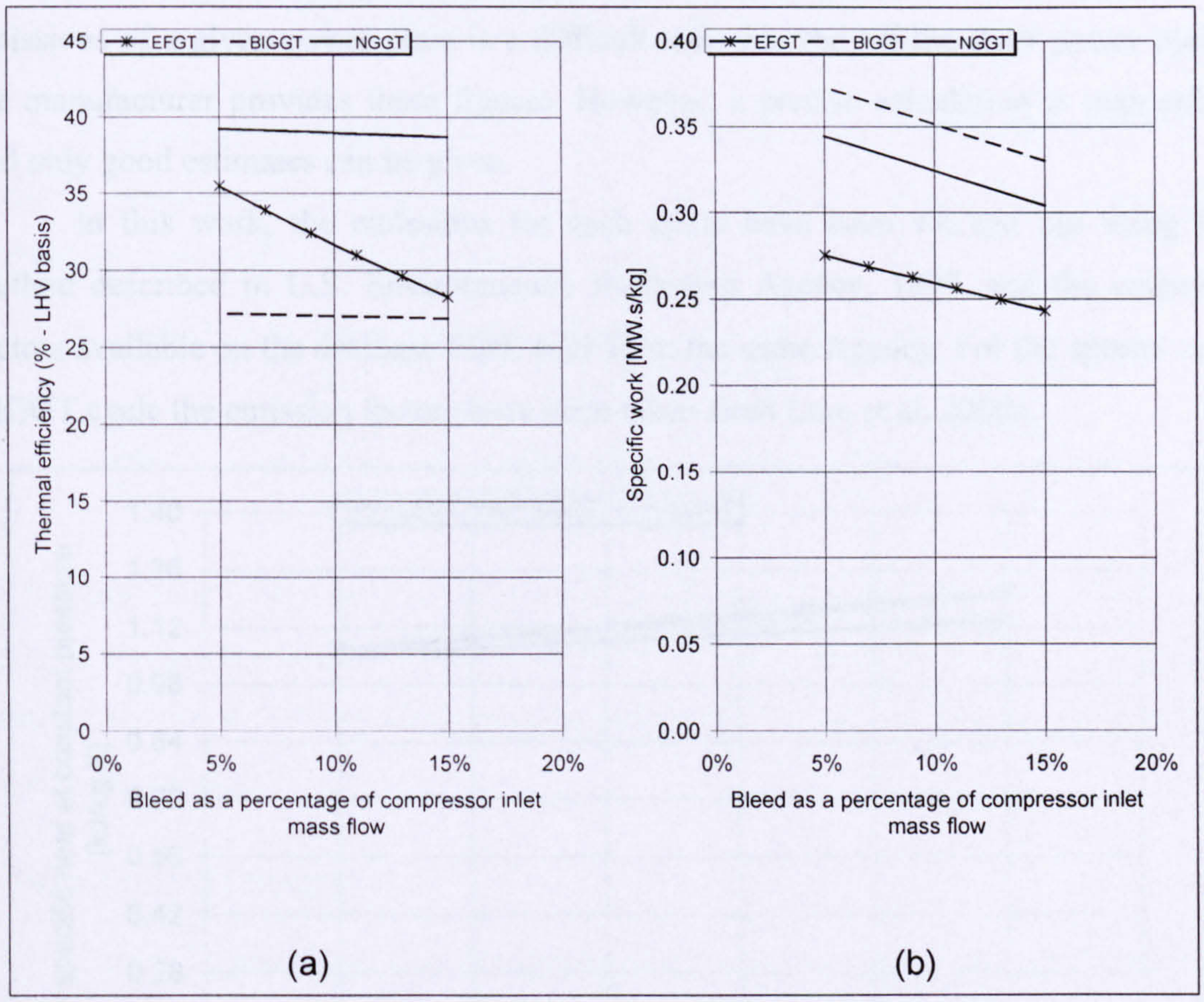

Figure 33 – Comparison of the sensitivity to bleeding between NGGT, BIGGT, and EFGT engines: (a) thermal efficiency and (b) specific work

In Figure 33 (b) the sensitivity to bleeding of those cycles regarding changes in specific power is shown. All cycles have their specific power penalised by the mixing of air bled from the compressor and the after-combustor flow. The EFGT engine suffers has a larger percentage decrease due to its already low specific power, fact explained by the smaller mass flow being expanded in its turbine, compared to the other two cycles.

It is worth pointing out that, due to the cleanness of the air going into the expander, the EFGT is likely to need less bleeding for cooling than the normal gas turbine engine.

The emissions issue

One of the major concerns involving the development of a new power plant is the amount of pollutants generated due to combustion. The accurate estimate of the emissions of a given power plant is a difficult task. For the off-the-shelf power plants the manufacturer provides these figures. However, a precise calculation is impossible and only good estimates can be given.

In this work, the emissions for each cycle have been worked out using the method described in U.S. Environmental Protection Agency, 1997, and the emission factors available on the database FIRE 6.23 from the same Agency. For the special case BIGGT cycle the emission factors have been taken from Lora et al. 2000a.

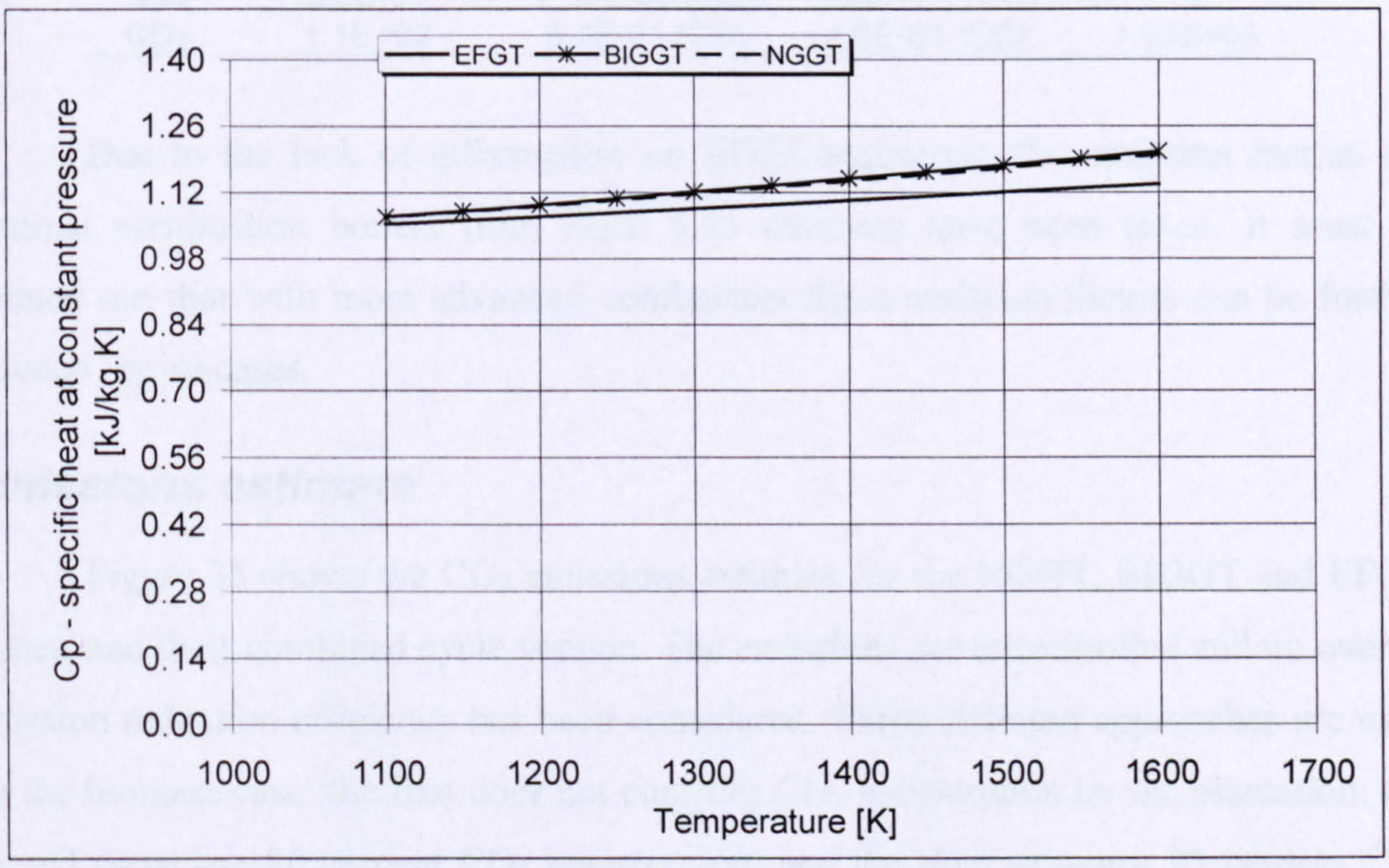

Figure 34 – Specific heat variation for the hot gases for the NGGT, BIGGT, and EFGT cases

Definition of an emission factor

An emission factor is a tool that is used to estimate air pollutant emissions to the atmosphere. It relates the quantity of pollutants released from a source to some activity associated with those emissions. The following general equation is used to estimate the emissions from a given source:

$$E = A \times EF \times \left[1 - \left(\frac{ER}{100}\right)\right] \qquad \textbf{[34]}$$

where $E \equiv$ emissions;

$A \equiv$ activity rate;

$EF \equiv$ uncontrolled emission factor;

$ER \equiv$ overall emission reduction efficiency, %.

None of the emissions calculated in this work take into consideration the overall emission reduction efficiency, i.e., $ER = 0$. The emission factors for the fuels and technology used in this thesis are shown in Table 17.

Table 17 – Emission factors for emission estimates in biomass cycles

	NGGT [lb/MBtu$_{fuel}$]	BIGGT [kg/kWh][29]		EFGT [lb/ton$_{fuel}$]
NO_x	3.2E-01	2.30E-03 (SC)	1.38E-03 (CC)	1.2
CO_2	1.1E+02	6.7E-01 (SC)	4.0E-01 (CC)	1.56E+03

Due to the lack of information on EFGT emissions, the emission factors for external combustion boilers from FIRE 6.23 database have been taken. It must be pointed out that with more advanced combustors these emission factors can be further reduced for all cases.

Emissions estimate

Figure 35 shows the CO_2 emissions estimate for the NGGT, BIGGT and EFGT cycles, and their combined cycle version. The emissions are uncontrolled and no overall emission reduction efficiency has been considered. Three different approaches are used for the biomass case: the first does not consider CO_2 reabsorption by the plantation; the second considers 80 percent CO_2 reabsorption; and the third assumes 95 percent CO_2 reabsorption.

It is clear that the BIGGT cycle has the highest CO_2 emissions when reabsorption is not considered, and the NGGT cycle has the lowest. Considering 80 percent reabsorption the two biomass fuelled simple cycles already present a much lower CO_2 emission. The reabsorption rate of 95 percent is usual in most emission analysis for biomass fuelled cycles (Lora, 2001).

[29] SC – simple cycle; CC – combined cycle

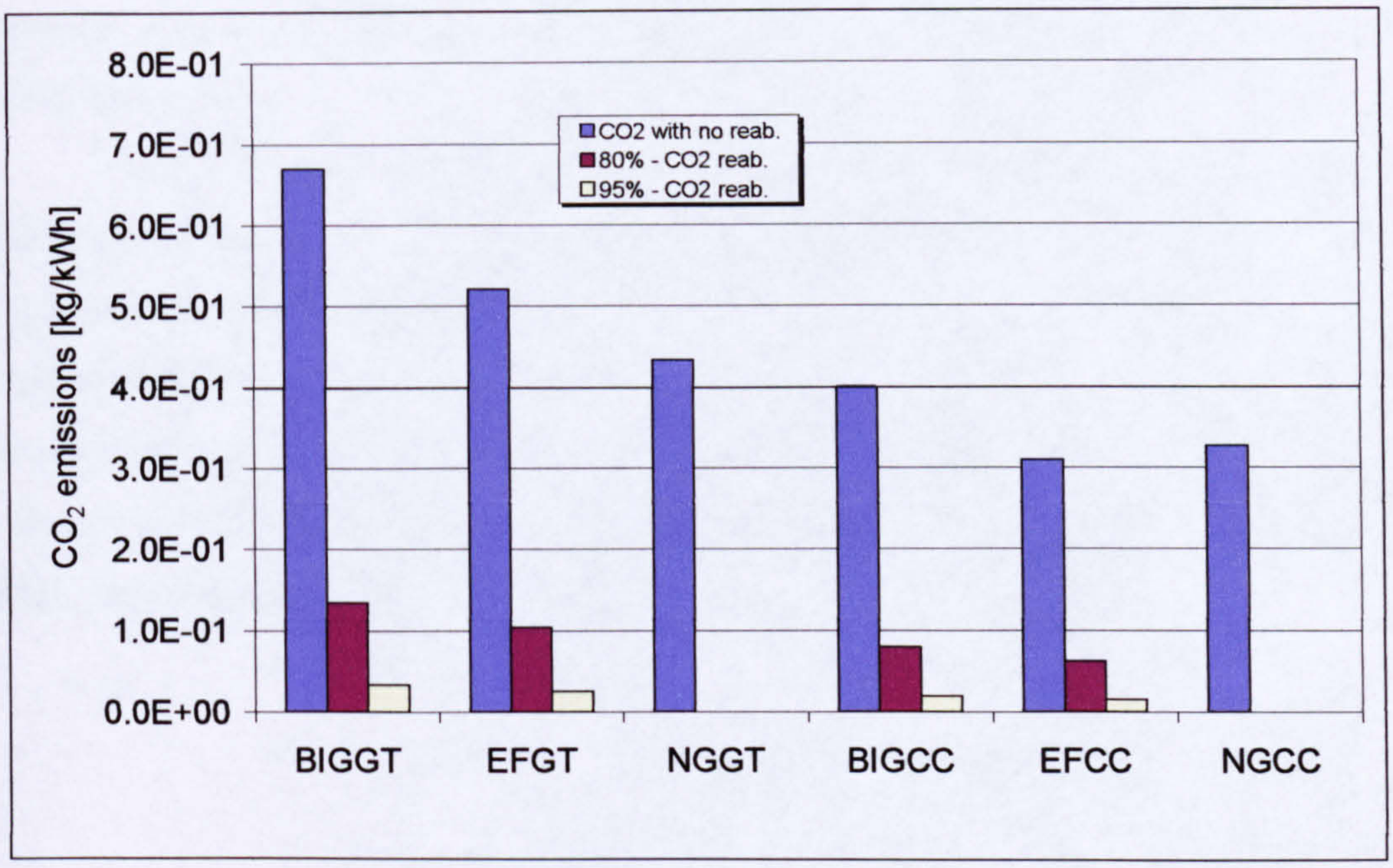

Figure 35 – CO_2 emissions estimate for NGGT, BIGGT, and EFGT cycles, and their combined cycle version

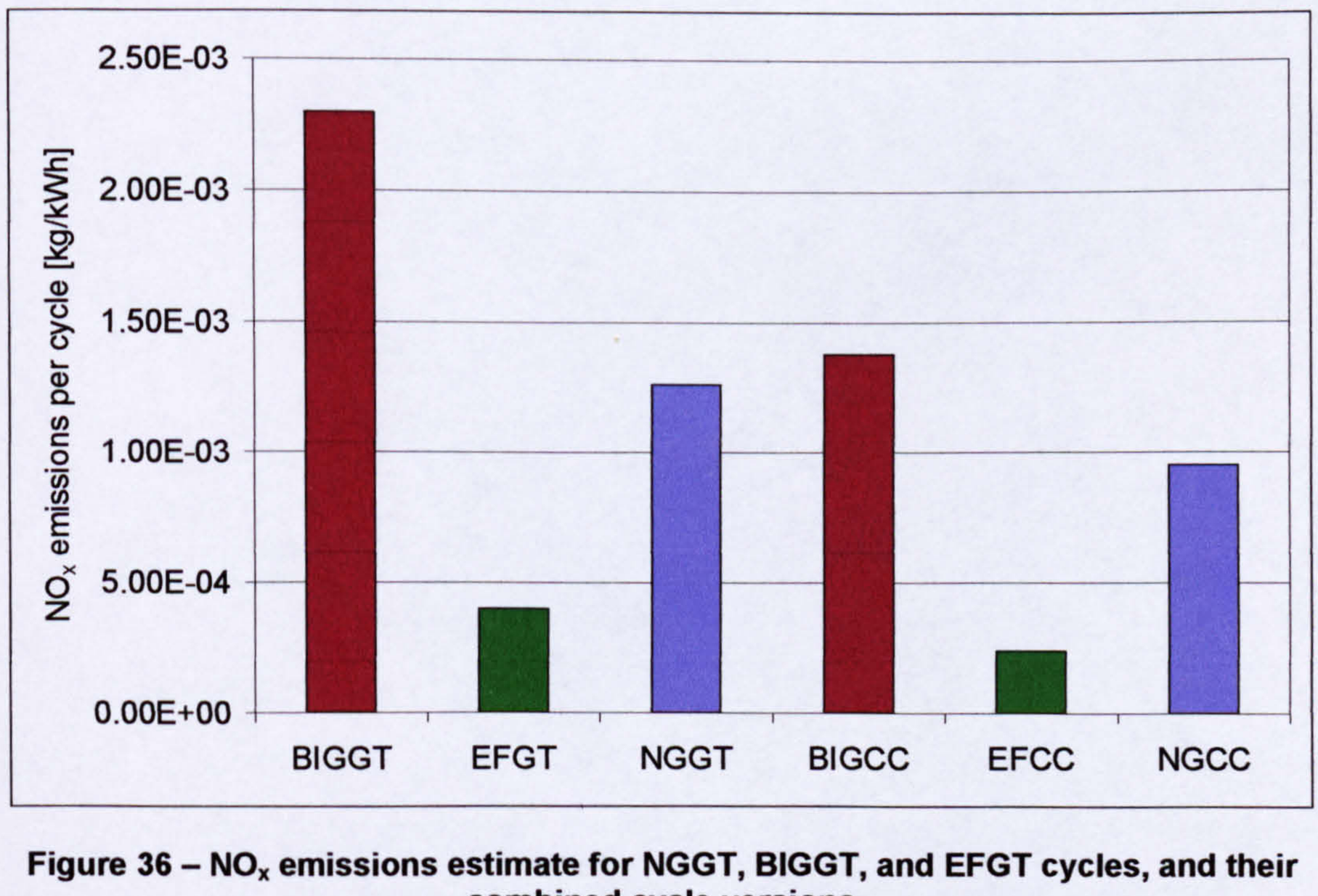

Figure 36 – NO_x emissions estimate for NGGT, BIGGT, and EFGT cycles, and their combined cycle versions

Yet in Figure 35, it is worthy of note that the externally fired combined cycle (EFCC) shows the lowest CO_2 emission of all cycles. The higher exhaust temperature explains this behaviour in the EFGT cycle compared with its counterparts, which

increases the steam cycle efficiency, and thus the overall thermal efficiency of the combined cycle.

Figure 36 shows the NO_x emissions estimate for the studied cycles and their combined cycle versions. The EFGT cycle presents the lowest NO_x emission in both simple and combined cycle. On the other hand, the BIGGT cycle shows the highest amount of NO_x emission. The emissions of NO_x for the EFGT cycle in the present work must be underestimated due to the fact that the bed temperature for the fluidised bed boiler combustor (FBC) in this case is higher than in normal steam cycle FBC, for which the emission factors were assessed.

CHAPTER IV – THE COMBIN ED CYCLE

Introduction

In order to take advantage of the heat available at the exhaust of the gas turbine, the simple cycle can be combined with another type of cycle, in which case the gas turbine is called topping cycle and the other bottoming cycle. The most common bottoming cycle is the steam cycle. In this configuration the hot gas from the turbine exhaust is redirected into a heat recovery steam generator (HRSG) where steam is raised to move a steam turbine (Figure 37).

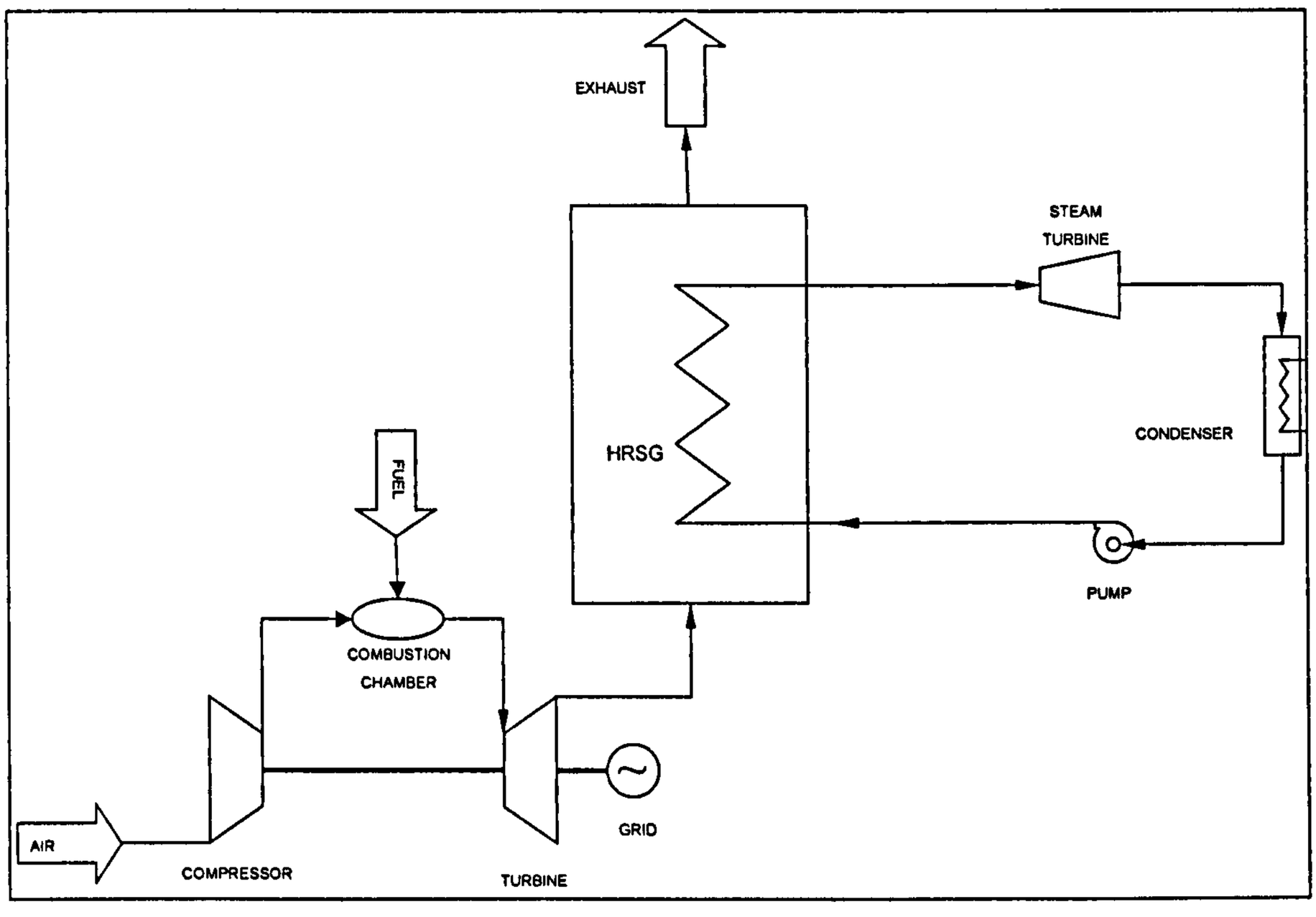

Figure 37 – Scheme of a gas trubine/combined cycle

Replacement of the water/steam with organic fluids, such as ammonia, has been suggested in the literature (Codeceira-Neto, 1999) due to potential advantages over water for low exhaust gas temperatures. However, as gas turbine exhaust temperatures increase with new developments, these advantages become marginal. Another point to be considered is the potential environmental hazard.

Although the gas turbine combined cycle was first mentioned in the 1960s (Horlock, 1995a), it was not until the 1970s that the gas turbine entry temperature, and

consequently the exhaust temperature, became high enough for combined cycle applications (Kehlhofer, R. H., Warner, J., Nielsen, H., and Bachmann, R., 1999). At that time combined cycles were built with typical electrical efficiencies of 40 percent (Bolland, 1991).

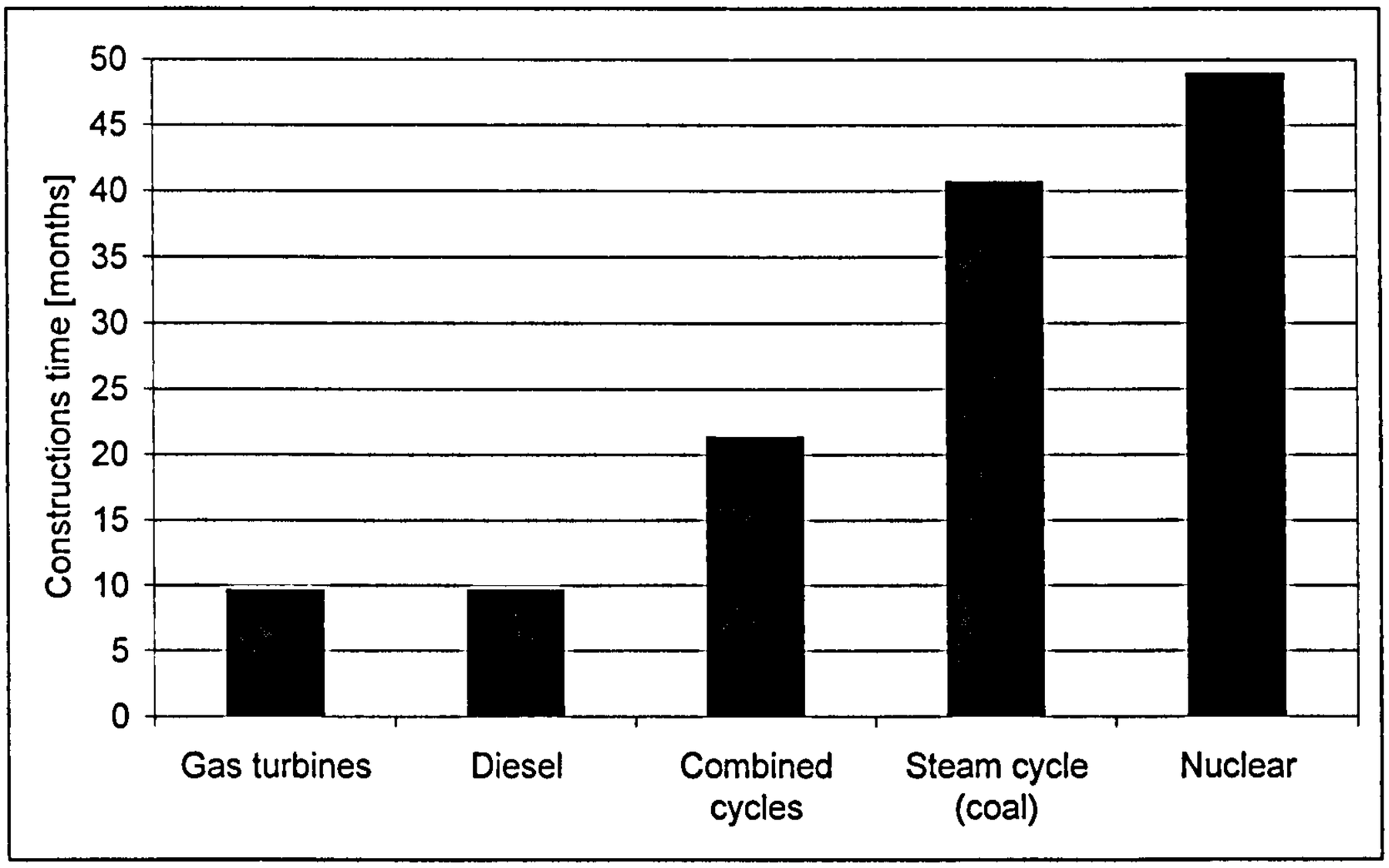

Figure 38 – Construction time for different power plants, from "notice to proceed" to "commercial operation" (Kehlhofer, R. H., Warner, J., Nielsen, H., and Bachmann, R., 1999)

The bottoming steam cycle of a combined heat and power (CHP) plant can operate basically in three different ways:

1. *As a source of heat and power*: in this mode the HRSG uses the heat available in the gas turbine exhaust and generates high-pressure steam. The steam is thus expanded in a back-pressure steam turbine, which has one or more bleedings in some of its stages to provide heat to process. In some variations, the condensed steam is also used as a heat source. The steam turbine, in its turn, also generates shaft power, which can either be used directly to move pumps, mills, etc., or an electricity generator.
2. *As a source of heat only*: the HRSG is used to raise low-pressure steam to be distributed to the manufacturing process or district heating.

3. *As source of electricity only*: in this mode, both the topping and the bottoming cycles are solely for the generation of electricity. No heat is delivered either for process or district heating.

The high efficiency, the time of construction (Figure 38), and the low emissions per MW make the combined cycles a very competitive type of power plant in current deregulated electricity markets. In this new scenario, cost is an essential factor for success, and one way to reduce costs is to increase efficiency, also contributing to the reduction of emissions.

The combined cycle for power generation only, and not the combined heat and power (CHP) version, has been chosen as the subject of this chapter due to the size of the gas turbine considered for the purposes of the present work, which make the combined cycle economically feasible.

Single pressure mode

The simplest configuration of a combined cycle is the single pressure scheme. In this cycle, the HRSG generates steam for the steam turbine at only one pressure level.

There are four main components in this cycle: gas turbine, HRSG, steam turbine, and condenser (or cooling system).

Gas turbine

The gas turbine is a key component in the combined cycle plant, contributing to approximately two thirds of the power produced. It has two roles:

1. Generate power;
2. Supply heat at its exhaust to the steam bottoming cycle.

These two tasks are contradictory in the sense that if one tries to increase the mechanical drive efficiency of a given gas turbine, the result will be a decreased heat content in the exhaust (Dechamps, 1999), as seen in the temperature-entropy (T-s) diagram of Figure 39. In order to increase efficiency, one increases the pressure ratio of the gas turbine cycle; considering the same turbine entry temperature (*TET*) the gas

turbine exhaust (T_{exh}) is decreased ($T_{exh2} < T_{exh1}$), supplying less heat to the bottoming cycle.

For power generation applications either single-shaft or two-shat units are usually specified. However, the performance of the two types at off-design is going to be quite different, regarding the combined cycle application, due to differences in the exhaust flow and temperature as load is reduced.

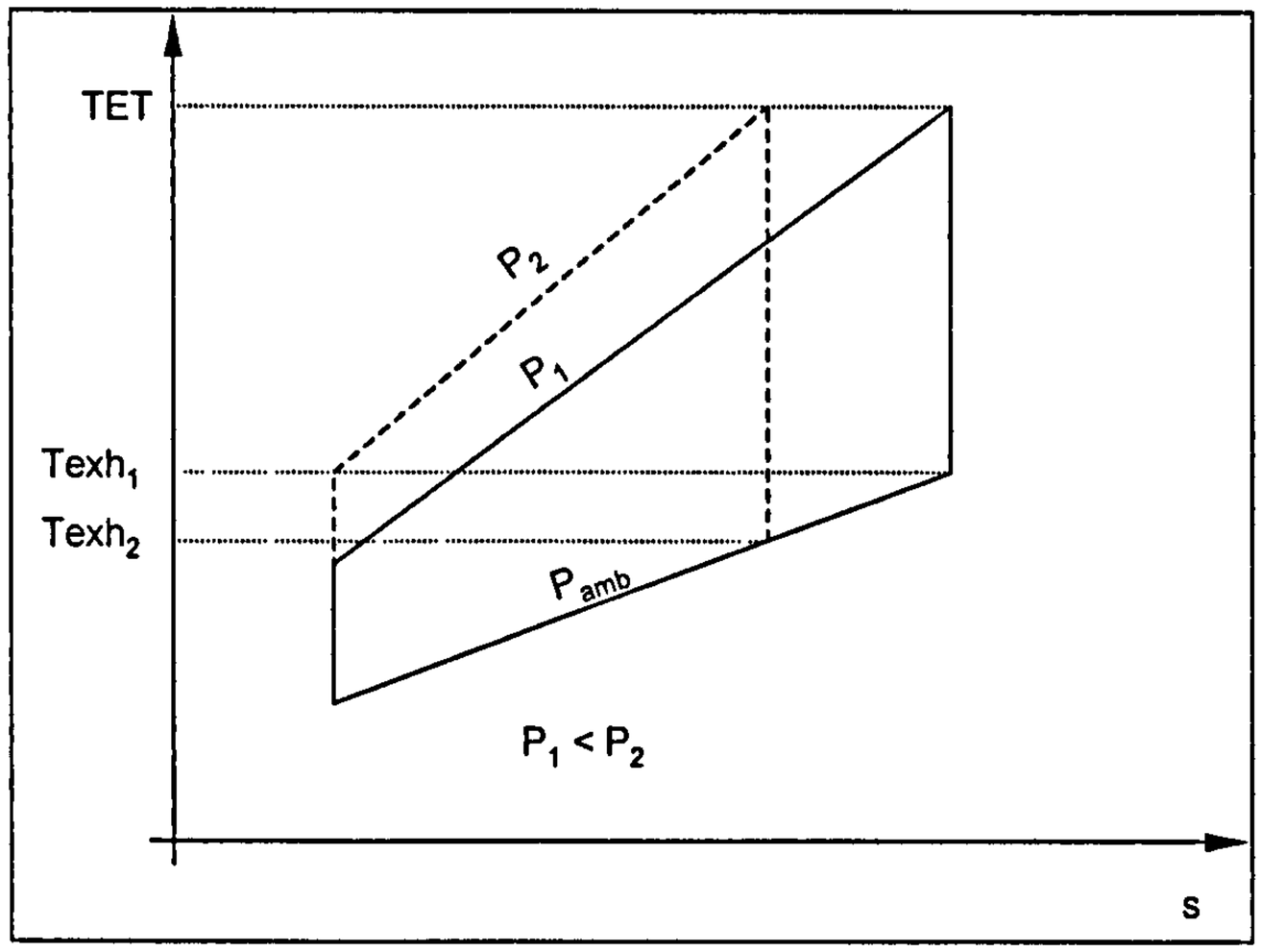

Figure 39 – T-s diagram comparing two gas turbine cycles of the same TET

The essentially constant mass flow and compressor power in a single-shaft unit result in a larger decrease of exhaust temperature for a given reduction in power that would not happen in a multi-shaft turbine, where variations are much smaller than in a single-shaft. It is worth pointing out that both single- and multi-shaft engines have been successfully used in CHP and combined cycle applications (Cohen, H., Rogers, G. F. C., and Saravanamuttoo, H. I. H., 1996).

Gas turbines with more complicated designs, including intercooler and recuperator, are not used in combined cycle applications, for these engines have low exhaust temperatures; moreover they alone present superior efficiencies when compared with simple cycles.

Gas turbine performance is well discussed in the literature and more information about this component, including detailed description of the performance of one- and multi-shaft engines, can be found in Cohen, H., Rogers, G. F. C., and Saravanamuttoo,

H. I. H., 1996, Najjar, 1997, Walsh, P. P. and Fletcher, P., 1998, and Boyce, M. P., 2001.

Heat Recovery Steam Generator (HRSG)

The HRSG consists of three sections (Figure 40):

1. *The economiser*: the feed water is heated to a temperature close to its saturation point.
2. *The evaporator*: the heated feed water is evaporated at a constant temperature and pressure in the evaporating loop. In this loop, the water and saturated steam are separated.
3. *The superheater*: the saturated steam is superheated to the desired steam temperature.

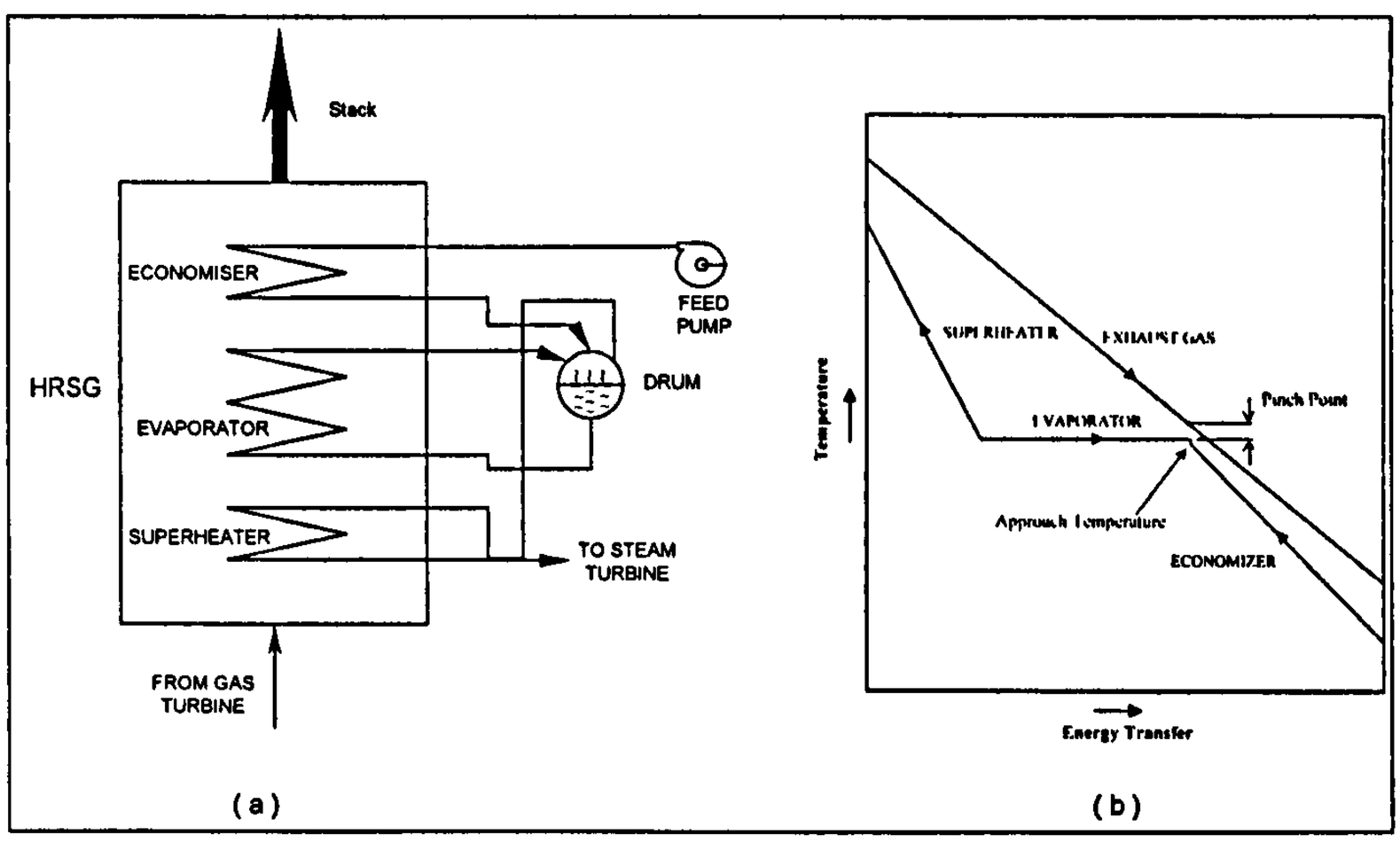

Figure 40 – (a) Diagram of single pressure HRSG and (b) heat transfer diagram for a single pressure HRSG

The more important parameters for the HRSG are:

1. The operating pressure, selected to provide the best possible heat recovery and combined cycle performance.
2. The feed water temperature, which must be sufficiently high to prevent the condensation on the HRSG tubes, avoiding corrosion.

3. The superheated steam temperature, which is limited both by the turbine limitations and the gas temperature at the turbine exhaust.
4. The superheater pinch point, which is the temperature difference between the hot gas and the superheated steam temperature.
5. The evaporator pinch point temperature difference between the gas and the saturated steam at the evaporator.
6. The approach point temperature difference, which is the saturation temperature in the evaporator and in the drum, minus the temperature of the water at the economiser outlet. Having steam in the economiser can be dangerous – salt deposition, control, stability –, for this reason the design is usually made with a safety margin of about 2 to 10°C (Dechamps, 1999).

The HRSG can be of different types such as once-through forced circulation, assisted circulation (vertical boiler), natural circulation (horizontal boiler), natural circulation (vertical boiler). For a comprehensive discussion on HRSGs, please refer to Kehlhofer, R. H., Warner, J., Nielsen, H., and Bachmann, R., 1999, Dechamps, 1999, and Ganapathy, V., 1991.

Steam turbine

The task of the steam turbine is to produce power through the expansion of superheated steam to the condensing pressure (Dechamps, 1999).

The main requirements for a modern combined cycle steam turbine are:

1. High efficiency;
2. Short start-up times;
3. Short installation times;
4. Floor-mounted installation (Kehlhofer, R. H., Warner, J., Nielsen, H., and Bachmann, R., 1999).

The first combined cycle plants used to adopt the steam turbines developed for conventional steam cycles, either as a repowering method or as an application of those. Compared with conventional steam turbines, combined cycle steam turbines have less

or no bleed, shorter start-up times, smaller power output, lower live steam pressures (100-160 bar).

The main parameters that define the steam turbine performance are:

1. The operating pressure;
2. The maximum inlet temperature;
3. The inlet mass flow;
4. The operating back-pressure;
5. The exhaust steam quality (qualities below 0.87-0.88 cause erosion problems due to droplet formation) (Dechamps, 1999).

Condenser and cooling system

The task of the condenser – essentially a heat exchanger – is to condense the steam/water mixture leaving the steam turbine exhaust. The condensed water can then be compressed with very small energy consumption.

The condenser is the heart of the cooling system, which can be classified as follows:

1. *Direct air-cooling in an air cooled condenser*: no cooling water is required; however, the power output and efficiency of the power plant are reduced due to the high vacuum levels required. This system is usually a solution for places where water is scarce or not available, or in order to minimise environmental impact to local water sources.
2. *Indirect air-cooling with a wet or hybrid cooling tower*: requires water to replace evaporation and blow-down losses. The amount of water demanded depends on the exhaust steam flow of the steam turbine.
3. *Direct water-cooling*: the water comes from a river or the sea. This system requires water in an amount 40-60 times larger than the indirect cooling. After serving as a sink, the water is returned to the water source.

Hybrid solutions can be also employed, depending on the needs of the power plant. More information on cooling systems can be found elsewhere (Dechamps, 1999, and Kehlhofer, R. H., Warner, J., Nielsen, H., and Bachmann, R., 1999).

Supplementary firing

Supplementary firing is the process of burning additional fuel with the exhaust gas from the gas turbine in order to increase power output, usually at the expense of the cycle efficiency. Supplementary firing is appropriate for HRSGs because there is usually sufficient oxygen content in the exhaust gas to act as combustion air[30]. As the turbine entry temperature (*TET*) increases, the exhaust temperature, and the need for the supplementary firing decreases. As mentioned by Dechamps, 1999, its use is more common for cogeneration applications, where the gas turbine produces power and its exhaust is used for steam generation for process heating.

Single pressure combined cycle performance

Gas turbines are the main component of combined cycles. As a general approximation these engines are responsible for two thirds of the total power output of the combined cycle. With no supplementary firing, the gas turbine – or gas turbines, for the cycle can have one or more engines – dictates the performance of the combined cycle, as it is the source of heat for the bottoming steam cycle. It is clear then that the same factors that affect the gas turbine performance will have an impact on the whole combined cycle. The main parameters to affect the combined cycle performance are:

1. Gas turbine pressure ratio (*PR*);
2. Gas turbine entry temperature (*TET*);
3. Steam pressure;
4. Ambient temperature.

---

[30] In an open cycle gas turbine with a single stage combustion, only 30-50 percent of the oxygen contained in the air is used for combustion (Kehlhofer, R. H., Warner, J., Nielsen, H., and Bachmann, R., 1999).

Gas turbine pressure ratio and gas turbine entry temperature

As described in Figure 39, PR and *TET* affect the gas turbine exhaust temperature (T_{exh}). The higher the pressure ratio the lower the T_{exh} for a constant *TET*; increasing *TET* increases T_{exh}. Thus, the effects of both *PR* and *TET* in the combined cycle performance can be summarised if one analyses the effect of T_{exh} alone, as demonstrated in equation **[35]**[31] and depicted in Figure 41:

$$T_{exh} = TET\left[1-\eta_t\left(1-PR^{\frac{\gamma}{\gamma-1}}\right)\right] \qquad \textbf{[35]}$$

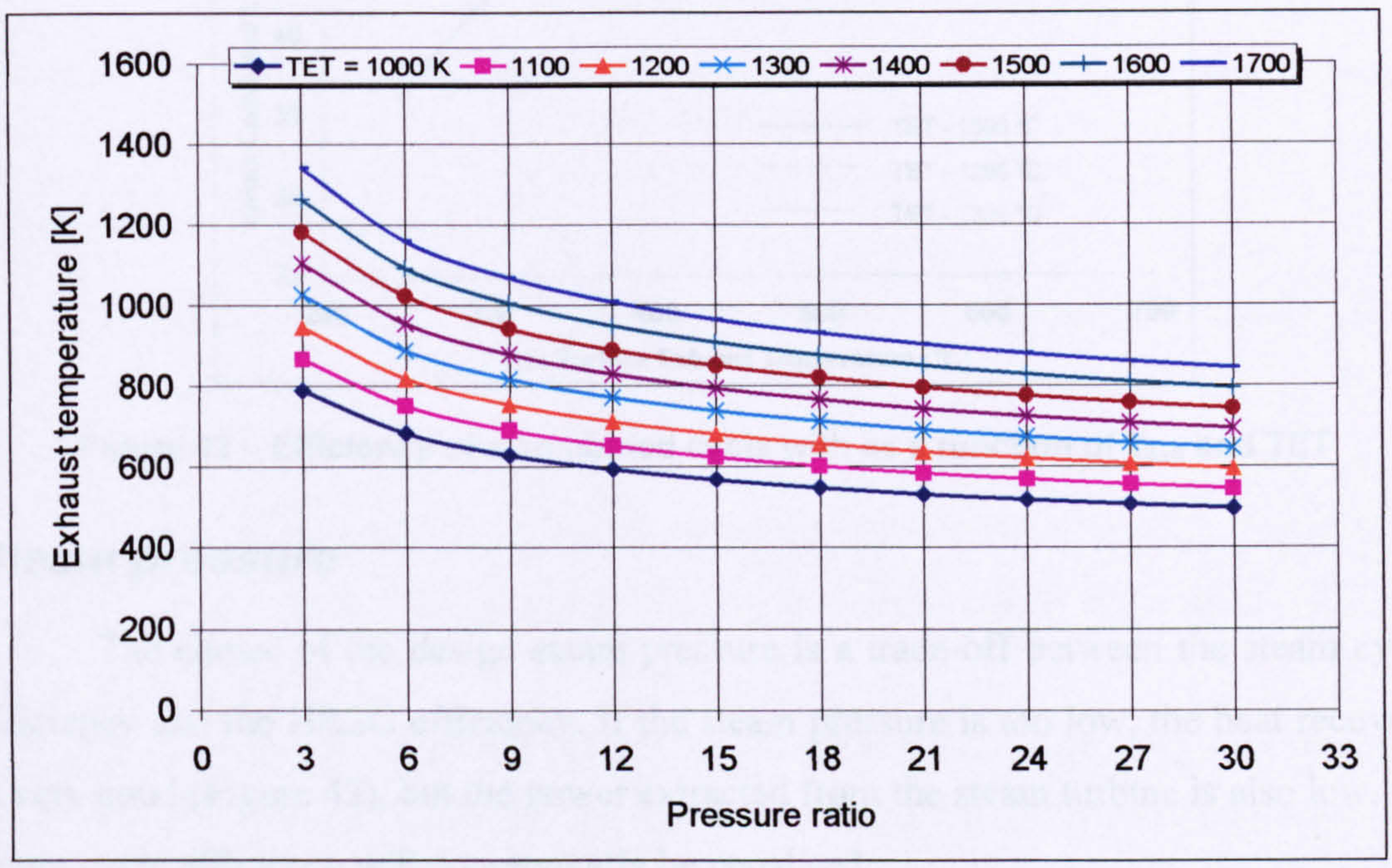

Figure 41 – Gas turbine exhaust temperature as a function of pressure ratio and *TET*

Figure 42 shows the efficiency of a single pressure combined cycle as a function of T_{exh} and *TET*. It is seen that the combined cycle efficiency increases as *TET* increases. Considering a line of constant *TET* it is seen that there is an optimum T_{exh}. This is due to the fact that in order to achieve high T_{exh} it is necessary to decrease turbine efficiency, thus from a certain value of T_{exh} the gas turbine engine efficiency overtakes the benefit of the steam cycle.

---

[31] Equation **[35]** assumes that the losses at intake, exhaust and combustor are negligible.

For economic reasons, current gas turbines are generally optimised with respect to maximum efficiency. However, quite often this optimum is not far from the optimum efficiency of the combined cycle plant. As a result, most of the gas turbines available today are optimally suited for combined cycle applications, as can be seen in Horlock, 1995b.

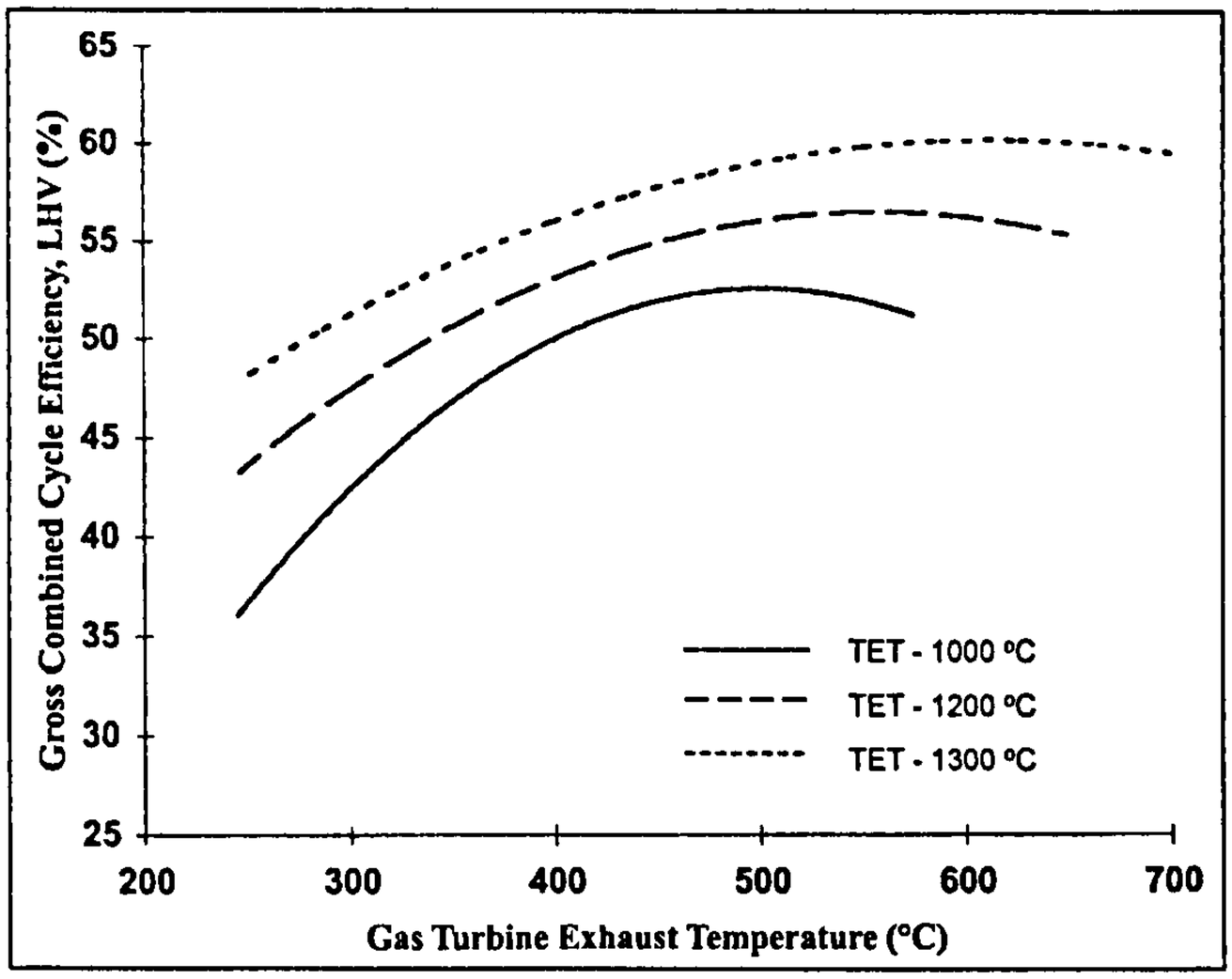

Figure 42 – Efficiency of a combined cycle with as a function of T_{exh} and TET

Steam pressure

The choice of the design steam pressure is a trade-off between the steam cycle efficiency and the HRSG efficiency. If the steam pressure is too low, the heat recovery is very good (Figure 43), but the power extracted from the steam turbine is also low, the steam cycle efficiency will consequently be penalised.

Expanding the steam from a high pressure will give high steam turbine output and good steam cycle efficiency. However, the heat recovery is poor due to the higher evaporation temperature, thus, less steam will be produced and the stack temperature will be high.

In general the total amount of live steam can also influence the optimum live steam pressure because it influences steam turbine efficiency and size. The optimum steam pressure also depends on the T_{exh}.

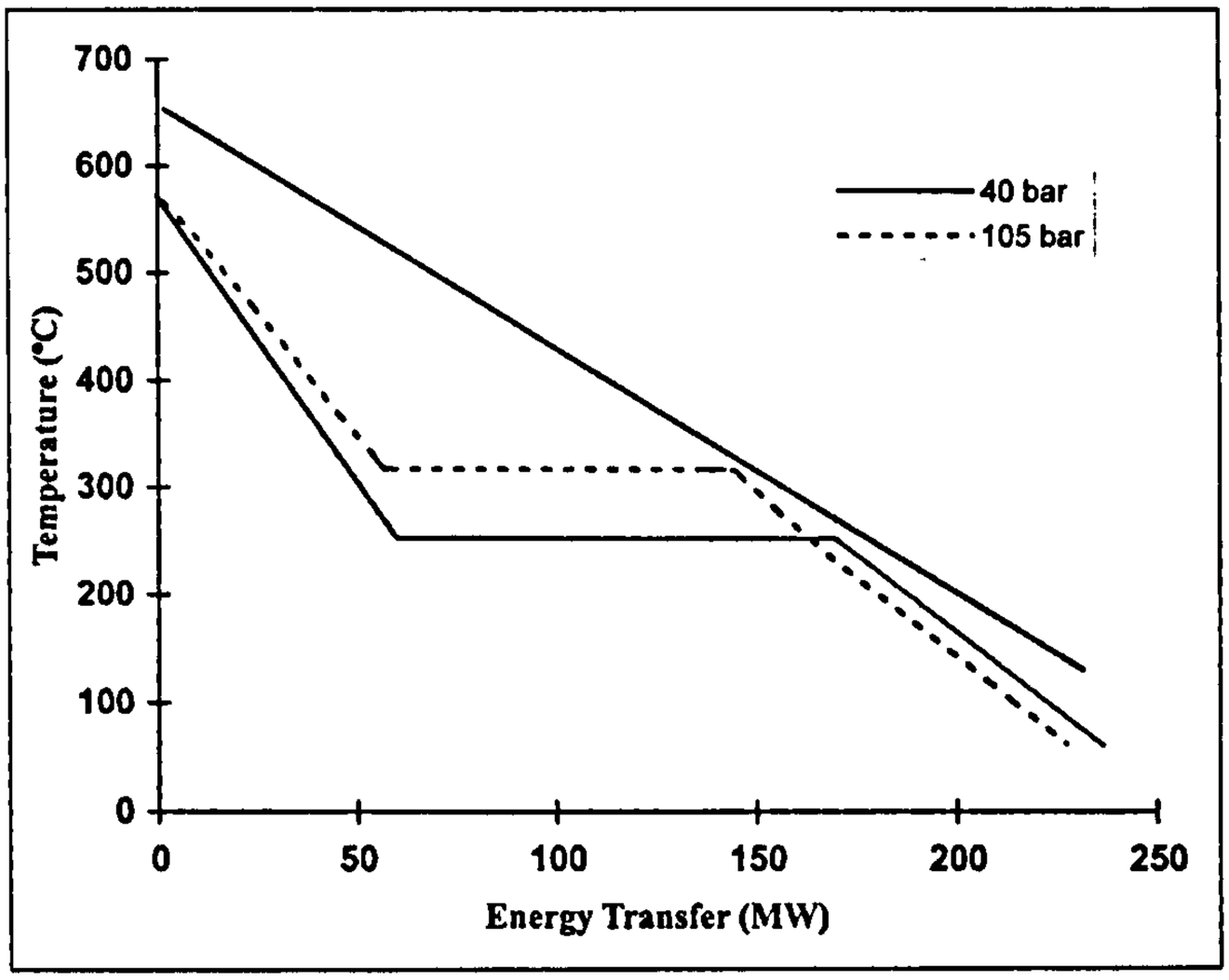

Figure 43 – Comparison between single pressure combined cycle operating at different live steam pressures

Ambient temperature

Ambient air temperature significantly affects gas turbine performance in the following ways:

1. Hot air reduces the density of the air and thereby the air mass flow contained in the given volume flow, affecting the power output for a given TET and PR.
2. The specific volume of the air increases in proportion to the intake temperature, increasing the power consumed by the compressor, without a corresponding increase in turbine output.
3. As the air temperature rises and the mass flow decreases the pressure ratio within the gas turbine is reduced.

Figure 44 (a) shows the effect of the ambient air temperature on the combined cycle efficiency, relative to design-point. It is seen that the gas turbine alone is more affected by an increase in ambient air temperature. The steam process efficiency is increased due to an increase in the compressor outlet, leading to a higher T_{exh}. This more than compensates for the low efficiency of the gas turbine, resulting in a slight enhancement in the combined cycle efficiency.

Figure 44 (b), on the other hand, shows that the gas turbine has a major role in the combined cycle regarding power output. This is because changes in mass flow of air and exhaust gases are more dominant than changes in the exhaust gas temperature (Kehlhofer, R. H., Warner, J., Nielsen, H., and Bachmann, R., 1999).

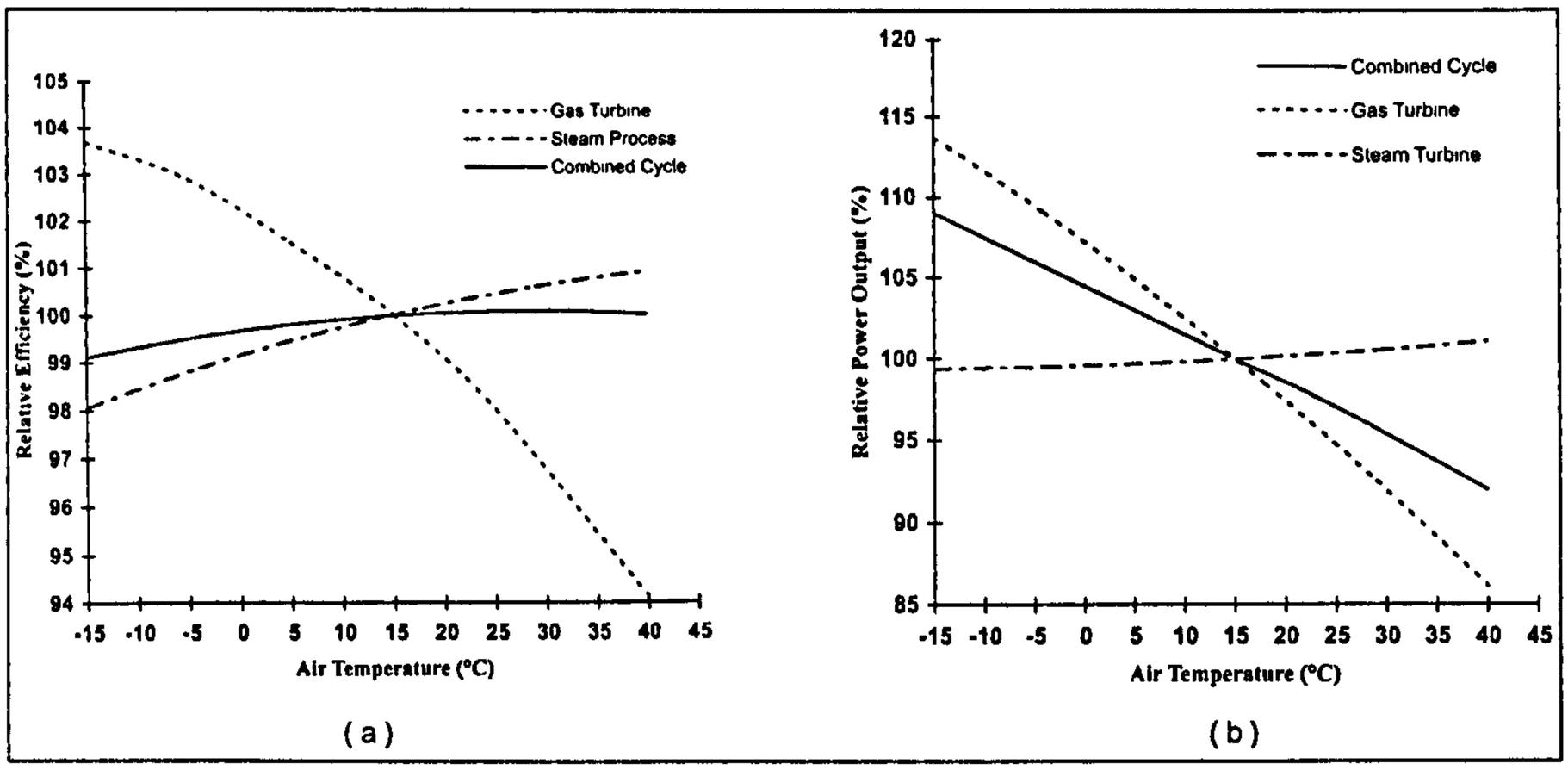

Figure 44 – Effect of the ambient air temperature on the combined cycle performance

Off-design behaviour

When a combined cycle operates without supplementary firing, the efficiency of the cycle depends very much on the gas turbine performance. There are two ways to reduce power output (Dechamps, 1995):

1. Reduce *TET* first, then close compressor variable inlet guide vanes (VIGVs);
2. Close VIGVs first, until the mass flow is reduced to 75 percent of the design value, then further reduce the gas turbine fuel flow with the VIGVs fully closed, i.e., with the air mass flow at 75 percent of its design value.

The impact of these methods is different for the gas turbine and the combined cycle. In the case of the gas turbine alone the reduction of *TET* is more suitable for a good part-load performance due to the fact that the compressor isentropic efficiency drops by around 5 percent when VIGVs are fully closed. This happens because the high pressure stages of the compressor have only a fraction of the design mass flow, as demonstrated by Dechamps, 1999.

When operating in combined cycle mode, the best way to reduce the output is to close the VIGVs first and then decrease *TET*. This change in operation is because the T_{exh} is better maintained when closing VIGVs than when reducing *TET* (Dechamps, 1995).

Figure 45 shows a comparison between the performance of the gas turbine and the combined cycle at part-load, related to their design-point performance. It is clearly seen that the efficiency of the gas turbine engine alone degrades much faster than the combined cycle.

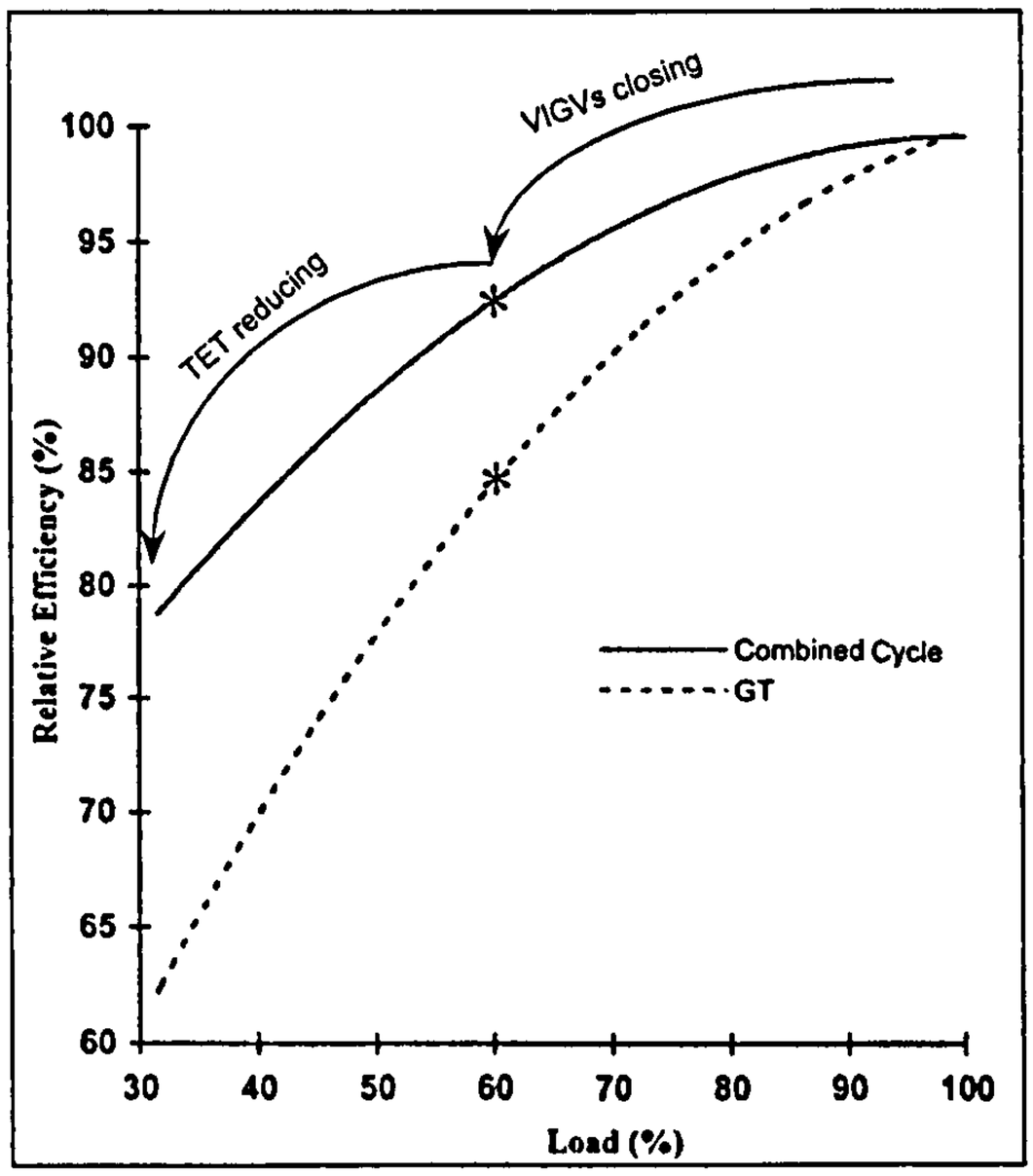

Figure 45 – Off-design efficiency for gas turbine and combined cycle (Kehlhofer, R. H., Warner, J., Nielsen, H., and Bachmann, R., 1999)

Another important parameter is the steam quality. As already mentioned this value should not be less then 0.88-0.89, otherwise erosion problems would arise. Because controlling VIGVs better maintains the gas turbine exhaust temperature, in this case when the VIGVs are fully closed the quality is even higher than that at full load.

In the *TET* control case, on the other hand, the steam quality drops continuously as soon as the output is reduced. Therefore, it is advisable to choose the design parameters of the cycle in such a way as to maintain an acceptable steam quality at part-load.

A combined cycle can have more than one gas turbine, in which case the part-load performance is controlled by shutting down one or more engines. In the case where

the power plant has four engines the following sequence is usual practice (Kehlhofer, R. H., Warner, J., Nielsen, H., and Bachmann, R., 1999):

1. Down to 75 percent → parallel reduction in load on all four gas turbines;
2. At 75 percent → one gas turbine is shut down;
3. Down to 50 percent → parallel reduction in load on the three remaining gas turbines;
4. At 50 percent → a second gas turbine in shut down; etc.

In this mode of operation, the efficiency at 75, 50, and 25 percent is lower than at full load. If there are four independent combined cycles, then the full load efficiency is maintained when one or more cycle is shut down, because the other steam turbines will be operating at full load.

It is not the aim of this work to make any further analysis on other combined cycle configurations such as dual and triple pressure. Detailed information on other configurations can be found elsewhere (Dechamps, 1995; Horlock, J. H., 1992, Dechamps, 1999, Kehlhofer, R. H., Warner, J., Nielsen, H., and Bachmann, R., 1999, and Zwebek, 2002).

CHAPTER V – THERMOECO NOMIC PRINCIPLES

Why exergy?

Energy is conserved in every device or process. It cannot be destroyed. Energy entering with fuel, electricity, streams of matter, etc., can be accounted for in the products and by-products. This is a First Law view of energy. The idea that something can be destroyed is useful. It should not be applied to energy however, but to something else. That "something" has been given the name exergy, and is derived from the Second Law of Thermodynamics.

The exergy analysis allows the identification and quantification of the losses within the cycle components, helping to arrive at a decision on which component needs the biggest enhancement. In real processes, the exergy outputs will always be less than those of the inputs because of irreversibilities and losses, which are especially significant in processes such as combustion, heat transfer (in heat exchangers), mixing, and nozzle discharge flow (Brilliant, 1995).

Defining exergy

Since two systems are at different states there is the opportunity to develop work as they are allowed to come into equilibrium. If we call one of these systems environment, **exergy**, or availability, is defined as the maximum theoretical useful work (shaft or electrical work) obtainable as the systems interact to equilibrium; heat transfer occurring with the environment only. Alternatively, exergy is the minimum theoretical useful work required to form a quantity of matter from substances present in the environment, and to bring the matter to a specific state (Bejan, A., Tsatsaronis, G., and Moran, M., 1996).

Exergy can be destroyed and generally is not conserved. A limiting case is when exergy would be completely destroyed, as would occur if a system were to come into equilibrium with the environment spontaneously with no provision to generate work (Moran et al. 1994). The capability to develop work existing initially would be completely wasted in the spontaneous process. Moreover, since no work needs to be

done to effect such a spontaneous change, we may conclude the value of exergy, $\dot{E}$, is at least zero and therefore cannot be negative. Thus:

$$\dot{E} \geq 0 \qquad \textbf{[36]}$$

Environment and dead state

Any system, such as a turbine or a pump in a power plant, operates surrounded by conditions such as temperature, pressure, humidity, etc., which are not included in the system. Inside the surroundings is the environment. In this special portion of the surroundings, which is considered large in extent and homogeneous in temperature and pressure, all parts are at rest relative to one another, and the intensive properties do not change significantly as a result of any process considered. The environment is considered free of irreversibilities.

When one or more properties – pressure, temperature, chemical composition, velocity, or elevation – of a system is different from those of the environment, there is a chance to develop work bringing the system into a state of equilibrium with the environment. There are two types of equilibrium states that are considered in exergy analysis; the restricted dead state and the true dead state. In the first case system and environment have the same temperatures and pressures, and this is called thermomechanical equilibrium. In the second case, the true dead state, beyond the thermomechanical equilibrium, there is also the chemical equilibrium.

Furthermore, related to these dead states are physical exergy, which includes mechanical exergy, thermal exergy, kinetic exergy, and potential exergy; and chemical exergy, which is made of the additional terms needed to define the work obtained in going to chemical equilibrium, after thermomechanical equilibrium is obtained (Brilliant, 1995).

Considering a system under pressure P, and temperature T and the environment at pressure P_o, and temperature T_o, the exergy of this system is:

$$\dot{E} = \dot{E}^{PH} + \dot{E}^{KN} + \dot{E}^{PT} + \dot{E}^{CH} \qquad [37]$$

where $\dot{E}$ ≡ is the total exergy rate of the system;

$\dot{E}^{PH}$ ≡ is the physical exergy;

$\dot{E}^{KN}$ ≡ is the kinetic exergy;

$\dot{E}^{PT}$ ≡ is the potential exergy;

$\dot{E}^{CH}$ ≡ is the chemical exergy of the system.

Neglecting the kinetic exergy and the potential exergy, the exergy of a system becomes:

$$\dot{E} = \dot{E}^{PH} + \dot{E}^{CH} \qquad [38]$$

The physical exergy is given by the following expression:

$$\dot{E}^{PH} = \dot{m}[(h - h_o) - T_o(s - s_o)] \qquad [39]$$

where h_o and s_o are the specific enthalpy and the specific entropy respectively, of the same material stream at temperature T_o and pressure P_o.

The molar chemical exergy of a mixture of ideal gases is calculated as a function of the molar chemical exergy of the n^{th} chemical constituent of the mixture (Tsatsaronis, 1993), as follows:

$$\bar{e}^{CH} = \sum_n x_n \bar{e}_n^{CH} + \bar{R} T_o \sum_n x_n \ln x_n \qquad [40]$$

where x_n is the mole fraction of the n^{th} substance in the mixture, $\bar{e}_n^{CH}$ is the molar chemical exergy of the n^{th} substance in the mixture, and $\bar{R}$ is universal gas constant. An

extensive discussion on chemical exergy, as well as values of chemical exergy for several chemical compounds, can be found in Kotas, T. J., 1985.

The choice of the reference state for exergy calculations is very important for the results of the exergy evaluation of a given system. The reference state and environment chosen as a basis for this work is represented in Table 18. The choice of this reference state has to do with the average ambient conditions in Brazil. A more detailed discussion on the choice of the reference state can be found in Munoz et al. 1999 and Gallo et al. 1990.

Table 18 – Environment and reference state chosen

P_o = 1.01325 bar, T_o = 298.15 K	
Substance	**Mole fraction**
Ar	0.0094
N_2	0.7790
O_2	0.2095
CO_2	0.0003
$H_2O_{(v)}$	0.0019

Standard chemical exergy of fuels

Gaseous fuels

If the chemical exergy of the component gases of a gaseous fuel is not tabulated, this value can be easily calculated by considering an idealised reaction of the substance with other reference substances for which the chemical exergy is known. Thus, considering the simple example of the reaction of a hydrocarbon, C_aH_b, with oxygen, O_2, both at T_o and P_o:

$$C_aH_b + \left(a + \frac{1}{4}b\right)O_2 \rightarrow aCO_2 + \frac{1}{2}bH_2O \qquad \textbf{[41]}$$

In this case the molar chemical exergy of the fuel, $\overline{e}_f^{CH}$, will by given by:

$$\overline{e}_f^{CH} = \overline{HHV}_{(T_o,P_o)} - T_o\left[\left(\sum x.\bar{s}\right)_r - \left(\sum x.\bar{s}\right)_p\right]_{(T_o,P_o)} + \left[\left(\sum x.\overline{e}^{CH}\right)_p - \left(a + \frac{b}{4}\right)\overline{e}_{O_2}^{CH}\right]$$

[42]

where $\overline{HHV} \equiv$ is the molar higher heating value of the fuel;

$x \equiv$ is the mole fraction of the compound;

$\bar{s} \equiv$ is the molar entropy of the compound;

r and $p \equiv$ are subscripts for reactants and products respectively.

In this thesis; however, due to the large amount of gaseous species present in gasified biomass, the calorific value of such fuel – the lower heating value(*LHV*) and the higher heating value (*HHV*) – is calculated as follows:

$$C_a H_b O_d N_e Ar_f S_g + O_2 \Rightarrow \beta CO_2 + \gamma H_2O_{(v)} + \psi N_2 + \varepsilon SO_2 + \varphi Ar \qquad \textbf{[43]}$$

The enthalpy of reaction at the standard state (P_o = 1 atm, T_o = 298.15 K) is equal to the difference between the enthalpies of the reactants and products measured at the standard state (Saad, M., 1997):

$$\Delta H^0 = \left(\sum_i \nu_i \bar{h}_i^0\right)_p - \left(\sum_i \nu_i \bar{h}_i^0\right)_r \qquad \textbf{[44]}$$

where $\Delta H^0 \equiv$ enthalpy of reaction;

$\bar{h}^0 \equiv$ enthalpy of formation per mole;

$\nu \equiv$ number of moles of a component. The subscripts p and r stand for products and reactants, respectively.

A negative value of ΔH^0 means that the process is exothermic, which is typical in combustion processes.

The heating value of a fuel is numerically equal to the enthalpy of combustion, but has opposite sign. The *HHV* is obtained when all the water vapour in the products is condensed at the reference temperature, T_o. When the water is in the vapour state, the *LHV* is obtained.

The standard chemical exergy of a mixture of gases is calculated as described earlier (equation **[40]**). For a gaseous fuel, the chemical exergy is calculated using the following formula (Bejan, A., Tsatsaronis, G., and Moran, M., 1996):

$$\overset{-CH}{e} = -\Delta G + \left\{ \sum_{p} n\overset{-CH}{e} - \sum_{r} n\overset{-CH}{e} \right\} \qquad \textbf{[45]}$$

where $\Delta G \equiv$ the change in Gibbs function for the reaction, regarding each substance as separate at temperature T_o and pressure p_o;

$n \equiv$ moles of reactants (r) and products (p) per mole of substance whose chemical exergy is being evaluated.

Solid fuels

The chemical exergy of solid fuels can be calculated using the method presented by Kotas, T. J., 1985. For dry organic substances contained in solid fossil fuels consisting of C, H, O, and N, with a mass ratio of oxygen to carbon of less than 0.667, the following expression was obtained in terms of mass ratios:

$$\varphi_{dry} = 1.0437 + 0.1882\frac{h}{c} + 0.0610\frac{o}{c} + 60.0404\frac{n}{c} \qquad \textbf{[46]}$$

where c, h, o, and n are the mass fractions of C, H, O, and N, respectively. Within the restriction regarding the upper limit of $\frac{o}{c}$, equation **[46]** is applicable to a wide range of industrial solid fuels, but not to wood. The accuracy of the expression is estimated to be better than ±1 percent (Kotas, T. J., 1985).

For fuels with the mass ratio $2.67 > \frac{o}{c} > 0.667$, which includes wood, equation **[46]** becomes:

$$\varphi_{dry} = \frac{1.0438 + 0.1882\frac{h}{c} - 0.2509\left(1 + 0.7256\frac{h}{c}\right) + 0.0383\frac{n}{c}}{1 - 0.3035\frac{o}{c}} \qquad \textbf{[47]}$$

This expression, which will be used throughout this thesis, is estimated to be accurate to within ±1 percent (Kotas, T. J., 1985).

Finally, the standard chemical exergy of the solid fuel becomes (Kotas, T. J., 1985):

$$e^{CH} = \varphi_{dry}\left(LHV + 2442w\right) + 9417s \qquad \textbf{[48]}$$

where e^{CH} ≡ is the chemical exergy of a solid fuel, [kJ/kg];

LHV ≡ is the lower heating value of the fuel, [kJ/kg];

w ≡ is the mass fraction of moisture in the fuel;

s ≡ is the mass fraction of sulphur in the fuel.

Equation **[48]** accounts for the presence of moisture and sulphur, considered as a free element.

The value of chemical exergy for several chemical compounds can be found in Kotas, T. J., 1985.

Exergy destruction and exergy loss ratios

Two important parameters in exergy analysis are the rates of exergy destruction ($\dot{E}_D$) and exergy loss ($\dot{E}_L$). Those two variables provide thermodynamic measures of the system inefficiencies. Related to these measures, respectively, are the exergy destruction ratio (y_D)and the exergy loss ratio (y_L).

The exergy destruction is always equal to the product of entropy generation and the temperature of the surroundings. Thus:

$$\dot{E}_D = T_o \dot{S}_{gen} \qquad \textbf{[49]}$$

where T_o is the surroundings temperature and $\dot{S}_{gen}$ is the entropy generation, which is the difference of entropy, $\Delta \dot{S}$, in a given component. Or:

$$\dot{E}_D = \sum_{i}^{n} \dot{m}_i e_i - \sum_{e}^{n} \dot{m}_e e_e \qquad \textbf{[50]}$$

where $\dot{m}$, is the mass flow of stream "*i*" or "*e*" (the indexes "*i*" and "*e*" stand for inlet and outlet respectively), e is the stream specific exergy, and n is the number of streams of a component.

For a system consisting of n subsystems, e.g. a power plant, the total exergy destruction ($\dot{E}_{D,tot}$), is equal to the sum of exergy destruction in all subsystems, or system components, $E_{D,k}$, $k = 1,\ldots,n$ (Tsatsaronis, 1993):

$$\dot{E}_{D,tot} = \sum_{k=1}^{n} \dot{E}_{D,k} \qquad [51]$$

A change in exergy destruction in one subsystem, in general, affects the exergy destruction in other subsystems too.

Since the total energy is conserved in an energy balance, there is no First Law analogous to exergy destruction. The exergy destruction represents the real energy waste that cannot be identified through an energy balance (Tsatsaronis, 1993). Thus, it can be said that the First Law quantifies energy and the Second Law, through exergy, qualifies energy.

The rate of exergy destruction in a system component can be compared with the exergy rate of the fuel provided to the overall system, $E_{f,tot}$, giving the exergy destruction ratio:

$$y_D = \frac{\dot{E}_D}{\dot{E}_{f,tot}} \qquad [52]$$

The exergy loss ratio is defined similarly to the exergy destruction ratio comparing the loss to the exergy of the fuel provided to the overall system, thus:

$$y_L = \frac{\dot{E}_L}{\dot{E}_{f,tot}} \qquad [53]$$

The exergy efficiency

Exergy efficiency is a very important variable that helps to determine how effectively the exergy input in a component or power plant is being transformed into

useful work. There are several approaches to calculating exergy efficiency; for example, one approach defines exergy efficiency as the ratio of the sum of the exergy exiting to the sum of the exergy entering; appropriate only for steady state devices. Another approach is that of task efficiencies. Task efficiency is the ratio of the theoretical minimum input required by the First and Second Laws to accomplish a given task to the actual input for a particular means.

In this work the exergy efficiency (ε) is given by:

$$\varepsilon = \frac{\dot{E}_p}{E_f} = 1 - \frac{\dot{E}_D + \dot{E}_L}{\dot{E}_f} \qquad \textbf{[54]}$$

where E_f is the "fuel" exergy rate and $\dot{E}_p$ is the product exergy rate.

The Second Law efficiency (or exergy efficiency) gives a finer understanding of performance than thermal efficiency (η). In computing η, the same weight is assigned to energy whether it is shaft work or a stream of low temperature fluid. Furthermore, it centres attention on reducing losses to improve efficiency. The parameter ε weighs energy flows by accounting for each in terms of exergy, or availability. It stresses that both losses and internal irreversibilities need to be dealt with to improve performance. In many cases it is the irreversibilities that are more significant and the more difficult to deal with (Moran, M., 1982).

For a more comprehensive discussion on the several exergy efficiency methods refer to Moran, M., 1982, Szargut, 2000, and Kotas, T. J., 1985.

Components exergy efficiencies

This section brings out the exergy efficiency related to some power plant components such as the compressor, pump, turbine, gasifier and combustion chamber, and heat recovery steam generator (HRSG) (Table 19).

Compressor and pump

The purpose of these devices is to increase the flow rate of exergy from inlet to outlet using mechanical or electrical power ($\dot{W}$), so that, in this case:

$$\dot{E}_p = E_2 - E_1 \text{, and } \dot{E}_f = \dot{W} \qquad \textbf{[55]}$$

Hence, according to the definition adopted for exergy efficiency:

$$\varepsilon = \frac{\dot{E}_2 - E_1}{\dot{W}} \qquad \textbf{[56]}$$

Turbine

The purpose of this device is to generate power ($\dot{W}$) by decreasing the flow rate of exergy from inlet to outlet, hence:

$$\dot{E}_p = W \text{, and } \dot{E}_f = \dot{E}_1 - \dot{E}_2 \qquad \textbf{[57]}$$

Thus:

$$\varepsilon = \frac{\dot{W}}{\dot{E}_1 - \dot{E}_2} \qquad \textbf{[58]}$$

Gasifier and combustion chamber

The purpose of the combustion reaction in the chamber is, primarily, to increase the thermal exergy difference between the reaction products and the reactants at the expense of chemical exergy of the fuel (Tsatsaronis, 1993). Thus:

$$E_p = \dot{E}_3 \text{, and } \dot{E}_f = \dot{E}_1 + \dot{E}_2 \qquad \textbf{[59]}$$

And:

$$\varepsilon = \frac{\dot{E}_3}{\dot{E}_2 + \dot{E}_1} \qquad \textbf{[60]}$$

Heat recovery steam generator (HRSG)

This device is intended to increase the exergy rate between inlet and outlet for the feedwater/steam stream, using heat released by exhaust gases from a gas turbine as input of exergy. Hence:

$$E_p = \left(\dot{E}_4 - \dot{E}_3 \right) + \left(\dot{E}_6 - \dot{E}_5 \right), \text{ and } \dot{E}_f = \dot{E}_1 - \dot{E}_2 \qquad \textbf{[61]}$$

And:

$$\varepsilon = \frac{\left(\dot{E}_4 - E_3 \right) + \left(E_6 - \dot{E}_5 \right)}{E_1 - \dot{E}_2} \qquad \textbf{[62]}$$

Heat exchangers

Depending on the purpose of the heat exchanger its product and fuel will vary accordingly, so its exergy efficiency can be defined in different ways (Bejan, A., Tsatsaronis, G., and Moran, M., 1996). For the purpose of this thesis the following definition will be used:

The purpose of the heat exchanger approach is to increase the exergy of a cold stream at the expense of the exergy of a hot stream, assuming the heat transfer occurs above T_o (Table 19). Thus:

$$\dot{E}_p = \dot{E}_2 - \dot{E}_1 \text{ and } \dot{E}_f = \dot{E}_3 - \dot{E}_4 \qquad \textbf{[63]}$$

And:

$$\varepsilon = \frac{\dot{E}_2 - \dot{E}_1}{\dot{E}_3 - \dot{E}_4} \quad \text{(heat exchanger; } T_1 \geq T_o\text{)} \qquad \textbf{[64]}$$

Table 19 – Exergy rates associated with fuel and product for selected components at steady state (Bejan, A., Tsatsaronis, G., and Moran, M., 1996)

Component	Comp., pump or fan	Turbine or expander	Combustion chamber	Heat exchanger	HRSG
Schematic	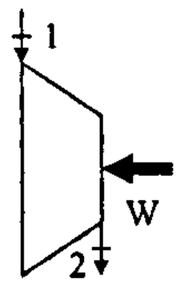	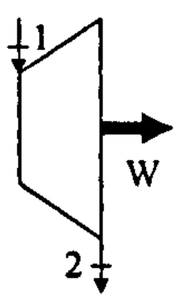	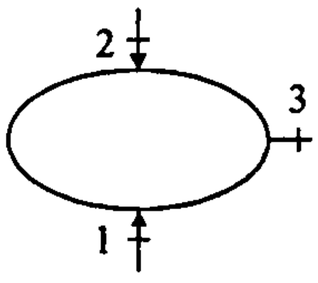	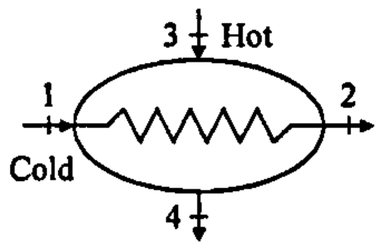	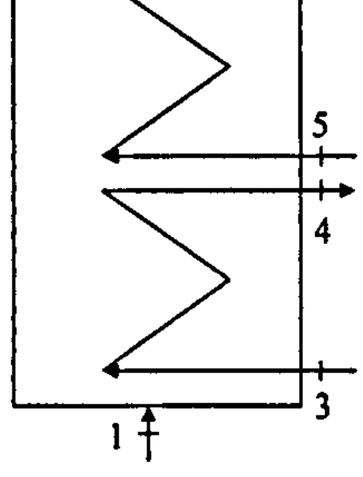
Exergy rate of product, $\dot{E}_p$	$\dot{E}_2-\dot{E}_1$	$\dot{W}$	$\dot{E}_3$	$\dot{E}_2-\dot{E}_1$	$\left(\dot{E}_4-\dot{E}_3\right)+\left(\dot{E}_6-\dot{E}_5\right)$
Exergy rate of fuel, E_f	$\dot{W}$	$\dot{E}_1-\dot{E}_2$	$\dot{E}_1+\dot{E}_2$	$\dot{E}_3-\dot{E}_4$	$\dot{E}_1-\dot{E}_2$

The thermoeconomic analysis method chosen is that proposed by Bejan, A., Tsatsaronis, G., and Moran, M., 1996. Given the cost related to each piece of equipment and the cost of fuel, it is possible to build a system of linear equations, the solution of which produces the cost of each cycle stream.

The use of the relative cost difference – which expresses the relative increase in the average cost per exergy unit between fuel and product of a component, and the exergoeconomic factor – provides the relative significance of each kind of cost source, and will aid in the plant optimisation at component level.

Exergy costing

In a conventional economic analysis a cost balance is usually formulated for the overall system operating at steady state:

$$\dot{C}_{p,tot} = \dot{C}_{f,tot} + \dot{Z}^{CI}_{tot} + \dot{Z}^{OM}_{tot} \qquad \textbf{[65]}$$

expressing the fact that the cost rate associated with the product of the system ($\dot{C}_{p,tot}$) equals the total rate of expenditures made to generate the product, that is, the fuel cost rate ($\dot{C}_{f,tot}$) and the cost rates associated with capital investment ($\dot{Z}_{tot}^{CI}$), and the operating and maintenance cost ($\dot{Z}_{tot}^{OM}$).

In exergy costing a cost is associated with exergy stream. Thus, for entering and exiting streams of matter with associated rates of exergy transfer ($\dot{E}_i$ and $\dot{E}_e$), power ($\dot{W}$), and exergy transfer rate associated with heat transfer ($\dot{E}_q$), are written:

$$\dot{C}_i = c_i \dot{E}_i = c_i \left(\dot{m}_i e_i \right) \quad \textbf{[66]}$$

$$\dot{C}_e = c_e \dot{E}_e = c_e \left(\dot{m}_e e_e \right) \quad \textbf{[67]}$$

$$\dot{C}_w = c_w \dot{W} \quad \textbf{[68]}$$

$$\dot{C}_q = c_q \dot{W} \quad \textbf{[69]}$$

where c_i, c_e, c_w, and c_q are the average costs per unit of exergy in monetary units per unit of energy; in the present work, dollars per gigajoule ($/GJ).

An exergy cost balance applied to the *k*th component in a system would have the form:

$$\sum_e \left(c_e \dot{E}_e \right)_k + c_{w,k} \dot{W}_k = c_{q,k} \dot{E}_{q,k} + \sum_i \left(c_i \dot{E}_i \right)_k + \dot{Z}_k \quad \textbf{[70]}$$

where

$$\dot{Z}_k = \dot{Z}_k^{CI} + \dot{Z}_k^{OM} \quad \textbf{[71]}$$

The exergy rates exiting and entering the *k*th component are calculated using the exergy analysis explained earlier in this chapter. The element $\dot{Z}_k$ is obtained by first calculating the capital investment and O&M costs associated with the *k*th component

and then computing the levelised values[32] of these costs per unit of time of system operation.

Figure 46 shows a comparison between energy and exergy costing for a steam turbine exhaust. It is seen in the exergy costing curve that the high-pressure (high-temperature) steam is valued more highly per unit of mass than low-pressure (low-temperature) steam. Moreover, the cost per unit of mass rapidly approaches zero as the thermodynamic usefulness of the steam (the quality of the energy contained in the steam) approaches zero. The curve based on energy costing, on the other hand, does not take into consideration the quality of the energy contained in the exhaust steam.

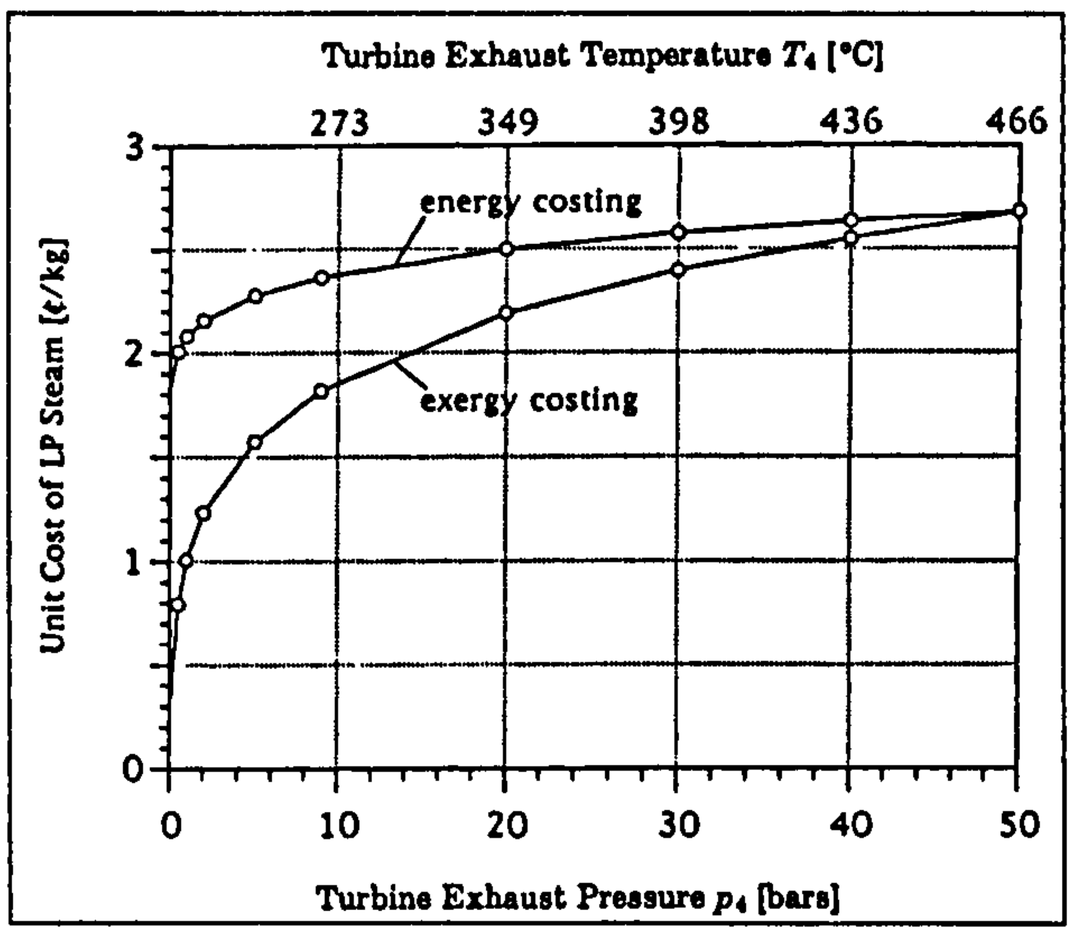

Figure 46 – Cost of low-pressure steam per unit of mass as a function of the turbine exhaust conditions (Bejan, A., Tsatsaronis, G., and Moran, M., 1996)

Table 20 shows the cost rate balances for all the relevant devices for this thesis. As a rule, $n-1$ auxiliary relations are needed for components with n exiting exergy streams.

Relative cost difference

The relative cost difference expresses the relative increase in the average cost per exergy unit between fuel and product of the component, and is given by the following expression:

[32] Details on the economic evaluation are discussed later in Appendix B.

$$r_k = \frac{c_{p,k} - c_{f,k}}{c_{f,k}} \qquad [72]$$

Table 20 – Cost rates associated with fuel and product as well as auxiliary thermoeconomic realtions for selected components (Bejan, A., Tsatsaronis, G., and Moran, M., 1996)

Component	Comp., pump or fan	Turbine or expander	Combustion chamber	Heat exchanger	HRSG
Schematic	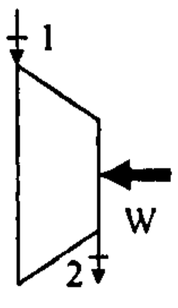	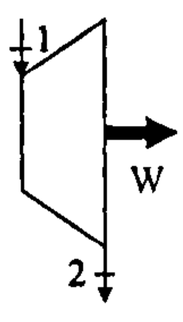	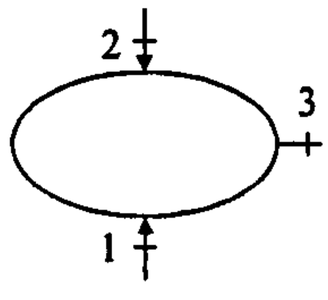	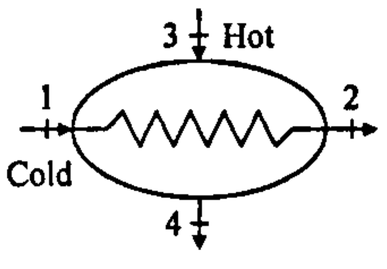	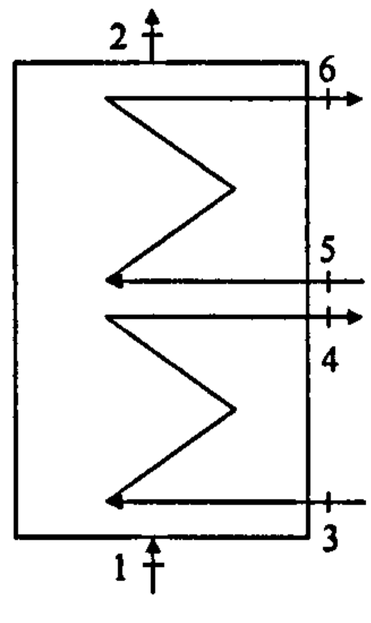
Cost rate of product, $\dot{C}_p$	$\dot{C}_2 - \dot{C}_1$	$\dot{C}_w$	$\dot{C}_3$	$\dot{C}_2 - \dot{C}_1$	$\left(\dot{C}_4 - \dot{C}_3\right) + \left(\dot{C}_6 - \dot{C}_5\right)$
Exergy rate of fuel, $\dot{C}_f$	$\dot{C}_w$	$\dot{C}_1 - \dot{C}_2$	$\dot{C}_1 + \dot{C}_2$	$\dot{C}_3 - \dot{C}_4$	$\dot{C}_1 - \dot{C}_2$
Auxiliary relations	None	$c_2 = c_1$	None	$c_3 = c_4$	$\frac{\dot{C}_6 - \dot{C}_5}{\dot{E}_6 - \dot{E}_5} = \frac{\dot{C}_4 - \dot{C}_3}{\dot{E}_4 - \dot{E}_3}$
Variable calculated from cost balance	c_2	c_w	c_3	c_2	c_4 or c_6

Exergoeconomic factor

The exergoeconomic factor states the importance of each cost source of a given component within a system, and is expressed as follows:

$$f_k = \frac{\dot{Z}_k}{\dot{Z}_k + c_{f,k}\left(\dot{E}_{D,k} + \dot{E}_{L,k}\right)} \qquad [73]$$

A low value of the exergoeconomic factor calculated for a major component suggests that cost savings in the entire system might be achieved by improving the component efficiency (reducing exergy destruction) even if the capital investment for this component will increase. On the other hand, a high value of this factor suggests a decrease in the investment costs of this component at the expense of its exergetic efficiency. Typical values of f_k are:

1. $f < 55\%$ for heat exchangers;
2. $35\% > f > 55\%$ for compressors and turbines;
3. $f > 70\%$ for pumps (Bejan, A., Tsatsaronis, G., and Moran, M., 1996).

Aggregation level

The level at which the cost balances are formulated affects the results of a thermoeconomic analysis. In thermal design it is recommended that the lowest possible aggregation level be used, i.e., the components should be analysed individually. Depending on the component, it may even be appropriate to distinguish between the various processes taking place within the component (Bejan, A., Tsatsaronis, G., and Moran, M., 1996).

Components costs

The equations for the compressor **[74]**, combustor **[75]**, and expander **[76]** costs are based on Bejan, A., Tsatsaronis, G., and Moran, M., 1996. However the coefficients for each equation have been changed, using the regression analysis tool in Excel®, in order to approximate the gas turbine purchase costs given by Farmer, 1999, such that the coefficients would fit the average curve in Figure 47. An error of 16% is found for the power range used in the present work.

This method has been applied also by Massardo et al. 2000 and Agazzani et al. 1997a for thermoeconomic analysis of gas turbines; the equations these authors used are different from equations presented in this thesis.

$$PEC_{comp} = \frac{C_{11}\dot{m}_{air}}{C_{12} - \eta_{is}} \times R_c \times \ln\left(R_c\right) \quad \textbf{[74]}$$

$$PEC_{cc} = \left[\frac{C_{21}\dot{m}_{out}}{C_{22} - \left(1 - \Delta P_{cc}\right)}\right] \times \left[1 + \exp\left(C_{23}T_4 - C_{24}\right)\right] \quad \textbf{[75]}$$

$$PEC_t = \left(\frac{C_{31}\dot{m}_g}{C_{32} - \eta_{is}}\right) \times \ln\left(R_t\right) \times \left[1 + \exp\left(C_{33}T_4 - C_{34}\right)\right] \quad \textbf{[76]}$$

with $C_{11} = 87.7163\left[\frac{\$ \cdot s}{kg}\right]; C_{12} = 0.9136$

$C_{21} = 119.85\left[\frac{\$ \cdot s}{kg}\right]; C_{22} = 1.0133$

$C_{23} = 0.010\left[K^{-1}\right]; C_{24} = 26.40$

$C_{31} = 614.9154\left[\frac{\$ \cdot s}{kg}\right]; C_{32} = 0.9972$

$C_{33} = 0.025\left[K^{-1}\right]; C_{34} = 54.4$

The ceramic heat exchanger cost is estimated using equation **[77]** given by Ranasinghe et al. 1989, with the coefficient also modified to fit figures in Consonni et al. 1996d:

$$PEC_{CerHx} = k\left(A\right)^{0.60} \quad \textbf{[77]}$$

where k = 56961.60 [$.m$^{-1.2}$].

The gasifier cost is based on the data from Bridgwater, 1995. Equation **[78]** represents the cost for an atmospheric gasification systems:

$$PEC_{gasif} = 2.90 \times 10^6 \left(3.6 \times \dot{m}_b\right)^{0.70} \quad \textbf{[78]}$$

It has been assumed that equation **[78]** includes the cleaning system, which can be seen in Craig et al. 1996 for capital costs of the low-pressure utility gas turbine.

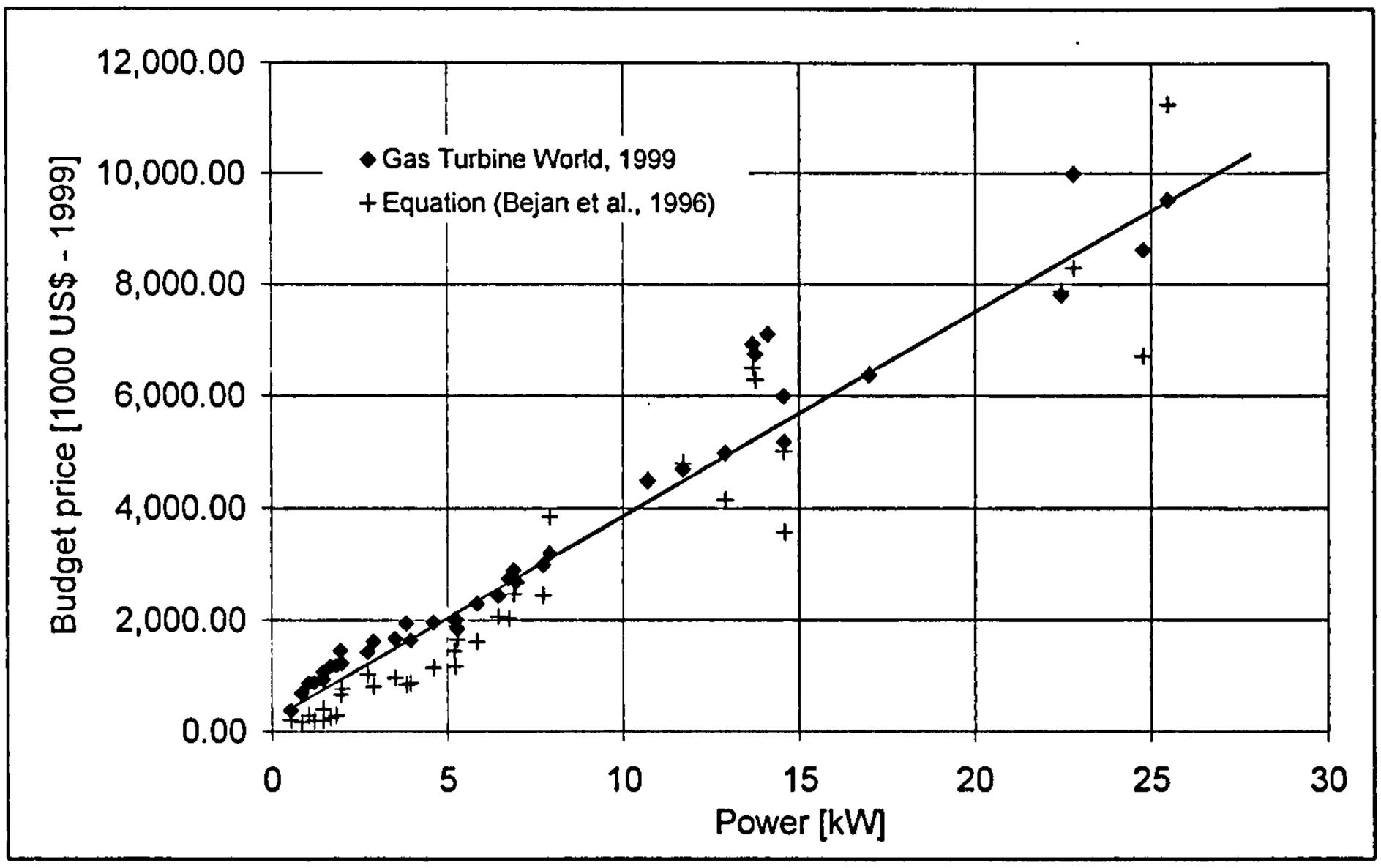

Figure 47 – Budget price of gas turbine engines (Farmer, 1999)

Validation for the economic analysis code

The validation for the economic analysis code has been carried out using the example given by Bejan, A., Tsatsaronis, G., and Moran, M., 1996, using the method proposed by the same authors, described in the Appendix B of this thesis. The same purchased-equipment-cost was given the developed code and the errors presented for all variables were negligible. Such errors occurred principally because the authors round the figures up.

As seen in Table 21, the results from the code developed are in agreement with the example found in the literature. The largest error is found for the O&M costs, and the reason is that the authors do not make explicit the method used to calculate their O&M charges. Nevertheless, the code is robust for assessing the economic performance of the system proposed in this work.

Table 21 – Validation of final results for economic analysis

	Error
Carrying charges	-4.03%
Fuel costs	-0.02%
O&M costs	6.34%
Total required revenue	0.19%

Exergy analysis

An exergy analysis has been conducted in order to identify the main components that cause losses to the cycle at design-point. First the sensitivity of the exergy destruction ratio (y_D) to pressure ratio is presented for each cycle, followed by a sensitivity of y_D to *TET*.

The thermochemical dead state has been assumed to be T_o = 298.15 K and P_o = 101325 Pa. The environment composition used is that presented in Table 18.

Sensitivity of exergy destruction ratio to pressure ratio

The sensitivity of the y_D to pressure ratio for the NGGT cycle is shown in Figure 48. As expected the combustor is the component with the largest exergy destruction ratio. The main sources of irreversibilities in the combustion process are heat transfer and loss, mixing, and incomplete combustion (Kotas, T. J., 1985). These immense losses basically mean that a large amount of energy present in the fuel, with great capacity to generate useful work, is being wasted.

One way of reducing this large entropy generation is to preheat both fuel and oxidant. That explains why the combustor y_D decreases whilst y_D for all other components is increasing. The higher the pressure ratio the higher the compressor outlet temperature, i.e., the oxidant, air in this case, has been preheated.

Exergy destruction ratio increases in the other components, mainly in the compressor, because an increase in pressure leads to an increase in entropy generation. However, this increase in y_D for the compressor and turbines is negligible when compared with the combustor y_D.

Figure 49 shows the exergy destruction ratio for the components in the BIGGT cycle. In this cycle the gasifier produces the highest y_D. As mentioned before, this device is the main source of losses in this cycle.

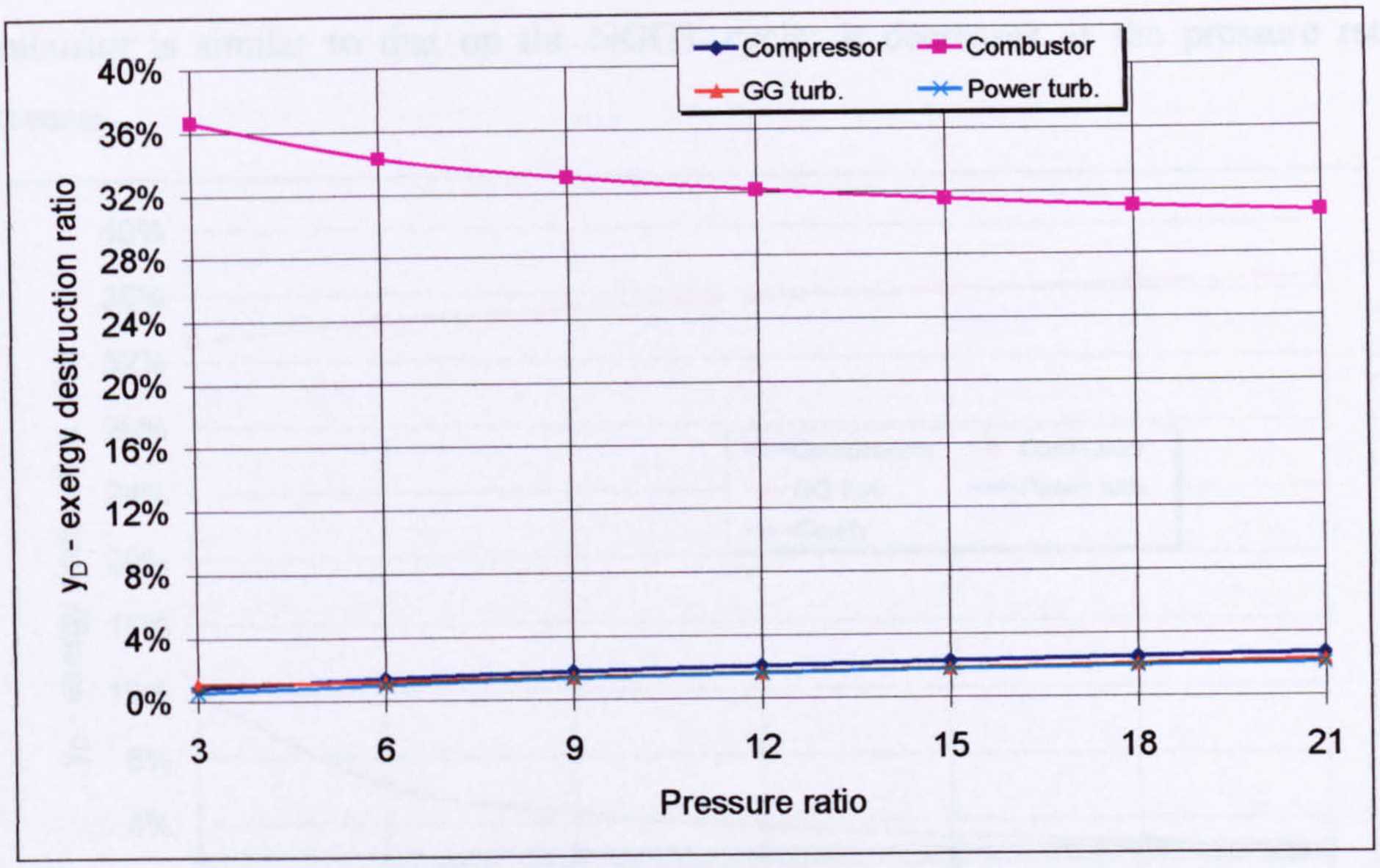

Figure 48 – Exergy destruction ratio sensitivity to pressure ratio for NGGT cycle

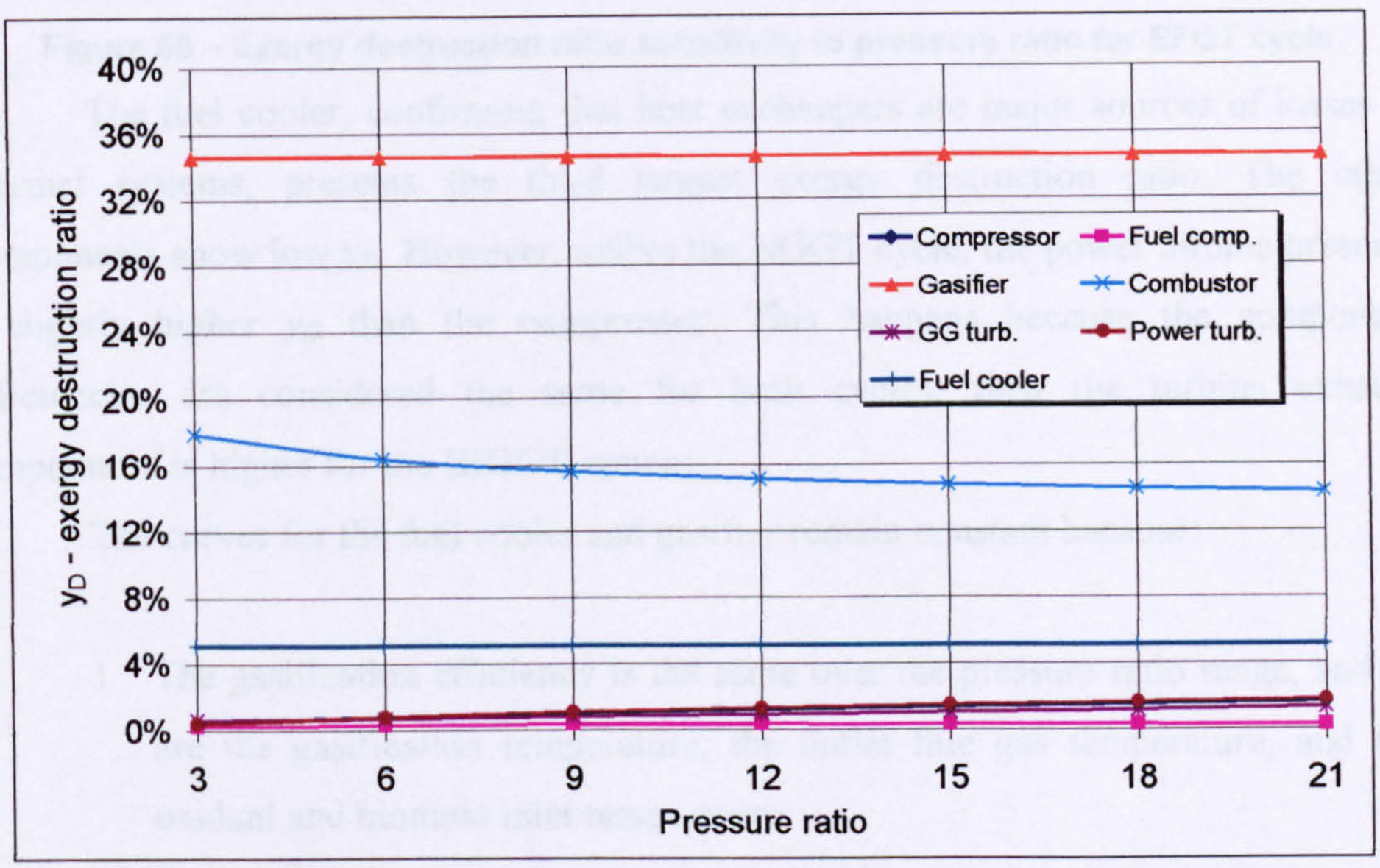

Figure 49 – Exergy destruction ratio sensitivity to pressure ratio for BIGGT cycle

It is interesting to note that the combustor presents half of the exergy destruction ratio of the natural gas cycle. This is explained by the fact that, in this cycle, the fuel itself is preheated, although it has released part of its energy in the fuel cooler, a heat exchanger that cools the fuel before compression. The trend of the y_D curve for the

combustor is similar to that on the NGGT cycle; it decreases as the pressure ratio increases.

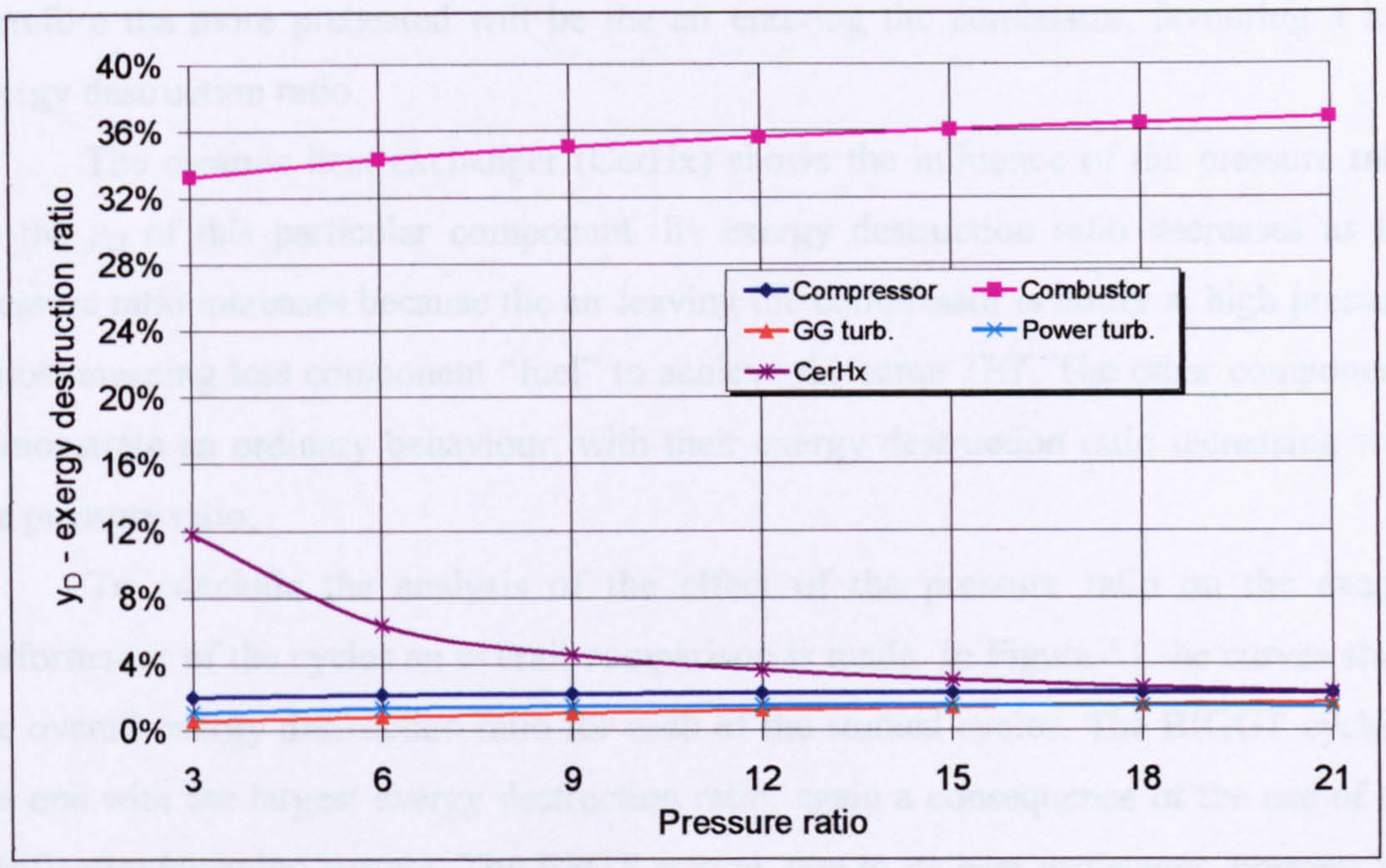

Figure 50 – Exergy destruction ratio sensitivity to pressure ratio for EFGT cycle

The fuel cooler, confirming that heat exchangers are major sources of losses in thermal systems, presents the third largest exergy destruction ratio. The other components show low y_D. However, unlike the NGGT cycle, the power turbine presents a slightly higher y_D than the compressor. This happens because the component efficiencies are considered the same for both cycles, then the turbine exhaust temperature is higher for the BIGGT system.

The curves for the fuel cooler and gasifier remain constant because:

1. The gasification efficiency is the same over the pressure ratio range, and so are the gasification temperature, the outlet flue gas temperature, and the oxidant and biomass inlet temperature.
2. The fuel cooler receives and delivers the biogas at the same temperature and pressure regardless the pressure ratio.

The EFGT cycle has some differences from the previous analysed cycles due to the presence of the heat exchanger. As seen in Figure 50, the combustor shows an increase in its exergy destruction ratio, instead of a reduction.

In the EFGT cycle the combustor is placed after the free power turbine. In this situation, the lower the pressure ratio the higher the turbine exhaust temperature, therefore the more preheated will be the air entering the combustor, favouring a low exergy destruction ratio.

The ceramic heat exchanger (CerHx) shows the influence of the pressure ratio on the y_D of this particular component. Its exergy destruction ratio decreases as the pressure ratio increases because the air leaving the compressor is hotter at high pressure ratios, meaning less component "fuel" to achieve the same *TET*. The other components demonstrate an ordinary behaviour, with their exergy destruction ratio increasing with the pressure ratio.

To conclude the analysis of the effect of the pressure ratio on the exergy performance of the cycles an overall comparison is made. In Figure 51 the curves show the overall exergy destruction ratio for each of the studied cycles. The BIGGT cycle is the one with the largest exergy destruction ratio, again a consequence of the use of the gasification/cleaning system. The EFGT engine, due to its heat exchanger, presents the second largest overall y_D. From all cycles the EFGT is the most sensitive to pressure ratio up to $PR = 9$.

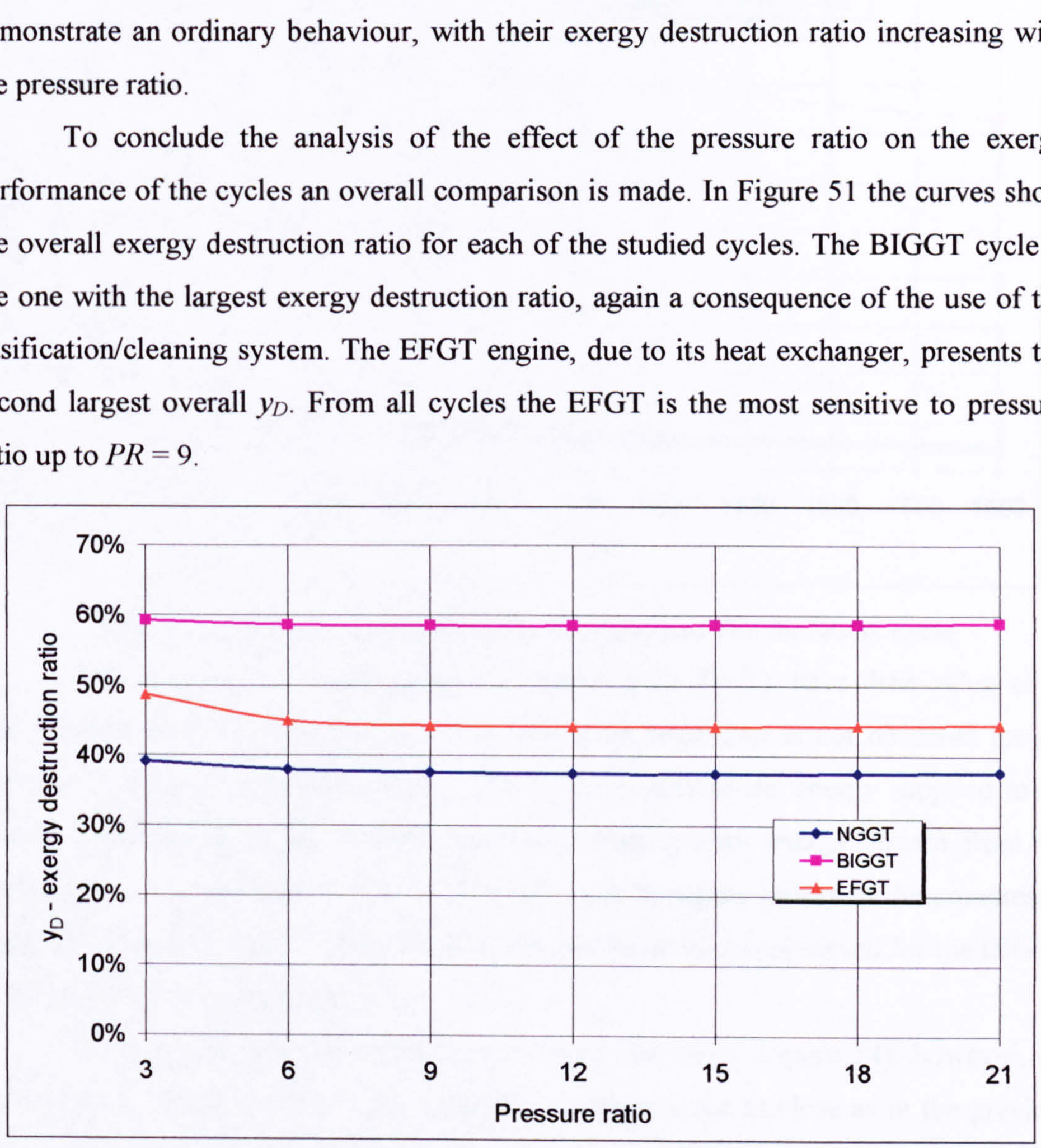

Figure 51 – Sensitivity of the overall exergy destruction ratio to pressure ratio

Sensitivity of exergy destruction ratio to turbine entry temperature

It is seen in Figure 52 that, in the NGGT cycle, the combustor shows a decreasing exergy destruction ratio as the *TET* decreases, demonstrating that high *TET*s diminish irreversibilities within this device, i.e., there is an increase in the quality of the energy supplied by the combustor.

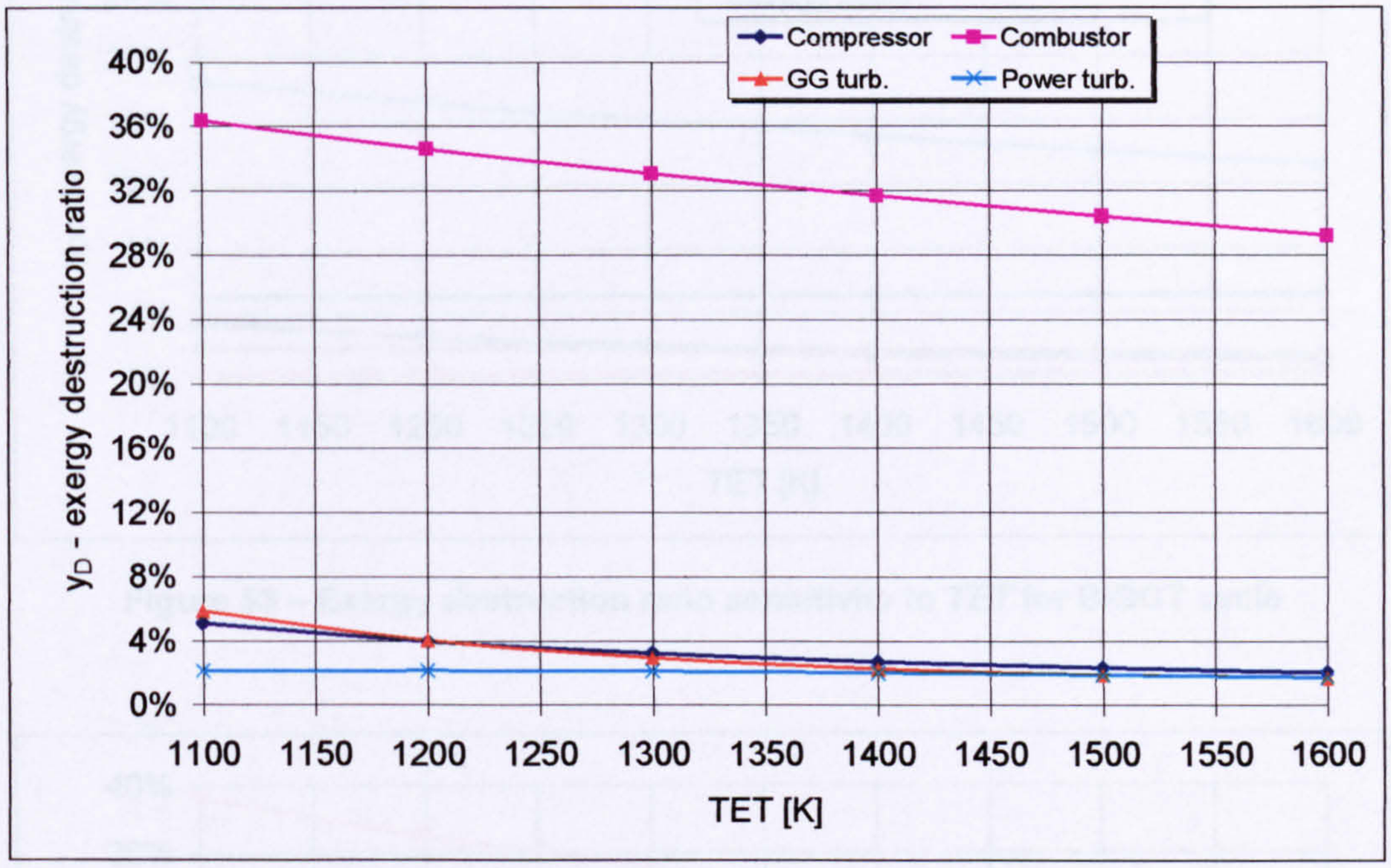

Figure 52 – Exergy destruction ratio sensitivity to *TET* for NGGT cycle

The compressor and gas generator turbine (*GG Turb.*), have their value of y_D decreased as the *TET* increases; however, the same behaviour is not observed for the free power turbine. Again this effect is due to the quality of the energy supplied to the devices. The gas generator turbine receives a high quality energy stream from the combustor; because the main role of this turbine is to supply power to the compressor the latter follows the turbine performance. Similar behaviour is observed for the BIGGT components, as shown in Figure 53.

In the EFGT cycle the behaviour pattern is the same (Figure 54); however, the curves for the compressor and gas generator turbine are not as close as in the previous two cycles. This fact demonstrates that the compressor is receiving a high quality energy stream – with a high exergy content – to produce a stream with a low exergy

content, which is sent to the heat exchanger – a device known for the losses it imposes – and then to the gas generator turbine.

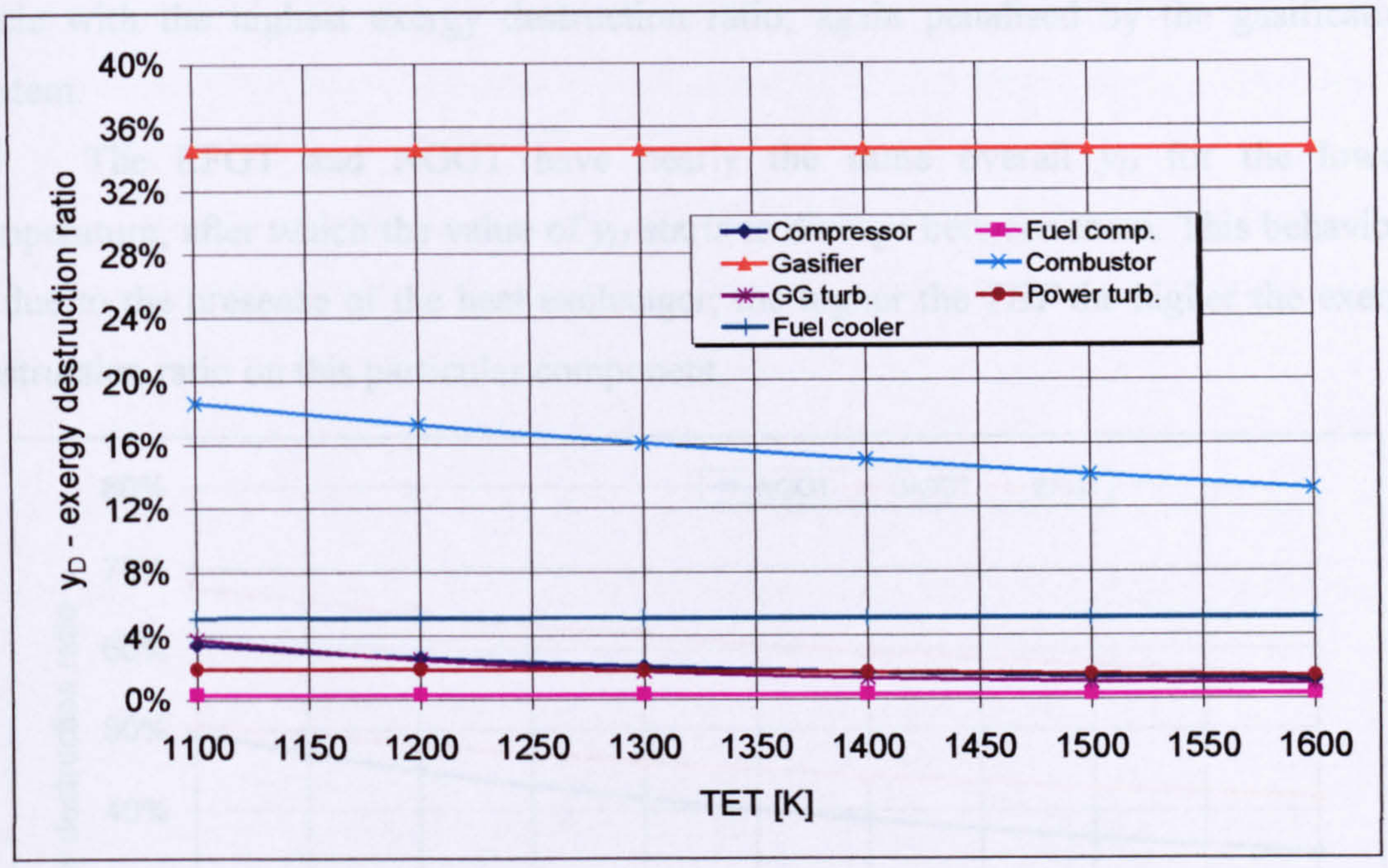

Figure 53 – Exergy destruction ratio sensitivity to *TET* for BIGGT cycle

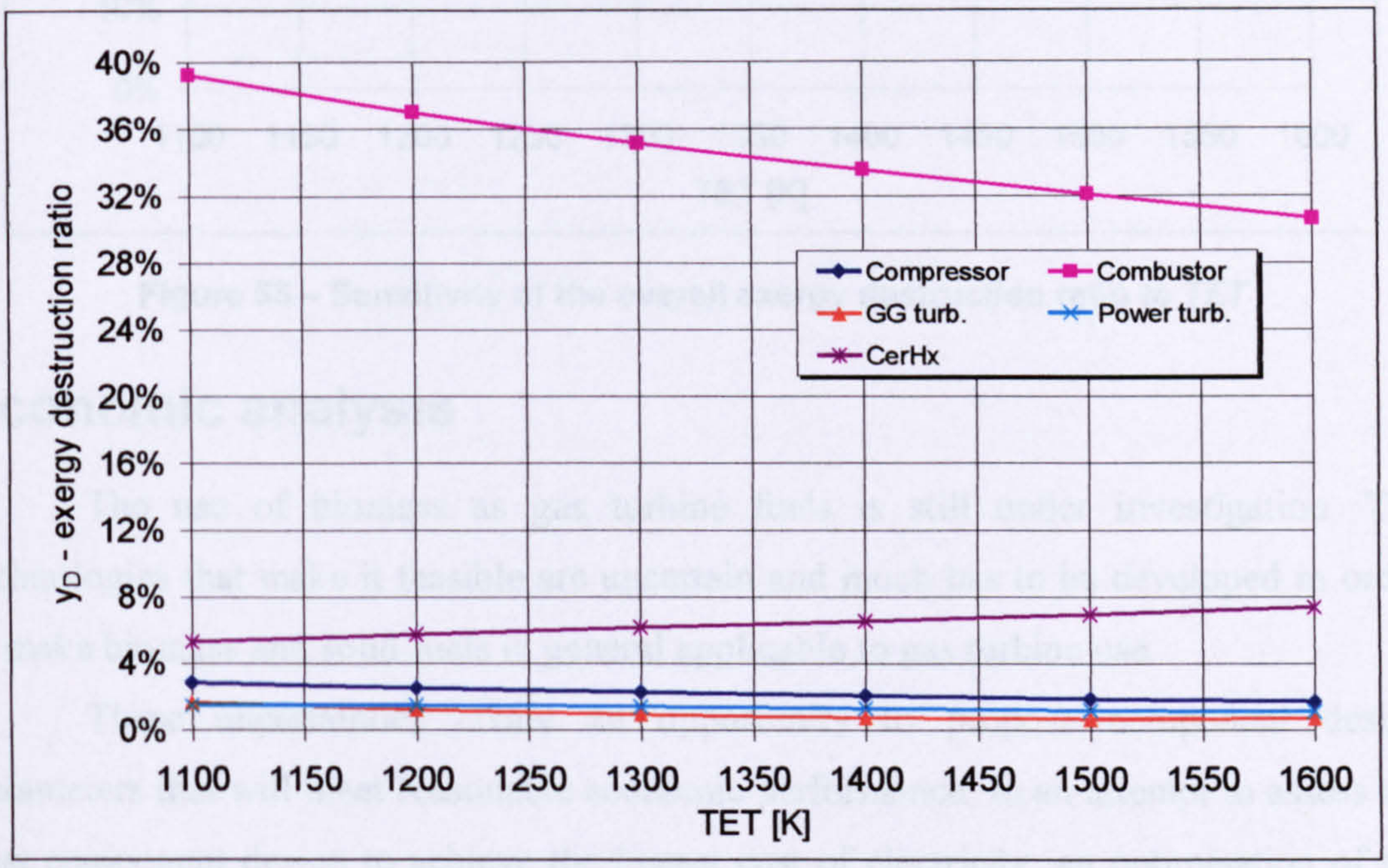

Figure 54 – Exergy destruction ratio sensitivity to *TET* for EFGT cycle

The losses due to the use of the heat exchanger are well depicted in the curve presented in Figure 54 for that device: an increase of about 50 percent in the value of y_D.

Finally a comparison between the sensitivity of the overall exergy destruction ratio to *TET* for the three studied cycles is presented in Figure 55. The BIGGT is the cycle with the highest exergy destruction ratio, again penalised by the gasification system.

The EFGT and NGGT have nearly the same overall y_D for the lowest temperature, after which the value of y_D starts to diverge between them. This behaviour is due to the presence of the heat exchanger; the higher the *TET* the higher the exergy destruction ratio on this particular component.

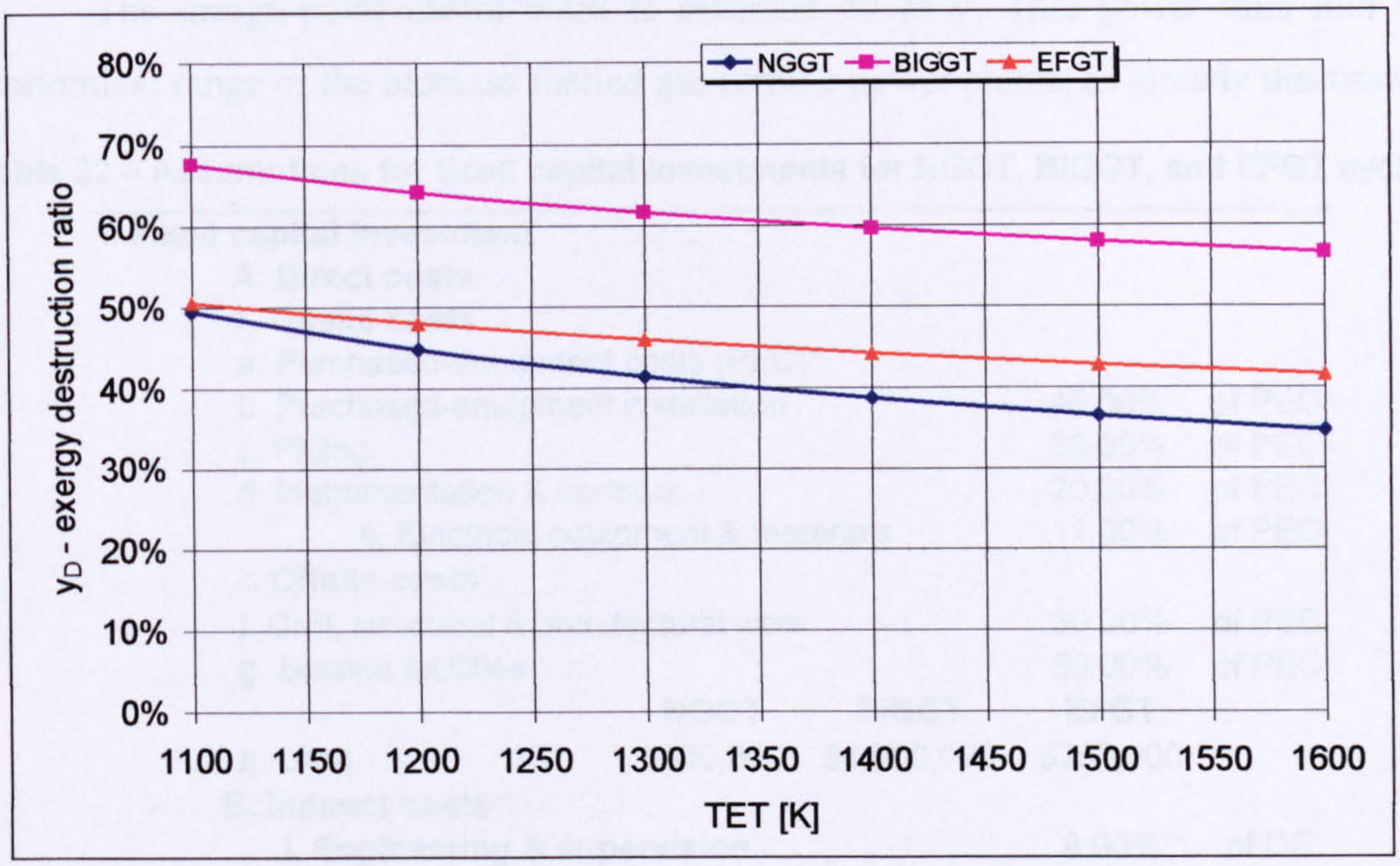

Figure 55 – Sensitivity of the overall exergy destruction ratio to *TET*

Economic analysis

The use of biomass as gas turbine fuels is still under investigation. The technologies that make it feasible are uncertain and much has to be developed in order to make biomass and solid fuels in general applicable to gas turbine use.

These uncertainties create an opportunity to propose component design parameters that will meet reasonable economic performance. In an attempt to assess the best component design to achieve the lowest cost of electricity, an optimisation of the BIGGT and EFGT cycles has been carried out. The economic analysis makes use of the equations and methodology already presented, and the assumptions used to estimate the fixed capital investment, common to the three cycles, are presented in Table 22.

These assumptions are based on the guidance given by Bejan, A., Tsatsaronis, G., and Moran, M., 1996. The land cost for the NGGT is the same suggested by those authors; however, for the BIGGT an assumption of twice the land cost for the NGGT has been assumed due to the size of such a plant. For the EFGT cycle a land cost 50 percent above the land cost for the NGGT has been assumed.

It must be pointed out again that the NGGT cycle has not been optimised and the design parameters for this cycle have been chosen such that they are in accordance with the present technology for aeroderivative gas turbines.

The design-point useful work is assumed 40 MW. This power falls into the economical range of the biomass fuelled gas turbine power plants, as already discussed.

Table 22 – Assumptions for fixed capital investments for NGGT, BIGGT, and EFGT cycles

I. Fixed capital investment				
A. Direct costs				
1. Onsite costs				
a. Purchased-equipment costs (PEC)*				
b. Purchased-equipment installation			45.00%	of PEC
c. Piping			35.00%	of PEC
d. Instrumentation & controls			20.00%	of PEC
e. Electrical equipment & materials			11.00%	of PEC
2. Offsite costs				
f. Civil, structural & architectural work			30.00%	of PEC
g. Service facilities			50.00%	of PEC
	NGGT	**BIGGT**	**EFGT**	
h. Land	$500,000	$1,000,000	$750,000	
B. Indirect costs				
i. Engineering & supervision			8.00%	of DC
j. Construction costs & contractors profit			15.00%	of DC
k. Contingency	15.00%	of the sum of items i and j		

Table 23 shows the assumptions made for the calculation of required revenue for each cycle. The inflation and escalation rates are comparable with the Brazilian economy at the time this thesis was written, so is the fuel price (Arrieta et al. 2000). Operating and maintenance, O&M, are based on Boyce, M. P., 2001. Although that author does not present O&M costs for biomass cycles, it has been assumed that the BIGGT cycle has about the same O&M costs as the simple cycle gas turbine oil fired. The EFGT cycle bears the same O&M costs as the simple cycle turbine crude fired.

These assumptions have been made based on the fact that the BIGGT cycle will have a relatively clean fuel entering the gas turbine and in the EFGT cycle, although no combustion products have contact with turbine parts, the ceramic heat exchanger will

contribute to increase O&M costs. Figure 56 shows how the cost of electricity behaves as a function of one of both the variable and the fixed O&M[33]; each curve represents one cycle. It is seen that within the range that has been assumed for the annual fixed O&M costs, the impact in the final CoE is negligible. However, the influence of the annual variable O&M is more substantial.

Table 23 – Assumptions for the calculation of required revenue for NGGT, BIGGT, and EFGT cycles

1a.	Average general inflation rate (%)				5.0%
b.	Average nominal escalation rate of all (except fuel) costs (%)				5.0%
c.	Average nominal escalation rate of fuel costs (%)				6.0%
2a.	Beginning of the design & construction period				January 1, 1996
b.	Date of commercial operation				January 1, 1998
3a.	Plant economic life (years)				20
b.	Plant life for tax purposes (years)				15
4.	Plant financing fractions & required returns on capital:				
	Type of financing	Common Equity	Preferred Stock	Debt	
	Financing fraction (%)	35.0%	15.0%	50.0%	
	Required annual return (%)	15.0%	11.7%	10.0%	
	Resulting average cost of money (%)			12.0%	
5a.	Average combined income tax rate (%)				38.00%
b.	Average property tax rate (%)				1.50%
c.	Average insurance rate (%)				0.50%
6.	Average capacity factor (%)				85%
			NGGT	BIGGT	EFGT
7.	Labour positions for O&M		30	35	30
8.	Average labour rate ($/h)				28.0
			NGGT	BIGGT	EFGT
9.	Annual fixed O&M costs	[$/MWh]	0.23	0.25	0.25
10.	Annual variable O&M costs	[$/MWh]	5.8	6.2	13.5
11.	Unit cost of fuel ($/GJ) (LHV based)		4.0 (NGGT)		0.42 (BIGGT)
12.	Allocation of plant facilities investment to the individual years of design & construction				
	January-96	December-96			40%
	January-97	December-97			60%

- Assumptions:
  MACRS depreciation used for tax purposes.
  Straight-line depreciation used for company purposes.
  Net salvage value equal zero.
  No investment tax credit and no grants in aid of construction.
  Revenue levelling occurs with before-tax average cost of money.

[33] When analysing the variable O&M costs, the fixed O&M costs are considered zero; and vice-versa.

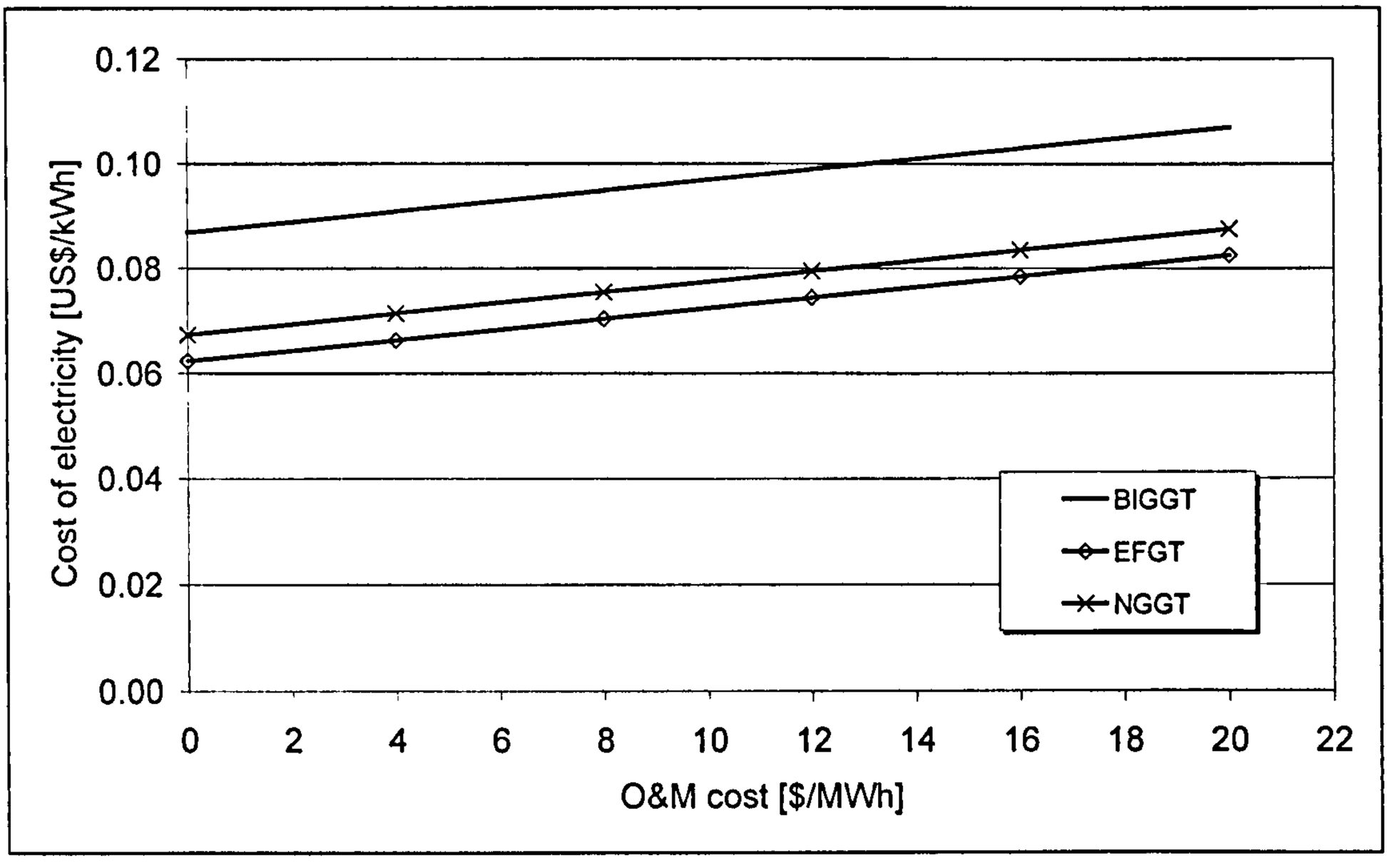

Figure 56 – The impact of the operating and maintenance cost in the final cost of electricity

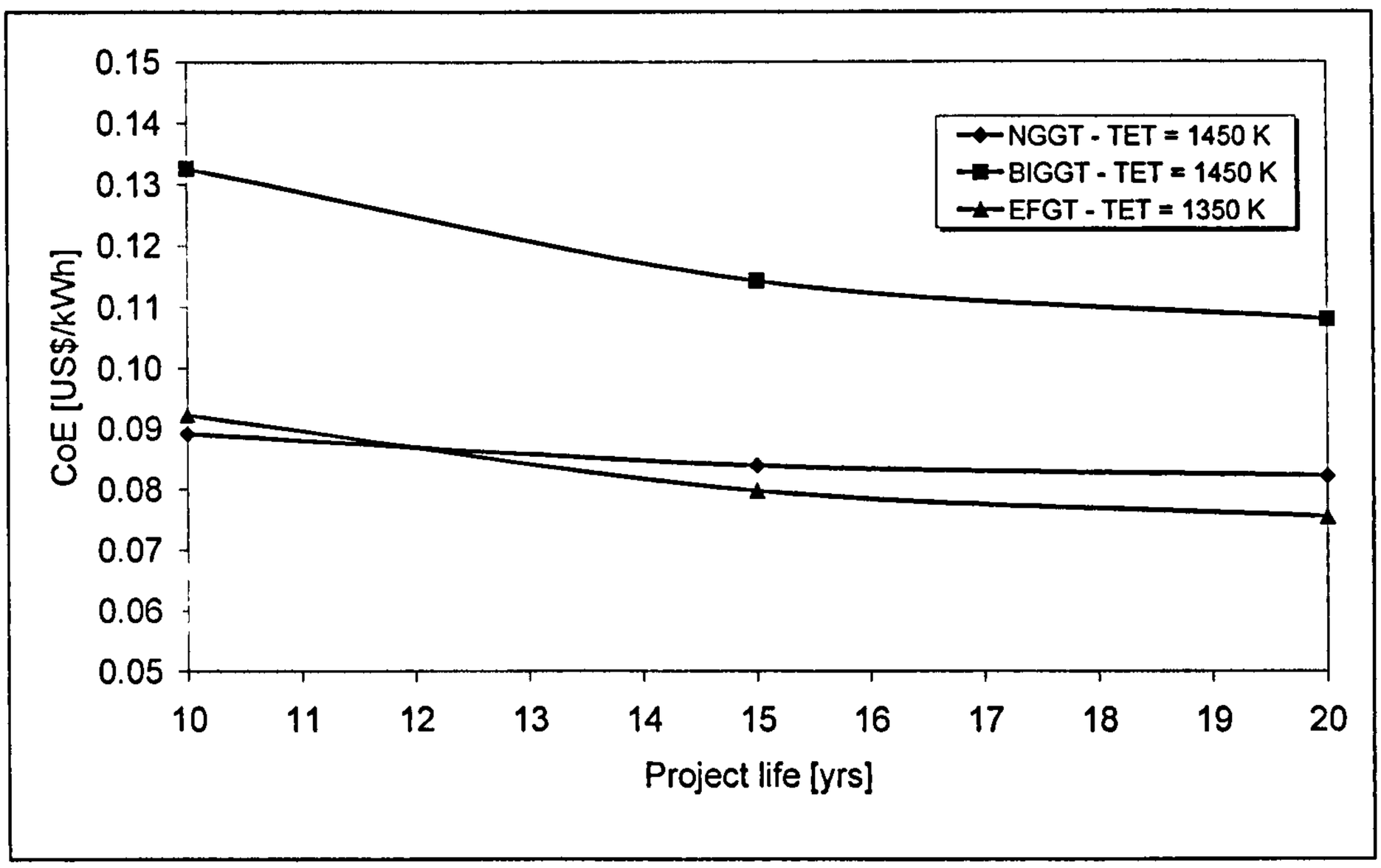

Figure 57 – Cost of electricity vs. project life for BIGGT and EFGT compared with NGGT

Figure 57 depicts the cost of electricity (CoE) for different project lives. The BIGGT cycle shows the highest CoE of all. The NGGT and EFGT are comparable, and for project lives above 12 years the CoE produced by the EFGT cycle is even lower than

the NGGT, suggesting that this cycle, although with a very expensive heat exchanger, can be a competitive alternative to natural gas systems.

However, Figure 58 suggests that the BIGGT cycle can also be competitive with the current natural gas technology. It is clear from that figure that there is a range of fuel prices within which both biomass-fuelled engines are competitive with natural gas. For instance, if the biomass fuel has a zero cost[34] for the utility company the CoE for the EFGT is already less than the CoE for the NGGT at its normal price (US$ 4.00 per GJ). Regarding the BIGGT case, it becomes competitive when the natural gas reaches a price of US$6.00/GJ. This may happen, for example, when emissions taxation, such as carbon tax (Traverso et al. 2002), is applied to the NGGT power plant.

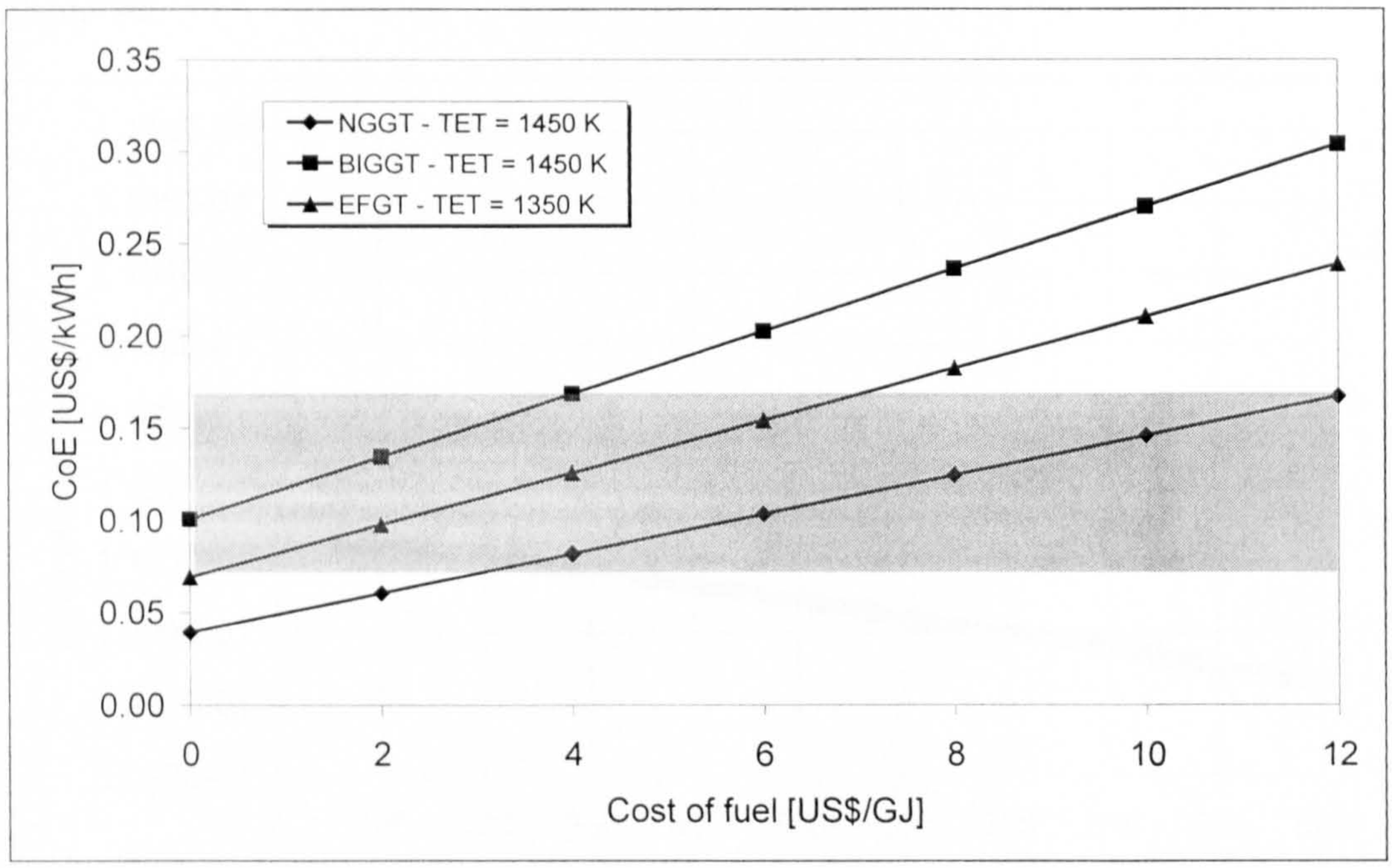

Figure 58 – Sensitivity to fuel price for NGGT, BIGGT, and EFGT cycles

Optimisation

For the optimisation, the technique known as Genetic Algorithms (Appendix A) has been applied, followed by a hill-climbing method. The reason to apply the hill-climbing method is simple. Because GAs use probabilistic rules to find the optimum point of a function, each time the code is run it generates a different optimum, such that

---

[34] A zero or negative cost can be achieved when the utility is paid to remove the residues which can be used as fuel in the power plant.

it is necessary to run the code several times and find the optimum from these runs. However, the output from GAs give a very good approximation of the region where the global optimum point is located; this is reached in the first run, thus avoiding the hill-climbing to find a local optimum. The application of this combined algorithm is referred to as hybrid algorithm (HA).

Figure 59 shows the evolution of the generations on the GA code for the minimisation of the cost of electricity for a BIGGT cycle. The best result in the first generation is well above the best result in the second generation from which the GA quickly moves towards the optimum. The last generation optimum is fed into a hill-climbing algorithm, which in turn finalises the optimisation, giving the results presented in Table 24.

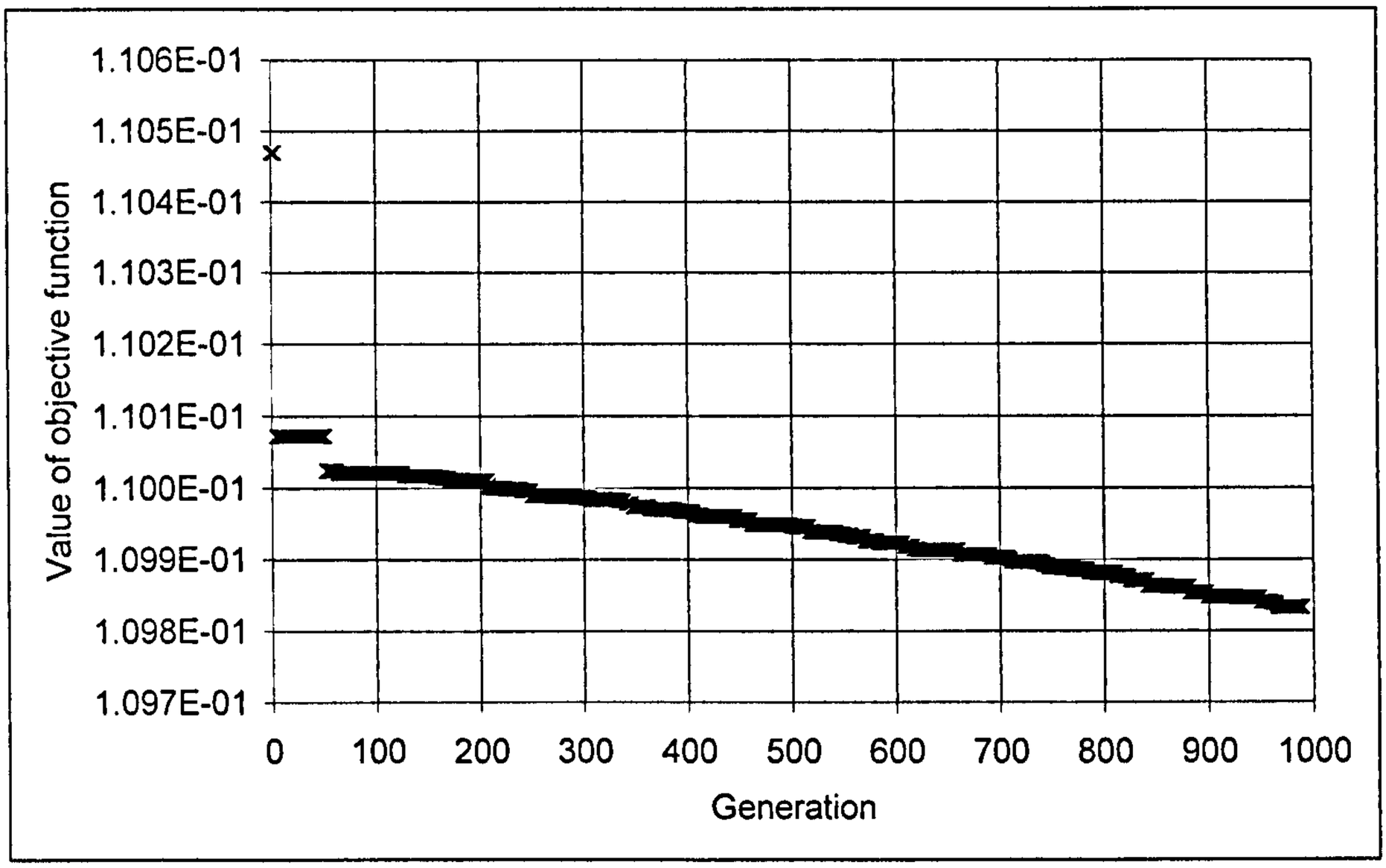

Figure 59 – Evolution of the GA code on the minimisation of CoE for a BIGGT cycle

The constraints for the optimisation are:

$$3 \le PR \le 20 \qquad 0.86 \le \eta_{\infty c} \le 0.91$$

$$1150 \le TET_{EFGT} \le 1350K \qquad 0.84 \le \eta_{\infty t} \le 0.88$$

$$1150 \le TET_{BIGGT} \le 1450K \qquad 0.80 \le \varphi_{CerHx} \le 0.95$$

Figure 60 shows the evolution of the optimisation for the EFGT cycle. Again the last generation best result is fed into a hill-climbing algorithm in order to refine the result, which is shown in Table 24.

The pressure ratio (*PR*) has been constrained between 3 and 20 because is unlikely that the first pilot plants will use state-of-the-art technology in order to minimise risks. The *TET* has been constrained in the EFGT cycle mainly due to limitations imposed by the ceramic heat exchanger, which will experience very high temperature in its hot side (1540 K). The ranges for compressor polytropic efficiency ($\eta_{\infty c}$) and turbine polytropic efficiency ($\eta_{\infty t}$) are due to limitations in the purchased-equipment cost equations. The efficiencies in those equations are isentropic efficiencies and they appear in the denominator to each equation; a value given to the code above the higher limit in the constraints would lead either to a zero or a negative denominator. These limits have been chosen based on the charts presented by Walsh, P. P. and Fletcher, P., 1998 and are shown in Figure 61.

Table 24 – Optimised parameters for the BIGGT and EFGT cycles

	NGGT	BIGGT	EFGT
PR	18.0	11.86	6.56
$\dot{m}_{air}$ **[kg/s]**	118.83	110.24	159.71
***TET* [K]**	1450	1450	1350
Cooling flow	6% of inlet flow	6% of inlet flow	None
$\eta_{\infty c}$	0.90	0.86	0.87
$\eta_{\infty t}$	0.88	0.88	0.88
$(\Delta P/P_{in})_{cc}$	0.04	0.04	0.04
η_{cc}	0.99	0.99	0.99
φ_{CerHX}	-	-	0.80
η_{gasif}	-	0.75	-
Life [yr]	20	20	20
c_{fuel} **[$/GJ]**	4.0	0.42	0.42
RESULTS			
CoE optimised			
η	38.20%	23.49%	29.21%
ε	36.59%	22.81%	27.76%
y_D	40.05%	50.27%	42.16%
CoE [$/kWh]	0.07	0.09	0.07

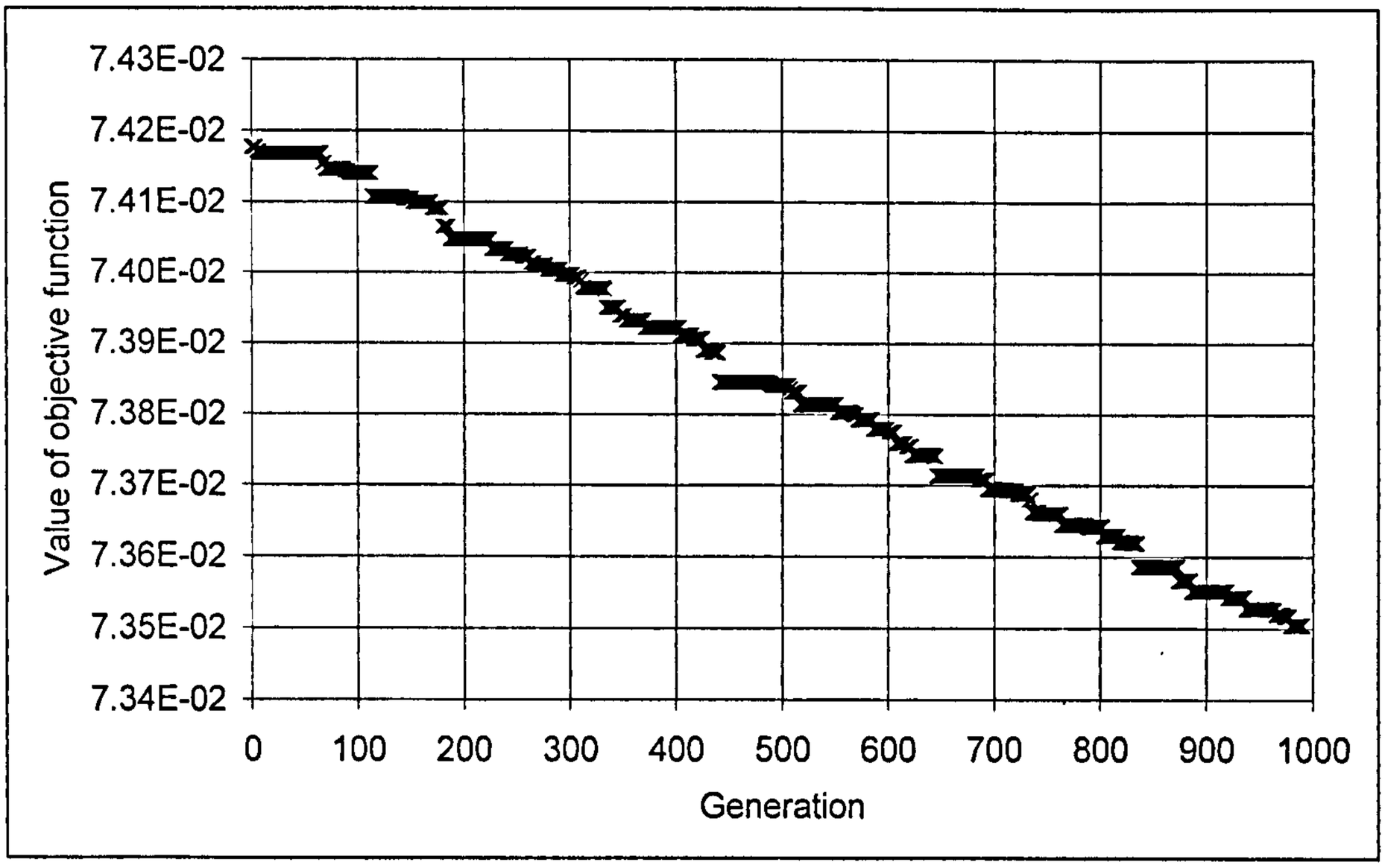

Figure 60 – Evolution of the GA code on the minimisation of CoE for an EFGT cycle

It is seen in Table 24 that the optimised EFGT cycle is competitive with natural gas, despite the very high cost to the ceramic heat exchanger considered in this study. Of course, technological barriers must be overcome.

In order to find the best alternative for investment an analysis regarding the required revenue (RR) for each cycle has been carried out on a 20-year investment basis (Table 25). The NGGT and the BIGGT cycles are the extremes as far as RR analysis is concerned, the BIGGT system being 32 percent higher than the NGGT. Although the EFGT requires more revenue than the NGGT cycle, the RR for this system is only 7 percent higher than the reference cycle.

Table 25 – Required revenue for each investment on a 20-years basis

	Required revenue
NGGT	$21,917,378.91
BIGGT	$29,027,401.52
EFGT	$23,333,035.42

Exergoeconomic analysis

Some devices, although economically optimised, are not at their highest thermodynamic productivity. A decision must be made in order to identify the devices

that can have their thermodynamic performance further enhanced. The exergoeconomic analysis helps with these decisions.

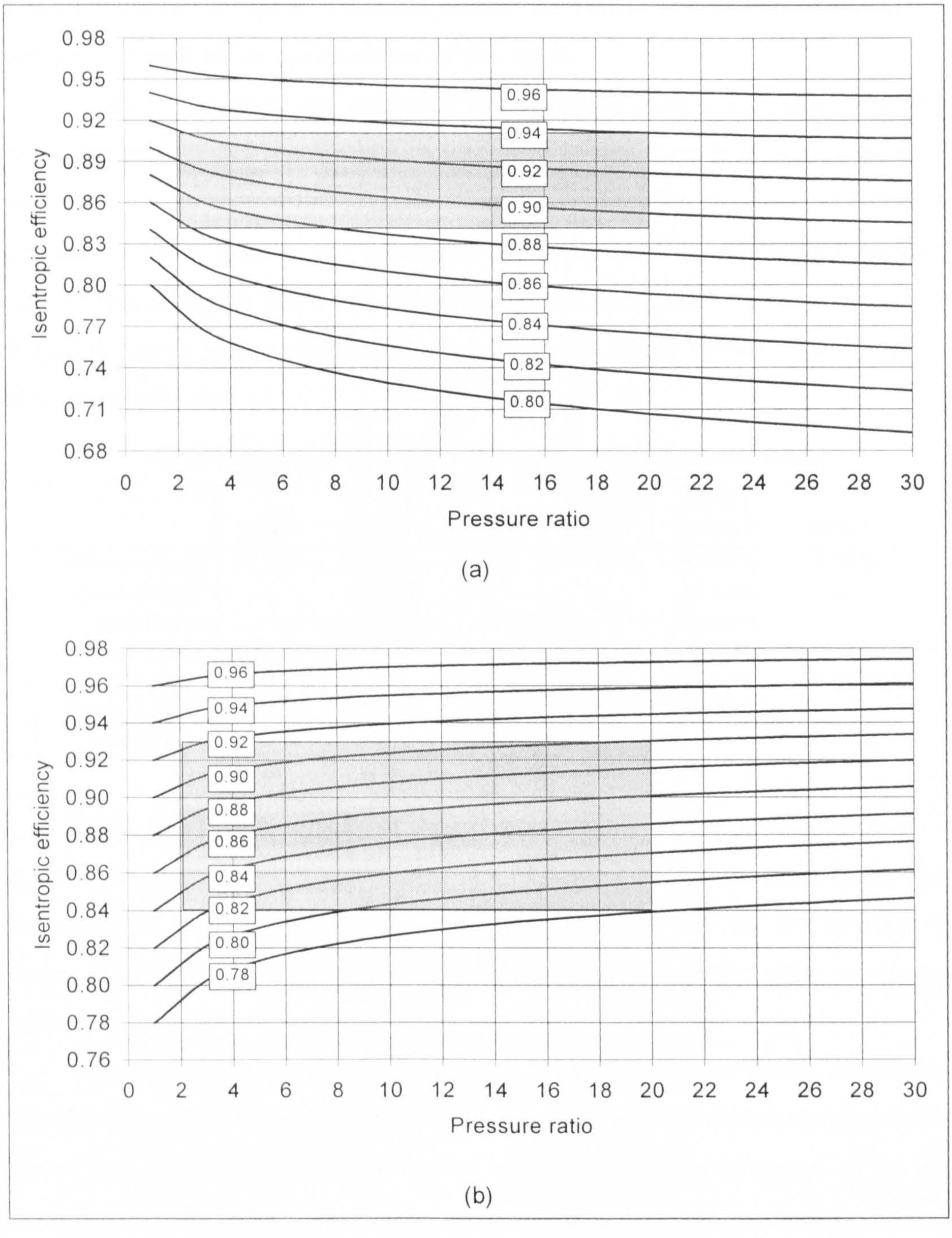

Figure 61 – Search space for the polytropic efficiencies (lines) of (a) compressor and (b) turbine

In this section an exergoeconomic assessment of the three cycles will be performed, and the results are shown in the following paragraphs. Two main parameters are used to carry out this analysis, the aforementioned *relative cost difference* (r), which

expresses the relative increase in the average cost per exergy unit, and the *exergoeconomic factor* (*f*), which states the importance of each cost source of a component within the cycle. Table 26 shows the values of the two aforementioned parameters for each of the cycles object of this thesis.

Let us first analyse the reference cycle, NGGT. The combustor presents the highest relative cost difference of all cycles, meaning that there is a relative increase of almost 400% in the cost of the stream leaving the combustion chamber. The other two cycles show a lower value of this parameter due to the fact that in both biomass-fuelled cycles the fuel exergy is much lower than the natural gas. Summing up, it means that a high quality energy source, the natural gas with a high exergy content, is not being well used by the combustor.

Table 26 – Relative cost difference and exergoeconomic factor

	r [%]			f [%]		
	NGGT	BIGGT	EFGT	NGGT	BIGGT	EFGT
Compressor	65.28%	23.67%	0.16%	96.97%	84.76%	77.52%
Fuel comp.	---	19.13%	---	---	87.13%	---
Gasifier	---	890.88%	---	---	98.46%	---
Combustor	390.97%	19.55%	42.82%	33.33%	8.30%	49.97%
GG Turb.	11.36%	7.59%	7.34%	89.36%	79.19%	87.43%
Power Turb.	15.13%	8.71%	9.58%	91.17%	83.83%	85.94%
CerHx	---	---	159.47%	---	---	97.81%

On the other hand, looking at the exergoeconomic factor for the combustor it is seen that it offers room for improvements in the NGGT case, but the gains in the overall cycle would be negligible. However, the very low value of *f* for the BIGGT cycle indicates that for this cycle an improvement in the combustor performance may improve the cost savings in the entire system.

A surprising result is that of the gasifier. Although it incurs severe augmentation on the flue gas stream average cost, as indicated by its relative difference cost, the high figure of the exergoeconomic factor for this cycle indicates that little gain on the whole cycle will be achieved by improving the performance of the gasification island. It actually suggests that a decrease in investment cost to the gasifier is acceptable at the expense of its exergetic efficiency.

The same can be said about the ceramic heat exchanger (CerHx) in the EFGT case. This device presents a very high value of relative cost difference; however, its exergoeconomic factor is equally high. A less efficient CerHx would not bring benefits

to the system as a whole, and a decrease in its investment cost is welcome, again at the expense of the exergetic efficiency.

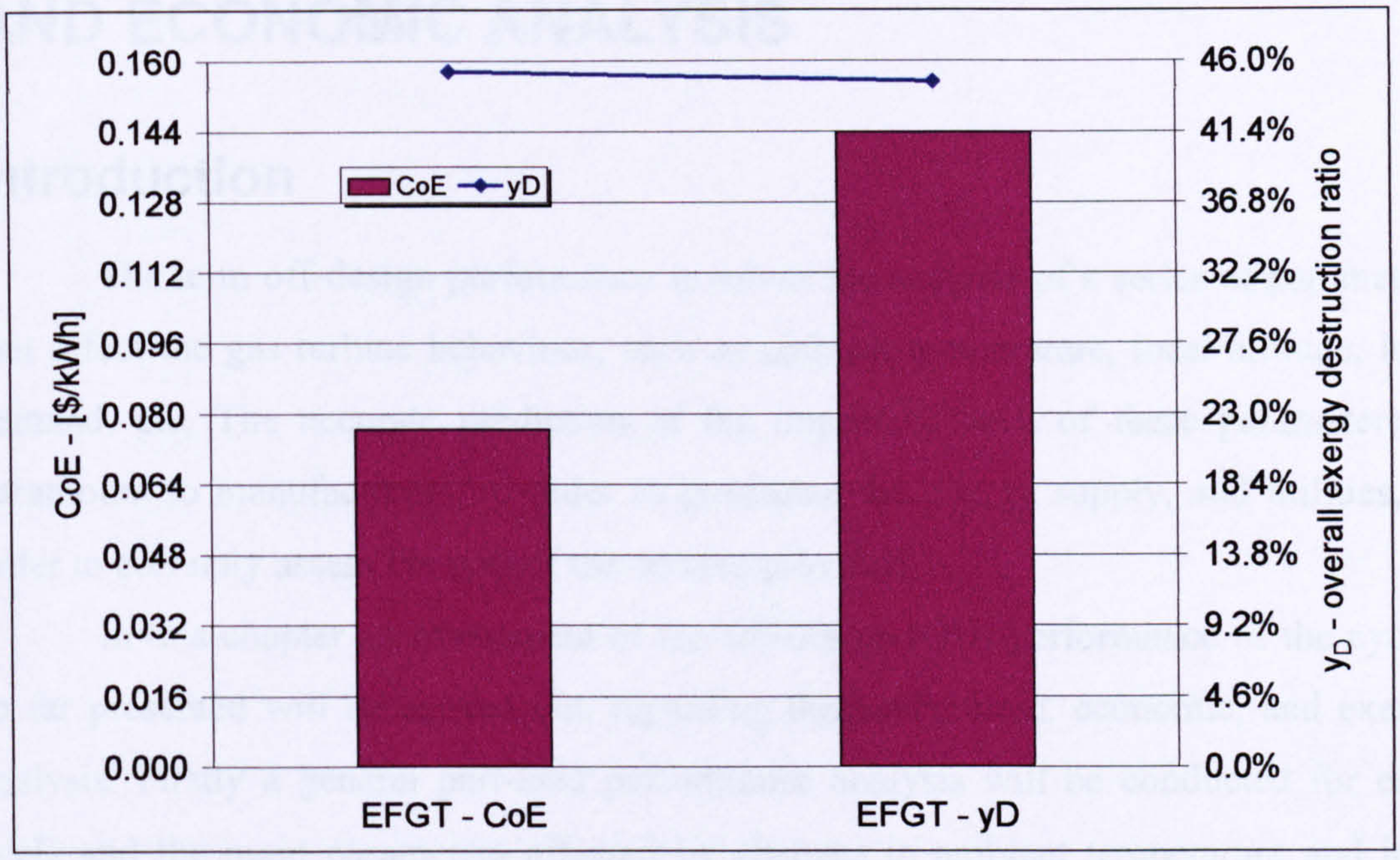

Figure 62 – Comparison between CoE and overall y_D for CoE optimised EFGT cycle and y_D optimised EFGT cycle

In order to illustrate this fact, an optimisation (minimisation) of the overall exergy destruction ratio has been conducted. Indeed, it is seen in Figure 62 that the reduction in the overall y_D is marginal, whereas the cost of electricity for the EFGT cycle increased by 100% when such a minimisation is conducted. Mainly because the effectiveness of the CerHx must be increased in order to reduce its y_D, consequently its surface area must be augmented, and so must the cost of this device.

The relative cost difference has been reduced from 159.47 percent to 99.34 percent after the optimisation. However the exergoeconomic factor has been marginally increased from 97.81 percent to 98.34 percent.

CHAPTER VI – OFF-DESIGN PERFORMANCE AND ECONOMIC ANALYSIS

Introduction

The term off-design performance involves the analysis of a series of parameters that affect the gas turbine behaviour, such as ambient temperature, local altitude, load demand, etc. The accurate prediction of the impact of each of these parameters is paramount to manufacturers, in order to guarantee the energy supply, and utilities, in order to correctly assess the cost of the service provided.

In this chapter an assessment of the off-design (OD) performance of the cycles so far presented will be carried out, regarding thermodynamic, economic, and exergy analysis. Firstly a general part-load performance analysis will be conducted for each cycle and the main parameters affected by changes in ambient temperature and load demand. A more specific analysis, following a typical Brazilian demand curve, is carried out for three main locations, and involves the thermodynamic and economic assessment for each cycle operating at and supplying energy to these different locations.

General off-design performance

As far as ambient conditions are concerned the parameter that has the most impact on the gas turbine performance is the ambient temperature (T_{amb}). Figure 63 shows the effect of this parameter on the main performance indicators.

The behaviour shown in Figure 63 is typical in gas turbine engines, and so can be generalised to non-reheat conventional cycles. As seen, power output reduces as T_{amb} increases due to the decrease in air density. This lower density means that the engine is swallowing less air than in design conditions, so less power is produced; efficiency is also reduced. The same behaviour is demonstrated by the pressure ratio.

As the flow rate and pressure ratio increase with reduction in T_{amb}, at very low temperatures the engine control system has to act to avoid unacceptable mechanical loads or pressure ratios. This is done by closing the VIGVs, and usually happens for temperatures below 5°C (Dechamps, 1999).

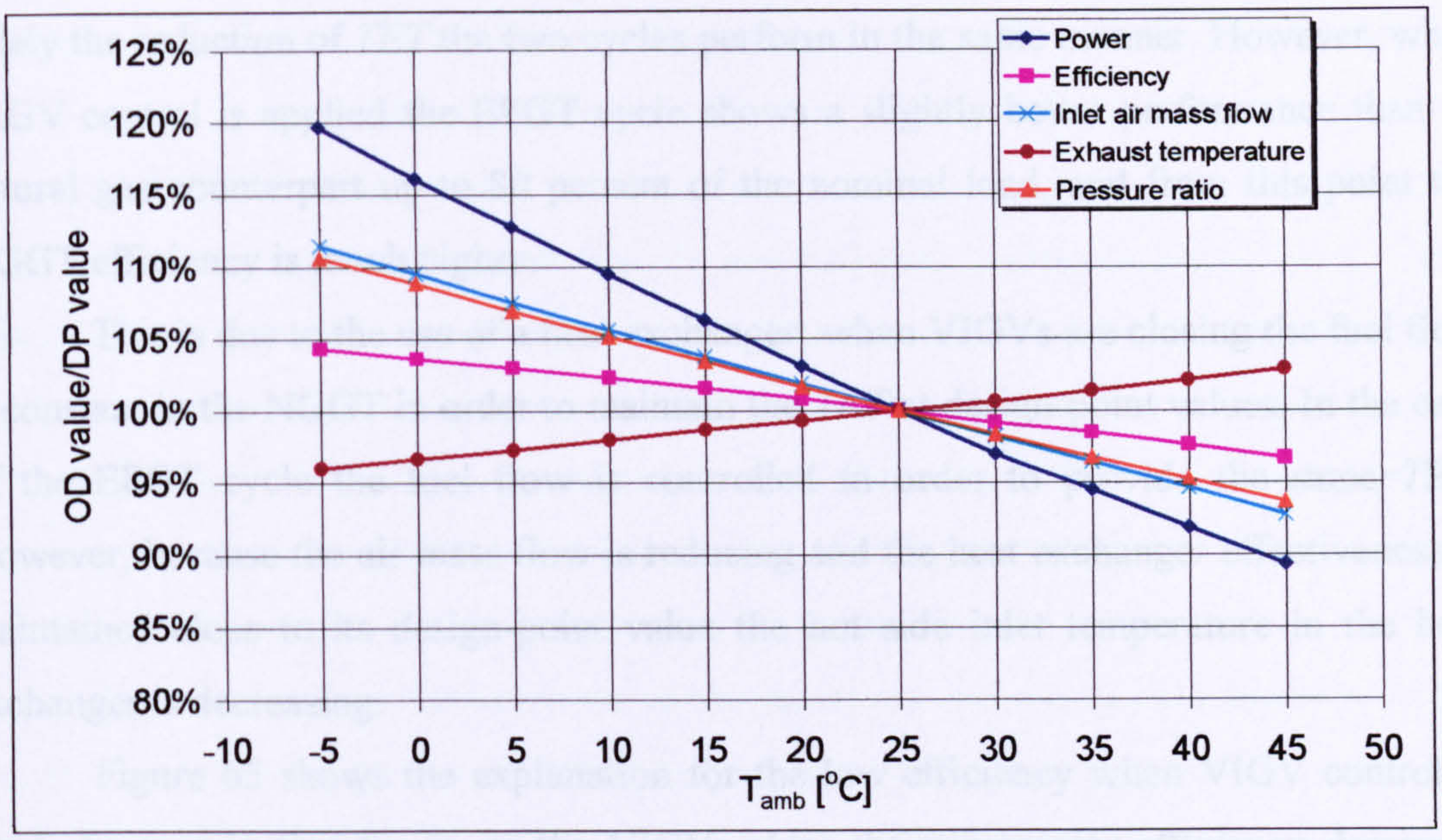

Figure 63 – Effect of ambient temperature on gas turbine performance

Part-load performance involves the analysis of the engine operating at different power demands. There are two types of control to achieve part-load performance; one is the reduction of the turbine entry temperature (*TET*) and the other strategy is to close VIGVs up to a certain load and then start to reduce *TET*.

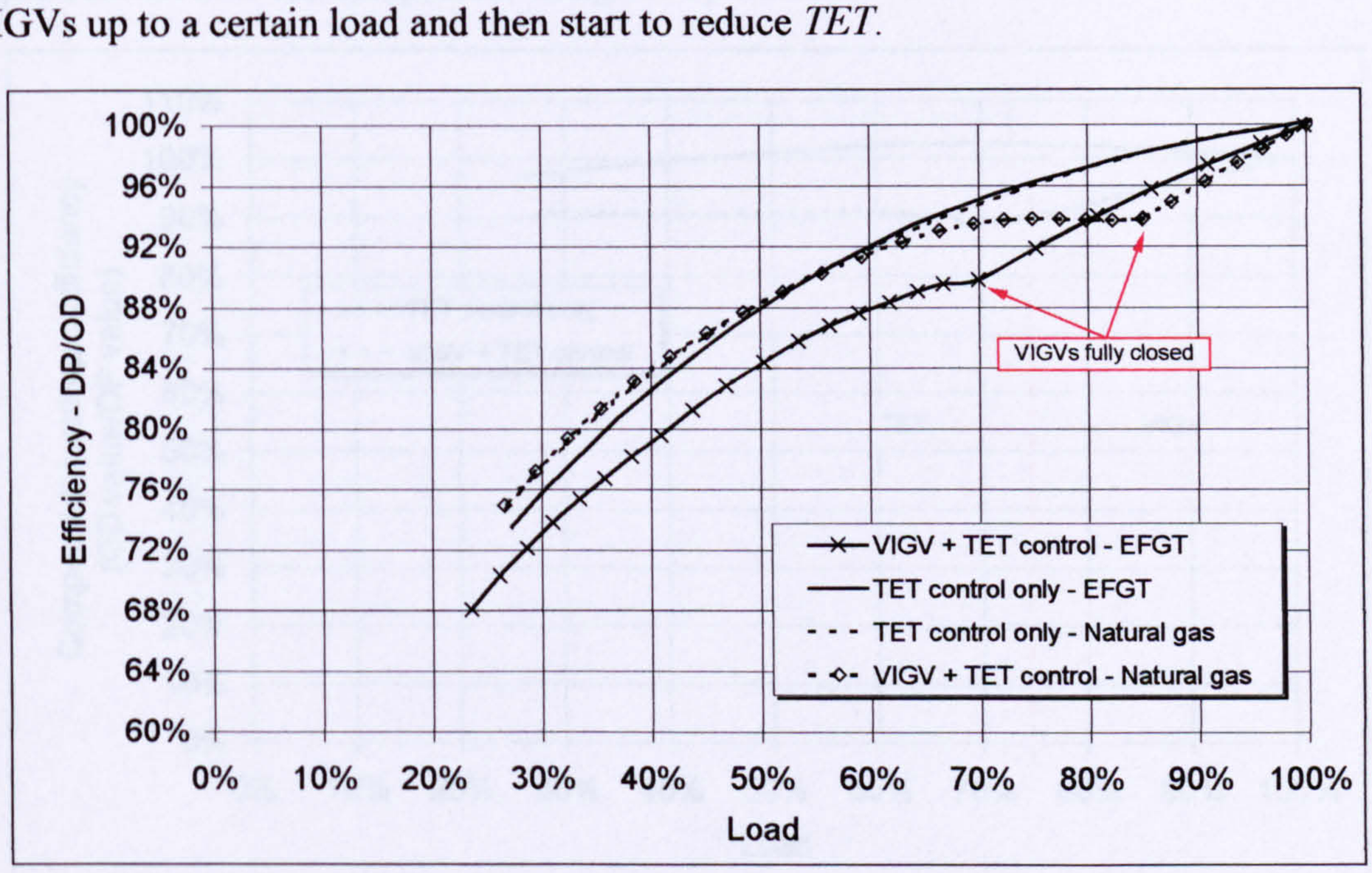

Figure 64 – Part-load efficiency comparison between NGGT and EFGT cycles

Figure 64 shows a comparison between efficiencies of the NGGT and EFGT cycles operating at part-load conditions – the curves for the BIGGT cycle present the same shape as the natural gas. It is seen in that figure that when the strategy adopted is

solely the reduction of *TET* the two cycles perform in the same manner. However, when VIGV control is applied the EFGT cycle shows a slightly better performance than its natural gas counterpart up to 80 percent of the nominal load, and from this point the NGGT efficiency is much higher.

This is due to the use of a heat exchanger; when VIGVs are closing the fuel flow is constant in the NGGT in order to maintain the *TET* at design-point values. In the case of the EFGT cycle the fuel flow is controlled in order to provide the same *TET*. However, because the air mass flow is reducing and the heat exchanger effectiveness is maintained close to its design-point value the hot side inlet temperature in the heat exchanger is decreasing.

Figure 65 shows the explanation for the low efficiency when VIGV control is used. As seen in that figure, as the VIGVs close the compressor efficiency decreases substantially up to 10 percent. Although this figure illustrates the compressor efficiency behaviour for the EFGT cycle, the NGGT and BIGGT cycles show the same trend, that is, the *TET* control makes the engine more efficient at part-load conditions. This is dependent on how the compressor design is optimised.

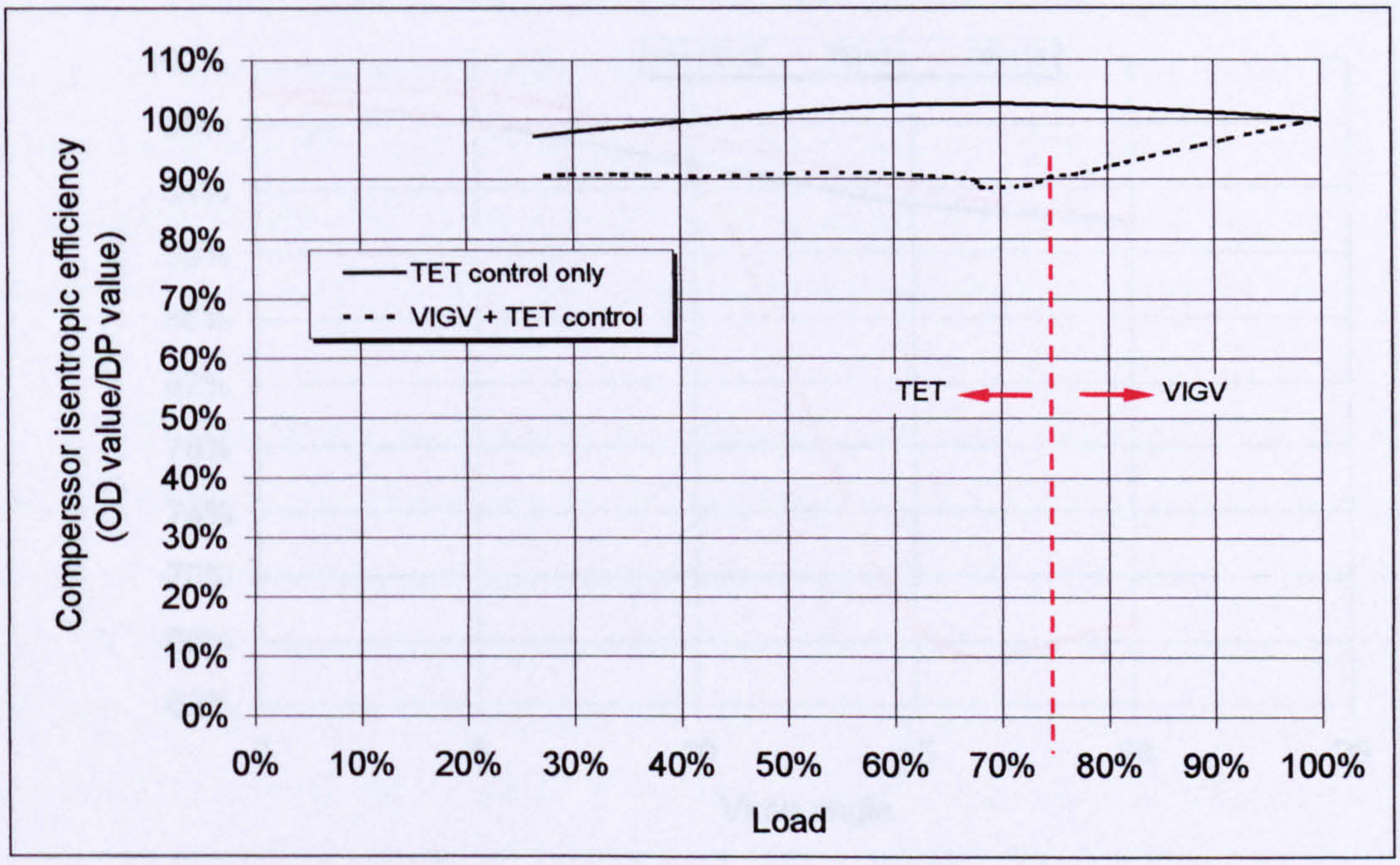

Figure 65 – Compressor isentropic efficiency variation with load for the EFGT cycle

When the VIGVs of a compressor are positioned at an angle different from their design-point angle, the map of characteristics of the compressor displaces up or down,

depending on whether the VIGVs are closing or opening. This displacement alters the operating parameters of the compressor, and is very difficult to be accurately calculated.

GateCycle® uses especial formulae for calculating the new mass flow, pressure ratio, and efficiency for the new VIGVs angle (Enter Software, Inc., 1995). These relationships are based on the original map of characteristics of the compressor being used, plus several inputs from the user of the software. This introduces a great amount of inaccuracies to the results calculated by these formulae. Even if the user has had previous experiences with VIGV variations on a specific compressor, it is very unlikely that a different compressor would behave in the same manner.

Figure 66 shows the variation of the isentropic efficiency as a function of the compressor VIGVs angle for an EFGT cycle. The map for pressure ratios less than eight (PR<8) has been used in the present work, for the optimised design of this cycle has a pressure ratio of around 6.5; it is seen that this map gives sensible results for this cycle. The map of characteristics for pressure ratio 18 (PR=18) does not encourage its use for such low pressure ratios. However, for the conventional NGGT cycle all the maps behave in a sensible way (Figure 67).

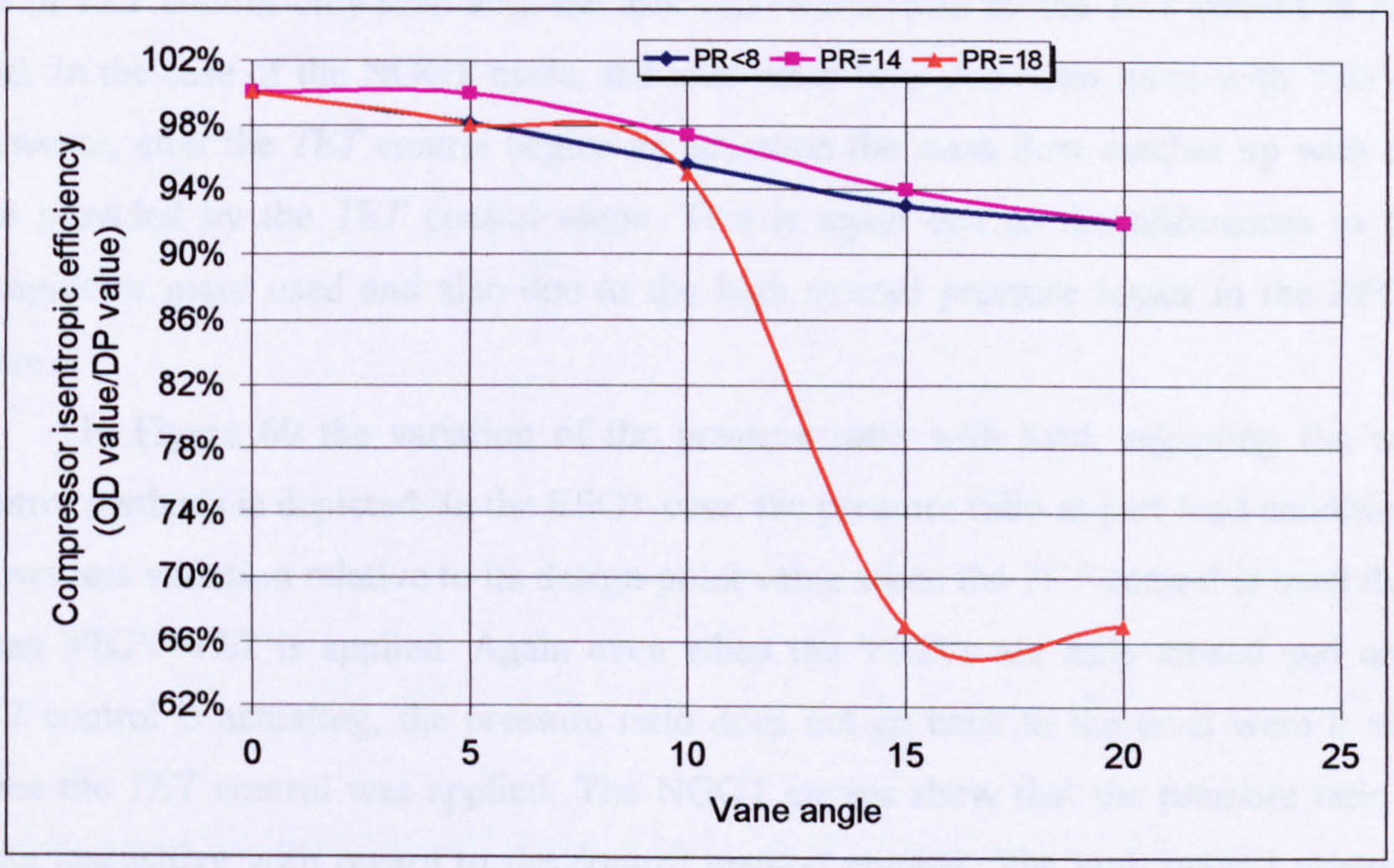

Figure 66 – Compressor isentropic efficiency as a function of the VIGVs angle for different compressors in an EFGT cycle

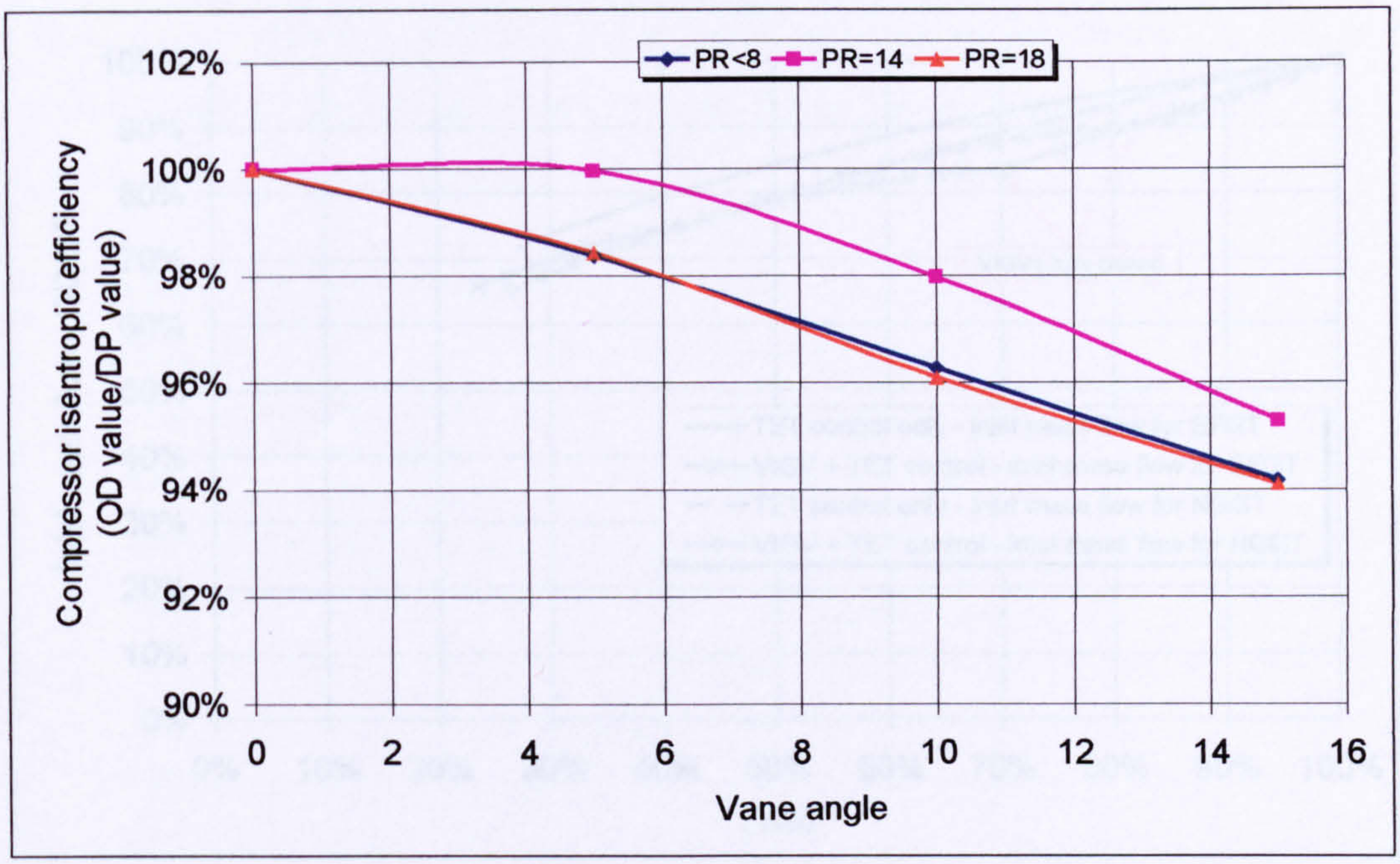

Figure 67 - Compressor isentropic efficiency as a function of the VIGVs angle for different compressors in a NGGT cycle

The variation of the inlet air mass flow is shown in Figure 68. The curves regarding the EFGT cycle demonstrate that the inlet mass flow decreases less with the use of *TET* control only than with the use VIGVs followed by the *TET* control at part load. In the case of the NGGT cycle, the inlet mass flow decreases more with VIGVs. However, after the *TET* control begins its actuation the mass flow catches up with the one provided by the *TET* control alone. This is again due to the differences in the compressor maps used and also due to the high overall pressure losses in the EFGT cycle.

In Figure 69 the variation of the pressure ratio with load, regarding the two control methods is depicted. In the EFGT case, the pressure ratio at part load conditions shows less variation relative to its design-point value when the *TET* control is used than when VIGV+*TET* is applied. Again even when the VIGVs are fully closed and only *TET* control is actuating, the pressure ratio does not go back to the level were it was when the *TET* control was applied. The NGGT curves show that the pressure ratio is quite insensitive with regard to the control method applied. The high overall pressure losses in the EFGT cycle explain the difference of behaviour between this cycle and the NGGT cycle.

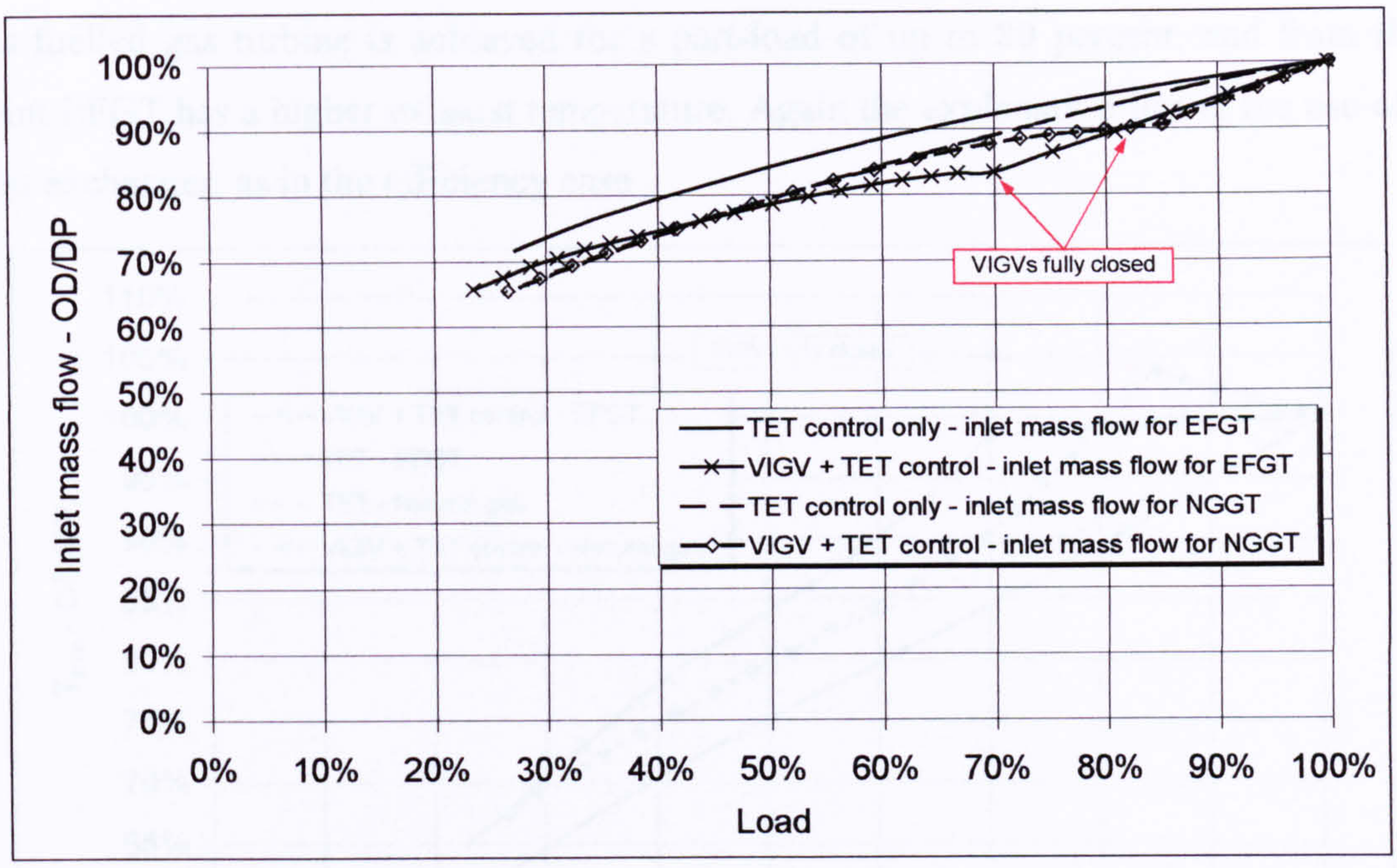

Figure 68 – Inlet mass flow behaviour with *TET* control and VIGV+*TET* control for the NGGT and the EFGT cycles

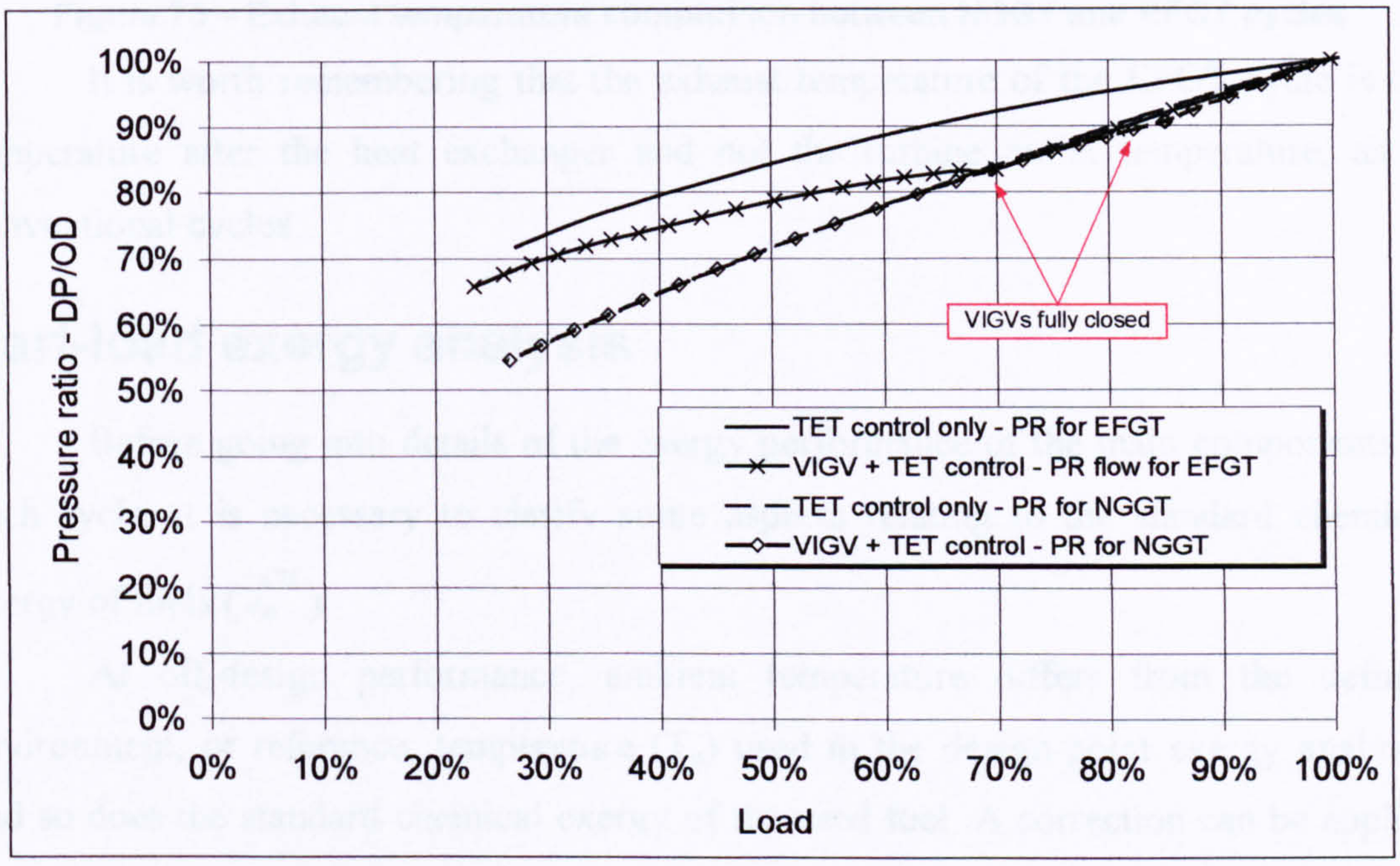

Figure 69 – Pressure ratio behaviour with *TET* control and VIGV+*TET* control for the NGGT and the EFGT cycles

An interesting data for combined cycle applications is the exhaust temperature at part-load (Figure 70). When *TET* control is applied the NGGT cycle has a higher T_{exh} than the EFGT, indicating that a better performance for combined cycle using natural

gas fuelled gas turbine is achieved for a part-load of up to 80 percent, and from that point EFGT has a higher exhaust temperature. Again the explanation lies in the use of a heat exchanger, as in the efficiency case.

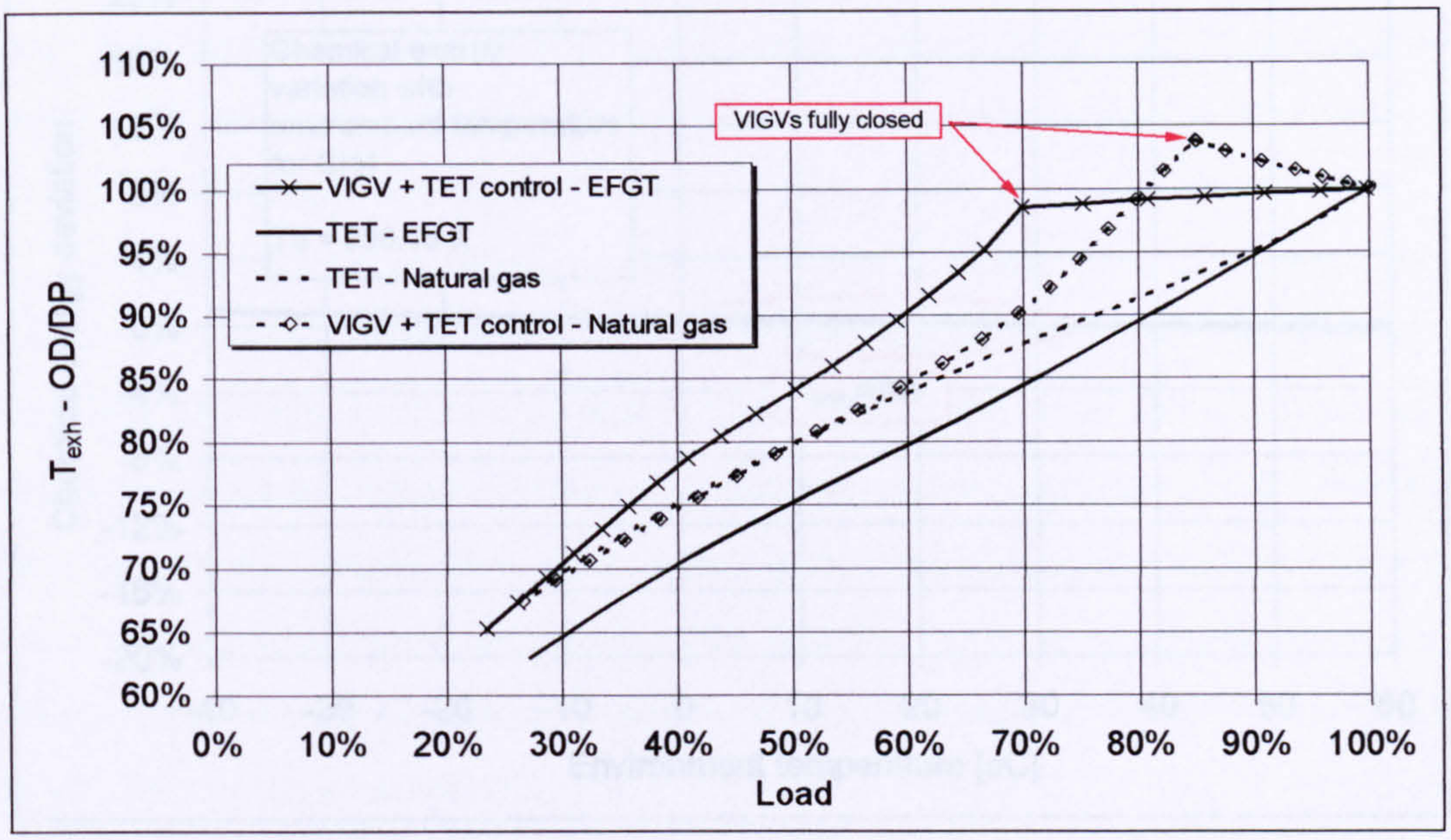

Figure 70 – Exhaust temperature comparison between NGGT and EFGT cycles

It is worth remembering that the exhaust temperature of the EFGT cycle is the temperature after the heat exchanger and not the turbine outlet temperature, as in conventional cycles.

Part-load exergy analysis

Before going into details of the exergy performance of the main components of each cycle, it is necessary to clarify some aspects relating to the standard chemical exergy of fuels ($\overline{e}_o^{CH}$).

At off-design performance, ambient temperature differs from the defined environment, or reference, temperature (T_o) used in the design-point exergy analysis, and so does the standard chemical exergy of the used fuel. A correction can be applied to this variation as suggested by Kotas, T. J., 1985.

However, in this work it is assumed that this change is negligible. Using the same expression proposed by Kotas, T. J., 1985, it is possible to demonstrate that, indeed, within the ambient temperature range of this work, the influence of T_{amb} in the

standard chemical exergy of the fuel can be neglected without major consequences to the results (Figure 71).

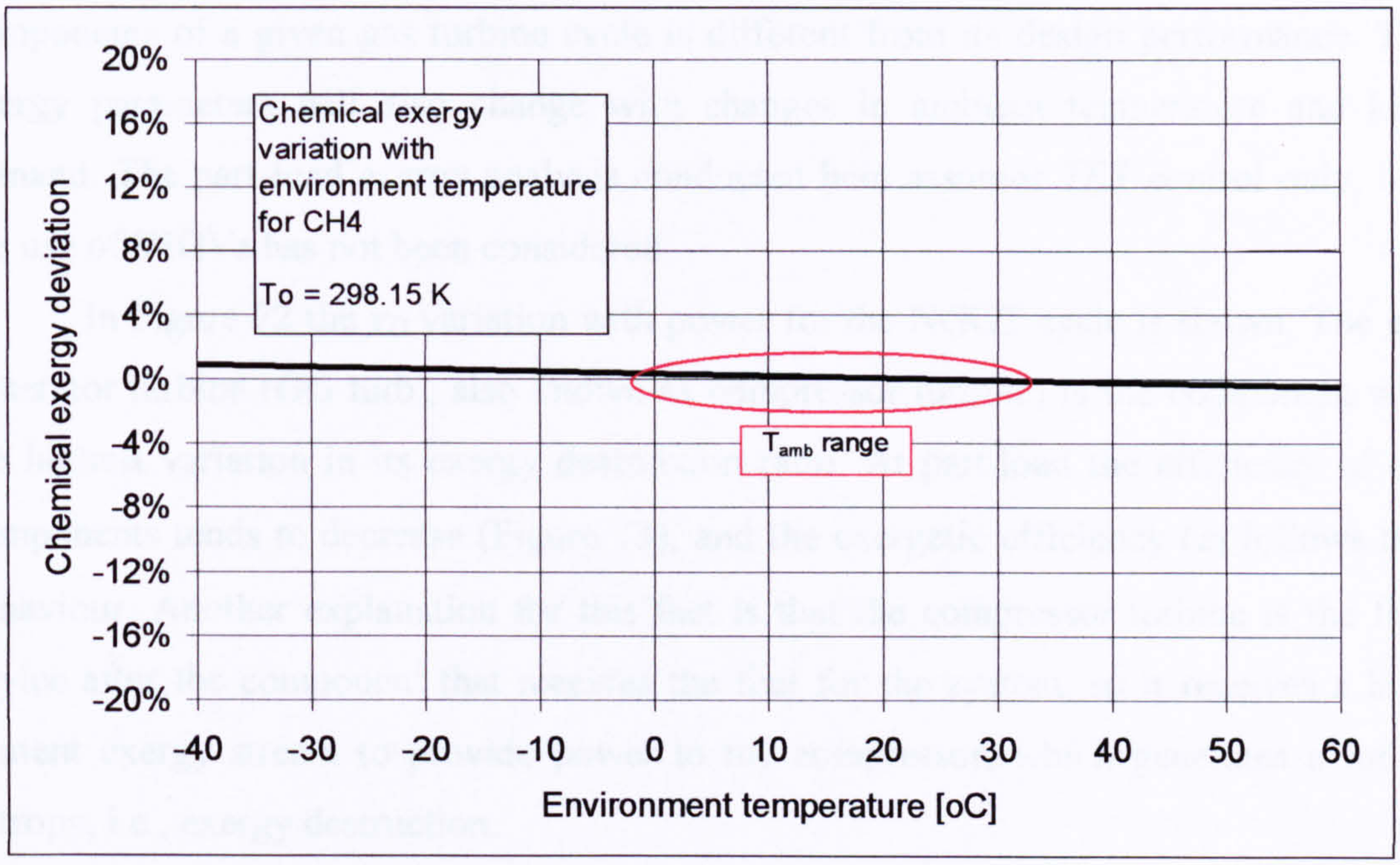

Figure 71 – Effect of T_{amb} on the standard chemical exergy of CH_4

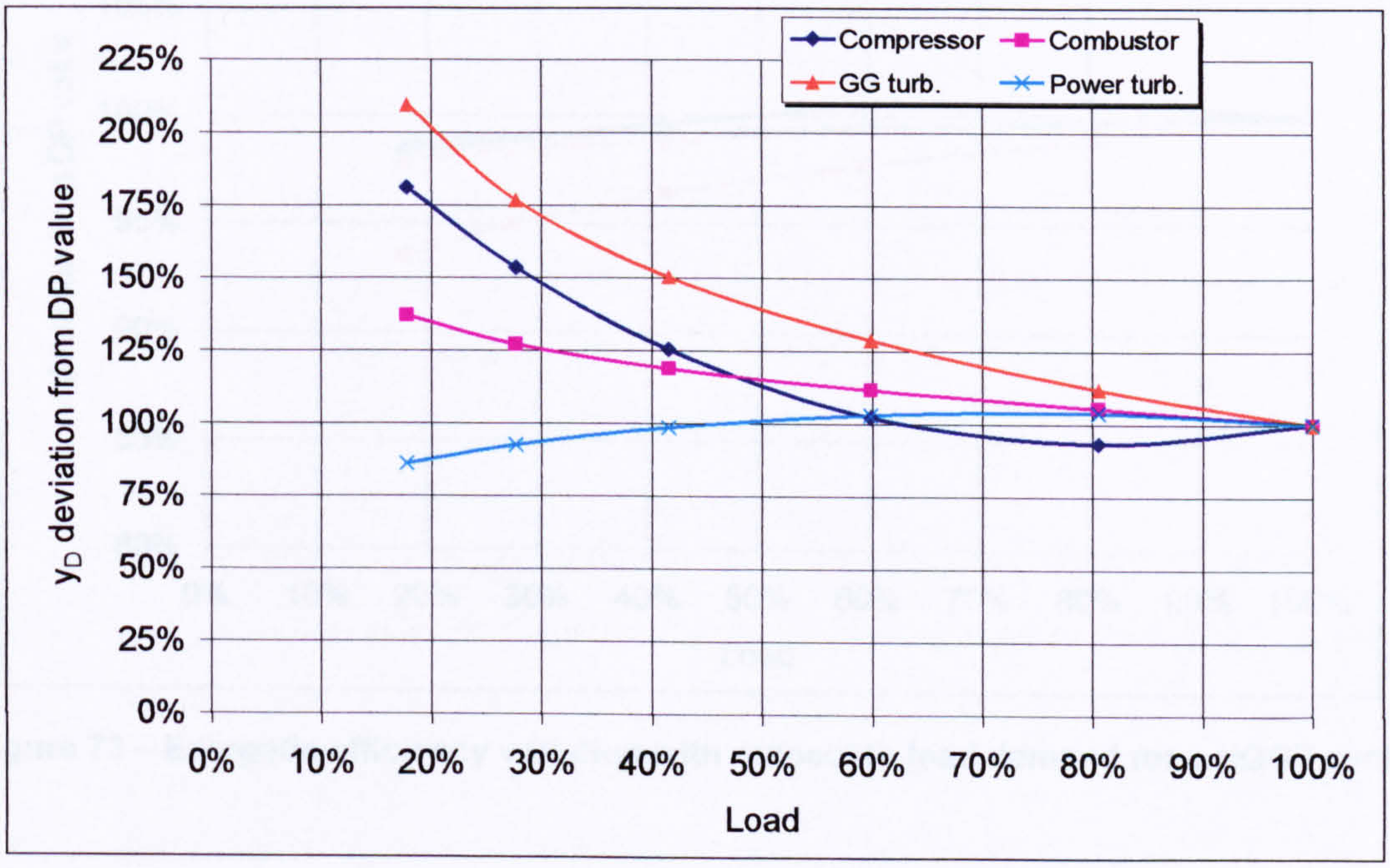

Figure 72 – Part-load exergy destruction ratio for the NGGT cycle

Exergy destruction ratio at part-load operation

As previously mentioned, at off-design conditions the behaviour of the components of a given gas turbine cycle is different from its design performance. The exergy parameters will also change with changes in ambient temperature and load demand. The part-load exergy analysis conducted here assumes *TET* control only, i.e., the use of VIGVs has not been considered.

In Figure 72 the y_D variation with power for the NGGT cycle is shown. The gas generator turbine (GG turb., also known as compressor turbine) is the component with the highest variation in its exergy destruction ratio. At part-load the efficiency of the components tends to decrease (Figure 73), and the exergetic efficiency (ε) follows this behaviour. Another explanation for this fact is that the compressor turbine is the first device after the component that receives the fuel for the system, so it receives a high content exergy stream to provide power to the compressor, which generates a lot of entropy, i.e., exergy destruction.

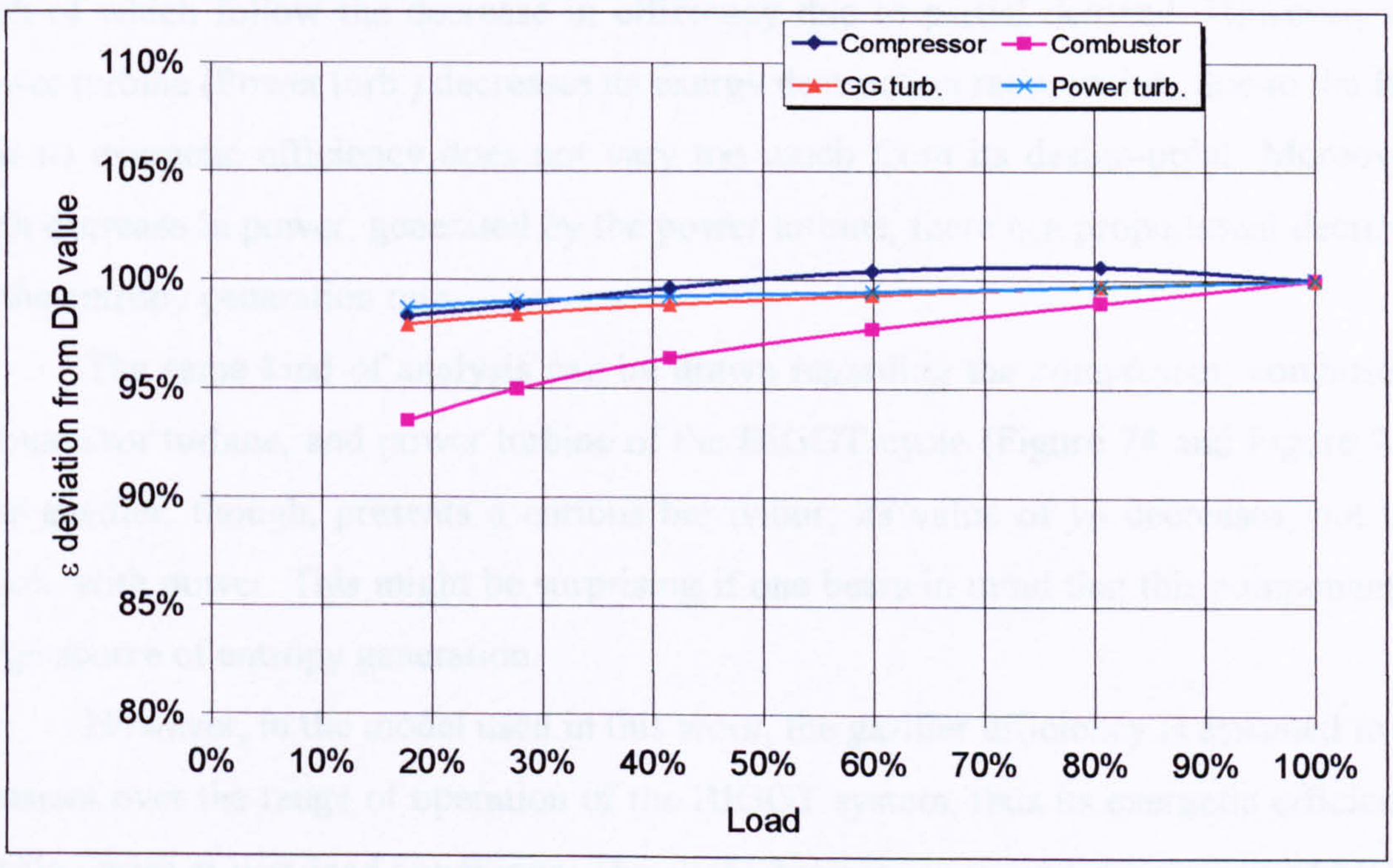

Figure 73 – Exergetic efficiency variation with respect to load demand for a NGGT cycle

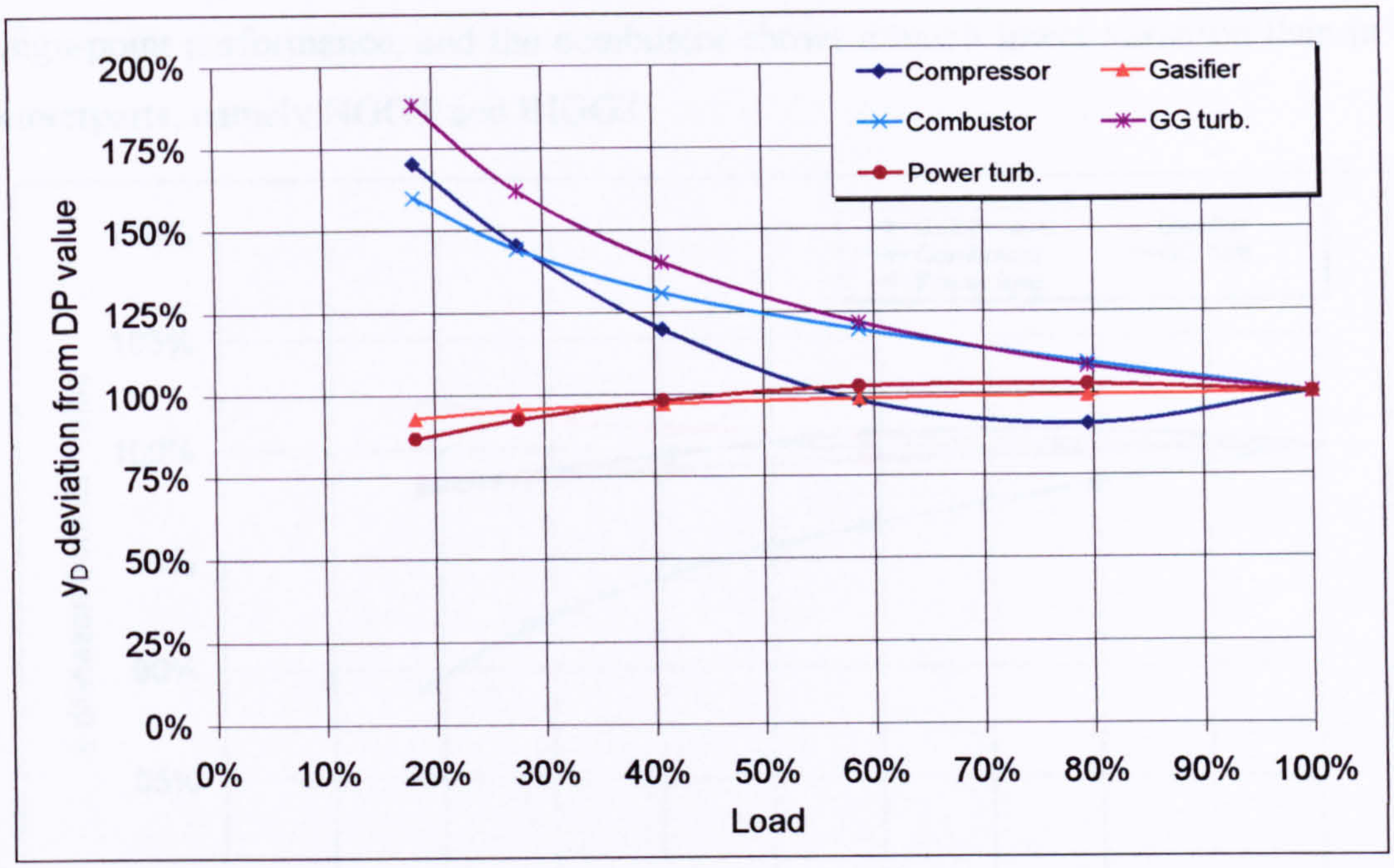

Figure 74 – Part-load exergy destruction ratio for the BIGGT cycle

The same behaviour can be observed for the compressor and the combustor; both of which follow the decrease in efficiency due to partial demand. However, the power turbine (Power turb.) decreases its exergy destruction ratio, mainly due to the fact that its exergetic efficiency does not vary too much from its design-point. Moreover, with decrease in power, generated by the power turbine, there is a proportional decrease in the entropy generation rate.

The same kind of analysis can be drawn regarding the compressor, combustor, compressor turbine, and power turbine of the BIGGT cycle (Figure 74 and Figure 75). The gasifier, though, presents a curious behaviour; its value of y_D decreases, not too much, with power. This might be surprising if one bears in mind that this component is large source of entropy generation.

However, in the model used in this work, the gasifier efficiency is assumed to be constant over the range of operation of the BIGGT system, thus its exergetic efficiency hardly varies at part-load conditions. The slight decrease in y_D and ε is explained by the fact that at low power settings less fuel is demanded from the engine, therefore the entropy generation rate during the gasification process is lower.

Regarding the EFGT cycle (Figure 76 and Figure 77), two main observations can be made. The ceramic heat exchanger (CerHx) doesn't move too far from its

design-point performance, and the combustor shows a much lower variation than in its counterparts, namely NGGT and BIGGT.

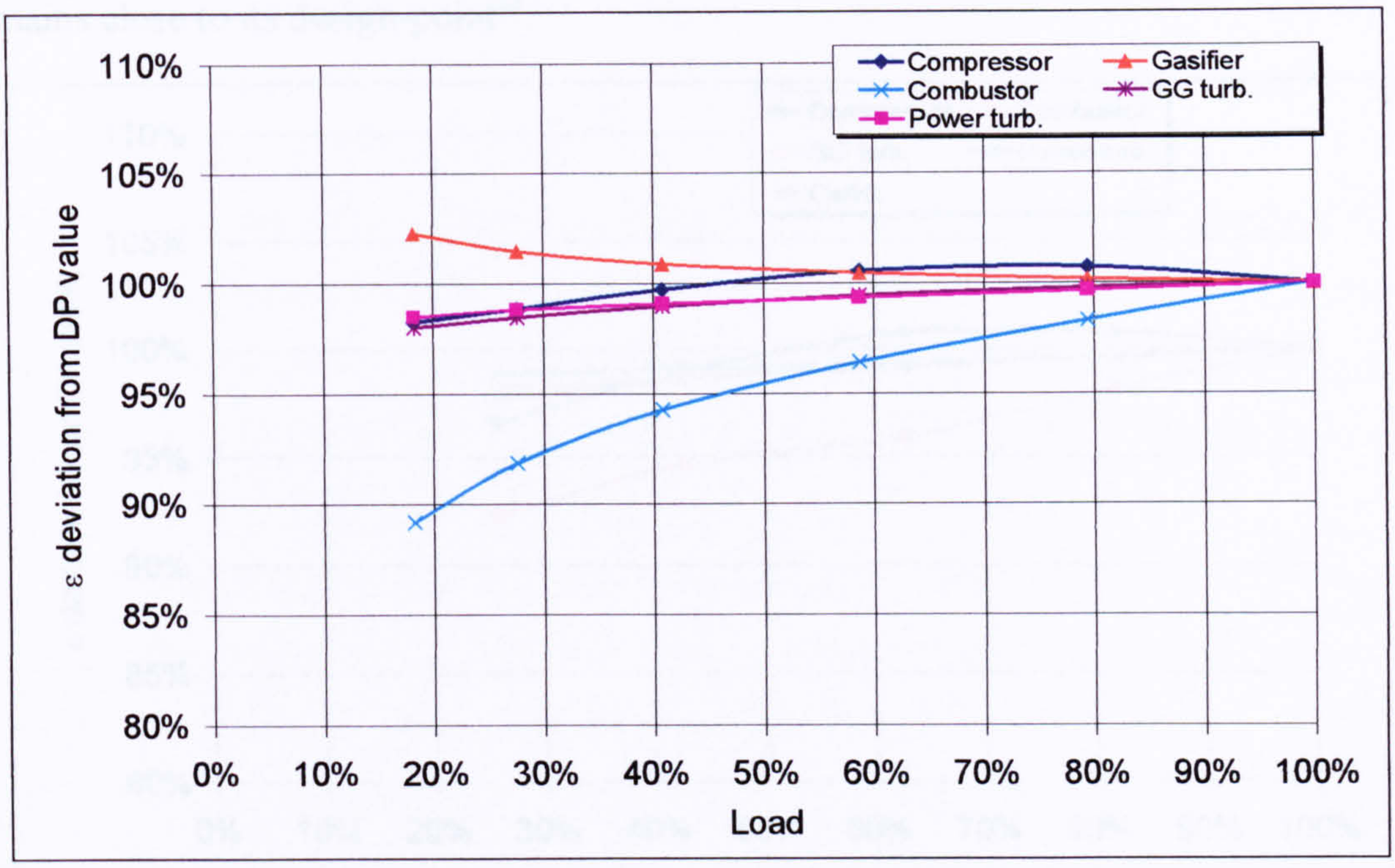

Figure 75 – Exergetic efficiency variation with respect to load demand for a BIGGT cycle

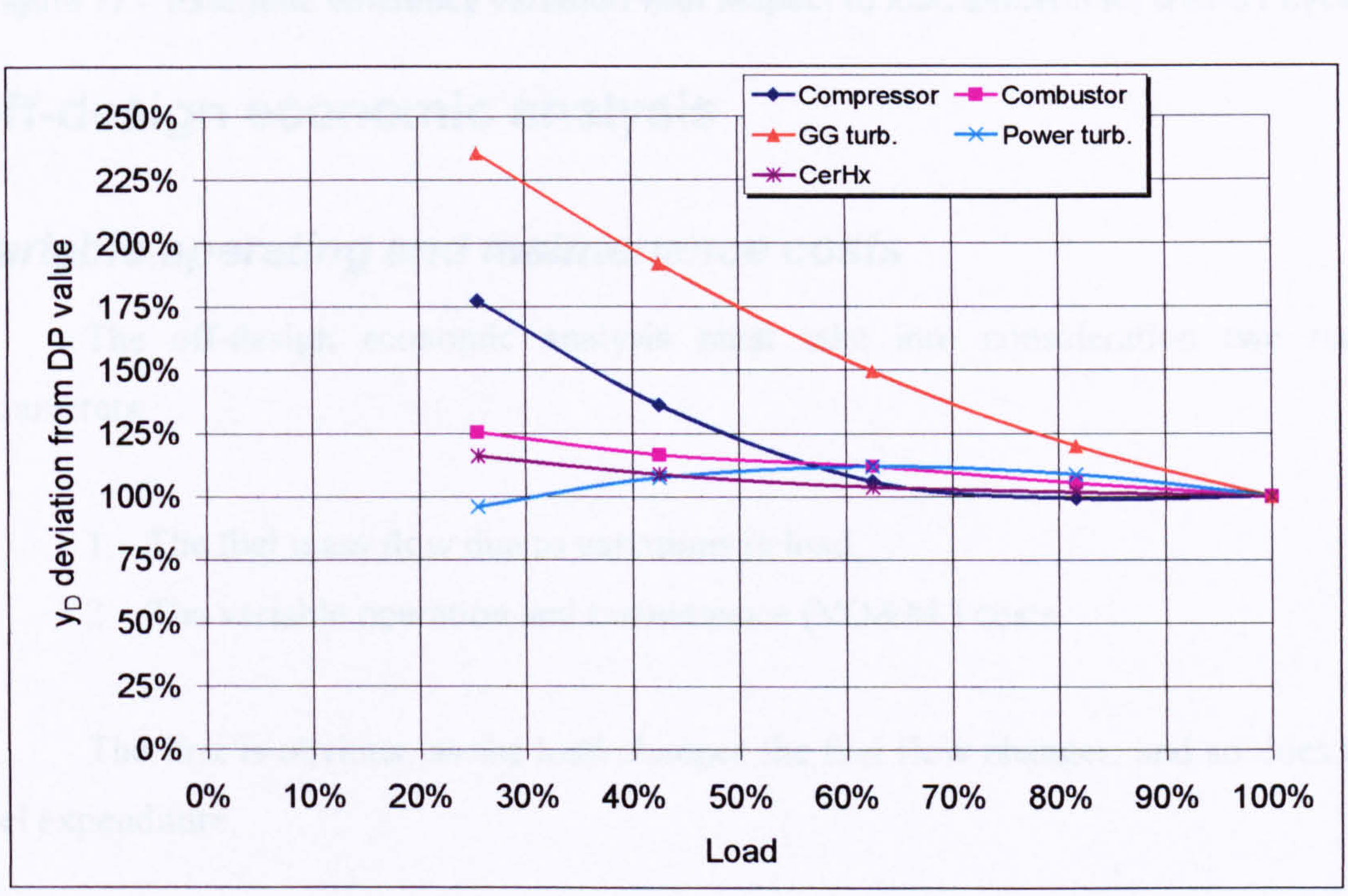

Figure 76 – Part-load exergy destruction ratio for the EFGT cycle

In the combustor case this happens because the air going into this device is preheated, and, as mentioned previously, one of the ways to decrease exergy destruction

in the combustor is to preheat the oxidant and/or the fuel. In the heat exchanger case, its effectiveness does not change significantly; consequently its exergetic efficiency remains close to its design-point[35].

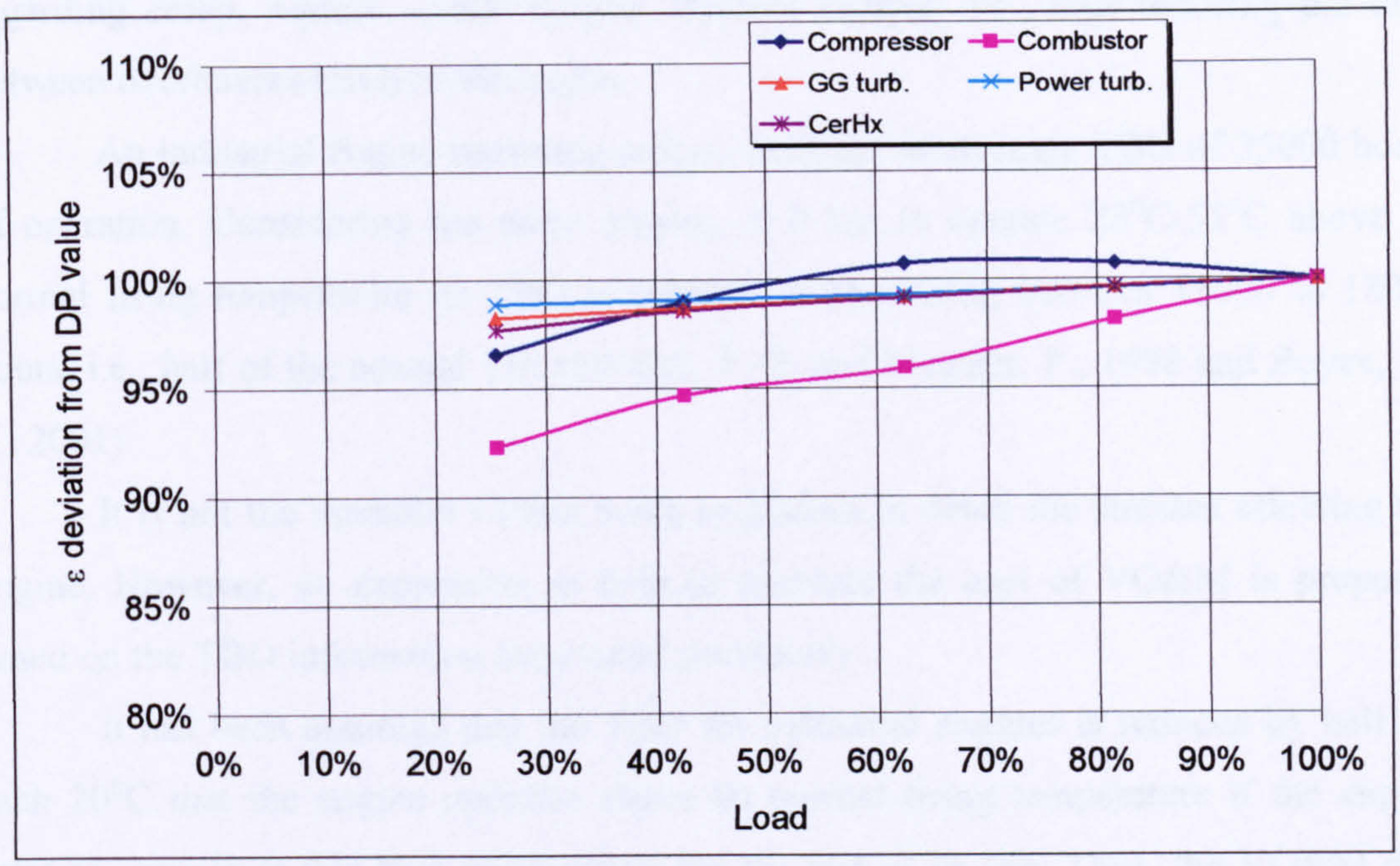

Figure 77 – Exergetic efficiency variation with respect to load demand for a EFGT cycle

Off-design economic analysis

Variable operating and maintenance costs

The off-design economic analysis must take into consideration two main parameters:

1. The fuel mass flow due to variations in load;
2. The variable operation and maintenance (VO&M) costs.

The first is obvious; as the load changes the fuel flow changes, and so does the fuel expenditure.

---

[35] For a comprehensive explanation on the off-design performance calculations for the heat exchanger, please refer to Enter Software, Inc., 1995

The second is more difficult to assess. Let us first consider that the demand is higher than the nominal power and that no power augmentation device is installed. To increase power output the engine *TET* must be increased. This causes problems regarding creep, rupture, cyclic fatigue, thermal fatigue, etc., thus reducing the time between overhauls (TBO) of the engine.

An industrial engine operating at base load has an average TBO of 35000 hours of operation. Considering the same engine, if it has to operate 28°C-55°C above its normal firing temperature its TBO is reduced to something between 15000 to 18000 hours, i.e., half of the normal TBO (Walsh, P. P. and Fletcher, P., 1998 and Boyce, M. P., 2001).

It is not the intention of this work to discuss in detail the stresses affecting the engine. However, an expression to help to estimate the cost of VO&M is proposed based on the TBO information mentioned previously.

It has been assumed that the TBO for industrial engines is reduced by half for each 20°C that the engine operates above its normal firing temperature if the engine were to operate at this high temperature for the rest of its life. Thus, the VO&M cost would double in that situation. When the engine operates below its normal firing temperature the TBO is not affected. It has also been assumed that the hot parts of the engine are the main cause of stoppage.

Thus:

$$if \begin{cases} \Delta TET \le 0.0 \Rightarrow VO\&M_{OD} = VO\&M_{DP} \\ \Delta TET > 0.0 \Rightarrow VO\&M_{OD} = VO\&M_{DP} \times \left(1 + \frac{t_{op}}{TBO}\right)^{k} \end{cases} \qquad \textbf{[79]}$$

where $k = \dfrac{\Delta TET}{\Delta TET_{ref}}$;

$\Delta TET \equiv$ difference between the DP *TET* and the OD *TET*, i.e., $TET_{OD} - TET_{DP}$;

$\Delta TET_{ref} \equiv$ temperature difference used as reference, in this case $\Delta TET_{ref} = 20^{o}C$;

$t_{op} \equiv$ time the engine operated at off-design *TET*;

$OD \equiv$ refers to off-design point;

$DP \equiv$ refers to design-point.

Equation **[79]** is depicted in Figure 78. It is clearly seen how an increase in *TET* to attend demand is reflected in the VO&M costs. This figure considers an operation time equal to the TBO of the engine; however, it is extremely unlikely that the engine will operate for long periods under *TET*s above its design-point value, mainly due to creep and temperature variations in the hot sections of the engine (Cookson, 2001). In general at peak-load the engine will operate for few minutes (maybe few hours) under such conditions.

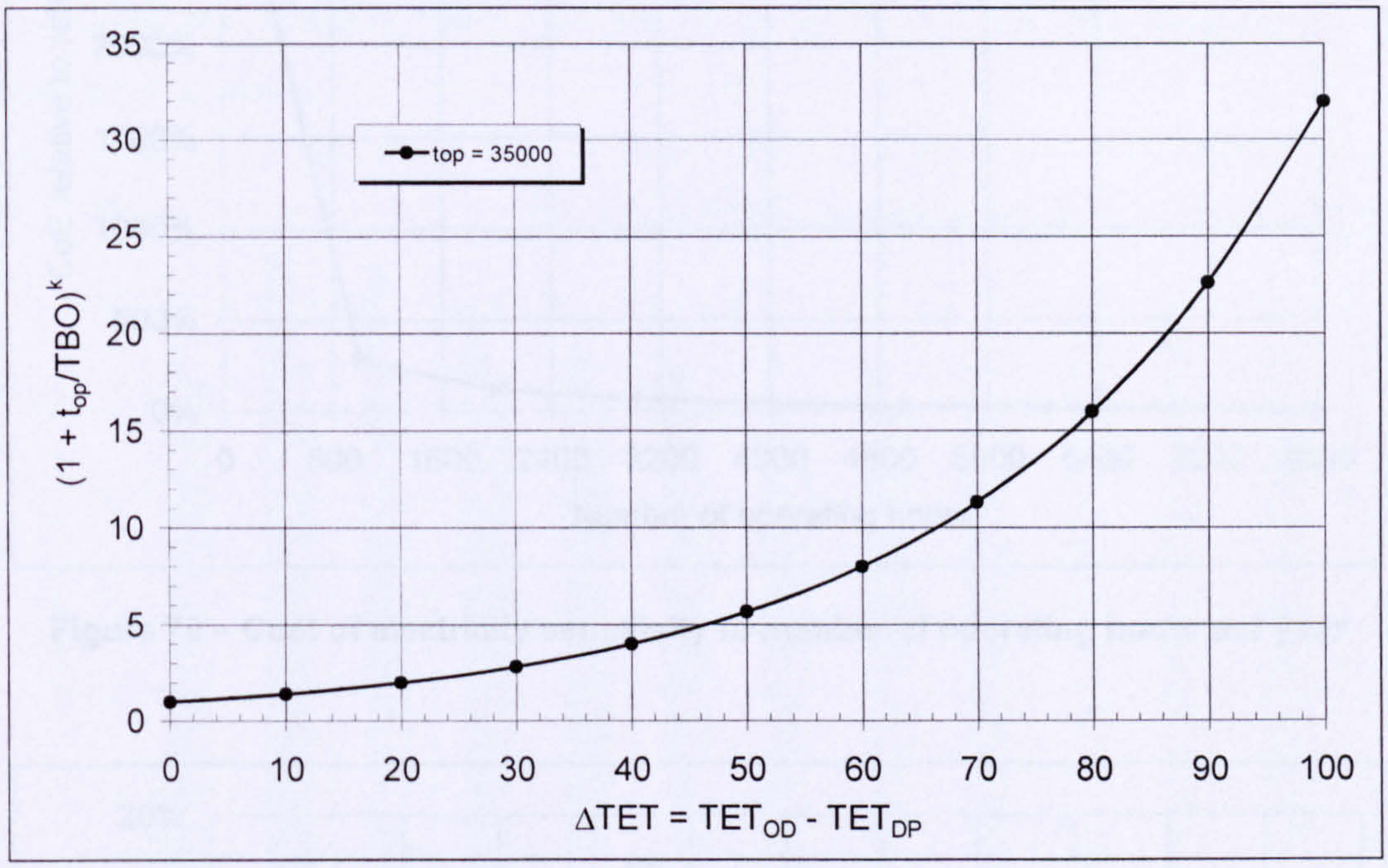

Figure 78 – Increase in the VO&M costs as a function of off-design *TET*

It is also interesting to see how the cost of electricity changes with the number of operating hours during a year. Figure 79 shows such an analysis for a natural gas fired simple cycle. It can be seen that an engine that would operate as a peak-load machine four hours a day would mean an increase in CoE of more than 200 percent.

Such an analysis is not meaningful for the BIGGT and EFGT cases. For the first, purchased-equipment costs are too high, and for the second, thermal inertia is too large to supply immediate electricity demand.

The demand curve

For the OD economic analysis it is assumed that the demand curve is the same regardless of the location; the only parameter which changes is the ambient temperature. The demand curve (Figure 80) has been obtained from a major Brazilian power

producer and for confidentiality reasons its name will not be mentioned; suffice to say that this electricity supplier attends major cities in the country. This demand curve shows the monthly average for electricity consumption.

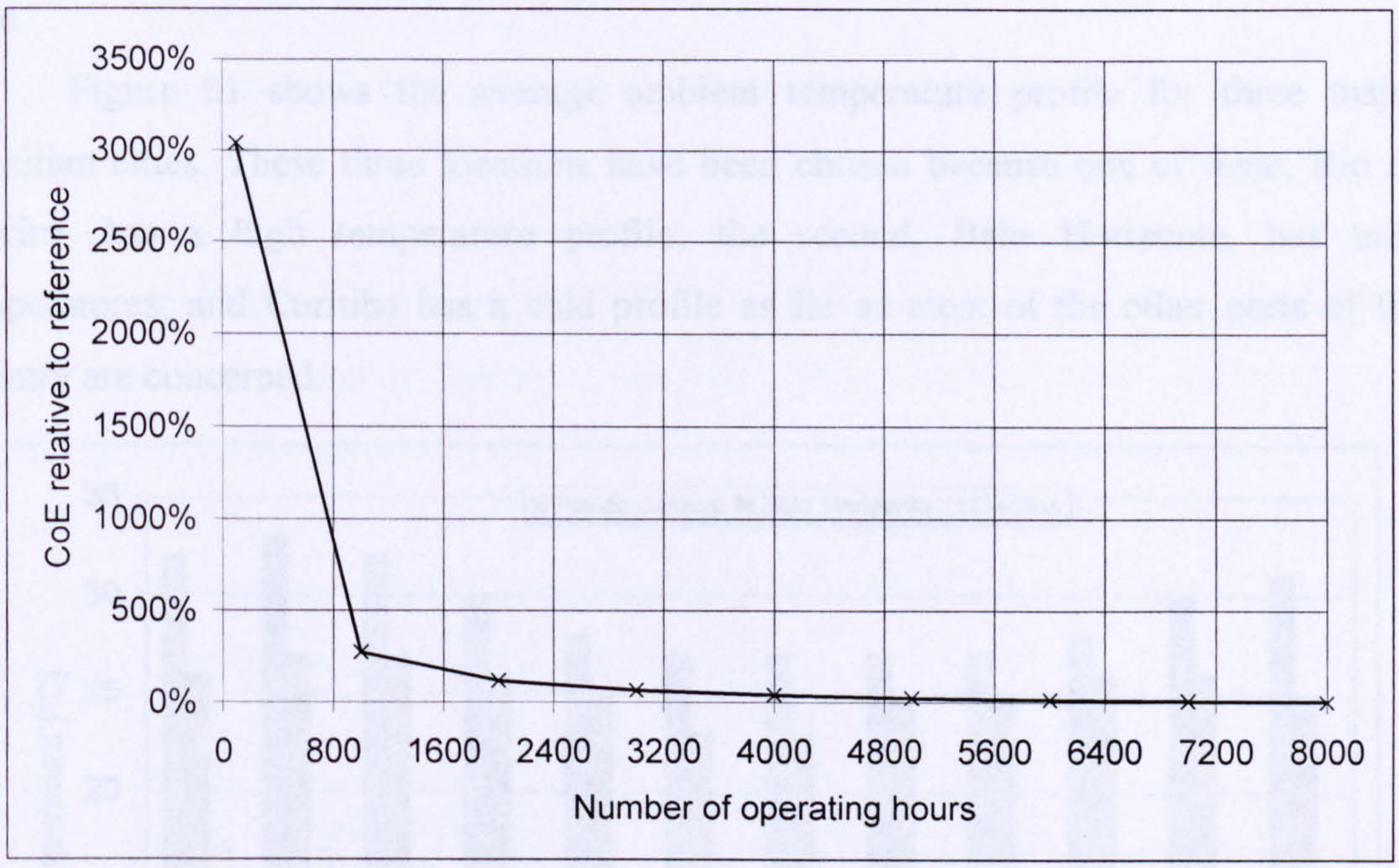

Figure 79 – Cost of electricity sensitivity to number of operating hours per year

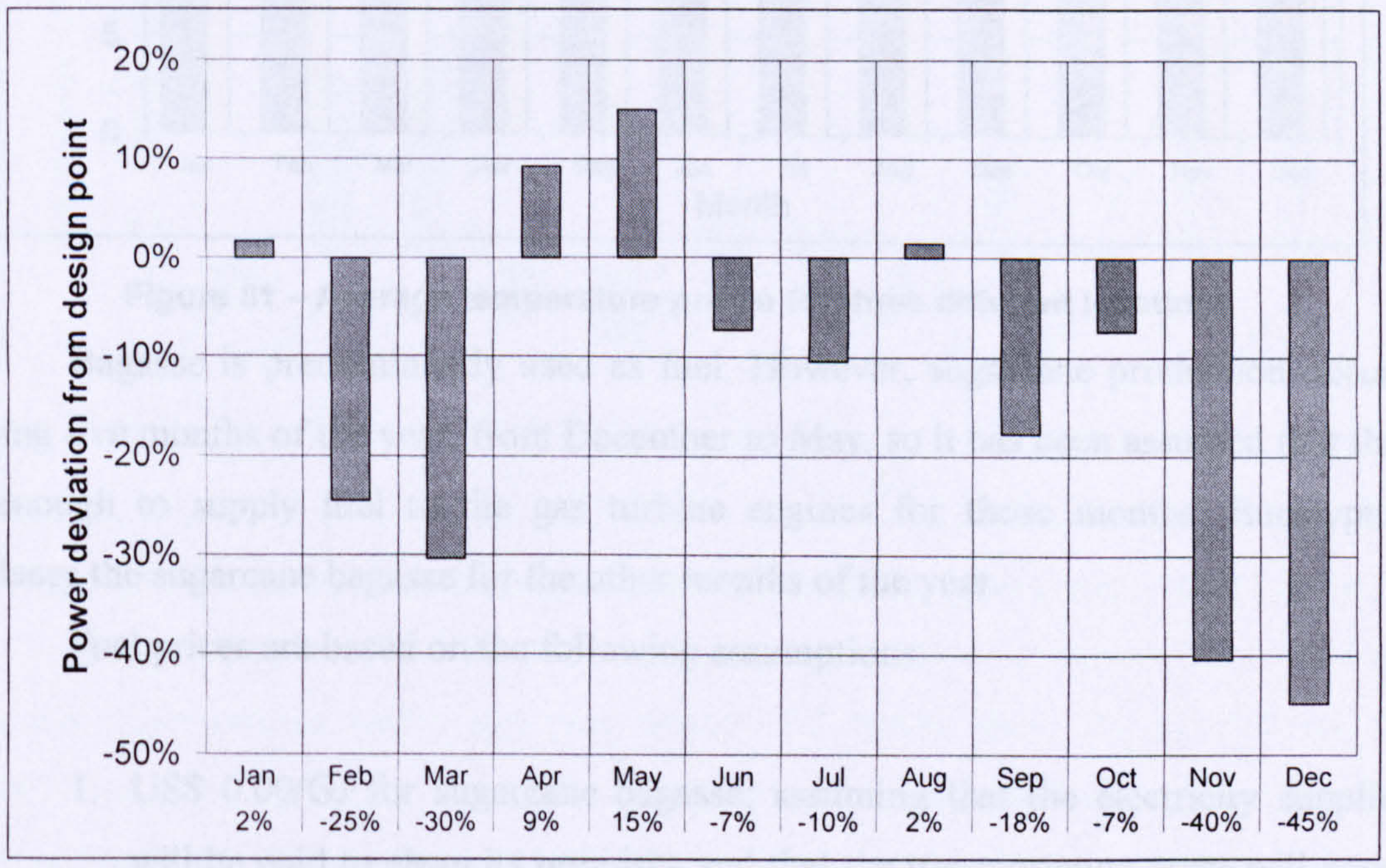

Figure 80 – Typical electricity demand curve in south-eastern region of Brazil

The aim is to assess the cost of electricity for each month. It is assumed that the engine operates at the monthly number of hours at that power setting. However, using the method described earlier this calculation can be conducted for different periods of time.

Figure 81 shows the average ambient temperature profile for three major Brazilian cities. These three locations have been chosen because one of them, Rio de Janeiro, has a high temperature profile; the second, Belo Horizonte, has mild temperatures; and Curitiba has a cold profile as far as most of the other parts of the country are concerned.

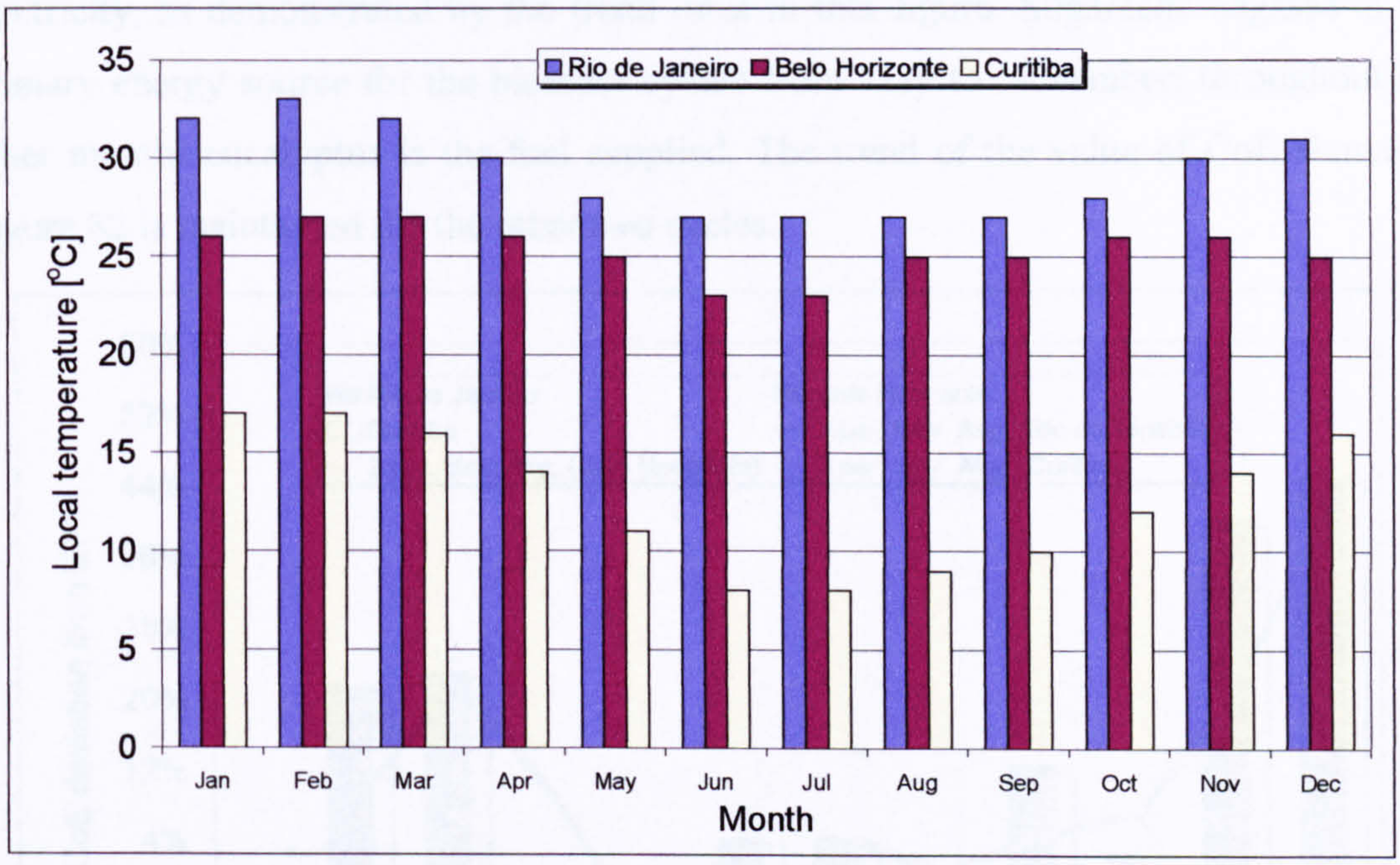

Figure 81 – Average temperature profile for three different locations

Bagasse is predominantly used as fuel. However, sugarcane production occurs during five months of the year, from December to May, so it has been assumed that that is enough to supply fuel to the gas turbine engines for those months. Eucalyptus replaces the sugarcane bagasse for the other months of the year.

Fuel prices are based on the following assumptions:

1. US$ 0.00/GJ for sugarcane bagasse; assuming that the electricity supplier will be paid to clean its premises and that the transportation costs will equal the amount paid.

2. US$ 2.00/GJ for eucalyptus; assuming a worst case scenario. According to Lora et al. 2000b, the prices for eucalyptus range from US$ 0.54/GJ to US$ 2.19/GJ depending on the region and plantation technology, so the value chosen is considered sensible.
3. US$ 4.00/GJ for natural gas. That is the average price for natural gas in Brazil.

Figure 82 shows the monthly CoE for each location. It is seen that, for the same demand curve, ambient temperature does not have a great impact on the cost of electricity, as demonstrated by the trend lines in that figure. Sugarcane bagasse is the primary energy source for the biomass cycles from May to November; throughout the other months eucalyptus is the fuel supplied. The trend of the value of CoE shown in Figure 82 is maintained for the other two cycles.

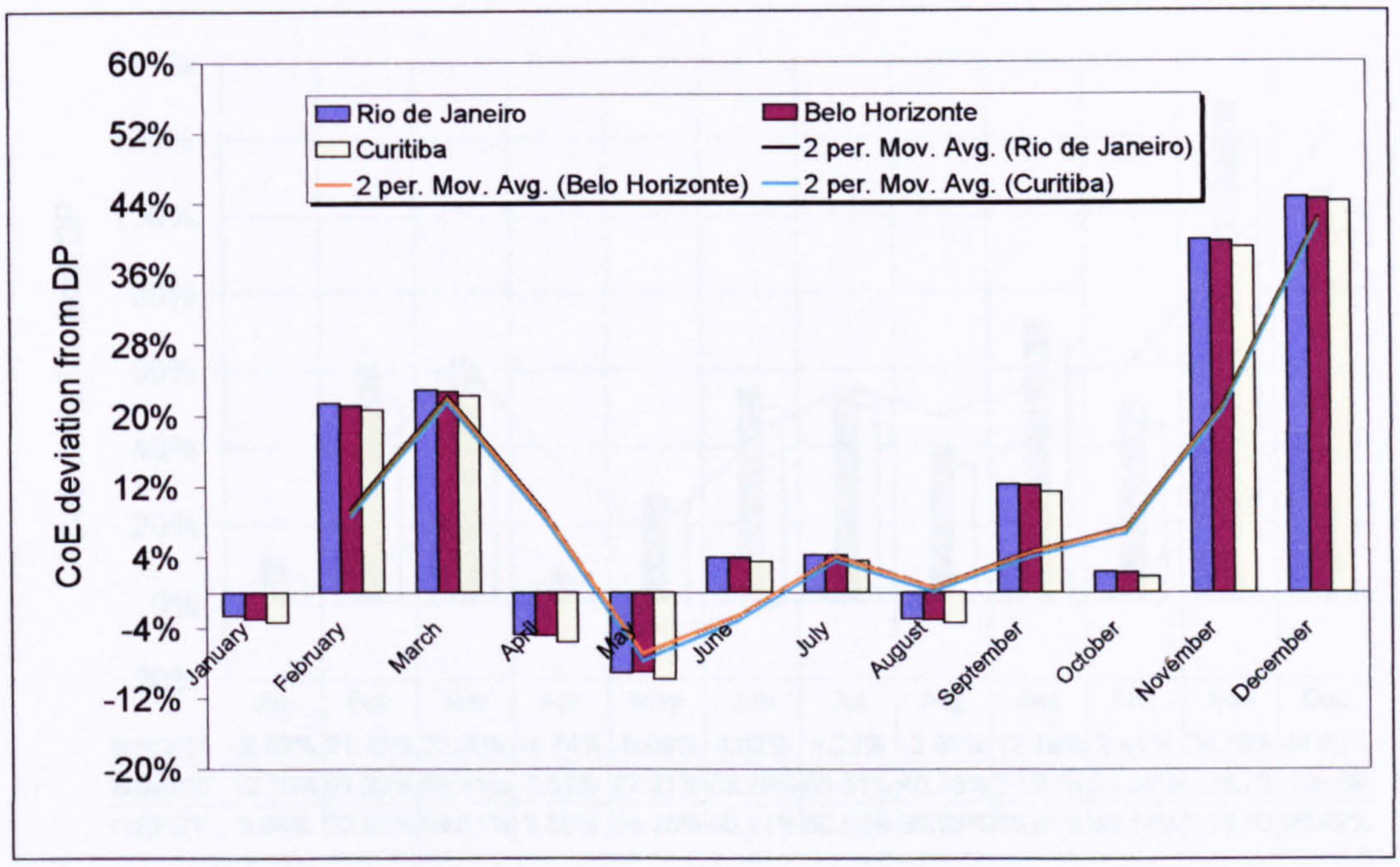

Figure 82 – Monthly cost of electricity for each location when using a NGGT cycle

Figure 83 shows the CoE when each cycle operates at various load demands and ambient temperatures within one-year period. All cycles show the same trend, the NGGT being the cycle that shows the lowest variation from the design-point CoE. The interesting fact is that the lowest CoE is found for the highest power settings, and vice-versa. This suggests that the variation in *TET* to attend the power demanded has little

influence on the final CoE. The only parameters that seem to have an impact on the CoE value are the fuel utilisation, and the purchased-equipment costs.

Even thermal efficiency does not seem to influence the value of CoE, indicating that for a short-term period it would be worthwhile maintaining the engine at high temperatures without any great impact on the final CoE.

However, it can be observed that the design-point economic analysis is not enough to give a clear picture of the costs of a power plant during its lifetime, and a more detailed, maybe a real-time, evaluation of these costs could have a great impact on the annual economic performance of the plant.

In an environment of fierce competition this real-time information about the real CoE could make a great difference to the financial life of the utility company. On the other hand the absence of such data could be disadvantageous during negotiations with buyers.

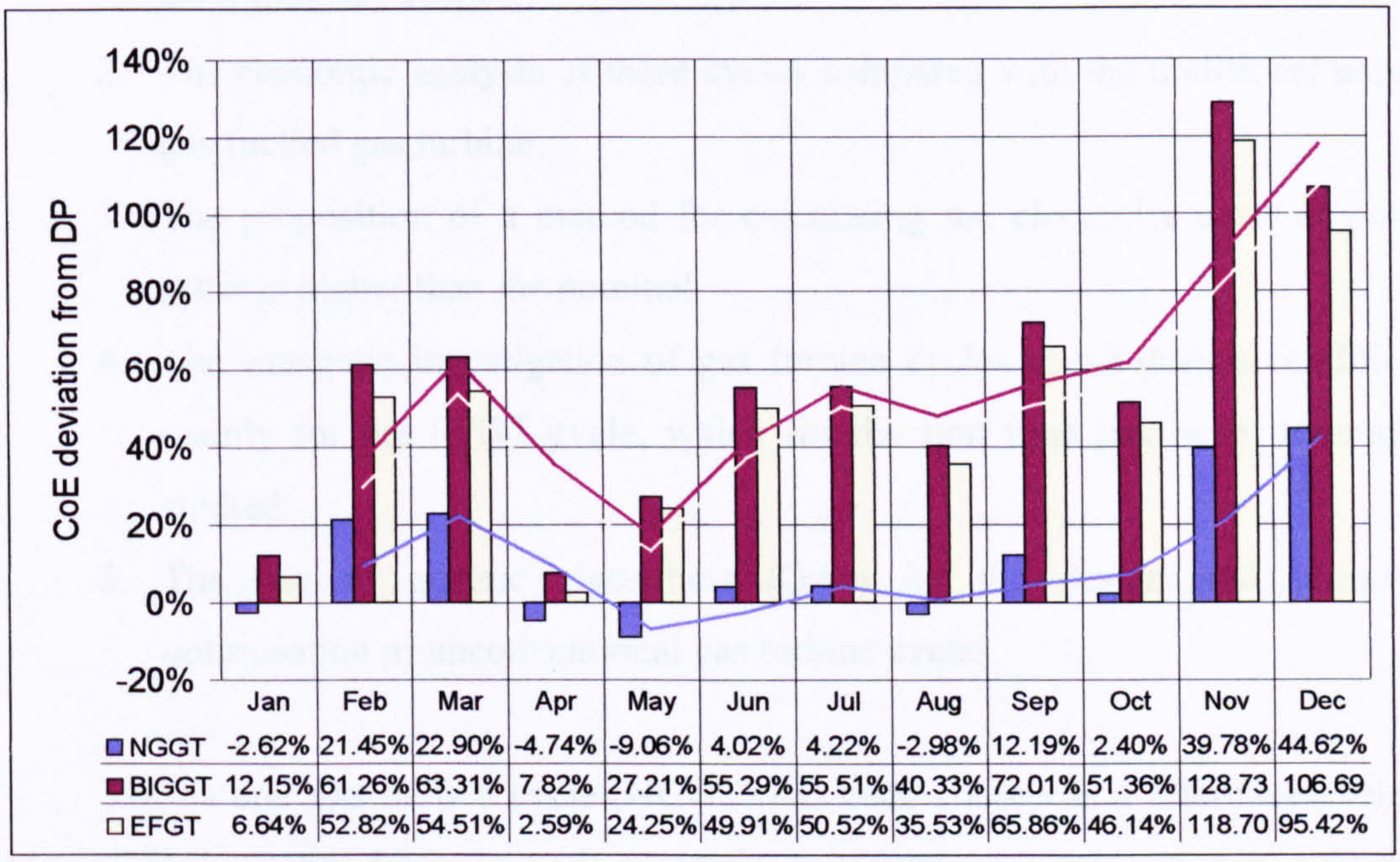

Figure 83 – Cost of electricity at different loads and ambient temperatures for each cycle

CHAPTER VII – CONCLUSIONS AND FURTHER WORK

Conclusions

The aim of this thesis, as mentioned in the introduction, is to propose, analyse, and compare new methods of using biomass fuels in gas turbines. The proposed cycles must be competitive with the current natural gas fuelled gas turbines, not only from the thermodynamic point of view, but also from the economic standpoint.

The main contributions of this work are:

1. The design and off-design assessment of alternative gas turbine cycles using solid biomass as fuel.
2. The economic analysis of these cycles compared with the traditional natural gas fuelled gas turbine.
3. The proposition of a method for calculating the electricity costs at power settings higher than the nominal.
4. The exergetic investigation of gas turbine cycles at off-design conditions, mainly for the EFGT cycle, which for the first time has been thoroughly studied.
5. The use of genetic algorithms (GAs) for the design and economic optimisation of unconventional gas turbine cycles.

The natural gas fuelled cycle (NGGT) has been chosen as a reference cycle in terms of both thermodynamic and economic performance. The biomass integrated gasification gas turbine cycle (BIGGT) and the externally fired gas turbine cycle (EFGT) have been compared with the NGGT system.

Two variants of the alternative cycles, the intercooled and recuperated biomass integrated gasification gas turbine (BIGICR), and the intercooled externally fired gas turbine (ICEFGT), have also been analysed. However, due to their complexity, the costs associated with these systems are higher than the costs associated with their basic configurations, namely BIGGT and EFGT.

Several aspects related to the chosen cycles were carefully studied, such as power delivered, thermal efficiency, exergetic analysis of individual components, as well as the whole cycle, emissions, purchased-equipment-costs, and cost of electricity. The summary of the findings for the studies carried out in this thesis will be summarised in the paragraphs that follow.

The design-point thermodynamic analysis revealed that the use of biomass fuels in gas turbines is feasible and the efficiency levels achieved can be as high as the natural gas cycle. The BIGGT cycle shows lower efficiency when compared with the NGGT and EFGT cycles due to the penalties imposed by the gasification and fuel cleaning systems. Nevertheless, it has reached a certain level of maturity that makes it possible to implement this technology, as demonstrated by the various projects in operation and in construction or analysis phase around the world, described earlier. The variants BIGICR and ICEFGT show higher efficiencies than their simple cycle counterparts, and are even comparable with the NGGT cycle at certain pressure ratios. However, they are very complex and expensive cycles.

The EFGT cycle proved to be more efficient than the BIGGT cycle. Furthermore, its efficiency is comparable with that of the NGGT cycle within a certain temperature and pressure ratio range. The technology level of this cycle has not allowed it to become commercially available yet, mainly due to material constraints. However, due to its very promising performance, several researchers are looking at materials that could withstand the high temperatures demanded in order to achieve performance levels comparable with ordinary cycles. The prospects are good and the best material for this application seems to be ceramics.

The effect of bleeding on the cycles has also been studied, and it has been revealed that the EFGT cycle is more sensitive to bleeding than its two other counterparts. An average decrease of 2 percent in thermal efficiency per 2 percent increase in the amount bled from the compressor has been estimated. The other two cycles – NGGT and BIGGT – are much less sensitive to bleeding. This is due to the fact that the *Cp* of the air is considerably lower than the *Cp* of the combustion gases. When the "cold" air bled from the compressor mixes with the hot air from the heat exchanger, for the EFGT cycle, its specific heat decreases further than in the case of the other two

cycles, NGGT and BIGGT, where the mixture is between the combustion products, which have a high *Cp*, and the air, producing a mixture with a higher *Cp*.

The heat exchanger in the EFGT is the critical component in this cycle. The analysis of the use of intercooling in the EFGT cycle showed that too high a decrease in the compressor delivery temperature leads the combustor to increase its exit temperature to unbearable limits for the ceramic heat exchanger. This component also introduces pressure losses that make this cycle more sensitive to off-design behaviour than normal gas turbine cycles.

In the BIGGT cycle the fuel compressor is a major power consumer due to the very large amount of fuel to be injected into the combustion chamber. The power demanded for fuel compression is up to 27 percent of the shaft power in the free power turbine. The use of pressurised gasification systems may decrease this value. However, it is worth pointing out that this type of gasification system must considerably increase the already high costs of the BIGGT cycle.

The optimisation carried out demonstrated the economic competitiveness of both biomass cycles. Despite the high cost of its ceramic heat exchanger, the EFGT cycle seems to be very promising in terms of cost of electricity (CoE), practically the same value was found for both the NGGT and the EFGT cycles; beyond that the required revenue (RR) is not much higher than the NGGT cycle, only 7 percent higher.

The BIGGT cycle is more expensive in terms of both, CoE – 29 percent higher than the NGGT – and RR – 32 percent higher RR than the NGGT cycle. However it has been demonstrated that the right incentives, such as emissions taxation, mainly carbon taxation, which would increase the fuel price, can make this cycle competitive with the currently used natural gas cycle.

As far as the optimisation is concerned, the technique applied, the hybrid algorithm (HA) which is a fusion of the novel technique GA and a hill climbing method, proved to be suitable for power plant optimisation. Due to the use of a HA the convergence does not take as long as a normal GA would take. Moreover, a power plant can be a an extremely noisy function when represented mathematically, in this respect the robustness of the GA in finding the global optima instead of local is an immense advantage.

Regarding emissions, when CO_2 reabsorption is considered, the biomass fuelled cycles have a much superior performance, with very low CO_2 emissions. In terms of NO_x emissions the EFGT cycle presents the lowest amount per kilowatt-hour. On the other hand, the BIGGT cycle has the largest NO_x emissions, with the NGGT cycle in between the two biomass fuelled power plants. The NO_x emissions for the EFGT cycle must have been underestimated due to the fact that the bed temperature for the fluidised bed combustor in this study is higher than in normal steam cycle fluidised bed boilers, for which the emission factors used were assessed.

The exergy analysis identified the major sources of irreversibilities in the two biomass cycles. In the BIGGT cycle the gasifier and combustor are the major sources of entropy generation, i.e., exergy destruction. However, further analysis using the exergoeconomic factor shows that little improvement would be achieved with more investment to increase the efficiency of these components.

In the EFGT case the combustor and the ceramic heat exchanger are the major contributors to exergy destruction. Again, the exergoeconomic factors of these components suggest little improvements with further investments.

In an attempt to minimise the overall exergy destruction ratio (y_D) of both BIGGT and EFGT cycles, it is seen that too high a price – nearly 100 percent increase in the cost of electricity – must be paid in order to achieve little improvement – more or less 2 percent reduction. This happens because in order to reduce y_D, the efficiencies in the components must be increased, consequently the cost of these devices increase proportionately.

The off-design analysis shows that the EFGT and BIGGT cycles follow the trend of a conventional gas turbine. A decrease in ambient temperature increases the power generated and vice-versa. The part-load performance is also similar to the conventional cycle, the difference being that the EFGT seems to maintain greater efficiency than the other two cycles for power settings up to 80 percent of nominal load.

The part-load exergy analysis revealed the major sources of losses within the cycles. The compressor turbine (or gas generator turbine) is the component that presents the highest exergy destruction ratio variation from its design-point for all cycles, followed by the compressor and the combustor. In the EFGT cycle, although the heat exchanger is a large entropy generator, under part-load conditions this device does not

change its exergy destruction ratio much, due to the nearly constant effectiveness at part-load operation.

The method proposed for the calculation of the variable operating and maintenance costs (VO&M) seems to be useful and consistent with the literature available. However the lack of experimental data makes it impossible to fine-tune the equations and their coefficients at the present time.

When the gas turbine engine is used as a peak-load electricity supplier, neither the BIGGT nor the EFGT seem to be suitable. The first has a very large capital cost, making its operation for a few hours per year economically infeasible. The EFGT has a large thermal inertia and would not start as quickly as the natural gas fuelled turbines.

A study of a typical demand curve in Brazil showed that the *TET* has little influence on the final cost of electricity, the amount of power demanded being the main parameter to affect it. However, in the present study the cumulative effects that higher-than-nominal power settings have on the cost of electricity have not been taken into consideration. A more in-depth analysis of this parameter could reveal more.

Further work

Computer codes that can optimise the off-design using the proposed hybrid algorithm are recommended. Due to the instabilities of the methods used for off-design simulation, it is recommended that the off-design analysis itself be conducted using the hybrid algorithm.

The lack of experimental data in the variable operating and maintenance costs do not allow the validation or adjustment of the method proposed, thus a link with a utility company which could supply this information is recommended. Nevertheless, the method seems sound with basic theories of gas turbine life prediction.

The components of the EFGT and BIGGT in this work are assumed to be working under their design conditions. However, compressor and turbines in a pilot project, of an EFGT for instance, will use components designed for a normal gas turbine cycle. These components, therefore, will be working in the EFGT cycle at off-design conditions, thus an analysis of conventional gas turbine components working attached to unconventional engines is recommended.

The thermodynamic and economic comparison between the series EFCC and the parallel EFCC is recommended, bearing in mind the large difference of temperature between the heat exchanger exhaust and the gas turbine exhaust (400 K for the optimum pressure ratio of 15).

REFERENCES

1. Anonymous (1999) Rotating or Reciprocating. *Power Plant Technology Operations & Maintenance* (April/May):26-31.

2. Anonymous (2001) *International Turbomachinery Handbook 2000/2001* Turbomachinery Publications.

3. Agazzani, A. and Massardo, A.F. (1997a) A Tool for Thermoeconomic Analysis and Optimization of Gas, Steam, and Combined Plants. *Journal of Engineering for Gas Turbines and Power* **119**, 885-892.

4. Agazzani, A., Massardo, A.F. and Frangopoulos, C.A. (1997b) Environmental Influence on the Thermoeconomic Optimization of a Combined Plant with NOx Abatement. *Series GT* ALL

5. Alves, M.A.C., Carneiro, H.F.F.M., Barbosa, J.R., Travieso, L.E., Pilidis, P. and Ramsden, K.W. (2001) An Insight on Intercooling and Reheat Gas Turbine Cycles. *Proceedings of the Institution of Mechanical Engineers - Part A Journal of Power and Energy* **215**, 163-172.

6. Arrieta, F. P and Lora, E. S.(2000) Thermoeconomic Analysis of BIGCC Cogeneration Plant.

7. Bejan, A., Tsatsaronis, G. and Moran, M. (1996) *Thermal Design and Optimization*, John Wiley & Sons, Inc.

8. Bettagli, N., Desideri, U. and Fiaschi, D. (1995) A Biomass Combustion-Casification Model: Validation and Sensivity Analysis. *Journal of Energy Resources Technology - ASME* **Vol. 117**, 329-336.

9. Bhattacharya, S.C. (1993) State-of-the-art of Utilizing Residues and Other Types of Biomass as an Energy Source. *RERIC International Energy Journal* **15**,

10. Bolland, O. (1991) A Comparative Evaluation of Advanced Combined Cycle

Alterantives. *Journal of Engineering for Gas Turbines and Power* **Vol. 113**, 190-197.

11. Boyce, M.P. (2001) *Gas Turbine Engineering Handbook*, Gulf Professional Publishing.

12. Bridgwater, A.V. (1995) The Technical and Economic Feasibility of Biomass Gasification for Power Generation. *Fuel* **74**, 631-653.

13. Brilliant, H. M.(1995) Second Law Analysis of Present and Future Gas Turbine Engines. **Report AIAA 95-3030**

14. Carcasci, C. and Facchini, B. (2000) Comparison Between Two Gas Turbine Solutions to Increase Combined Power Plant Efficiency. *Energy Conversion & Management* **41**, 757-773.

15. Carpentieri, A.E. and Silva, A. (1998) WBP/SIGAME - The Brazilian BIG-GT Demonstration Project: Actual Status and Perspectives. *Biomass and Bioenergy* **15**, 229-232.

16. Codeceira-Neto, A. (1999) Assessment of Novel Power Generation Systems for the Biomass Industry. Cranfield University.
Notes: PhD Thesis

17. Codeceira-Neto, A. and Pilidis, P.(1999) A Comparative Exergy Analysis of Advanced Power Cycles Using Biomass Fuel.

18. Coelho, S. T., Moreira, J. R., Campos, I. A., and Oliveira, A. C.(1999) Proposals for the Improvement of Biomass Participation in the Brazilian Energy Matrix: the Declaration of Recife".

19. Cohen, H., Rogers, G.F.C. and Saravanamuttoo, H.I.H. (1996) *Gas Turbine Theory*, Addison Wesley Longman Limited.

20. Consonni, S. and Larson, E.D. (1996a) Biomass-Gasifier/Aeroderivative Gas Turbine Combined Cycles: Part A - Technologies and Performance

Modeling. *Journal of Engineering for Gas Turbines and Power* **118**, 507-515.

21. Consonni, S. and Larson, E.D. (1996b) Biomass-Gasifier/Aeroderivative Gas Turbine Combined Cycles: Part B - Performance Calculations and Economic Assessment. *Journal of Engineering for Gas Turbines and Power* **118**, 516-525.

22. Consonni, S. and Macchi, E.(1996c) Externally Fired Combined Cycles (EFCC). Part B: Alternative Configurations and Cost Projections

23. Consonni, S., Macchi, E., and Farina, F.(1996d) Externally Fired Combined Cycles (EFCC). Part A: Thermodynamics and Technological Issues. **96-GT-92**

24. Cookson, R.A. (2001) SME/PPA/RAC/1898, UK: Cranfield University. Notes: Lecture notes

25. Cortez, L.A.B. and Lora, E.S. (1997) *Tecnologias de Conversao Energetica da Biomassa*, ABEU/EDUA. Notes: in Portuguese

26. Craig, K.R. and Mann, M.K. (1996) Cost and Performance Analysis of Biomass-Based Integrated Gasification Combined Cycle (BIGCC) Power Systems. NREL/TP-430-21657, NREL.

27. Craig, K. R., Mann, M. K., and Bain, L. R.(1994) Cost and Performance Potential of Advanced Integrated Biomass Gasification Combined Cycle Power Plant. **9**

28. Dechamps, P.J. (1995) Part-load Operation of Combined Cycle Plants with and without Sumpplementary Firing. *Journal of Engineering for Gas Turbines and Power* **Vol. 117**, 475-483.

29. Dechamps, P.J. (1999) Combined Cycle Gas Turbine - Lecture Notes. Cranfield University.

Notes: Notes from the CC short course

30. Desrosiers, R. (1981) *Biomass Gasification: Principles and Technology - Thermodynamics of Gas-Char Reactions*, New Jersey, USA: Noyes Data Corporation.

31. Ellis, T.M.R., Philips, I.R. and Lahey, T.M. (1997) *Fortran90 Programming*, Addison Wesley Longman Limited.

32. Elmegaard, B. and Qvale, B.(2002) Analysis of Indirectly Fired Gas Turbine for Wet Biomass Fuels Based on Commercial Micro Gas Turbine Data. New York: ASME. (2002)

33. Enter Software, I. (1995) *GateCycle User's Guide*

34. Ergudenler, A., Ghaly, A.E., Hamdullahpur, F. and Al-Taweel, A.M. (1997) Mathematical Modeling of a Fluidized Bed Straw Gasifier: Part I - Model Development. *Energy Sources* **19**, 1065-1084.

35. Farmer, R. (1999) Small-to-medium size turbogenset budget pricing levels up 5% to 8%. *Gas Turbine World* **May-June** 12-14.

36. Ferreira, S.B. (1998) Análise das Condições de Operação de Turbinas a Gás Industriais Utilizando Biomassa Gaseificada. Escola Federal de Engenharia de Itajuba.
Notes: in Portuguese

37. Ferreira, S.B. and Pilidis, P. (2001a) Comparison of Externally Fired and Internal Combustion Gas Turbine Using Biomass Fuel. *Journal of Energy Resources Technology - ASME*
Notes: To be published in the ASME- JERT in December 2001

38. Ferreira, S. B., Pilidis, P., and Nascimento, M. A. R.(2001b) A Comparison of Different Gas Turbine Concepts Using Biomass Fuel.

39. Gallo, W.L.R. and Milanez, L.F. (1990) Choice of a Reference State for Exergetic

Analysis. *Energy* **15**, 113-121.

40. Ganapathy, V. (1991) *Waste heat boiler deskbook*, GA: Fairmont Press.

41. Gayraud, S. (1998) Design of a Decision Support System for Combined Cycle Schemes. Cranfield University.

42. Goldberg, D.E. (1989) *Genetic Algorithms in Search, Optimization, and Machine Learning*, Addison-Wesley Publishing Company, Inc.

43. Grefenstette, J. J. and Baker, J. E.(1989) How Genetic Algorithms Work: A Critical Look at Implicit Paralellism.

44. Hajela, P. (1999) Nongradient Methods in Multidisciplinary Design Optimization - Status and Potential. *Journal of Aircraft* **Vol. 36**, 255-265.

45. Hall, D.O. and House, J. (1995) Biomass: an Environmentally Acceptable Fuel for the Future. *Proceedings of the Intution of Mechanical Engineers* **209**, 203-213.

46. Holland, J.H. (1975) *Adaption in Natural and Artificial Systems*, Ann Arbor: University of Michigan Press.

47. Horlock, J.H. (1992) *Combined Power Plants - Including Combined Cycle Gas Turbine (CCGT) Plants*, Pergamon Press.

48. Horlock, J.H. (1995a) Combined Power Plants - Past, Present, and Future. *Journal of Engineering for Gas Turbines and Power* **Vol. 117**, 608-616.
Notes: The 1994 Calvin Winsor Rice Lecture

49. Horlock, J.H. (1995b) The Optimum Pressure Ratio for a Combined Cycle Gas Turbine Plant. *Journal of Power and Energy* **Vol. 209**, 259-264.

50. Hughes, W.E.M. and Larson, E.D. (1998) Effect of Moisture Content on Biomass - IGCC Performance. *Journal of Engineering for Gas Turbines and Power* **Vol. 120**, 455-459.

51. Instituto Brasileiro de Geografia e Estatistica - IBGE (2001) Energy. vol. 9, IBGE.

52. Instituto de Economia Agricola. Estatisticas de Producao Vegetal, por Escritorio de Desenvolvimento Rural, Estado de Sao Paulo, 2000. 2001. 2001. Notes: in Portuguese

53. Jolly, A.J., O'Doherty, T. and Bates, C.J. (1998) COHEX: a computer model for solving the thermal energy exchange in an ultra high temperature heat exchanger. Part A: computational theory. *Applied Thermal Engineering* **18,** 1263-1276.

54. Junior Isles (1998) Bahia: Where the Wood Comes Good. *PEi* 71-75.

55. Kehlhofer, R.H., Warner, J., Nielsen, H. and Bachmann, R. (1999) *Combined Cycle Gas & Steam Turbine Power Plants*, PennWell Publishing Company.

56. Kotas, T.J. (1985) *The Exergy Method of Thermal Plant Analysis*, Butterworths.

57. KrishnaKumar, K. (1992) AIAA-92-4462-CP, AIAA.

58. Lahaye, P. G. and Zabolotny, E. R.(1989) Externally Fired Combined Cycle (EFCC

59. Larson, E.D. (1993) Technology for Electricity and Fuels from Biomass. *Annual Review of Energy and Environment* **18,** 567-630.

60. Larson, E.D. and Marrison, C.I. (1997) Economic Scales for First-Generation Biomass-Gasifier/Gas Turbine Combined Cycles Fueled from Energy Plantations. *Journal of Engineering for Gas Turbines and Power* **119,** 285-290.

61. Larson, E.D., Svenningosn, P. and Bjerle, I. (1989) Biomass Gasification for Gas Turbine Power Generation. In: Anonymouspp. 695-737. England: Chartwell-Bratt.

62. Larson, E. D. and Williams, R. H.(1988) Biomass-Fired Steam-Injected Gas

Turbine Cogeneration. New York: ASME.

63. Lefebvre, A.H. (1998) *Gas Turbine Combustion*, Taylor & Francis.

64. Leite, A.D. (1997) *A Energia do Brasil*, Editora Nova Fronteira.
Notes: in Portuguese

65. Levine, J.S. (1991) *Global Biomass Burning: Atmospheric, Climatic, and Biospheric Implications*, MIT - Massachusetts Institute of Technology.

66. Li, K.W. and Priddy, A.P. (1985) *Power Plant System Design*, John Wiley & Sons, Inc.

67. Lora, E. S. Re: Duvidas. Ferreira, S. B. 2001.
Notes: in Portuguese

68. Lora, E.S., Arrieta, F.P., Carpio, R.C.C. and Nogueira, L.A.H. (2000a) Clean Production: Efficiency and Environment. *International Sugar Journal* **102**, 343-351.

69. Lora, E. S. and Nogueira, L. A. H. Technoeconomic Evaluation of Gasification Technologies for Small Scale Electricity Generation form Biomass. 2000b.

70. Luzzatto, C., Morgana, A., Chaudourne, S., O'Doherty, T. and Sorbie, G. (1997) A New Concept Composite Heat Exchanger to be Applied in High-Temperature Industrial Processes. *Applied Thermal Engineering* **17**, 789-797.

71. Man, K.F., Tang, K.S. and Kwong, S. (1999) *Genetic Algorithms Concepts and Design*, Springer Verlag.

72. Mansaray, K.G., Al-Taweel, A.M., Ghaly, A.E., Hamdullahpur, F. and Ugursal, V.I. (2000) Mathematical Modeling of a Fluidized Bed Rice Husk Gasifier: Part I - Model Development. *Energy Sources* **22**, 83-98.

73. Massardo, A.F. and Scialo, M. (2000) Thermoeconomic Analysis of Gas Turbine Based Cycles. *Journal of Engineering for Gas Turbines and Power* **122**,

664-671.

74. Mathieu, P. and Dubuisson, R. (2002) Performance Analysis of a Biomass Gasifier. *Energy Conversion & Management* **43**, 1291-1299.

75. Mayer, D.G., Belward, J.A., Widell, H. and Burrage, K. (1999) Survival of the fittest - genetic algorithms versus evolution strategies in the optimization of systems models. *Agricultural Systems* **60**, 113-122.

76. McBride, B.J., Gordon, S. and Reno, M.A. (1993) NASA Technical Memorandum 4513, USA: NASA.

77. McGowin, C., Hughes, E. and Holt, N. (1998) TR-111xxx, Electric Power Research Institute - EPRI.

78. McKendry, P. (2002a) Energy Production from Biomass (Part 1): Overview of Biomass. *Biosource Technology* 37-46.

79. McKendry, P. (2002b) Energy Production from Biomass (Part 3): Gasification Technologies. *Biosource Technology* 55-63.

80. McNeely, M. (2001) Engine Orders Go Through the Roof. *Diesel and Gas Turbine Worldwide* (October):28-36.

81. Michalewicz, Z. (1996) *Genetic Algorithms + Data Structures = Evolution Programs*, Springer Verlag.

82. Michalewicz, Z. and Fogel, D.B. (2000) *How to solve it: Modern heuristics*, Springer Verlag.

83. Ministerio das Minas e Energia - Brazilian Government (2001) Brazilian National Energy Balance. Brazil: Ministry of Energy.

84. Moran, M. (1982) *Availability analysis: a guide to efficient energy use*, Englewood Cliffs, N.J: Prentice-Hall.

85. Moran, M. and Sciubba, E. (1994) Exergy Analysis: Principles and Practice.

Journal of Engineering for Gas Turbines and Power **Vol. 116**, 285-290.

86. Munoz, J.R. and Michaelides, E.E. (1999) The Impact of the Model of the Environment in Exergy Analyses. *Journal of Energy Resources Technology - ASME* **121**, 268-276.

87. Najjar, Y.S.H. (1997) Comparison of Performance for Cogeneration Systems Using Single- or Twin-shaft Gas Turbine Engines. *Journal of Thermal Engineering* **Vol. 17**, 113-124.

88. Neilson, C.E. (1998) LM2500 Gas Turbine Modifications for Biomass Fuel Operation. *Biomass and Bioenergy* **15**, 269-273.

89. Neilson, C.E., Shafer, D.G. and Carpentieri, A.E. (1999) LM2500 Gas Turbine Fuel Nozzle Design and Combustion Test Evaluation and Emission Results with Simulated Gasified Wood Product Fuels. *Journal of Engineering for Gas Turbines and Power* **121**, 600-606.

90. Newby, R.A. and Bannister, R.L. (1998) A Direct Coal-Fired Combustion Turbine Power System Based on Slagging Gasification With In-Situ Gas Cleaning. *Journal of Engineering for Gas Turbines and Power* **Vol. 120**, 450-454.

91. Nogueira, L.A.H., Lora, E.S., Trossero, M.A. and Frisk, T. (2000) *Dendroenergia: Fundamentos e Aplicacoes*, Brazil: ANEEL/MCT/PNUD.
Notes: in Portuguese

92. Nogueira, L. A. H. and Walter, A. C. S.(1995) Experiências de Geração de Energia Elétrica a Partir de Biomassa no Brasil: aspectos técnicos e econômicos. Biomass folderp.
Notes: in Portuguese

93. Oliveira, P. C. and Nascimento, M. A. R.(1999) Analise Termodinamica e Economica de Ciclos com Biomassa Gaseificada.
Notes: in Portuguese

94. Quaak, P., Knoef, H. and Stassen, H. (1999) *Energy from Biomass: A Review of*

Combustion and Gasification Technologies, The World Bank.

95. Ramsden, K.W. (2002) *Symbols, Abbreviations and Terms in Common Use for Gas Turbine Engines*, UK: School of Engineering - Cranfield University.

96. Ranasinghe, J., Aceves-Saborio, S. and Reistad, G.M. (1989) Irreversibility and Thermoeconomics Based Design Optimization of a Ceramic Heat Exchanger. *Journal of Engineering for Gas Turbines and Power* **111**, 719-727.

97. Saad, M. (1997) *Thermodynamics: Principles and Practice*, Prentice-Hall International, Inc.

98. Schmitz, W. and Hein, D.(2000) Concepts for the Production of Biomass Derived Fuel Gases for Gas Turbine Applications.

99. Secretaria de Politica Agricola - Brasil. Estatisticas Agricolas. 2001. 2001. Notes: in Portuguese

100. Singh, R. (1998) Combustors - Lecture Notes. Cranfield University.

101. Solomon, P.R., Serio, M.A., Cosgrove, J.E., Pines, D.S., Zhao, Y., Buggeln, R.C. and Shamroth, S.J. (1996) A Coal-Fired Heat Exchanger for an Externally Fired Gas Turbine. *Journal of Engineering for Gas Turbines and Power* **Vol. 118**, 23-31.

102. Souza-Santos, M.L. (1989) Comprehensive Modelling and Simulation of Fluidized Bed Boilers and Gasifiers. *Fuel* **Vol. 68**, 1507-1521.

103. Steen, M. and Ranzani, L. (2000) Potential of SiC as a heat exchanger material in combined cycle plant. *Ceramics International* **26**, 849-854.

104. Stevens, D.J. (2001) NREL/SR-510-29952, USA: NREL - National Renewable Energy Laboratory.

105. Stoll, H.G. (1989) *Least-cost Electric Utility Planning*, John Wiley & Sons, Inc.

106. Szargut, J. (2000) Discussion:"The Impact of the Model of the Environment in Exergy Anlyses". *Journal of Energy Resources Technology - ASME* **122**, 248

107. Tariq, A.S. and Purvis, M.R.I. (1996) NOx Emissions and Thermal Efficiencies of Small Scale Biomass-Fuelled Combustion Plant with Reference to Porcess Industries in a Developing Country. *International Journal of Energy Research* **Vol. 20**, 41-55.

108. Traverso, A., Massardo, A. F., Santarelli, M., and Cali, M.(2002) A New Gereralised Carbon Exergy Tax: an Effective Rule to Control Global Warming.

109. Tsatsaronis, G. (1993) Thermoeconomic Analysis and Optimization of Energy Systems. *Proc. Energy Combust. Sci.* **19**, 227-257.

110. Turn, S.Q. (1999a) Biomass Integrated Gasifier Combined Cycle Technology: Application in the Sugar Cane Industry. *International Sugar Journal* **101**, 267-272.

111. Turn, S.Q. (1999b) Biomass Integrated Gasifier Combined Cycle Technology: II - Application in the Sugar Cane Industry. *International Sugar Journal* **101**, 316-322.

112. Turn, S.Q. (1999c) Biomass Integrated Gasifier Combined Cycle Technology: III - Application in the Sugar Cane Industry. *International Sugar Journal* **101**, 368-374.

113. Turnbull, J.H. (1996) Strategies for Achieving a Sustainable, Clean and Cost-effective Biomass Resource. *Biomass and Bioenergy* **10**, 93-100.

114. U.S. Environmental Protection Agency (1997) EPA-454/R-95-015, USA: EPA.

115. Walsh, P.P. and Fletcher, P. (1998) *Gas Turbine Performance*, Blackwell Science.

116. Walter, A. and Overend, R.P. (1999) Financial and Environmental Incentives:

Impact on the Potential of BIG-CC Technology at the Sugar-Cane Industry. *Renewable Energy* **16**, 1045-1048.

117. Wang, Y. and Kinoshita, C.M. (1993) Kinetic Model of Biomass Gasification. *Solar Energy* **Vol. 51**, 19-25.

118. Ward, M.E., Metcalfe, A.G. and Dapkunas, S.J. (1983) Ceramic Tube Heat Exchanger Technology Development for Indirect-Fired Gas Turbine Cycle. *Journal of Engineering for Power* **Vol. 105**, 310-316.

119. West, R. and Kreith, F. (1988) Economic Analysis of Solar Thermal Energy Systems. In: Anonymouspp. 19-27. Massachusetts Institute of Technology.

120. Widell, H. (1997) GENIAL 1.1: A Friendly Function Optimizer based on Evolutionary Algorithms - User Manual

.

121. Wright, A. (1991) Genetic Algorithms for Real Parameter Optimisation. In: Anonymouspp. 205-218. San Mateo, CA, USA: Morgan Kaufmann.

122. Zwebek, A.I. (2002) Combined Cycle Performance Deterioration Analysis. Cranfield University.
Notes: PhD Thesis

APPENDIX A – APPLICATION S OF GENETIC ALGORITHMS

Introduction

Genetic Algorithms are adaptive methods that may be used to solve search and optimisation problems. These problems have widespread applications, including optimisation of simulation models, fitting curves to data, solving systems of non-linear equations, engineering design, and control problems (Goldberg, D. E., 1989), and also setting weights on neural networks. They have been successfully applied to solve problems as those listed, which can present non-differentiable mathematical equations, and consequently cannot be solved by using conventional methods like hill-climbing or derivative based techniques.

GAs form a subset of evolutionary techniques, and are based on the genetic processes of biological organisms. They use operations found in natural genetics to guide their way through a search space.

Over many generations, natural populations evolve according to the principles of natural selection and "survival of the fittest", first clearly described by Charles Darwin in his book "The Origin of Species". By adapting this natural process to scientific problem solving, genetic algorithms are able to evolve solutions to mathematical problems, if they have been suitably encoded.

An optimisation process consists of adjusting inputs to a mathematical model representing the problem in order to find the minimum or maximum value of the solution of the problem as the output. The input consists of parameters. The mathematical model to be evaluated uses an objective function, here called fitness function, which represents the value of the solution. The output is the fitness. The parameters often have constraints and incorporate equalities and inequalities to the optimisation process.

Interpreting the results means analysing various measures of fitness over time. The most significant fitness indicators, which can be compared across generations, are the fitness of the set of parameters, which are the best (worst) in each generation, and the average fitness of the whole population. Generation here is defined as the time

period between different application of genetic operators. Population is defined as the various sets of different parameters considered in the application of the algorithm.

Genetic algorithms allow a population composed of many individuals to evolve under specified selection rules, to a state that maximises or minimises the fitness function. The method was developed by Holland, J. H., 1975, and finally popularised by one of his students, David Goldberg (Goldberg, D. E., 1989). Nowadays, genetic algorithms are increasing in popularity as a search and optimisation technique.

Some of the advantages of genetic algorithms are described as follows:

1. They optimise with continuous or discrete parameters;
2. They do not require derivative information;
3. They are well suited for parallel computers;
4. They optimise parameters in complex mathematical models.

```
procedure traditional GA
begin
        i=0
        initialize population(i) of n chromosomes
        evaluate population(i)
        do
        begin
                i=i+1
                select m chromosomes from population(i-1)
                apply operator(s) to m chromosomes
                insert m chromosomes into population(i)
                evaluate population(i)
        end
        until (termination condition)
end
```

```
procedure GENIAL
begin
        i=0
        initialize population(i) of n chromosomes
        evaluate population(i)
        do
        begin
                i=i+1
                do
                begin
                        select operator
                        select k* chromosomes from
                        population(i-1)
                        apply operator to selected
                        chromsomes and generate f* child
                        chromosomes
                end
                until (m children have been generated)
                insert m children into population(i)
                evaluate population(i)
        end
        until (termination condition)
end
```

Figure 84 – Comparison between usual procedure and GENIAL's procedure (Widell, H., 1997)

Most authors report that GAs are computationally demanding, which may have been true until some years ago. The code used in this thesis is a refinement of the traditional techniques (Figure 84), and run in a AMD, 1.2GHz, 512 Mb RAM, took, on average five minutes to converge. With the development of more powerful machines GAs can become as quick as any other conventional method.

Since genetic algorithms are based on a random process, there is no possibility of predicting their efficiency on a given problem.

The strength of the method adopted by GENIAL lies in the fact that it is easy to change operators that are already implemented in the code, as can be seen in Figure 85. This software proved to be reliable and robust (Mayer et al. 1999).

Formal definition

GAs are search algorithms based on the mechanics of natural selection and natural genetics. They combine survival of the fittest among string structures with a structured yet randomised information exchange to form a search algorithm with the innovative flair of human search. In every generation a new set of artificial creatures (strings) is created using bits and pieces of the fittest of the old set (Goldberg, D. E., 1989). Although randomised, GAs efficiently use historical information to improve the new generation of "offspring".

As an overview on how the GAs work we can explain it as a three phased process:

1. First population is randomly generated;
2. Some individuals are selected for "reproduction" (crossover);
3. Some individuals are selected for "mutation".

As seen in Figure 85, the first population is randomly generated, then some individuals go through the selection operation, which selects the individuals according to rules defined in the fitness function. The selected individuals undergo the crossover operation, and again some individuals are selected for mutation, after which a second generation has been generated[36]. The process is repeated again and again, until the criterion for "convergence" is met.

GAs compared with traditional methods

GAs are different from traditional methods in four basic ways:

[36] The operators for selection, crossover and mutation are discussed in detail in later sections of this chapter.

1. *GAs work with a coding of the parameter set, not the parameters themselves*: Imagine that there is a black box with five switches on it. The switches can be adjusted so that each gives a value 0 or 1, or *on* or *off*. The black box (the function to be optimised) outputs a value depending on the combination of the position of the switches. The objective is to maximise the output value from the black box. The only information the GA code needs to know is the combination of the switches and the output value, nothing else has to be said about the "function" (Goldberg, D. E., 1989).

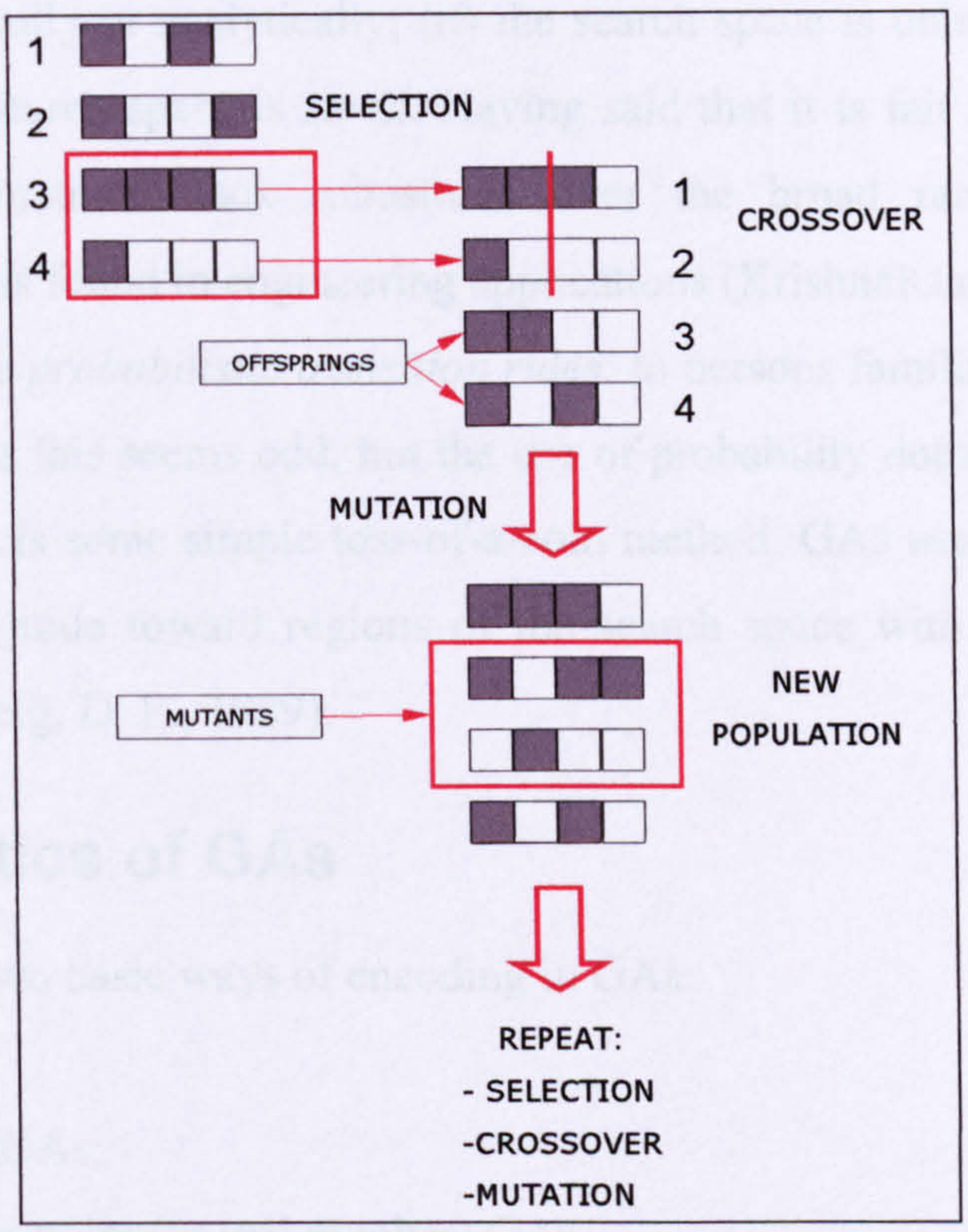

Figure 85 – Scheme of GA operators

2. *GAs search from a population of points, not a single point*: most of the traditional optimisation techniques use a "point-to-point" approach to locate the optimum point (a peak, maximum, or a valley, minimum). This approach; however, is dangerous because it can lead to the location of false optimal points within a multimodal search space. The power of GAs derives from their implicit parallelism, i.e., the simultaneous allocation of search effort to many regions of the search space according to sound principles (Grefenstette et al. 1989).

3. *GAs do not depend on auxiliary knowledge, like derivatives*: GAs are "blind", they only require payoff values (objective function values) associated with individual strings (Goldberg, D. E., 1989), making them a broadly based scheme. On the other hand, traditional techniques rely on, for example, derivatives, like gradient techniques. This also contributes to the robustness of the GAs because they do not see discontinuities in the functions. Traditional techniques (also called calculus-based techniques) work well on problems in which: (i) the gradients are well defined, either numerically or analytically; (ii) the search space is unimodal; (iii) the order of the search space is small. Having said that it is fair to say that calculus-based methods lack robustness over the broad range of optimisation functions found in engineering applications (KrishnaKumar, 1992).
4. *GAs use probabilistic transition rules*: to persons familiar with deterministic methods this seems odd, but the use of probability does not suggest that the method is some simple toss-of-a-coin method. GAs use random choice as a toll to guide toward regions of the search space with likely improvement (Goldberg, D. E., 1989).

Characteristics of GAs

There are two basic ways of encoding in GAs:

1. Binary GAs;
2. Floating-point (or real number) GAs.

Both algorithms have the same path to modelling genetic recombination and natural selection. The binary GAs represent parameters as an encoded binary string of zeroes, 0, and ones, 1, and work with the binary strings to solve the optimisation problem. On the other hand, floating-point GAs, also called continuous GAs, work with real numbers to solve the optimisation problem.

Several empirical comparisons between binary GAs and floating-point GAs have shown better performance for the floating-point GA (Michalewicz, Z., 1996). However, the performance obtained in using these two types of genetic algorithms

depends very much on the problem and details of the algorithm being used. At the present time, there are no rigorous guidelines for predicting which type of genetic algorithm will work best, and both approaches are currently in use.

When using a binary GA, each parameter requires many bits of 0s and 1s to fully represent it. When the number of parameters is large, the size of the strings grows quickly. Furthermore, since binary GAs have their precision limited by the binary representation of parameters, using floating-point numbers allows representation to the machine precision.

Moreover, floating-point GAs have the advantage of requiring less storage than binary GAs because a single floating-point number represents the parameter instead of the string of integers represented by the number of bits. Another consideration, which is worth noting, is the accurate representation of the floating-point parameter. GENIAL 1.1 is a floating-point GA.

It is not the intention of this chapter to discuss in depth the methods used for the operations carried out in a GA software package. This information can be easily found in the open literature (Goldberg, D. E., 1989, Wright, 1991, Man, K. F., Tang, K. S., and Kwong, S., 1999, and Michalewicz, Z. and Fogel, D. B., 2000). The following paragraphs are intended to give a brief overview of the operators used in a simple GA code.

Selection

The objective of the selection operator is to produce more fit members each generation, and to eliminate the less fit ones. A very simple approach to selecting fit members of a population is to assign each member a probability of selection (p_{sel}) on the basis of its fitness. If $F_v(i)$ is the fitness measure of the i^{th} member, then the one way to assign a probability of selection is:

$$p_i = \frac{F_v(i)}{\sum_{NPOP} F_v(i)} \qquad [80]$$

where $NPOP$ is the population size.

A new population pool of the same size as the original is created; however, the average fitness of the new population is higher. No new individuals (strings) are created

in this process; the less fit ones are simply eliminated and additional copies of the more fit designs are brought into the population (Hajela, 1999).

Crossover

The crossover process, also known as recombination, allows for an exchange of genetic material among members of the population. Its intention is to improve the fitness of the new population. There several ways to implement crossover in a population, the most common being the two point crossover (Figure 85 shows a one point crossover).

A probability of crossover (p_c) is defined to determine whether the operation should be applied to a chosen pair of mating strings. The different approaches for the crossover operation can be found in Michalewicz, Z., 1996 and Widell, H., 1997.

Mutation

Mutation safeguards the genetic search process from a premature loss of valuable genetic information during reproduction and crossover. The idea behind mutation is simply to choose a few members from the population pool according to a probability of mutation (p_m) and to randomly switch the genes of a given individual (Figure 85).

APPENDIX B – PRINCIPLES OF ECONOMICS

Principles of economics

In order to arrive at a good evaluation of the influence of the various thermodynamic parameters on the economics of a given power plant, it is necessary to carry out an economic analysis of the investment made and the final cost of electricity (CoE).

The final cost of electricity comprises several cost components, such as purchased-equipment costs (*PEC*), purchased-equipment installation (*PEI*), piping, land, etc. These costs can be divided into fixed costs and variable costs.

Estimation of the total capital investment (TCI)

In contrast to fuel and O&M costs, which are continuous or repetitive in nature, an investment cost is a one-off cost, and is therefore treated differently from fuel and O&M expenses.

It can be divided into fixed capital investment (*FCI*), and other outlays. The *FCI* in its turn can be subdivided into:

1. Direct costs (*DC*), which are all the permanent equipment, materials, labour, and other resources involved in the fabrication, erection, and installation of the permanent facilities;
2. Indirect costs (*IC*), which are not a permanent part of the facilities, but are required for the completion of the project.

Both direct and indirect *FCIs* can be estimated as percentages of *PEC* or *FCI*. In this work the *FCIs* are taken as percentages of *PEC*.

Other outlays comprise the start-up costs, working capital, licensing, research and development, and allowance for funds used during construction (*AFUDC*).

The *TCI* is the sum of the values of *FCI* and other outlays. Table 27 shows the breakdown of all costs involved in a project as part of the *TCI*.

Table 27 – Composition of the total capital investment (*TCI*)

I. Fixed-capital investment (*FCI*)
A. Direct costs (*DC*)
1. Onsite costs (*ONSC*)
* Purchased-equipment cost (*PEC*; 15-40% of *FCI*)
* Purchased-equipment installation (*PEI*, 20-90% of *PEC*; 6-14% of *FCI*)
* Piping (10-70% of *PEC*; 3-20% of *FCI*)
* Instrumentation and controls (6-40% of *PEC*; 2-8% of *FCI*)
* Electrical equipment and materials (10-15% of *PEC*; 2-10% of *FCI*)
2. Offsite costs (*OFSC*)
* Land (0-10% of *PEC*; 0-2% of *FCI*)
* Civil, structural, and architectural work (15-90% of *PEC*; 5-23% of *FCI*)
* Service facilities (30-100% of *PEC*; 8-20% of *FCI*)
B. Indirect costs (*IC*)
1. Engineering and supervision (25-75% of *PEC*; 6-15% of *DC*; 4-21% of *FCI*)
2. Construction costs including contractor's profit (15% of *DC*; 6-22% of *FCI*)
3. Contingencies (8-25% of the sum of the above costs; 5-20% of *FCI*)
II. Other outlays
A. Start-up costs (5-12% of *FCI*)
B. Working capital (10-20% of *FCI*)
C. Costs of licensing, research, and development
D. Allowance for funds used during construction (*AFUDC*)

Estimation of the FCI direct costs

Purchased-equipment costs (*PEC*)

The *PEC* component can be calculated using equations **[74]** to **[78]**, presented in a previous section of this chapter.

Purchased-equipment installation (*PEI*)

This includes freight and insurance for transportation, labour for unloading, handling, foundations, and all construction expenses directly related to the erection and connections of the equipment. In the absence of reliable information about this cost a value of 45 percent of *PEC* can be adopted (Bejan, A., Tsatsaronis, G., and Moran, M., 1996).

Piping

This includes all the material and labour costs required to complete the erection of all the piping used in the system. Its value can vary with the type of process involved:

1. For processes involving solids only an average value of 16 percent of *PEC* can be used.

2. For processes involving solids and fluids an average value of 31 percent of *PEC* is recommended.
3. For processes involving fluids only an average of 66 percent of *PEC* is normally adopted.

Instrumentation and controls

The value applied for this type of cost is dependent on the technological level of the instrumentation and control adopted. For steam power plants a value of 6-10 percent of *PEC* is typically adopted; however, due to increasing complexity and automation in the power plants a sensible value ranges from 6 to 40 percent. In the absence of reliable information an average value of 20 percent can be safely used in the calculations (Bejan, A., Tsatsaronis, G., and Moran, M., 1996).

Electrical equipment and materials

This cost includes materials and installations labour for ancillary systems such as substations, distribution lines, switch gears, emergency power supply, area lighting, etc. A typical value for this cost ranges from 10 to 15 percent. However, in the absence of reliable information the adoption of an average value of 11 percent is recommended.

Land

The cost of land depends very much on the location of the power plant and usually does not decrease with time, unlike the other costs. If land is to be purchased an average value of 10 percent of *PEC* can be adopted.

Civil, structural, and architectural work

In these costs are represented the total costs for all buildings, roads, sidewalks, fencing, landscaping, yard improvements, etc. The cost depends on whether the project is a new plant, a new unit at an existing site, or an expansion of an existing site, as summarised in Table 19.

Service facilities

Also known as auxiliary facilities this cost includes a variety of features related to the general utilities required to operate the plant such as fuel, water, steam, and

electricity (assuming that these are not produced by the plant), refrigeration, inert gas, sewage, waste disposal, environmental control, fire protection, equipment for shops, first aid, and cafeteria. It can range from 30 to 100 percent of *PEC*. An average value of 65 percent can be assumed in the absence of more information.

Table 28 – Cost of civil, structural, and architectural work as a percentage of *PEC* (Bejan, A., Tsatsaronis, G., and Moran, M., 1996)

Type of process plant	New plant at new site (% of *PEC*)	New unit at existing site (% of *PEC*)	Expansion of an existing site (% of *PEC*)
Solid processing	83	40	30
Solid-fluid processing	62	44	22
Fluid processing	60	20-33	21

Estimation of the FCI indirect costs

Engineering and supervision

This includes the cost for developing the detailed plant design and drawings, scale models, purchasing, engineering supervision and inspection, administration, travel, and consultant fees. An average value of 30 percent of *PEC* or 8 percent of *DC* can be assumed, according to Bejan, A., Tsatsaronis, G., and Moran, M., 1996.

Construction (including contractor's profit)

This cost is in addition to the construction charges previously discussed and includes expenses for temporary facilities and operations, tools, equipment, home office personnel located at the construction site, insurance, etc.

Contingencies

Designing a process plant, as in any other project, involves assumptions for costs and productivity. On the top of these assumptions there are other unpredictable factors that may affect the performance of the system, such as weather conditions, work stoppages, changes in the economy, transportation difficulties, and so forth. All these uncertainties represent potential risks to the project and are accounted for under the contingency factor, which ranges from 5 to 20 percent of the *FCI*.

Other outlays

Start-up costs

These costs are mainly associated with the design changes that have to be made after completion of completion of construction but before the plant can operate at design conditions. They include:

1. Labour;
2. Materials;
3. Equipment;
4. Overhead expenses to be used only during start-up times;
5. Loss of income during the time the system is not operating or operating at partial capacity (Bejan, A., Tsatsaronis, G., and Moran, M., 1996).

According to Bejan, A., Tsatsaronis, G., and Moran, M., 1996, for electric power plants the start-up costs are the sum of the following unescalated[37] values:

1. One month of fixed operating and maintenance costs;
2. One month of variable operating costs at full load;
3. One week of fuel at full load;
4. Two percent of the plant facilities investment (*PFI*), which is equal to the *FCI* minus land costs.

An average value of 10 percent of *FCI* may be used in the absence of reliable data.

Working capital

This represents the funds required to pay for the operating expenses before payment is received through the sale of the plant products. The working capital usually

---

[37] The concept of escalation will be explained later in this chapter.

represents 10-20 percent of the *TCI*; however, an average value of 15 percent can be applied if no information is available.

Licensing, research, and development

If a lump sum payment is required, costs associated with licensing and costs incurred in the past for research and development must be considered within the *TCI*.

Allowance for funds used during construction (*AFUDC*)

This represents the parts of the investment released between the beginning of the construction of the plant and the start-up. The *AFUDC* represents the time value of money[38] during construction. When the total design and construction period is known, the allocation of *FCI* to the individual years of this period is estimated and the interest rate is given, and so the *AFUDC* can be calculated using the concepts presented in the section Economic assessment.

Economic assessment

This section presents some engineering economy principles that help in the economic assessment of a given project. The concepts presented here have been thoroughly discussed in the literature, and further information can be found in Li, K. W. and Priddy, A. P., 1985, Bejan, A., Tsatsaronis, G., and Moran, M., 1996, and Gayraud, 1998.

Time value of money

One unit of currency in hand today is worth more than one unit of currency received one year from now because the unit of currency in hand today can be invested for the year. Thus, the cost assessment of a given investment must be calculated and compared at various points in time. The following paragraphs describe the main methods that allow the assessment of the evolution of a given investment.

---

[38] The concept of time value of money is presented later in this chapter.

Future value

When an amount of capital in present value (P) is invested today earning i percent of interest[39] per period of time and the interest is compounded at the end of each of n time periods, the investment will have a future value (F) that can be calculated by:

$$F = P(1+i)^n \qquad [81]$$

On the other hand, when evaluating investment on projects it is necessary to know the present value of funds that will be spent or received in the future. This present value is calculated by:

$$P = \frac{F}{(1+i)^n} \qquad [82]$$

Annuities

Annuity is a series of equal-amount money transactions occurring at equal time intervals (periods) (Bejan, A., Tsatsaronis, G., and Moran, M., 1996). The most common type of annuity is the ordinary annuity, which involves money transactions occurring at the end of each time interval. If A units of currency are invested at the end of each period earning i percent per period, the future value (of the annuity) accumulated at the end of the n^{th} period is:

$$F = A\frac{(1+i)^n - 1}{i} \qquad [83]$$

In the same fashion the present value of the annuity is defined:

$$\frac{P}{A} = \frac{(1+i)^n - 1}{i(1+i)^n} \qquad [84]$$

---

[39] Interest is the compensation paid for the use of borrowed money. It is also known as *rate of return* and *annual cost of money*.

or

$$CRF = \frac{A}{P} = \frac{i(1+i)^n}{(1+i)^n - 1} \qquad \textbf{[85]}$$

where $CRF \equiv$ capital-recovery factor, used to determine the equal amounts A of a series of n money transactions.

Equations **[83]** to **[85]** assume that the money transactions occur at the end of each time interval.

Salvage value

An asset of fixed capital cost will have a finite life. The economic life (or book life) of an asset is the best estimate of the length of time that the asset can be used. The salvage value of an asset is the estimated economic worth of the asset at the end of its economic life (Bejan, A., Tsatsaronis, G., and Moran, M., 1996). In this work the salvage value for all assets is assumed to be zero.

Inflation

Inflation is the rise in price levels associated with an increase in available goods and services of equal quality (Bejan, A., Tsatsaronis, G., and Moran, M., 1996).

When inflation occurs, costs change every period (year, month, or weeks, depending on the performance of the economy); usually every year. As a common practice the inflation rate for future periods represents an estimation. In this work a constant inflation rate of 6 percent per year for future periods is assumed.

Escalation

The escalation rate of an expenditure is the annual rate of expenditure change caused by factors such as resource depletion, increased demand, and technological advances. The first two factors lead to a positive real escalation rate, whereas the third factor results in a negative rate (Bejan, A., Tsatsaronis, G., and Moran, M., 1996).

Levelisation

The concept of levelisation is general and is defined as the use of time value of money arithmetic to convert a series of varying quantities to a financially equivalent

constant quantity (annuity) over a specified time interval. In other words, it consists of bringing all values to the same level in order to have the same basis of comparison.

Current vs. constant units of currency

An economic analysis can be carried out either in:

1. *Current currency*, by including the effect of inflation in projections of capital expenditures, fuels costs, and O&M costs or;
2. *Constant currency*, by excluding inflation and considering only real escalation rates in cost projections and the real cost of money (Bejan, A., Tsatsaronis, G., and Moran, M., 1996).

In general, a current currency analysis gives the impression that the project being analysed is more costly than we would expect based on today's cost values, whereas a constant currency analysis presents the project as less costly than it will ultimately be. The results of studies involving more than ten years are best presented in current currency. Longer term studies may be best presented in constant currency so that the effect of many years of inflation does not distort the costs to the point that they bear no resemblance to today's cost values (Bejan, A., Tsatsaronis, G., and Moran, M., 1996).

Depreciation

Depreciation is the parameter that takes into consideration the devaluation of a given asset due ageing (or use) due to several factors, the most important being:

1. Physical deterioration;
2. Technological advances;
3. Other factors that will lead to the retirement of the asset.

As depreciation is deducted from the taxable profit, it can substantially reduce income taxes.

Several methods can be used to calculate depreciation, as seen in Bejan, A., Tsatsaronis, G., and Moran, M., 1996, and Gayraud, 1998. It is not the object of this

work to discuss the merits of each method; suffice to say that the method known as straight line is the most common, and will be used throughout this thesis.

The annual depreciation is constant when the straight line method is used, and can be calculated using the following equation:

$$DP_i = \frac{C_0 - S}{n} \qquad [86]$$

where $DP_i \equiv$ depreciation rate at year i;

$C_0 \equiv$ total depreciable investment at the beginning of the economic life period;

$S \equiv$ salvage value;

$n \equiv$ tax life or economic life considered in the depreciation calculations (years).

The cumulative depreciation (CDP), allocation at the end of year z is:

$$CDP_z = \sum_{i=1}^{z} DP_i = (C_0 - S)\frac{z}{n} \qquad [87]$$

Project financing

A project can be financed in various ways:

1. *Long term liabilities*: these include bank loans, private loans, etc. In a long project, such as a power plant, for instance, it is common to sell bonds; a method known as debt financing.
2. *Common stock*: is part of common equity of the company, in the particular case of this thesis, the utility. The utility issues stock on the stock exchanges, which permits public ownership of the company.
3. *Preferred stock*: the difference between common stock and preferred stock is that the latte has a fixed yield associated with each offering and usually gives voting rights to the owner.
4. A combination of all methods cited in the previous items (1, 2, and 3), comprising the *composite cost of capital* (*CCC*), which is defined as:

$$CCC = \sum_i \zeta_i F_i \qquad [88]$$

where $\zeta \equiv$ is the share of the financing type *i* on the total capital requirement for the project, and

$F \equiv$ is the rate of return on the respective financing type *i* (Gayraud, 1998).

Comparison between alternative investments

There are several ways of evaluating alternative investments, such as:

1. Average rate of return;
2. Payback period;
3. Net present value;
4. Benefit-cost ratio;
5. Internal rate of return;
6. Repeatability;
7. Cotermination;
8. Capitalised-cost.

All of these methods have been exhaustively discussed in the literature (Bejan, A., Tsatsaronis, G., and Moran, M., 1996 and Gayraud, 1998).

However, the method used in this work is the so-called revenue requirement method. According to Stoll, H. G., 1989, and West et al. 1988, this is the most common method used in the utility industry.

This method divides the present value or annual value costs (less salvage values) associated with an energy system, adjusted for income taxes, by one minus the composite marginal income tax rate. This provides a measure of the before-tax revenue in present value required to cover the costs on an after-tax basis. The required revenue (*RR*) is calculated by the following formula (West et al. 1988):

$$RR = \frac{\left[\sum_{j=0}^{n} \frac{(C_j - S_j)}{(1+d)^j}\right]}{(1-t)} \qquad [89]$$

where $C_j \equiv$ is the cost of the system in the year j;

$S_j \equiv$ is the salvage value of the system in the year j;

$d \equiv$ is the discount rate;

$t \equiv$ is the marginal income tax rate, which is calculated by multiplying the income tax rate by the taxable income.

APPENDIX C – COEFFICIEN TS FOR CALCULATING GAS PROPERTIES

Table 29 – Coefficients for the calculation of physical properties of selected species at T < 1000 K (From McBride et al. 1993).

T<1000	a_1	a_2	a_3	a_4	a_5	b_1	b_2
CH_4	5.149876130E+00	-1.367097880E-02	4.918005990E-05	-4.847430260E-08	1.666939560E-11	-1.024664760E+04	-4.641303760E+00
C_2H_6	4.291424920E+00	-5.501542700E-03	5.994382880E-05	-7.084662850E-08	2.686857710E-11	-1.152220550E+04	2.666823160E+00
C_3H_8	4.211026200E+00	1.715998030E-03	7.061834720E-05	-9.195941160E-08	3.644213720E-11	-1.438121060E+04	5.609304910E+00
C_4H_{10}	6.147468060E+00	1.559473890E-04	9.679135170E-05	-1.254839100E-07	4.978165550E-11	-1.759944020E+04	-1.094098790E+00
C_5H_{12}	1.898367900E+00	4.120303700E-02	1.231217500E-05	-3.658950100E-08	1.504250900E-11	-2.009150000E+04	1.867907200E+01
C_2H_2	8.086810940E-01	2.336156290E-02	-3.551718150E-05	2.801524370E-08	-8.500729740E-12	2.642898070E+04	1.393970510E+01
C_7H_8	1.611914000E+00	2.111889020E-02	8.532214530E-05	-1.325668760E-07	5.594061090E-11	4.096519760E+03	2.029736140E+01
Ar	2.500000000E+00	0.000000000E+00	0.000000000E+00	0.000000000E+00	0.000000000E+00	-7.453750000E+02	4.379674910E+00
H_2	2.344331120E+00	7.980520750E-03	-1.947815100E-05	2.015720940E-08	-7.376117610E-12	-9.179351730E+02	6.830102380E-01
N_2	3.531005280E+00	-1.236609870E-04	-5.029994370E-07	2.435306120E-09	-1.408812350E-12	-1.046976280E+03	2.967474680E+00
O_2	3.782456360E+00	-2.996734150E-03	9.847302000E-06	-9.681295080E-09	3.243728360E-12	-1.063943560E+03	3.657675730E+00
CO_2	2.356773520E+00	8.984596770E-03	-7.123562690E-06	2.459190220E-09	-1.436995480E-13	-4.837196970E+04	9.901052220E+00
CO	3.579533470E+00	-6.103536800E-04	1.016814330E-06	9.070058840E-10	-9.044244990E-13	-1.434408600E+04	3.508409280E+00
NO	4.218598960E+00	-4.639881240E-03	1.104430490E-05	-9.340555070E-09	2.805548740E-12	9.845099640E+03	2.280610010E+00
N_2O	2.257168600E+00	1.130463380E-02	-1.367103500E-05	9.681620980E-09	-2.930555830E-12	8.741771460E+03	1.075791540E+01
NO_2	3.944039070E+00	-1.585474440E-03	1.665789840E-05	-2.047544780E-08	7.835032650E-12	2.896598650E+03	6.311962250E+00
NH_3	4.301778080E+00	-4.771273300E-03	2.193416190E-05	-2.298564890E-08	8.289922680E-12	-6.748063940E+03	-6.906443930E-01
H_2S	3.932347600E+00	-5.026090500E-04	4.592847300E-06	-3.180721400E-09	6.649756100E-13	-3.650535900E+03	2.315790500E+00
$H_2O(g)$	4.198640560E+00	-2.036434100E-03	6.520402110E-06	-5.487970620E-09	1.771978170E-12	-3.029372670E+04	-8.490322080E-01
$H_2O(l)$	7.255750050E+01	-6.624454020E-01	2.561987460E-03	-4.365919230E-06	2.781789810E-09	-4.188654990E+04	-2.882801370E+02
S_2	2.858575400E+00	5.175835500E-03	-6.549343400E-06	3.399864300E-09	-4.015676600E-13	1.441240200E+04	9.891278490E+00
SO_2	3.266533800E+00	5.323790200E-03	6.843755200E-07	-5.281004700E-09	2.559045400E-12	-3.690814800E+04	9.664651080E+00
SO_3	2.578038500E+00	1.455633500E-02	-9.176417300E-06	-7.920302200E-10	1.970947300E-12	-4.893175300E+04	1.226513840E+01

Table 30 – Coefficients for the calculation of physical properties of selected species at T > 1000 K (From McBride et al. 1993).

T>1000	a_1	a_2	a_3	a_4	a_5	b_1	b_2
CH_4	1.635526430E+00	1.008427950E-02	-3.369162540E-06	5.349586670E-10	-3.155188300E-14	-1.000564550E+04	9.993133260E+00
C_2H_6	4.046666740E+00	1.535387660E-02	-5.470393210E-06	8.778262280E-10	-5.231673050E-14	-1.244735120E+04	-9.686836070E-01
C_3H_8	6.667893630E+00	2.061202140E-02	-7.365530270E-06	1.184407610E-09	-7.069532100E-14	-1.627485210E+04	-1.318595030E+01
C_4H_{10}	9.445358340E+00	2.578580730E-02	-9.236191220E-06	1.486327550E-09	-8.878971580E-14	-2.011382165E+04	-2.634700760E+01
C_5H_{12}	1.354699800E+01	2.842178600E-02	-9.417464800E-06	1.389358900E-09	-7.421260900E-14	-2.457768000E+04	-4.702118500E+01
C_2H_2	4.658785040E+00	4.883965470E-03	-1.608287750E-06	2.469742260E-10	-1.386056800E-14	2.575940440E+04	-3.998347720E+00
C_7H_8	1.293947500E+01	2.669215580E-02	-9.684201080E-06	1.573921400E-09	-9.466704820E-14	-6.770357690E+02	-4.672553020E+01
Ar	2.500000000E+00	0.000000000E+00	0.000000000E+00	0.000000000E+00	0.000000000E+00	-7.453750000E+02	4.379674910E+00
H_2	2.932865790E+00	8.266079670E-04	-1.464023350E-07	1.541003590E-11	-6.888044320E-16	-8.130655970E+02	-1.024328870E+00
N_2	2.952576260E+00	1.396900570E-03	-4.926316910E-07	7.860103670E-11	-4.607553210E-15	-9.239486450E+02	5.871892520E+00
O_2	3.660960830E+00	6.563655230E-04	-1.411494850E-07	2.057976580E-11	-1.299132480E-15	-1.215977250E+03	3.415361840E+00
CO_2	4.636594930E+00	2.741319910E-03	-9.958285310E-07	1.603730110E-10	-9.161034680E-15	-4.902493410E+04	-1.935348550E+00
CO	3.048485830E+00	1.351728180E-03	-4.857940750E-07	7.885364860E-11	-4.698074890E-15	-1.426611710E+04	6.017097900E+00
NO	3.260712340E+00	1.191011350E-03	-4.291226460E-07	6.944814630E-11	-4.032956810E-15	9.921431320E+03	6.369005180E+00
N_2O	4.823188730E+00	2.626852790E-03	-9.584260580E-07	1.599912960E-10	-9.774169390E-15	8.073356620E+03	-2.202366000E+00
NO_2	4.884744290E+00	2.172416390E-03	-8.280790200E-07	1.574772930E-10	-1.051105490E-14	2.316484620E+03	-1.173570750E-01
NH_3	2.717096920E+00	5.568563380E-03	-1.768863960E-06	2.674172600E-10	-1.527314190E-14	-6.584519890E+03	6.092898370E+00
H_2S	2.745219900E+00	4.043460700E-03	-1.538451000E-06	2.752024900E-10	-1.859209500E-14	-3.419944400E+03	8.054674500E+00
$H_2O(g)$	2.677037870E+00	2.973183290E-03	-7.737696900E-07	9.443366890E-11	-4.269009590E-15	-2.988589380E+04	6.882555710E+00
$H_2O(l)$	0.000000000E+00	0.000000000E+00	0.000000000E+00	0.000000000E+00	0.000000000E+00	0.000000000E+00	0.000000000E+00
S_2	3.988606900E+00	5.577505100E-04	-5.018927800E-08	-1.547031900E-11	2.666177100E-15	1.419801500E+04	4.491191590E+00
SO_2	5.245136400E+00	1.970420400E-03	-8.037576900E-07	1.514996900E-10	-1.055800400E-14	-3.755822700E+04	-1.074048920E+00
SO_3	7.075737600E+00	3.176338700E-03	-1.353576000E-06	2.563091200E-10	-1.793604400E-14	-5.021137600E+04	-1.118751760E+01